Electronic Thesis and Dissertation Repository

9-20-2011 12:00 AM

Critical Stages in Viral Replication - Entry, Gene Regulation and Egress

Matthew S. Miller
The University of Western Ontario

Supervisor
Dr. Joe Mymryk
The University of Western Ontario

Graduate Program in Microbiology and Immunology
A thesis submitted in partial fulfillment of the requirements for the degree in Doctor of Philosophy
© Matthew S. Miller 2011

CRITICAL STAGES IN VIRAL REPLICATION – ENTRY, GENE REGULATION
AND EGRESS

(Spine title: Key Stages of viral replication: Entry, gene regulation and egress)

(Thesis format: Integrated Article)

by

Matthew Steven <u>Miller</u>

Graduate Program in Microbiology and Immunology

A thesis submitted in partial fulfillment
of the requirements for the degree of
Doctor of Philosophy

The School of Graduate and Postdoctoral Studies
The University of Western Ontario
London, Ontario, Canada

THE UNIVERSITY OF WESTERN ONTARIO
School of Graduate and Postdoctoral Studies

CERTIFICATE OF EXAMINATION

<u>Supervisor</u>   <u>Examiners</u>

_____   _____
Dr. Joe Mymryk   Dr. Vince Morris

<u>Supervisory Committee</u>

                                                          _____
                                                          Dr. Stephen Barr

_____
Dr. Joe Torchia

                                                          _____
                                                          Dr. Bonnie Deroo

_____
Dr. Rodney DeKoter

                                                          _____
                                                          Dr. Karen Mossman

The thesis by

Matthew Steven <u>Miller</u>

entitled:

**CRITICAL STAGES IN VIRAL REPLICATION – ENTRY, GENE REGULATION
AND EGRESS**

is accepted in partial fulfillment of the
requirements for the degree of
Doctor of Philosophy

_____   _____
           Date   Chair of the Thesis Examination Board

ii

Abstract

Despite the amazing biological diversity exhibited by viruses, their very existence relies upon their ability to overcome a set of common barriers. The nature of these barriers reflects the nature of viruses themselves. During their extracellular phase, viruses are metabolically inert obligate parasites. Upon encountering a host cell, productive infection necessitates that the virus successfully enter the cell, regulate the expression of its genes, and after assembling new progeny particles, egress such that the cycle of infection can continue. These three basic processes are not only attractive candidates for therapeutic intervention, but also reveal much about virus biology in the most basic sense. That is why these processes are the focus of the studies described herein. We have identified vimentin, an intermediate filament protein expressed primarily in cells of mesenchymal origin, as a cellular factor required for the efficient onset of human cytomegalovirus (CMV) infection in fibroblasts. We observed that an endotheliotropic (EC-tropic) strain of CMV relies more heavily on vimentin than the fibroblast-adapted strain, possibly reflecting different modes of entry utilized by these two strains. We have also performed the first functional study of the 55R E1A protein encoded by human adenovirus (HAdV). This protein was expressed at late times post-infection and was able to both transactivate expression of viral genes, and promote productive replication of HAdV in the absence of all other E1A isoforms. Finally, our focus returns to CMV where we describe a novel protein that we have dubbed ' nuclear rim-associated cytomegaloviral protein' (RASCAL). RASCAL is expressed with early-late kinetics and localizes to the nuclear rim, in deep intranuclear invaginations, and in unusual lamin B-positive vesicular structures at late times post-infection. RASCAL could be immunoprecipitated with pUL50, a member of the CMV nuclear egress complex (NEC) and pUL50 was sufficient to recruit RASCAL to the nuclear rim. These studies have illuminated novel processes through which two important human viruses enter cells, regulate viral gene expression and ultimately egress. Considered together, they have also expanded our understanding of three central aspects of virus biology upon which further studies can build.

KEYWORDS

Human cytomegalovirus, Human adenovirus, early region 1A (E1A), cytoskeleton, vimentin, viral entry, rim-associated cytomegaloviral protein (RASCAL), viral egress, nuclear egress complex, 9S E1A, 55R E1A

Co-Authorship Statement

Chapter 2 of this thesis was published in Journal of Virology **83**(14):7015-7028, July 2009. I was involved in performing all of the experiments.

Chapter 4 of this thesis was published in Journal of Virology **84**(13):6483-6496. I was involved in performing all experiments with the exception of those described in Fig. 4-2c,d, which were primarily performed by W. E. Furlong, and those described in Fig. 4-8 which were primarily performed by L. Hertel.

Dedication

""Forty-two" said Deep Thought, with infinite majesty and calm.

..."But it was the Great Question! The Ultimate Question of Life, the Universe and Everything," howled Loonquawl

..."Exactly," said Deep Thought. "So once you know what the question actually is, you'll know what the answer means."

-from "Hitchhiker's Guide to the Galaxy" by Douglas Adams

I dedicate this thesis to the many "teachers" I have had the privilege of encountering over the course of these early, formative years of my life: from my parents, family, girlfriend, friends, educators and advisors , to nature herself. Thank you for teaching me that asking the right questions in life is almost always far more important than having the right answers.

Acknowledgments

There are a great many people to whom I owe a great deal for any of the successes I have enjoyed during the completion of this work. Indeed, I am quite certain that none of this would have been possible without the contributions and support of those listed below.

I am forever deeply indebted to my supervisor, Dr. Joe Mymryk. His guidance as a supervisor, mentor and friend has played an instrumental role in both where I am today, and where I will go in the future. Dr. Mymryk belongs to that rarest breed of individuals whom one must admire both personally and professionally. The formative scientific lessons that I have learned from Dr. Mymryk are matched only by the humility, respect and deep concern for others that he demonstrates by example each day. I feel absolutely privileged to have been a part of his laboratory.

I would also like to thank Dr. Laura Hertel, who supervised the early part of my studies and played a formative role in my scientific development. Her attention to detail and demand for excellence have taught me valuable lessons about what it takes to succeed in this discipline.

I have been fortunate to have been surrounded by truly wonderful people during my time as a member of the Department of Microbiology & Immunology. I owe an enormous 'thank you' to my lab mates, who have not only been a great resource, but have also made the lab an exciting and enjoyable place to spend long days and sleepless nights. I would also like to thank my Advisory Committee members: Dr. Wayne Flintoff, Dr. Miguel Valvano, Dr. Rodney DeKoter and Dr. Joe Torchia. Their guidance and support have been invaluable through both successes and difficulties. Finally, I would like to thank all members of the department with whom I have had the privilege of interacting. You have been wonderful colleagues and great friends!

Of course, I would be nowhere without the amazing personal support network of my family and friends. My deepest heartfelt gratitude to my parents, Anne and Steve. Their constant love, support and sacrifices have allowed me to pursue my dream. This is a gift

that I fear I will never be able to repay. I also owe my sincere gratitude to my girlfriend, Kara. Her love, encouragement and most importantly, patience, have been a constant source of comfort and inspiration. I could not have completed this feat without her. The 'men' at Unit 98 have been my family away from home. They are largely responsible for my sanity through the best and worst of times. One could not ask for better housemates. Cheers, gentlemen! Sincere thanks as well to my grandparents, aunts, uncles, cousins and dear friends. You have all been instrumental contributors to my success.

Table of Contents

List of Figures (where applicable)

List of Abbreviations

Abbreviation	Meaning
Ab	Antibody
AP	Assembly protein
APIS	ATPase proteins independent of 20S
ATCC	American Type Culture Collection
BB	Blocking buffer
BRK	Baby rat kidney
CAR	Coxackie virus and Adenovirus receptor
CBP	CREB-binding protein
CDK	Cyclin-dependent kinase
CDK1	cdc2/Cyclin-dependent kinase 1
CMV	Human Cytomegalovirus
c-ORFs	Conserved open reading frames
CR	Conserved region
CtBP	C-terminal binding protein
DC	Dendritic cells
DE	Delayed early genes
DYRK	Dual specificity tyrosine phophorylation-regulated kinase
E1A	Early region 1A
E1B	Early region 1B
EBV	Epstein-barr virus
EC	Endothelial cells
EC-tropic	Endotheliotropic

ER	Endoplasmic reticulum
ERGIC	ER-golgi intermediate complex
g	Glycoprotein
GFAP	glial fibrillary acidic protein
GST	Glutathione S-transferase
HAdV	Human adenovirus
HAT	Histone acetyltransferase
HDAC	Histone deacetylase
HEK	Human embryonic kidney
HF	Human foreskin fibroblasts
HHV-5	Human Herpesvirus 5
hpi	hours post-infection
HPV	Human Papillomavirus
HSPGs	Heparin sulfate proteoglycans
HSV-1	Herpes Simplex Virus type I
IE	Immediate early genes
IF	Intermediate filaments
IFN	Interferon
INM	Inner nuclear membrane
KLH	Keyhole limpet hemocyanin
L	Late genes
LBR	Lamin B receptor
LDS	Lithium dodecyl sulfate
MEF	Mouse embryonic fibroblast
MLP	Major late promoter

MoRFs	Molecular recognition features
MTOC	Microtubule organizing centre
MW	Molecular weight
NEC	Nuclear egress complex
NPC	Nuclear pore complex
NR	Nuclear receptor
ONM	Outer nuclear membrane
ORFs	Open reading frames
pAP	Precursor of the assembly protein
PBS	Phosphate buffered saline
PFA	Phosphonoformic Acid
PKA	Protein kinase A
PKC	Protein kinase C
pPR	Precursor of the maturational protease
PR	Maturational protease/assemblin
PVDF	Polyvinylidene difluoride
R	Residues
RASCAL	Rim-associated cytomegaloviral protein
Rb	Retinoblastoma
SDS	Sodium dodecyl sulphate
siS8	S8 silencing RNA
STAT	Signal transducers and activators of transcription
TBP	TATA-binding protein
TBS	Tris-buffered saline
TMD	Transmembrane domain

TR	Thyroid hormone receptor
UL	Unique long
US	Unique short

Chapter 1 INTRODUCTION

1.1 Preface

"The aim of science is to seek the simplest explanation of complex facts. We are apt to fall into the error of thinking that the facts are simple because simplicity is the goal of our quest. The guiding motto in the life of every natural philosopher should be "Seek simplicity and distrust it.""-*Alfred North Whitehead (1861-1947) English Mathematician and Philosopher-from **Concepts of Nature***

The above quote by Alfred North Whitehead should not only serve as an important reminder to all those seeking to unravel nature's complexities, but should resonate with particular strength amongst virologists. At a glance, the focus of our studies would seem exceedingly simple: biological particles composed of small strands of nucleic acids with limited coding potential encased within a proteinaceous shell, some of which are surrounded by lipid envelopes, others which are not. In isolation, these particles are metabolically inert - unable to perform even the most basic functions associated with life, including self-replication. However, in the context of a host cell, an organism or indeed, an entire ecosystem, these seemingly simple particles perform a dazzlingly diverse array of functions, many of which have shaped, and continue to shape every aspect of life on this planet.

Herein, the author shall focus his attention on three essential processes common amongst all viruses: entry, gene regulation and egress. The first and last processes were investigated in the context of human cytomegalovirus infection, whereas gene regulation was studied in the context of human adenovirus infection. In each case, the author sought to arrive at the simplest explanation which rectifies a series of complex observations. It is

the sincere hope of the author that during the course of these studies, areas that were previously poorly understood have become illuminated, and that once completed, we will find many more questions to ask, and perhaps even arrive at a few answers.

1.2   Human Cytomegalovirus

1.2.1   General Characteristics

CMV, also known as Human Herpesvirus 5 (HHV-5) belongs to the family *herpesviridae*, and is a member of the betaherpesvirus subfamily. These viruses exhibit strict species specificity and productively infect many differentiated cell types, including fibroblasts, endothelial cells (EC), epithelial cells, macrophages and dendritic cells (DC) (48, 67, 88, 129, 134, 199, 228). In fact, it is easier to mention the few cell types that do not seem to support productive CMV infection; these include lymphocytes and polymorphonuclear leukocytes (80, 200-201). CMV has been shown to use many different entry receptors (98) and permissiveness to infection seems to be determined at a post-penetration step (199, 202). Serial passaging of clinical isolates on human foreskin fibroblasts (HF) has resulted in the accumulation of mutations which improves growth of these strains on HF, while concomitantly decreasing their tropism for other cell types, such as EC and DC (31, 50, 135, 142-143). These strains are now called 'laboratory-adapted,' and many were intially passaged on HF with the hope that they would become attenuated and could then be used for the generation of a vaccine (73). Unfortunately, this strategy was largely unsuccessful. However, new vaccine strategies have been developed over the past several years and are currently the focus of active investigation (191).

Infection by CMV is ubiquitious in the adult population, though frequency of infection is higher in less-developed countries. Primary infection usually occurs early in life and is especially prevalent in childcare settings. In immunocompetent individuals, primary infection is generally asymptomatic. However, severe disease often develops during reactivation of CMV in immunocompromised individuals, especially transplant recipients undergoing immunosuppressive drug regimes. This generally occurs because like other herpesviruses, CMV is able to establish latency within the host following primary infection, and periodically reactivates throughout the rest of the host's life. In addition, CMV is somewhat unique among herpesviruses in that transplacental transmission occurs naturally. This type of transmission is much more common in women who experience primary infection during pregnancy, as opposed to those who experience a reactivation from latency (62, 123, 136).

1.2.2   Virion Structure

Like all herpesviruses, the CMV virion is composed of a double-stranded DNA genome enclosed within a proteinaceous, icosohedral capsid. The capsid itself is surrounded by another, less structured proteinaceous layer called the tegument (or matrix). The tegument consists of approximately 30 virus-encoded proteins, most of which are phosphorylated, as well as some other cellular proteins and various RNAs. While many proteins are found in the tegument, the most abundant are pp65 (encoded by UL83), pp71 (encoded by UL82) and pp150 (encoded by UL32) at 15%, 9% and 9% abundance by mass, respectively (225). These tegument proteins serve two primary functions. The first is to assist in the structural assembly and disassembly of the virion during entry and

egress. The second is to subvert the cell's normal response to infection, thereby creating an environment which is conductive to viral replication (136).

In addition to making contacts with the capsid, tegument proteins also interact with the viral envelope and the proteins embedded therein. The mature virion envelope is ultimately derived from the endoplasmic reticulum (ER)/ER golgi intermediate complex (ERGIC). In terms of facilitating viral entry, the most essential envelope proteins encoded by CMV share significant homology with those encoded by other herpesviruses. These proteins form distinct complexes on the viral envelope commonly termed glycoprotein (g)B, gH:gL and gM:gN (27, 39). gB is expressed on the envelope as a disulfide-linked homodimer. It is responsible for the initial interaction between the virion and heparan sulfate proteoglycans present on the surface of target cells, as well as cell-to-cell transmission and fusion of infected cells (136). It is also the major target of the neutralizing antibody response and has thus received attention as a vaccination candidate (69, 108). Together, these components generate a virion of approximately 200-300 nm in diameter (136).

1.2.3   Genome

The CMV genome is composed of a unique long (U_L) and a unique short (U_S) sequence flanked by internal and terminal repeats. This arrangement of repeats promotes isomerization of the genome, leaving four possible combinations of infectious genomes (Fig. 1-1). These genomes range in size from 196-241 kbps, depending on the particular strain in question. The termini of the genome contain conserved packaging signals (*pac-1* and *pac-2*) which are recognized during encapsidation and determine the site of

concatamer cleavage (136). There is also a large origin of replication (*ori*Lyt) located between genes UL57 and UL69 which is necessary for lytic replication of the viral genome (6, 23, 122). CMV is estimated to contain about 140 genes, approximately 80 of which are necessary for replication in fibroblasts (53, 245). The rest of the genes are thought to be involved in processes including cell-type specific tropism, temperance or immune modulation. Currently recognized ORFs have been characterized by a set of arbitrary criteria, most notably an insistence on undisrupted coding regions and for the coding of polypeptides greater than 100 amino acids in size. Recent studies have re-examined the historical annotation of CMV genomes and have resulted in the identification of a number of putative open reading frames (ORFs) that were previously unrecognized. Several of these ORFs are conserved among multiple clinical isolate and have thus been dubbed 'conserved ORFs (c-ORFs) (47, 50, 142).

1.2.4   Entry and Tropism

1.2.4.1   Factors associated with viral tropism

Herein, we shall define 'entry' as all processes from the time of initial viral binding to the expression of immediate early genes. The process of CMV entry into a host cell begins with binding of gB to surface heparin sulfate proteoglycans (HSPGs) (39). Depending on the cell type being studied, gH:gL:gO or gH:gL:UL128-131 complexes are then required to promote higher affinity binding with one of the many known CMV receptors and/or downstream fusion of the viral envelope with the cellular membrane (98). In fact, the UL128-131 locus has been mapped as a major viral determinant of CMV tropism. The

gH:gL:UL128-131A complex is required for endocytic uptake of CMV virions into EC and epithelial cells, and in some cases this is followed by pH-dependent fusion of the viral envelope with the endocytic vesicle, which facilitates capsid release into the cytoplasm (159, 183-184). Interestingly, HF-adapted CMV strains are often found to have acquired large deletions or mutations in this region which inevitably result in loss of tropism breadth. For example, the common laboratory adapted strain, AD169, harbours a frameshift mutation in UL131A which results in the production of a truncated protein and subsequent loss of EC tropism (1, 3, 81, 230). While the specific mutations acquired by other laboratory-adapted strains differ subtly, the restricted tropism that results is common.

Numerous cellular factors also contribute to CMV tropism, though they have not yet been fully described. Strikingly though, penetration into the cell does not seem to be a major barrier. A myriad of cell surface receptors which facilitate CMV entry have been described throughout the years, though none appear to be absolutely required in all settings. These include various integrin family heterodimers: $\alpha2\beta1$, $\alpha6\beta1$ and $\alpha_v\beta3$ (58, 98, 230), platlet-derived growth factor-α receptor (205) and epidermal growth factor receptor, whose characterization as a bona-fide entry receptor has been controversial (97, 233).
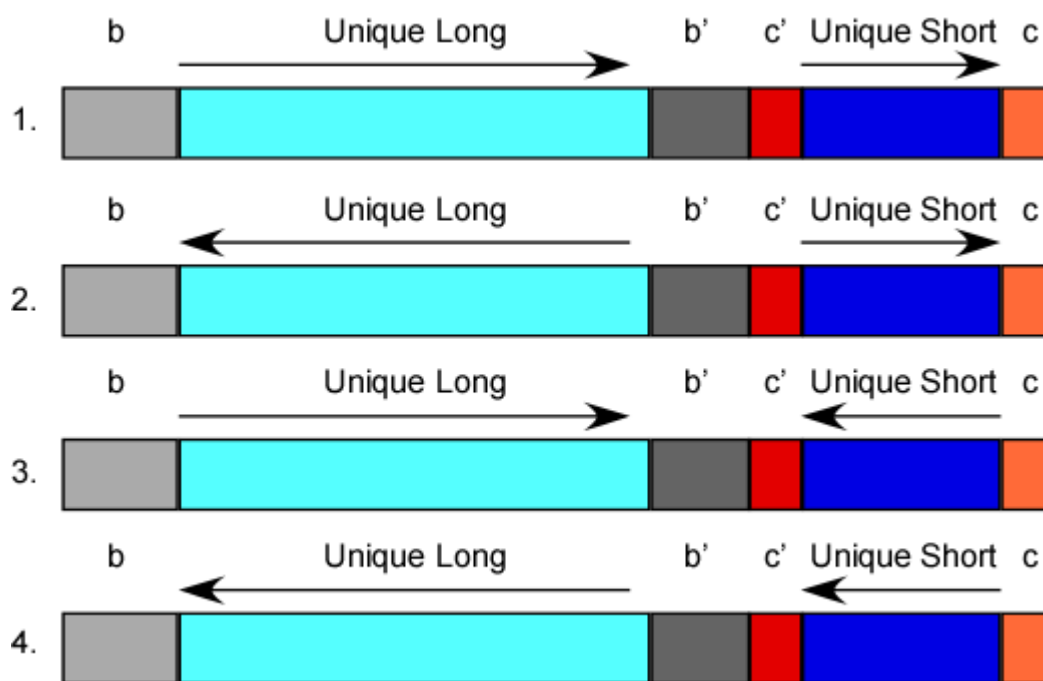
FIG. 1-1. Diagrammatic representation of the possible isomeric arrangements of the CMV genome. The unique long segment of the CMV genome contains the vast majority of CMV ORFs. It is flanked by a terminal repeat long (b) and an inverted repeat long (b'). The unique short region contains fewer ORFs, many of which encode proteins involved in immune evasion. The unique short region is flanked by an inverted repeat short (c') and a terminal repeat short (c). This genetic architecture allows for four possible isomeric arrangements of the CMV genome. The directionality of the U_L and U_S segments in each isoform are denoted by arrows.

1.2.4.2 Penetration of CMV virions in different cell types

Cytoplasmic release of AD169 capsids into HF occurs mainly through direct fusion of the viral envelope with the plasmalemma, although some studies have reported observing AD169 in phagolysosome-like structures within HF (40, 204). This may be explained by the fact that AD169 capsids express only the gH:gL:gO glycoprotein complex, and lack the gH:gL:UL128-131A complex which is known to be required for endocytic uptake of CMV in epithelial cells and EC (159, 183-184). The mechanism used by the EC-tropic strain TB40/E to enter fibroblasts has not been formally investigated, although it was assumed to be similar to AD169 despite the fact that TB40/E is able to express both gH:gL:gO and gH:gL:UL128-131A complexes (199). Recently, it has become clear that the cell type in which a viral strain is grown plays a major role in determining the tropism and spread of progeny virus. In fibroblast cultures, virus spread is mainly supernatant-driven, whereas in EC cells, spread is mainly focal. Closer inspections of the viruses released from these cells revealed that HF infected with an EC-tropic strain of CMV release virus capable of infecting both EC and HF. In contrast, EC infected with the same EC-tropic strain of CMV released virus that could readily infect HF, but was much poorer at infecting EC. This phenotype correlated with the amount of gH:gL:UL128-131A incorporated into the virions of virus found in the supernatant, with virions from HF-derived supernatants carrying significantly more of this complex. Further experiments demonstrated that all of these observations resulted from retention of EC-tropic virus expressing gH:gL:UL128-131A on/in EC cells (192).

1.2.4.3   The cytoskeleton and its role during CMV entry

The cellular cytoskeleton is composed of three major networks: microtubules, microfilaments and intermediate filaments. The basic units of microtubules are α- and β-tubulin heterodimers. These dimers assemble in a head-to-tail orientation to form protofilaments, 13 of which create a hollow microtubule with an outer diameter of 25 nm. These structures exhibit a defined polarity whereby the 'plus' end of microtubules is extremely dynamic and the 'minus' end is quite stable and is tethered to the microtubule organizing centre (MTOC) (102). Two classes of motor proteins facilitate transport along these 'cellular roadways.' Plus-ended motor proteins are called kinesins and this superfamily includes at least 45 members in mammalian cells. These proteins move cargo towards the cell periphery. They are composed of two heavy chains and two light chains (130). Minus-end transport (ie. toward the cell centre) is accomplished by dynein. The structure of dynein is complex, as each motor consists of two heavy chains, two intermediate chains and multiple intermediate light/light chains (168). Its processivity is stablized by a large protein complex called dynactin which interacts with specific cargo (223).

Microfilaments are the smallest of the cytoskeletal elements and their basic units consist of α-, β- and γ-actin. α-actin is found most commonly in the contractile elements of muscle tissue, whereas β- and γ-actin co-exist in most other cell types to generate microfilaments. Like microtubules, actin microfilaments have a definite polarity. ATP-bound actin monomers (G-actin) assemble into protofilaments (F-actin), two of which wind around one another to form a microfilament of 5-9 nm in diameter. The polarity of

these filaments can be detected by decoration microfilaments with myosin S1 fragments which create 'barbed' (+) and 'pointed' (-) ends. The actin motor proteins myosin V and myosin VI are largely responsible for the transport of cargo along microfilaments. Myosin V is a plus-end-directed motor protein that transports cargo to the cell surface, while mysoin VI carries endocytic vesicles inward (4).

As their name suggests, intermediate filaments (IF) have a diameter of about 10 nm, intermediate in relation to microfilaments and microtubules. The major role of IF proteins is to provide mechanical support for the cell, as there are no known motor proteins which transport cargo on them. All IF proteins have the same basic structure, globular N- and C-terminal domains surrounding an alpha-helical central rod. Individual IF proteins first dimerize in the rod domain to form a coiled coil. These dimers then polymerize in an antiparallel orientation, meaning that unlike microtubules and microfilaments, they do not exhibit polarity. There are approximately 70 IF genes which are subdivided into six types of IFs, whose characterization is based on protein structure and amino acid similarity. Acidic and basic keratins comprise the type I and II IFs, respectively. Type III IFs can form either homo- or heteropolymers; desmin, glial fibrillary acidic protein (GFAP), peripherin and vimentin belong to this group. Type IV IFs include α-internexin, synemin, syncoilin and the neurofilaments. The lamins (A, B and C), which provide structural support in the nucleus, comprise the type V IFs. Nestin is an example of a type VI IF and is expressed in many cell types during development, but generally does not persist into adulthood (56, 64).

The profile of IFs expressed by different cells vary. Some cells express only one type of IF, while others express several. This property has been exploited by scientists and medical practitioners such that certain IFs can now be used as biomarkers to monitor disease states. For example, vimentin is expressed specifically in mesenchymal cells, but not in epithelial cells. Thus, vimentin expression can be used to monitor mesenchymal to epithelial transition and epithelial to mesenchymal transition, which is a common process during the metastasis of many cancers (104).

Many viruses utilize and alter the cytoskeleton during infection. In certain cases, cytoskeletal elements must be depolymerized in order for large capsids to be transported through the cell body. In other cases, cytoskeletal elements are stabilized and exploited, along with their motor proteins, for capsid transport (49, 117). In the case of CMV, de-enveloped capsids associate with the microtubule network following capsid release into the cytoplasm. Microtubules then facilitate their transport toward the MTOC. Treatment of cells with microtubule depolymerizing agents nocodazole and colchicine severely hinders CMV infection, but also results in the structural collapse of vimentin, an important IF protein. Therefore, one must be cautious in the interpretation of such experiments (103, 154). At around the same time, depolymerization of the actin microfilament network is observed and may be necessary for efficient transport of capsids through the actin microfilament-dense cytosol (11, 101, 116). The role of the IF network during CMV entry has not been assessed.

The method by which capsids are transported from the MTOC to the nucleus is poorly understood, but eventually capsids are thought to dock at nuclear pores through which

they deposit their genomes. Though this has not been studied carefully in the context of CMV, elegant atomic force microscopy studies have been able to visualize Herpes Simplex Type I (HSV-1) capsids docked at the nuclear pore complex (NPC) depositing densely compacted rod-like structures (thought to be the HSV-1 genome) into the nucleus (196).

1.2.5   CMV Gene Expression

Following nuclear deposition of the viral genome, immediate-early (IE) gene expression is initiated. IE1 and IE2 proteins are the first to be expressed and are the major viral transactivating factors. In addition to the roles these proteins play in activating downstream viral genes, IE1 blocks signal transducers and activators of transcription (STAT) signaling in order to prevent interferon (IFN) activation while IE2 induces cell-cycle arrest and apoptosis (14, 160, 240-241). At approximately 6 hours post infection (hpi) IE proteins activate transcription of delayed-early (DE) genes. DE genes are expressed until 18-24 hpi, and many play important roles in initiation of viral DNA replication and modulation of the host cell environment to create a milieu which is conducive to viral replication (7, 237). Late (L) gene regulation is not well-studied in the context of CMV, but in general, L genes are characterized as those whose expression begins later than 24 hpi and/or are sensitive to inhibition of viral DNA synthesis (136). Most genes that belong to this class are involved in encapsidation, virion assembly and egress (164).

1.2.6   Encapsidation and Egress

1.2.6.1   Nucleocapsid assembly

Encapsidation takes place in the nucleus adjacent to CMV DNA replication compartments. The process is initiated by a set of conserved herpesvirus proteins: MCP, TRI1, TRI2, SCP and PORT, that together form a procapsid around the UL80.5 gene product, precursor of the assembly protein (pAP). Another protein, precursor of the maturational protease (pPR), is also required for DNA encapsidation and procapsid maturation to nucleocapsid. pPR is self-cleaved by the maturational protease (PR, also called assemblin) which is initially within the same peptide. PR is also responsible for cleavage of pAP to its various intermediate forms and its mature form, assembly protein (AP). PR, AP and intermediate pAP isoforms are all removed from nucleocapsids after packaging of viral DNA (68).

1.2.6.2   The nucleus as a barrier during CMV egress

After successful assembly of the nucleocapsid, a complex egress pathway ensues which eventually results in the envelopment of capsids and their release from the cell. Before reaching the cytoplasm, capsids must first traverse the nuclear envelope. This barrier consists of an inner and outer nuclear membrane, separated by a perinuclear space. Within the perinuclear space are several proteinaceous structures which link the two membranes and provide the nucleus with structural support. The NPC consists of a network of proteins called nucleoporins, which form channels linking the cytoplasm with the nucleoplasm. These complexes associate with other proteins and are tightly regulated

as they largely control the transport of materials into and out of the nucleus (52). However, viral capsids are too large to pass through these complexes. The perinuclear space is also rich in a rigid network of lamins which link the periphery of NPCs to chromatin. Together, these structures represent a formidable barrier through which the virus must escape.

1.2.6.3   The nuclear lamina

The nuclear lamins are type V IF proteins and include lamins A, B1, B2 and C. Lamin B1 and B2 are encoded by distinct genes, whereas lamins A and C result from differential splicing of the product encoded by the *lmnA* gene. Lamin B is mainly associated with the inner nuclear membrane (INM) and plays a critical role in maintenance of nuclear shape. Lamin A associates more specifically with the nucleoplasm, performing specialized roles and contributing to nuclear stiffness (28, 95, 109).

Lamins have the same conserved structural features as other members of the IF family. They are composed of a central alpha-helical rod domain flanked by globular head and tail regions. The rod domains of two individual lamin molecules dimerize in a parallel manner, and these dimers interact with one another to form longer lamin filaments and regular cross-connections (175). In addition to providing the nucleus with structural support, the lamina also serves as a scaffold for proteins which span the nuclear envelope, interact with chromatin or with structures present in the cytosol including lamin B receptor (LBR) and emerin, chromatin-modifying enzymes and transcription factors, as well as cytoskeleton-interacting proteins (137, 171).

Despite its role in mediating nuclear rigidity, the nuclear lamina is a dynamic structure and must reorganize at various stages throughout the cell cycle. The assembly and disassembly of the nuclear lamina is regulated by site-specific phosphorylation events by various kinases, including the cAMP-dependant kinases protein kinase A (PKA), protein kinase C (PKC) and cdc2/cyclin dependent kinase 1 (CDK1) (149). Lamin A/C is phosphorylated by CDK1 at Ser-22, Ser-390 and Ser-392 while lamin B is phosphorylated by CDK1 only at Ser-22 to promote disassembly of the nuclear lamina during mitosis (87, 149, 167). This strategy is also exploited by the viral NEC in order to facilitate capsid escape from the nucleus.

1.2.6.4   The CMV nuclear egress complex

The first stage of CMV egress is primary envelopment which occurs at the inner nuclear membrane. Following successful assembly of viral nucleocapsids and their accumulation proximal to the INM, the viral pUL97 kinase is recruited to the nuclear envelope by cellular p32, and also interacts with LBR (120). At this location, pUL97 phosphorylates lamins at CDK1 sites, leading to their local disruption (84). Lamin phosphorylation by UL97 generates a binding site for the cellular peptidyl-prolyl *cis/trans*-isomerase, Pin1. During CMV infection Pin1 relocalizes to viral replication centres and to the nuclear lamina (133). Disassembly of the nuclear lamina seems to promote the accumulation of viral proteins pUL53 and pUL50 (homologs of herpes simplex virus (HSV) proteins pUL31 and pUL34 and epstein-barr virus (EBV) proteins BFLF2 and BFLF1) to the nuclear membrane. These proteins interact with phosphorylated p32, lamin A/C and LBR to form the basic NEC (30, 131-132, 185). pUL50 is a type II integral membrane protein

that accumulates in the INM. It is required for the proper localization of pUL53 proximal to the INM and unlike its HSV homolog pUL34, it is sufficient to recruit PKC to the NEC. Recruitment of PKC aids in further disruption of the nuclear lamina in order to allow passage of primary enveloped capsids through the perinuclear space (131, 141).

Disassembly of the nuclear lamina results in marked morphological changes within the nucleus itself. In particular, large infoldings of the INM have been observed proximal to nucleocapsids and these areas seem to be where primary envelopment takes place (29, 43, 70, 194). Enveloped particles then enter the perinuclear space and are then thought to fuse with the outer nuclear membrane (ONM) resulting in de-envelopment (Fig. 1-2). It is likely that other viral and cellular factors contribute to the nuclear egress of CMV, but have yet to be identified. These factors may also aid in remodeling of the nucleus and/or the assembly, trafficking and maturation of virions.
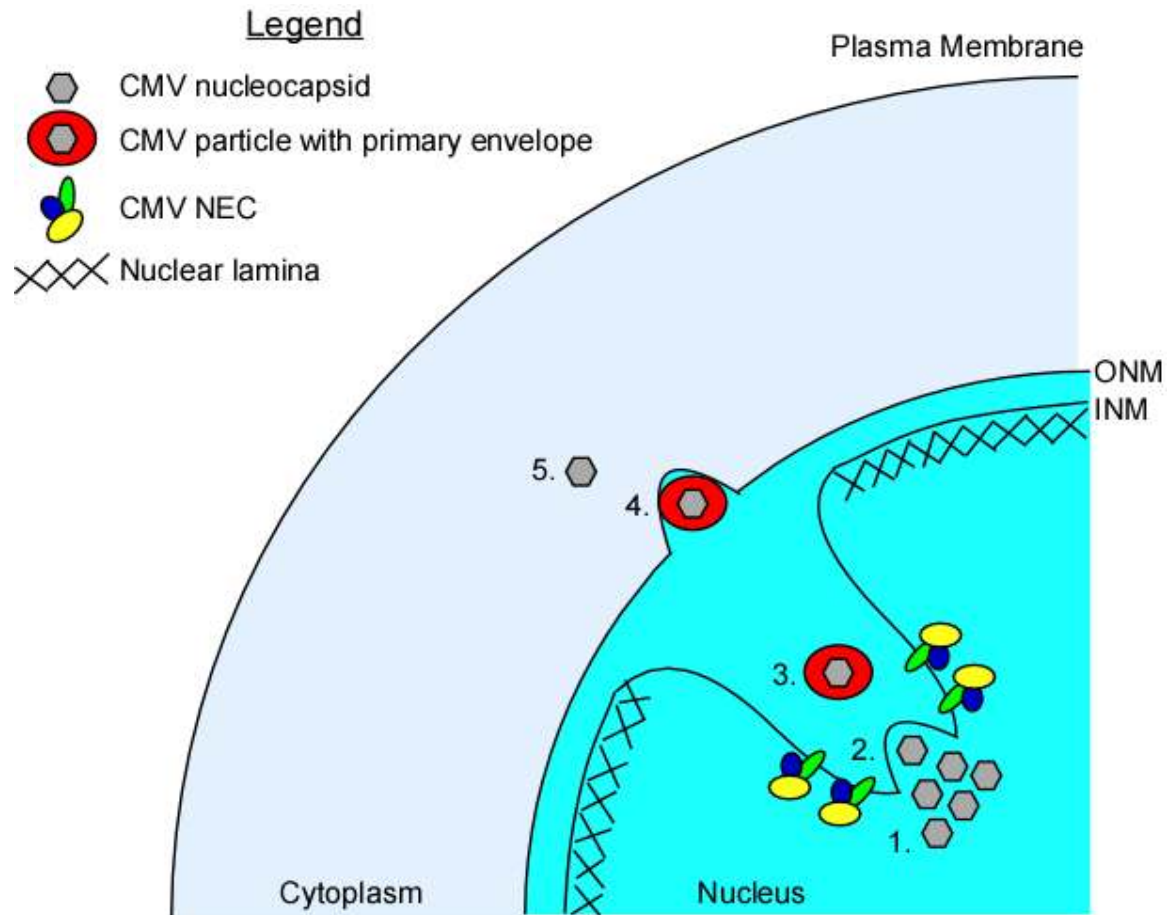
FIG. 1-2. Process of CMV nuclear egress. 1. The process of nuclear egress begins with assembly of the CMV NEC. This complex mediates disassembly of the nuclear lamina, which subsequently results in deep invaginations of the INM to regions of the nucleus containing viral nucleocapsids. 2. Nucleocapsids acquire their primary envelope by budding through in INM into the perinuclear space. 3. Viral particles containing primary envelopes move through the perinuclear space towards the ONM. 4. Particles that have undergone primary envelopment fuse with the ONM to facilitate nucleocapsid release into the cytoplasm. 5. De-enveloped nucleocapsids are transported through the cytoplasm and eventually acquire their secondary and final envelope, before being released at the plasma membrane.

1.2.6.5 Secondary envelopment and release

The vast majority of tegument proteins are thought to associate with the capsid during the cytoplasmic stage of egress. While the tegument is often considered to be amorphous, recent studies suggest that those proteins that associate most closely with the capsid may actually exhibit an icosohedral symmetry (128). Assembly of the capsid-proximal layers of the tegument seem to be mediated by a complex series of protein-protein interactions that exhibit a high degree of redundancy. This process may be nucleated by the UL48 gene product, a homolog of HSV-1 UL36 (or large tegument protein) which interacts with capsid pentons (124, 128). The UL32 gene product pp150 is another major tegument protein that plays a crucial role in virion maturation. pp150 associates with capsids in the nucleus and continues to accumulate at the cytoplasmic inclusion and locations of secondary envelopment and final maturation (48, 186, 188). Together with UL99-encoded pp28, these proteins form the basis of a transport complex which ultimately results in the secondary envelopment of nucleocapsids at cytoplasmic assembly compartments located adjacent to the nucleus. This compartment consists of a series of concentric rings that surround the MTOC, with trans-golgi network and endosome-derived rings located most centrally and golgi/ER-derived rings forming the periphery (45, 188, 198). This rearrangement causes the characteristic 'kidney bean' nuclear morphology observed at late times post-infection, and the 'owl's eye' cellular morphology typical of CMV infection. Once secondary envelopment has been completed, vesicles containing mature virions are transported to the cell membrane where the virus is released (136).

1.3 Human Adenovirus

1.3.1 General Characteristics

Adenoviruses were first discovered in 1952 as the etiological agents responsible for acute respiratory infections (89, 179). However, these infections are responsible for only a minority of childhood respiratory illnesses, which themselves are generally self-limiting. The most striking early observation involving adenovirus infections came in 1962, when Trentin and colleagues showed that HAdV-12 caused malignant tumors upon infection of newborn hamsters (220). This was the first example of an oncogenic human virus, although HAdV has never been shown to cause cancer in humans. Nevertheless, this observation sparked an explosion of interest in the field which led to the use of HAdV as a tool to understand many critical cellular processes and pathways including: mRNA splicing, regulation of gene expression, DNA replication and cell cycle control.

There are currently approximately 50 types (formerly serotypes) of HAdV, which are divided into 6 species (formerly subgroups) based on their ability to agglutinate red blood cells (178). Recently, the accuracy and utility of naming and characterizing HAdVs according to the traditional methods of serology and agglutination has come into question. This has sparked a debate in the field as to the design of a new naming convention for HAdVs that will serve both the clinical and basic science communities, and more accurately group viruses based on parameters which reflect the relationships among the viruses themselves (9, 96, 193).

1.3.2   Virion Structure

Unlike herpesviruses, HAdV particles are non-enveloped. The capsids are icosohedral in shape and approximately 90 nm in diameter, with fibers projecting from the vertices (181-182). 240 hexon (trimer of polypeptide II) capsomers and 12 penton capsomers constitute the major structural components of the virion (71). Fibers project from the penton base (hexamers of polypeptide III) and play an important role in receptor binding and entry (251). The minor capsid protein VI is important for endosomal escape (242).

Recent cryo-electron microscopy and crystallography studies have greatly enhanced understanding of HAdV capsid structure and assembly (115, 173). Protein IIIa is responsible for coordinating the penton base with its five surrounding hexon units through an interaction with the vertices of these subunits that together form group-of-six tiles. Protein IX acts as a network of 'ropes' linking hexons together to form group-of-nine tiles. These ropes also link group-of-nine tiles to one another, further contributing to capsid stability. Yet another underlying network, coordinated by protein IIIa and VIII, bind each group-of-six tile to five surrounding group-of-nine tiles (115, 173).

The viral DNA is condensed within the core by three basic, arginine-rich proteins: polypeptides V, VII and μ (8, 91, 180). Terminal protein is covalently bound to the 5'-ends of viral DNA by a phosphodiester bond between the β-hydroxyl group of serine 562 and the 5' hydroxyl of the terminal deoxycytosine (174, 203). Polypeptide VII is the most predominant core protein, with over 800 copies per virion (181, 187). The core also contains approximately 10 copies of the viral cysteine protease p23, which is responsible for cleavage of several virion precursor proteins during assembly and maturation (236).

Polypeptide V appears to link the virion core to the capsid via an interaction bridging the penton base and polypeptide VI (57).

1.3.3   Genome

The HAdV genome is approximately 36 kbp in size and is flanked by inverted terminal repeats which function as origins of replication during asymmetric synthesis of viral DNA (46, 177). The viral genome packaging sequence is composed of a series of repeats located between the left terminal inverted repeats and early region 1A (E1A) (75, 85). HAdV-2 was the first HAdV to have its genome sequenced completely (177), although subsequently many more complete sequences have been compiled for both HAdV and AdVs from other species.

The HAdV genome contains five early transcription units (E1A, early region 1B (E1B), E2, E3, and E4), three delayed-early units (IX, IVa2 and E2 late) and one late transcription unit (major late) which encode L1-L5. By convention, the map of the HAdV genome is depicted with E1A at the left end. While the sequence of most structural proteins is highly conserved, more variability is evident in early regions 1, 3, 4 and in the small virus-associated RNA (VA RNA), which is transcribed by RNA polyermase III (46). Genes are transcribed from both strands of viral DNA, with E1A, E1B, IX, major late, VA RNA and E3 transcribed from the rightward reading strand, while the leftward reading strand encodes E4, E2 and IVa2 (18).

All mRNAs transcribed by RNA polymerase II give rise to multiple species through alternative splicing and/or use of alternative poly(A) sites. The lack of a consistent terminology for naming of HAdV proteins has led to a confusing nomenclature whereby

some proteins are named according to the sedimentation coefficients of the mRNAs which encode them or the particular number of amino acids residues present in the protein (ie. E1A), others are named according to the molecular weight of the proteins themselves (ie. E1B and E3), the ORF from which they arise (ie. E4) or descriptively, according to their function (ie. E2) (18). For the sake of clarity herein, E1A isoforms shall be referred to according to the number of residues composing each isoform (ie. 289R, 243R, etc... in the case of HAdV-2/5).

1.3.4   Viral Entry and Egress

Most detailed studies of the HAdV infection cycle have been completed using HAdV-2. Thus, the following observations apply directly to HAdV-2 and more generally to other HAdVs. Initial HAdV attachment to cells is mediated by interaction of the fiber protein with coxsackie B virus and adenovirus receptor (CAR) (17). The penton base then binds integrin family members (specifically, $\alpha_v\beta_3$ and $\alpha_v\beta5$ which are present on most epithelial cells) via an RGD motif (239). The penton-integrin interaction results in release of the fibers and endocytosis of the fiber-less virion (144). As endosomes mature and acidify, partial disassembly of the virion is initiated and continued as virions are released into the cytosol (22, 170). The reducing environment inside of the cell activates the virion-associated viral protease, which cleaves protein VI, releasing the capsid from the viral core (79).

Following endosomal escape, viral particles are transported towards the nucleus on microtubules by dynein motor proteins (44, 77, 111, 118, 215). Viral particles then dock

at NPCs where disassembly is completed and viral genomes are deposited into the nucleus (78).

Expression of E1A begins almost immediately upon nuclear deposition of the viral genome (147). Transcription of E1A is initially controlled by a constitutive enhancer element (86) and once expressed, E1A activates the expression of downstream viral genes, as will be discussed extensively below.

Following extensive replication of the viral genome and production of structural virion components, virion assembly begins in the nucleus of host cells. Following their translation, hexon and penton monomers rapidly assembly into capsomers in the cytoplasm. They are then transported into the nucleus where assembly continues (18). HAdV DNA is packaged into virions starting at the left end of the genome, where the packaging signal is located (85). Precursor of the major histone-like protein (pVII) associates with viral DNA late during infection and may form a complex with core protein V and precursor of μ (235, 250). Packaging is promoted by viral IVa2, L1 52/55K and L4 22 kDa proteins (156, 165).

 Protein VI, VII, VIII, μ and terminal protein are cleaved by the viral cysteine protease, which is also packaged in the virion. This completes virion maturation and renders the particle infectious (217, 234).

Escape and spread of progeny virus is mediated through a variety of cooperating mechanisms. First, the viral L3 protease is able to cleave the IF protein cytokeratin K18, weakening the overall structural integrity of the cell (34). The 11.6 kDa E3 protein, also

known as 'adenovirus death protein' is an integral membrane glycoprotein and is highly expressed at late times post-infection (218). The protein localizes to the nuclear membrane, ER and golgi apparatus. It is known to interact with MAD2B, a regulator of the anaphase-promoting complex, though how this interaction results in cell death remains poorly understood (244). Finally, released, free fiber proteins bind to and prevent oligomerization of CAR at tight junctions. This is likely to promote viral spread and mediate access to the airway during respiratory infection (229).

1.3.5   E1A

1.3.5.1   General properties

For the sake of clarity, the following sections will focus on E1A of HAdV-2/5 unless otherwise specified. E1A is located at the left end of the HAdV genome and is the first transcription unit to be expressed after infection. The primary E1A transcript is alternatively spliced to generate 5 mRNA species which encode proteins of 289, 243, 217, 171 and 55 residues (R). Splicing maintains the reading frame of each isoform except 55R. Sequence comparison of the largest E1A isoform across multiple AdV serotypes revealed four regions of high conservation which have been dubbed 'conserved regions (CR) 1-4'. While 289R E1A possesses each of these regions, the smaller E1A isoforms may lack one or more CRs. 55R E1A is the only E1A isoform that lacks all four conserved regions (Fig. 1-3) (161).

E1A is essential for efficient infection of human cells, which reflects the diverse and complex functions it performs (99). In addition to activating viral gene expression, E1A also reprograms host cells, forcing them out of quiescence and into the cell cycle (15, 19,

61, 66). Since E1A does not exhibit DNA binding activity, it is able to perform these functions by binding to and subverting the normal function of over 50 cellular proteins. This has led to the description of E1A as a 'viral hub protein' (161).

Interactions between E1A and its many cellular partners occur mainly through molecular recognition features (MoRFs) or linear motifs. These are short segments of the primary amino acid sequence that exhibit a high degree of structural plasticity. Indeed, with the exception of CR3, E1A is thought to be intrinsically unstructured (60). Such flexibility allows E1A to adopt one of many possible conformations subsequent to binding of particular targets. Many of these MoRFs can also be found in the endogenous, cellular binding partners of E1A targets. Amazingly, these MoRFs often overlap in E1A, making for extremely dense regions of protein binding. Intuitively, only certain combinations of concurrent binding of E1A to its cellular targets is possible due to steric hindrance, and this property may be important in determining the novel complexes nucleated by E1A (161).
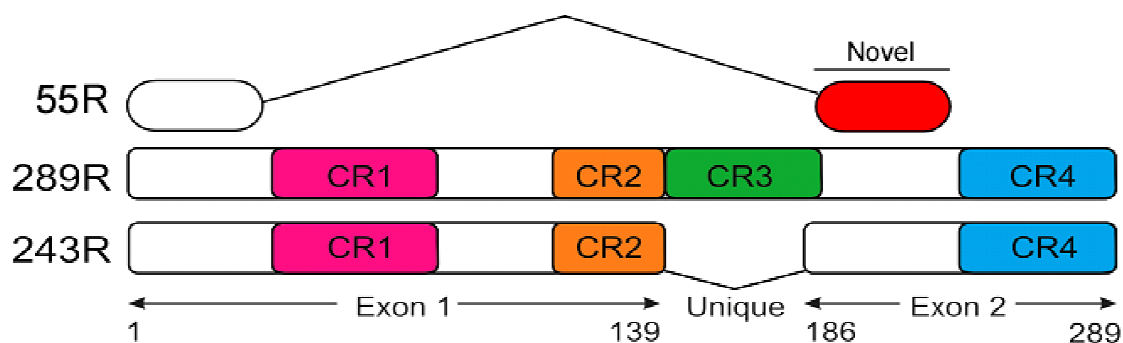
FIG. 1-3. Comparison of the 55R E1A isoform with CRs present in 289R and 243R E1A. The 55R E1A protein shares only the first 26 amino acids encoded by exon 1 with the larger E1A isoforms. Splicing of the 9S mRNA causes a frameshift in exon 2 of 55R E1A that results in a novel C-terminal amino acid sequence relative to the other E1A isoforms. 289R E1A, the largest E1A isoform, contains all 4 CRs. The 243R E1A isoform is different from 289R E1A only in that it lacks CR3.

1.3.5.2   E1A-induced cell cycle progression

The cells of the respiratory epithelium normally infected by HAdV are terminally differentiated, quiescent cells. Thus, they lack an abundance of many substrates required by HAdV during the replication cycle. To overcome this difficulty, the virus has evolved a variety of mechanisms which together force the host to re-enter the cell cycle, making it more conducive to viral replication. E1A plays a central role in this process by targeting cellular proteins that are key regulators of growth and cell cycle pathways, including retinoblastoma (Rb)-family proteins, p300/CREB-binding protein (CBP) and C-terminal binding protein (CtBP).

243R E1A, which lacks CR3 (a strong transcriptional activation domain), is sufficient to induce S-phase induction and cell cycle progression of contact-inhibited primary cells (26, 207, 248). Expressed alone, CR1 or CR2 is sufficient to induce S-phase, but both are required for progression into mitosis and for transformation in cooperation with E1B or activated RAS (93, 209). CR2 was shown to bind Rb and Rb family members p107 and p130 (13, 38, 55, 238). These proteins regulate the E2F family of transcription factors, many of which control cellular genes required for S-phase entry (including *CDK2*, cyclins A and E, and c-*MYC*) (54, 63, 146, 148, 221). E1A CR2 contains an LxCxE motif which binds with high affinity to the same pocket domain on Rb family proteins that is bound by E2Fs (148). Binding of E1A to Rb family proteins results in the release of E2Fs from Rb-mediated inhibition, resulting in constitutive activation of E2F-responsive promoters (21). In a normal context, Rb inhibition is relieved by phophorylation mediated by cyclin-dependant kinase (CDK)-cyclin complexes whose activity is stimulated by mitogens in G_1. Expression of CDK inhibitors which prevent Rb phosphorylation are

partially responsible for senescence, which is also detrimental to virus replication (16, 190, 210). Through bypassing these cellular pathways, CR2 ensures efficient S-phase entry, although other functions of E1A are required to push cells through the complete cell cycle (92).

While initiating relief of Rb-mediated E2F repression provides a solid mechanistic explanation for the ability of CR2 to induce S-phase progression, the way in which CR1 causes this same phenomenon is much less clear. One important contribution is likely the association of CR1 with the histone acetyltransferases (HAT) p300 and CBP (10, 13, 211, 232). In normal settings, p300/CBP are recruited to specific promoters via their interaction with various transcription factors where they activate transcription by acetylating histone tails or specific lysines present in other transcription factors (74). E1A binding to p300/CBP is actually tripartite, involving both the non-conserved N-terminus and CR1 (152, 162). Despite this knowledge, it is unclear how binding of E1A to p300/CBP contributes to S-phase induction. Binding may inhibit HAT activity, although even this point remains controversial (2, 32, 83). Interestingly, inhibition of p300 has been shown to markedly increase expression of MYC, which is important for G_0 to S transition (74). Effects such as this, although elusive, will be important to study more directly in order to better understand CR1-mediated S-phase induction and will likely yield important new knowledge of cell cycle regulation in general.

Many of the cellular factors targeted by E1A are responsible for regulating large networks of gene expression. This was most elegantly demonstrated in series of recent reports showing that E1A is able to reprogram the expression of virtually every gene

within the cell over the course of an infection (59, 90). The N-terminus of E1A contains a CoRNR box motif also found in nuclear receptor (NR) corepressors, which mediates interaction with NRs. This motif is responsible for the interaction of E1A with unliganded, but not liganded thyroid hormone receptor (TR) (125). Strikingly, despite binding in the corepressor mode, E1A is able to activate transcription from thyroid hormone response elements, effectively ensuring constitutive activation of TR-responsive genes in the presence and absence of hormone (94, 125-126, 189, 227).

Recently, 289R E1A was shown to activate E2F-responsive gene expression independently of binding Rb-family proteins. This is accomplished through targeting of E2F/DP-1 via a direct interaction with DP-1. 289R E1A appears to be recruited to E2F-responsive promoters by DP-1/E2F heterodimers, stimulating their activity. Interestingly, this effect seems to be most profound in the context of E2F4 and E2F5, both considered 'repressive' E2Fs (163). E1A is also able to eliminate p130-E2F4 and histone deacetylase (HDAC)1/2-mSin3B repressive complexes from the promoters of E2F-regulated genes in quiescent cells. This dramatically decreases H3K9 methylation of these promoters and correspondingly increases H3K9/14 acetylation, which ultimately results in increased transcription from E2F-regulated genes (161, 195). This may be yet another example of redundant targeting of a critical cellular pathway, and the ability of E1A to stimulate activation of genes that are normally repressed in quiescent cells.

The N-terminus and CR1 also bind a series of other chromatin remodeling complexes, including p400, Tip60, Gcn5, PCAF and TRAAP (65, 107, 150, 212). How interaction with these proteins and their associated complexes contributes to S-phase progression is

equally mysterious. A final set of less mysterious CR1 targets include the CDK inhibitors p21 and p27 (5, 33, 151). Binding of these inhibitors abrogates their association and inhibition of CDK-cyclin complexes, thereby promoting cell cycle progression.

The major target of CR4, found near the C-terminus of E1A, is CtBP (35). This protein acts as a transcriptional corepressor, and upon homodimerization and recruitment to a promoter by sequence-specific transcription factors, forms a silencing complex (36). Binding of E1A to CtBP derepresses target promoters and may result in recruitment of activating complexes, though this has not been tested directly (161). The only other factors that have currently been identified which bind CR4 are the dual specificity tyrosine phophorylation-regulated kinase 1A (Dyrk1A) and Dyrk1B. These kinases are involved in regulating proliferation, differentiation and cell survival (127). Their binding site on E1A overlaps that of CtBP, suggesting that binding of these two factors may be mutually exclusive. While the global effects of E1A-Dyrk binding have yet to be elucidated, E1A has been shown to stimulate Dyrk kinase activity *in vitro* (249). Interestingly, CR4 is required for E1A-mediated transformation of rodent cells in cooperation with E1B. However, it also suppresses oncogenic transformation in cooperation with activated *ras* (24, 51, 213-214). Delineating the molecular basis of these paradoxical phenotypes will provide important insights regarding the mechanism of E1A-induced transformation.

1.3.5.3   E1A-induced transcription of viral genes

The CR3 region of E1A functions as a strong activation domain when fused to the Gal4 DNA-binding domain and recruited to a Gal4 responsive promoter (113, 121). This

region is also important in stimulating transcription from the four early HAdV promoters, as mutations in CR3 substantially reduce the abundance of early viral transcripts (20, 99). 243R E1A (which lacks CR3) can stimulate a low level of early gene transcription, whereas 289R alone activates transcription of early promoters to the same level as wildtype (140, 243). Since E1A does not possess DNA binding activity itself, it associates with cellular transcription factors (through the C-terminal end of CR3) which bind HAdV early promoters (114). Each early promoter contains binding sites for cellular transcriptional activators upstream of the TATA-box (100).

Unlike most of E1A, CR3 appears to exhibit distinct structural features and forms a zinc finger domain (42). One of the major contributors to CR3-mediated transcriptional activation is MED23. MED23 is a subunit of the mediator complex, which is composed of approximately 30 total subunits. Mediator plays a key role in transcriptional activation and functions by bridging DNA-bound activators with the general transcriptional machinery, in particular, RNA polymerase II. This nucleates assembly of the preinitiation complex (112). CR3 binds MED23 both *in vitro* and *in vivo*, thereby recruiting the mediator complex to specific viral and cellular promoters and greatly enhancing transcriptional activity at these promoters (25, 72, 231).

243R E1A specifically activates the E2 early promoter (12, 169). This promoter contains two inverted E2F binding sites which are activated by E2Fs following E1A-mediated relief of Rb repression (12, 105-106, 169, 246). Free E2Fs interact with dimers of E4orf6/7, which greatly increases their affinity for the E2F binding sites found within the

viral E2 early promoter (41, 121, 153). As E2 products accumulate, viral DNA replication begins to occur and the late stage of viral gene expression begins.

Expression of most late HAdV transcripts is controlled by the major late promoter (MLP). This promoter exhibits low levels of activity during the early stages of infection and is activated several hundred fold at late times (197). Although activation of the MLP is understood to be mediated by binding of E1A to Sp1 and MAZ transcription factors (the MLP contains binding sites for both of these proteins), this does not account for the delayed kinetics of transcription from the MLP (158). Studies to date suggest that both *cis*- and *trans*-acting factors regulate these kinetics.

The *cis*-acting factor appears to rely on DNA replication, although the precise mechanism for regulation of kinetics remains poorly understood (216). It has been suggested that DNA replication may facilitate removal of protein VII, the basic protein that is associated with viral DNA that is translocated through the NPC, thereby allowing transcription factors access to the MLP (18). The fact that the transcription factor *USF* (also called *MLTF*) can only bind the MLP after onset of DNA replication provides further support for a *cis*-acting change in viral chromatin that is required for binding of factors that drive transcription from MLP (219).

The HAdV IVa2 protein has been implicated as a transactivator of the MLP. It binds in the +85 to +120 region upstream of the transcriptional initiation site and cooperates with *USF/MLTF* to enhance MLP activity (110, 119, 138-139, 157). IVa2 itself is expressed with delayed early kinetics and together with MLP, functions as an elegant molecular timer to control the kinetics of viral gene expression. The second viral transactivator of

the MLP appears to arise from an internally spliced mRNA arising from L4, although the mechanism underlying this action awaits further study (18, 155).

1.3.5.4 E1A interaction with the proteasome

Both 289R and 243R E1A have been shown to interact with, and affect the function of the proteasome. This was first demonstrated in 1999, when Grand and colleagues showed that E1A binds to hSug1 (S8), a component of the 19S regulatory subunit of the 26S proteasome. Surprisingly, HAdV-12 E1A was shown to inhibit activity of the 20S proteasome *in vitro*, but had little or no effect on the function of the 26S proteasome (76). Later studies would reveal that E1A could also interact with S4, another member of the 19S regulatory subunit of the 26S proteasome. S4 possesses ATPase activity and binding of E1A significantly reduced this activity. This reduction correlated with an increase in the half-life of p53 in the presence of the human papillomavirus (HPV) E6 protein. E6 is normally responsible for targeting p53 for proteasomal degradation during HPV infection. E1A-26S proteasome complexes could be found in both the nucleus and the cytoplasm, suggesting the E1A might alter proteasome function in both locations. The binding region for S4 and S8 was mapped to residues 4-25 on E1A. Strikingly, despite the fact that E1A was found to be a substrate for proteasomal degradation, binding to S4 or S8 was not required for this degradation to occur. In addition, degradation of E1A was found to be mediated by a C-terminal PEST domain and did not depend on ubiquitylation (222).

S8 also possesses ATPase activity and in addition to binding the E1A N-terminus, it can also interact specifically with CR3. Recruitment of S8 (and the 26S proteasome) to early

viral promoters by CR3 enhances its ability to stimulate transcription of early HAdV genes. The 20S proteasome can also be recruited by CR3, independent of S8 and the 26S proteasome. E1A, S8 and the 20S proteasome can all be found on HAdV early gene promoters and sequences. In fact, inhibition of proteasome function diminishes the ability of E1A to transactivate viral genes (172). Active proteasomal function is required for efficient transactivation by many cellular factors as well, including nuclear receptors and coactivators. Presumably, turnover of promoter-bound factors and dissociation of transcriptional complexes on certain genes must occur before transcriptional re-initiation can take place (145). Taken together, these observations suggest that efficient transactivation by E1A also requires proteasomal activity, and that E1A-mediated recruitment of the proteasome to viral promoters enhances transactivation of early viral genes.

1.3.5.5   55R E1A

The 55R isoform of E1A is generated from the 9S mRNA species, described over 30 years ago (20). It is the smallest E1A species and contrary to 289R and 243R E1A, it accumulates at late times of infection (166). While it is not entirely clear what causes the shift in splice site preference to generate 55R E1A at late times of infection, it appears to require replication of viral DNA. Interestingly, the 9S E1A mRNA species is not produced in 293 cells, which harbor an integrated copy of the left end (E1A and E1B) of the HAdV genome (206). 55R E1A is the only E1A species that does not contain any of the CRs. In addition, reconstitution of its splice junction results in a frame shift relative to all other E1A isoforms. As a result, 55R E1A shares its first 26 amino acids encoded in exon 1 with all other E1A isoforms. The remaining 29 amino acids encoded after the

splice junction linking exon 1 and exon 2 are read from a different reading frame and are therefore unique to the 55R E1A protein (176, 224, 226).

Despite historical knowledge of the 9S mRNA species and its kinetics of expression, the 55R E1A protein has never been studied directly. Therefore, almost nothing is known about its function. This is due, in large part, to the fact that none of the existing E1A antibodies (of which there are many), seem to recognize the 55R isoform. Early studies using 55R cDNA plasmids or mutant virus that could only express 55R E1A indicated that unlike the 289R and 243R isoforms, 55R E1A could not transform primary BRK cells when expressed in combination with activated *ras* (82, 247). Neither could it induce DNA synthesis in growth-arrested NIH 3T3 cells (208). This is not entirely surprising given the subsequent knowledge that 55R lacks all of the regions known to be required for E1A-induced transformation. 55R E1A also fails to stabilize p53 and induce apoptosis (37). Nevertheless, 55R E1A does share its first 28 amino acids (the first 26 encoded by exon 1, plus a V and L which are regenerated from sequences encoded by exon 2 as a consequence of the frameshift caused by splicing) with its larger E1A counterparts. Several proteins are known to bind (at least partially) in this region, including thyroid hormone receptor, TRRAP, S4 and S8 (161). 55R E1A may maintain interaction with these known targets of the larger E1A isoforms to either produce similar functional outcomes, or perhaps more interestingly, to cause novel outcomes. Finally, the C-terminal region of 55R E1A remains completely unexplored territory and is itself likely to interact with novel cellular targets that will expand our knowledge of HAdV biology and may also provide novel insights into biology of the cell.

1.4   Thesis Overview

Here, we explore three essential processes in the life of any virus: entry, gene regulation and egress. Entry is explored in the context of CMV infection. We have identified the IF vimentin as a host factor required for the efficient onset of CMV replication in HF. Our results demonstrate that the EC-tropic strain TB40/E is more negatively affected by disruption or absence of vimentin than the HF-adapted strain, AD169. In vimentin null cells, viral particles were observed to remain in the cytoplasm longer than in their wildtype counterparts. These findings suggest that vimentin may function during viral entry to facilitate viral trafficking and/or docking of viral particles to the NPC. In addition, our results suggest that more broadly tropic CMV strains, such as TB40/E, exhibit a higher degree of reliance on the vimentin cytoskeleton which may reflect fundamental differences in the process of entry of these strains.

In examining viral gene regulation, we turned our attention to HAdV. We have developed a novel antibody which allows for the direct study of the smallest E1A isoform, 55R E1A. We show that 55R E1A is able to stimulate viral replication relative to E1A null virus. Using a co-infection system, we found that in the context of 289R E1A, the effect of 55R E1A on viral replication was not dose-dependent. However, in the presence of 243R E1A, 55R E1A improved virus replication in a dose-dependent manner. This is due, at least in part, to the ability of 55R to stimulate viral gene expression. Interestingly, the profile of viral gene transactivation by 55R E1A is distinct from that of wildtype E1A. Finally, we show that 55R interacts with the S8 component of ATPase proteins independent of 20S (APIS), but not S4. Knockdown of S8 had a deleterious effect on the

growth of a virus expressing only 55R E1A. This is the first study to functionally characterize the 55R E1A protein, describe its effect on virus growth and identify a novel interaction between it and a cellular target. We are confident that this represents an exciting new field in the study of adenoviruses and that elucidating additional functions and cellular targets of 55R will yield important contributions to our understanding of the functions of E1A and of HAdV biology, in general.

In the final data chapter of this thesis, we turn our attention back to CMV in order to study the process of viral egress. We identify and describe a novel protein encoded by c-ORF29 which we have called RASCAL. Two isoforms of RASCAL were found to be encoded by different CMV strains. The majority of strains encode a 97 amino acid protein, while an extended 176 amino acid isoform is unique to strains Towne, Toledo, HAN20 and HAN38. RASCAL localizes to the nuclear rim, in deep intranuclear invaginations and in cytoplasmic vesicles at late times post-infection. These RASCAL-containing vesicles are positive for lamin B, strongly suggesting that they are derived from the nuclear membrane. The localization of RASCAL observed during infection was dependent on a member of the NEC, pUL50. Indeed, RASCAL could be co-immunoprecipitated with UL50, indicating that they are part of the same complex and strongly suggesting that RASCAL is a novel component of the CMV NEC. The presence of RASCAL in the Lamin B positive vesicles presents the intriguing possibility that RASCAL is also involved in steps of virion maturation subsequent to escape of nucleocapsids from the nucleus.

Taken together, these studies highlight three crucial stages of virus replication as exemplified by CMV and HAdV. The insights gained from this work are likely to have broader implications in our understanding of viral replication and cell biology. Although the utility of therapeutically targeting the specific proteins/pathways described herein has not yet been tested directly, any drug capable of interfering with the essential processes of viral entry, gene regulation or egress could serve as a potent antiviral agent. We hope that whether in the short or long-term, the knowledge gained from this work will advance our field and have a positive impact on human health.

1.5   References

1. **Adler, B., L. Scrivano, Z. Ruzcics, B. Rupp, C. Sinzger, and U. Koszinowski.** 2006. Role of human cytomegalovirus UL131A in cell type-specific virus entry and release. J Gen Virol **87:**2451-2460.

2. **Ait-Si-Ali, S., S. Ramirez, F. X. Barre, F. Dkhissi, L. Magnaghi-Jaulin, J. A. Girault, P. Robin, M. Knibiehler, L. L. Pritchard, B. Ducommun, D. Trouche, and A. Harel-Bellan.** 1998. Histone acetyltransferase activity of CBP is controlled by cycle-dependent kinases and oncoprotein E1A. Nature **396:**184-186.

3. **Akter, P., C. Cunningham, B. P. McSharry, A. Dolan, C. Addison, D. J. Dargan, A. F. Hassan-Walker, V. C. Emery, P. D. Griffiths, G. W. Wilkinson, and A. J. Davison.** 2003. Two novel spliced genes in human cytomegalovirus. J Gen Virol **84:**1117-1122.

4. **Alberts B, J. A., Lewis J, Raff M, Roberts K and Walter P (ed.).** 2002. Molecular Biology of the Cell, 4 ed. Garland Science, New York.

5. **Alevizopoulos, K., B. Catarin, J. Vlach, and B. Amati.** 1998. A novel function of adenovirus E1A is required to overcome growth arrest by the CDK2 inhibitor p27(Kip1). EMBO J **17:**5987-5997.

6. **Anders, D. G., M. A. Kacica, G. Pari, and S. M. Punturieri.** 1992. Boundaries and structure of human cytomegalovirus oriLyt, a complex origin for lytic-phase DNA replication. J Virol **66:**3373-3384.

7. **Anders, D. G., and L. A. McCue.** 1996. The human cytomegalovirus genes and proteins required for DNA synthesis. Intervirology **39:**378-388.

8. **Anderson, C. W., M. E. Young, and S. J. Flint.** 1989. Characterization of the adenovirus 2 virion protein, mu. Virology **172:**506-512.

9. **Aoki, K., M. Benko, A. J. Davison, M. Echavarria, D. D. Erdman, B. Harrach, A. E. Kajon, D. Schnurr, and G. Wadell.** 2011. Toward an integrated human adenovirus designation system that utilizes molecular and serological data and serves both clinical and fundamental virology. J Virol **85:**5703-5704.

10. **Arany, Z., D. Newsome, E. Oldread, D. M. Livingston, and R. Eckner.** 1995. A family of transcriptional adaptor proteins targeted by the E1A oncoprotein. Nature **374:**81-84.

11. **Arcangeletti, M. C., F. Pinardi, M. C. Medici, E. Pilotti, F. De Conto, F. Ferraglia, M. P. Landini, C. Chezzi, and G. Dettori.** 2000. Cytoskeleton involvement during human cytomegalovirus replicative cycle in human embryo fibroblasts. New Microbiol **23:**241-256.

12. **Bagchi, S., P. Raychaudhuri, and J. R. Nevins.** 1990. Adenovirus E1A proteins can dissociate heteromeric complexes involving the E2F transcription factor: a novel mechanism for E1A trans-activation. Cell **62:**659-669.

13. **Barbeau, D., R. C. Marcellus, S. Bacchetti, S. T. Bayley, and P. E. Branton.** 1992. Quantitative analysis of regions of adenovirus E1A products involved in interactions with cellular proteins. Biochem Cell Biol **70:**1123-1134.

14. **Bauer, D., and R. Tampe.** 2002. Herpes viral proteins blocking the transporter associated with antigen processing TAP--from genes to function and structure. Curr Top Microbiol Immunol **269:**87-99.

15. **Bayley, S., and J. Mymryk.** 1994. Adenovirus e1a proteins and transformation (review). Int J Oncol **5:**425-444.

16. **Ben-Porath, I., and R. A. Weinberg.** 2004. When cells get stressed: an integrative view of cellular senescence. J Clin Invest **113:**8-13.

17. **Bergelson, J. M., J. A. Cunningham, G. Droguett, E. A. Kurt-Jones, A. Krithivas, J. S. Hong, M. S. Horwitz, R. L. Crowell, and R. W. Finberg.** 1997. Isolation of a common receptor for Coxsackie B viruses and adenoviruses 2 and 5. Science **275:**1320-1323.

18. **Berk, A. J.** 2007. Adenoviridae, p. 2355-2394. *In* D. M. Knipe (ed.), Field's Virology, 5th ed. Lippincott Williams & Wilkins, Philadelphia, PA.

19. **Berk, A. J.** 2005. Recent lessons in gene expression, cell cycle control, and cell biology from adenovirus. Oncogene **24:**7673-7685.

20. **Berk, A. J., F. Lee, T. Harrison, J. Williams, and P. A. Sharp.** 1979. Pre-early adenovirus 5 gene product regulates synthesis of early viral messenger RNAs. Cell **17:**935-944.

21. **Blais, A., and B. D. Dynlacht.** 2004. Hitting their targets: an emerging picture of E2F and cell cycle control. Curr Opin Genet Dev **14:**527-532.

22. **Blumenthal, R., P. Seth, M. C. Willingham, and I. Pastan.** 1986. pH-dependent lysis of liposomes by adenovirus. Biochemistry **25:**2231-2237.

23. **Borst, E. M., and M. Messerle.** 2005. Analysis of human cytomegalovirus oriLyt sequence requirements in the context of the viral genome. J Virol **79:**3615-3626.

24. **Boyd, J. M., T. Subramanian, U. Schaeper, M. La Regina, S. Bayley, and G. Chinnadurai.** 1993. A region in the C-terminus of adenovirus 2/5 E1a protein is required for association with a cellular phosphoprotein and important for the negative modulation of T24-ras mediated transformation, tumorigenesis and metastasis. EMBO J **12:**469-478.

25. **Boyer, T. G., M. E. Martin, E. Lees, R. P. Ricciardi, and A. J. Berk.** 1999. Mammalian Srb/Mediator complex is targeted by adenovirus E1A protein. Nature **399:**276-279.

26. **Braithwaite, A. W., B. F. Cheetham, P. Li, C. R. Parish, L. K. Waldron-Stevens, and A. J. Bellett.** 1983. Adenovirus-induced alterations of the cell growth cycle: a requirement for expression of E1A but not of E1B. J Virol **45:**192-199.

27. **Britt, W. J., and S. Boppana.** 2004. Human cytomegalovirus virion proteins. Hum Immunol **65:**395-402.

28. **Broers, J. L., F. C. Ramaekers, G. Bonne, R. B. Yaou, and C. J. Hutchison.** 2006. Nuclear lamins: laminopathies and their role in premature ageing. Physiol Rev **86:**967-1008.

29. **Buser, C., P. Walther, T. Mertens, and D. Michel.** 2007. Cytomegalovirus primary envelopment occurs at large infoldings of the inner nuclear membrane. J Virol **81:**3042-3048.

30. **Camozzi, D., S. Pignatelli, C. Valvo, G. Lattanzi, C. Capanni, P. Dal Monte, and M. P. Landini.** 2008. Remodelling of the nuclear lamina during human cytomegalovirus infection: role of the viral proteins pUL50 and pUL53. J Gen Virol **89:**731-740.

31.   **Cha, T. A., E. Tom, G. W. Kemble, G. M. Duke, E. S. Mocarski, and R. R. Spaete.** 1996. Human cytomegalovirus clinical isolates carry at least 19 genes not found in laboratory strains. J Virol **70:**78-83.

32.   **Chakravarti, D., V. Ogryzko, H. Y. Kao, A. Nash, H. Chen, Y. Nakatani, and R. M. Evans.** 1999. A viral mechanism for inhibition of p300 and PCAF acetyltransferase activity. Cell **96:**393-403.

33.   **Chattopadhyay, D., M. K. Ghosh, A. Mal, and M. L. Harter.** 2001. Inactivation of p21 by E1A leads to the induction of apoptosis in DNA-damaged cells. J Virol **75:**9844-9856.

34.   **Chen, P. H., D. A. Ornelles, and T. Shenk.** 1993. The adenovirus L3 23-kilodalton proteinase cleaves the amino-terminal head domain from cytokeratin 18 and disrupts the cytokeratin network of HeLa cells. J Virol **67:**3507-3514.

35.   **Chinnadurai, G.** 2002. CtBP, an unconventional transcriptional corepressor in development and oncogenesis. Mol Cell **9:**213-224.

36.   **Chinnadurai, G.** 2007. Transcriptional regulation by C-terminal binding proteins. Int J Biochem Cell Biol **39:**1593-1607.

37.   **Chiou, S. K., and E. White.** 1997. p300 binding by E1A cosegregates with p53 induction but is dispensable for apoptosis. J Virol **71:**3515-3525.

38.   **Cobrinik, D.** 2005. Pocket proteins and cell cycle control. Oncogene **24:**2796-2809.

39.   **Compton, T.** 2004. Receptors and immune sensors: the complex entry path of human cytomegalovirus. Trends Cell Biol **14:**5-8.

40.   **Compton, T., R. R. Nepomuceno, and D. M. Nowlin.** 1992. Human cytomegalovirus penetrates host cells by pH-independent fusion at the cell surface. Virology **191:**387-395.

41.   **Cress, W. D., and J. R. Nevins.** 1994. Interacting domains of E2F1, DP1, and the adenovirus E4 protein. J Virol **68:**4213-4219.

42.   **Culp, J. S., L. C. Webster, D. J. Friedman, C. L. Smith, W. J. Huang, F. Y. Wu, M. Rosenberg, and R. P. Ricciardi.** 1988. The 289-amino acid E1A protein of adenovirus binds zinc in a region that is important for trans-activation. Proc Natl Acad Sci U S A **85:**6450-6454.

43.   **Dal Monte, P., S. Pignatelli, N. Zini, N. M. Maraldi, E. Perret, M. C. Prevost, and M. P. Landini.** 2002. Analysis of intracellular and intraviral localization of the human cytomegalovirus UL53 protein. J Gen Virol **83:**1005-1012.

44.	**Dales, S., and Y. Chardonnet.** 1973. Early events in the interaction of adenoviruses with HeLa cells. IV. Association with microtubules and the nuclear pore complex during vectorial movement of the inoculum. Virology **56:**465-483.

45.	**Das, S., A. Vasanji, and P. E. Pellett.** 2007. Three-dimensional structure of the human cytomegalovirus cytoplasmic virion assembly complex includes a reoriented secretory apparatus. J Virol **81:**11861-11869.

46.	**Davison, A. J., M. Benko, and B. Harrach.** 2003. Genetic content and evolution of adenoviruses. J Gen Virol **84:**2895-2908.

47.	**Davison, A. J., A. Dolan, P. Akter, C. Addison, D. J. Dargan, D. J. Alcendor, D. J. McGeoch, and G. S. Hayward.** 2003. The human cytomegalovirus genome revisited: comparison with the chimpanzee cytomegalovirus genome. J Gen Virol **84:**17-28.

48.	**Digel, M., K. L. Sampaio, G. Jahn, and C. Sinzger.** 2006. Evidence for direct transfer of cytoplasmic material from infected to uninfected cells during cell-associated spread of human cytomegalovirus. J Clin Virol **37:**10-20.

49.	**Dohner, K., and B. Sodeik.** 2005. The role of the cytoskeleton during viral infection. Curr Top Microbiol Immunol **285:**67-108.

50.	**Dolan, A., C. Cunningham, R. D. Hector, A. F. Hassan-Walker, L. Lee, C. Addison, D. J. Dargan, D. J. McGeoch, D. Gatherer, V. C. Emery, P. D. Griffiths, C. Sinzger, B. P. McSharry, G. W. Wilkinson, and A. J. Davison.** 2004. Genetic content of wild-type human cytomegalovirus. J Gen Virol **85:**1301-1312.

51.	**Douglas, J. L., and M. P. Quinlan.** 1995. Efficient nuclear localization and immortalizing ability, two functions dependent on the adenovirus type 5 (Ad5) E1A second exon, are necessary for cotransformation with Ad5 E1B but not with T24ras. J Virol **69:**8061-8065.

52.	**Drummond, S., and T. Allen.** 2004. Structure, function and assembly of the nuclear pore complex. Symp Soc Exp Biol**:**89-114.

53.	**Dunn, W., C. Chou, H. Li, R. Hai, D. Patterson, V. Stolc, H. Zhu, and F. Liu.** 2003. Functional profiling of a human cytomegalovirus genome. Proc Natl Acad Sci U S A **100:**14223-14228.

54.	**Dyson, N.** 1998. The regulation of E2F by pRB-family proteins. Genes Dev **12:**2245-2262.

55.	**Dyson, N., P. Guida, C. McCall, and E. Harlow.** 1992. Adenovirus E1A makes two distinct contacts with the retinoblastoma protein. J Virol **66:**4606-4611.

56.   **Eriksson, J. E., T. Dechat, B. Grin, B. Helfand, M. Mendez, H. M. Pallari, and R. D. Goldman.** 2009. Introducing intermediate filaments: from discovery to disease. J Clin Invest **119:**1763-1771.

57.   **Everitt, E., and L. Philipson.** 1974. Structural proteins of adenoviruses. XI. Purification of three low molecular weight virion proteins of adenovirus type 2 and their synthesis during productive infection. Virology **62:**253-269.

58.   **Feire, A. L., H. Koss, and T. Compton.** 2004. Cellular integrins function as entry receptors for human cytomegalovirus via a highly conserved disintegrin-like domain. Proc Natl Acad Sci U S A **101:**15470-15475.

59.   **Ferrari, R., M. Pellegrini, G. A. Horwitz, W. Xie, A. J. Berk, and S. K. Kurdistani.** 2008. Epigenetic reprogramming by adenovirus e1a. Science **321:**1086-1088.

60.   **Ferreon, J. C., M. A. Martinez-Yamout, H. J. Dyson, and P. E. Wright.** 2009. Structural basis for subversion of cellular control mechanisms by the adenoviral E1A oncoprotein. Proc Natl Acad Sci U S A **106:**13260-13265.

61.   **Flint, J., and T. Shenk.** 1997. Viral transactivating proteins. Annu Rev Genet **31:**177-212.

62.   **Frere, P., M. Pereira, G. Fillet, and Y. Beguin.** 2006. Infections after CD34-selected or unmanipulated autologous hematopoietic stem cell transplantation. Eur J Haematol **76:**102-108.

63.   **Frolov, M. V., and N. J. Dyson.** 2004. Molecular mechanisms of E2F-dependent activation and pRB-mediated repression. J Cell Sci **117:**2173-2181.

64.   **Fuchs, E., and K. Weber.** 1994. Intermediate filaments: structure, dynamics, function, and disease. Annu Rev Biochem **63:**345-382.

65.   **Fuchs, M., J. Gerber, R. Drapkin, S. Sif, T. Ikura, V. Ogryzko, W. S. Lane, Y. Nakatani, and D. M. Livingston.** 2001. The p400 complex is an essential E1A transformation target. Cell **106:**297-307.

66.   **Gallimore, P. H., and A. S. Turnell.** 2001. Adenovirus E1A: remodelling the host cell, a life or death experience. Oncogene **20:**7824-7835.

67.   **Gerna, G., F. Baldanti, and M. G. Revello.** 2004. Pathogenesis of human cytomegalovirus infection and cellular targets. Hum Immunol **65:**381-386.

68.   **Gibson, W.** 1996. Structure and assembly of the virion. Intervirology **39:**389-400.

69. **Gicklhorn, D., M. Eickmann, G. Meyer, M. Ohlin, and K. Radsak.** 2003. Differential effects of glycoprotein B epitope-specific antibodies on human cytomegalovirus-induced cell-cell fusion. J Gen Virol **84:**1859-1862.

70. **Gilloteaux, J., and M. R. Nassiri.** 2000. Human bone marrow fibroblasts infected by cytomegalovirus: ultrastructural observations. J Submicrosc Cytol Pathol **32:**17-45.

71. **Ginsberg, H. S., H. G. Pereira, R. C. Valentine, and W. C. Wilcox.** 1966. A proposed terminology for the adenovirus antigens and virion morphological subunits. Virology **28:**782-783.

72. **Gold, M. O., J. P. Tassan, E. A. Nigg, A. P. Rice, and C. H. Herrmann.** 1996. Viral transactivators E1A and VP16 interact with a large complex that is associated with CTD kinase activity and contains CDK8. Nucleic Acids Res **24:**3771-3777.

73. **Gonczol, E., and S. Plotkin.** 2001. Development of a cytomegalovirus vaccine: lessons from recent clinical trials. Expert Opin Biol Ther **1:**401-412.

74. **Goodman, R. H., and S. Smolik.** 2000. CBP/p300 in cell growth, transformation, and development. Genes Dev **14:**1553-1577.

75. **Grable, M., and P. Hearing.** 1992. cis and trans requirements for the selective packaging of adenovirus type 5 DNA. J Virol **66:**723-731.

76. **Grand, R. J., A. S. Turnell, G. G. Mason, W. Wang, A. E. Milner, J. S. Mymryk, S. M. Rookes, A. J. Rivett, and P. H. Gallimore.** 1999. Adenovirus early region 1A protein binds to mammalian SUG1-a regulatory component of the proteasome. Oncogene **18:**449-458.

77. **Greber, U. F., and H. Kasamatsu.** 1996. Nuclear targeting of SV40 and adenovirus. Trends Cell Biol **6:**189-195.

78. **Greber, U. F., M. Suomalainen, R. P. Stidwill, K. Boucke, M. W. Ebersold, and A. Helenius.** 1997. The role of the nuclear pore complex in adenovirus DNA entry. EMBO J **16:**5998-6007.

79. **Greber, U. F., P. Webster, J. Weber, and A. Helenius.** 1996. The role of the adenovirus protease on virus entry into cells. EMBO J **15:**1766-1777.

80. **Grefte, A., M. C. Harmsen, M. van der Giessen, S. Knollema, W. J. van Son, and T. H. The.** 1994. Presence of human cytomegalovirus (HCMV) immediate early mRNA but not ppUL83 (lower matrix protein pp65) mRNA in polymorphonuclear and mononuclear leukocytes during active HCMV infection. J Gen Virol **75 (Pt 8):**1989-1998.

81.   **Hahn, G., M. G. Revello, M. Patrone, E. Percivalle, G. Campanini, A. Sarasini, M. Wagner, A. Gallina, G. Milanesi, U. Koszinowski, F. Baldanti, and G. Gerna.** 2004. Human cytomegalovirus UL131-128 genes are indispensable for virus growth in endothelial cells and virus transfer to leukocytes. J Virol **78:**10023-10033.

82.   **Haley, K. P., J. Overhauser, L. E. Babiss, H. S. Ginsberg, and N. C. Jones.** 1984. Transformation properties of type 5 adenovirus mutants that differentially express the E1A gene products. Proc Natl Acad Sci U S A **81:**5734-5738.

83.   **Hamamori, Y., V. Sartorelli, V. Ogryzko, P. L. Puri, H. Y. Wu, J. Y. Wang, Y. Nakatani, and L. Kedes.** 1999. Regulation of histone acetyltransferases p300 and PCAF by the bHLH protein twist and adenoviral oncoprotein E1A. Cell **96:**405-413.

84.   **Hamirally, S., J. P. Kamil, Y. M. Ndassa-Colday, A. J. Lin, W. J. Jahng, M. C. Baek, S. Noton, L. A. Silva, M. Simpson-Holley, D. M. Knipe, D. E. Golan, J. A. Marto, and D. M. Coen.** 2009. Viral mimicry of Cdc2/cyclin-dependent kinase 1 mediates disruption of nuclear lamina during human cytomegalovirus nuclear egress. PLoS Pathog **5:**e1000275.

85.   **Hearing, P., R. J. Samulski, W. L. Wishart, and T. Shenk.** 1987. Identification of a repeated sequence element required for efficient encapsidation of the adenovirus type 5 chromosome. J Virol **61:**2555-2558.

86.   **Hearing, P., and T. Shenk.** 1983. The adenovirus type 5 E1A transcriptional control region contains a duplicated enhancer element. Cell **33:**695-703.

87.   **Heitlinger, E., M. Peter, M. Haner, A. Lustig, U. Aebi, and E. A. Nigg.** 1991. Expression of chicken lamin B2 in Escherichia coli: characterization of its structure, assembly, and molecular interactions. J Cell Biol **113:**485-495.

88.   **Hertel, L., V. G. Lacaille, H. Strobl, E. D. Mellins, and E. S. Mocarski.** 2003. Susceptibility of immature and mature Langerhans cell-type dendritic cells to infection and immunomodulation by human cytomegalovirus. J Virol **77:**7563-7574.

89.   **Hilleman, M. R., and J. H. Werner.** 1954. Recovery of new agent from patients with acute respiratory illness. Proc Soc Exp Biol Med **85:**183-188.

90.   **Horwitz, G. A., K. Zhang, M. A. McBrian, M. Grunstein, S. K. Kurdistani, and A. J. Berk.** 2008. Adenovirus small e1a alters global patterns of histone modification. Science **321:**1084-1085.

91.   **Hosokawa, K., and M. T. Sung.** 1976. Isolation and characterization of an extremely basic protein from adenovirus type 5. J Virol **17:**924-934.

92.   **Howe, J. A., and S. T. Bayley.** 1992. Effects of Ad5 E1A mutant viruses on the cell cycle in relation to the binding of cellular proteins including the retinoblastoma protein and cyclin A. Virology **186:**15-24.

93.   **Howe, J. A., J. S. Mymryk, C. Egan, P. E. Branton, and S. T. Bayley.** 1990. Retinoblastoma growth suppressor and a 300-kDa protein appear to regulate cellular DNA synthesis. Proc Natl Acad Sci U S A **87:**5883-5887.

94.   **Hu, X., and M. A. Lazar.** 1999. The CoRNR motif controls the recruitment of corepressors by nuclear hormone receptors. Nature **402:**93-96.

95.   **Hutchison, C. J., M. Alvarez-Reyes, and O. A. Vaughan.** 2001. Lamins in disease: why do ubiquitously expressed nuclear envelope proteins give rise to tissue-specific disease phenotypes? J Cell Sci **114:**9-19.

96.   **Imperiale, M. J., and L. W. Enquist.** 2011. What's in a Name? J Virol **85:**5245.

97.   **Isaacson, M. K., A. L. Feire, and T. Compton.** 2007. Epidermal growth factor receptor is not required for human cytomegalovirus entry or signaling. J Virol **81:**6241-6247.

98.   **Isaacson, M. K., L. K. Juckem, and T. Compton.** 2008. Virus entry and innate immune activation. Curr Top Microbiol Immunol **325:**85-100.

99.   **Jones, N., and T. Shenk.** 1979. An adenovirus type 5 early gene function regulates expression of other early viral genes. Proc Natl Acad Sci U S A **76:**3665-3669.

100.   **Jones, N. C., J. D. Richter, D. L. Weeks, and L. D. Smith.** 1983. Regulation of adenovirus transcription by an E1a gene in microinjected Xenopus laevis oocytes. Mol Cell Biol **3:**2131-2142.

101.   **Jones, N. L., J. C. Lewis, and B. A. Kilpatrick.** 1986. Cytoskeletal disruption during human cytomegalovirus infection of human lung fibroblasts. Eur J Cell Biol **41:**304-312.

102.   **Kavallaris, M.** 2010. Microtubules and resistance to tubulin-binding agents. Nat Rev Cancer **10:**194-204.

103.   **Klymkowsky, M. W., J. B. Bachant, and A. Domingo.** 1989. Functions of intermediate filaments. Cell Motil Cytoskeleton **14:**309-331.

104.   **Kokkinos, M. I., R. Wafai, M. K. Wong, D. F. Newgreen, E. W. Thompson, and M. Waltham.** 2007. Vimentin and epithelial-mesenchymal transition in human breast cancer--observations in vitro and in vivo. Cells Tissues Organs **185:**191-203.

105. **Kovesdi, I., R. Reichel, and J. R. Nevins.** 1986. E1A transcription induction: enhanced binding of a factor to upstream promoter sequences. Science **231:**719-722.

106. **Kovesdi, I., R. Reichel, and J. R. Nevins.** 1986. Identification of a cellular transcription factor involved in E1A trans-activation. Cell **45:**219-228.

107. **Lang, S. E., and P. Hearing.** 2003. The adenovirus E1A oncoprotein recruits the cellular TRRAP/GCN5 histone acetyltransferase complex. Oncogene **22:**2836-2841.

108. **Lantto, J., J. M. Fletcher, and M. Ohlin.** 2003. Binding characteristics determine the neutralizing potential of antibody fragments specific for antigenic domain 2 on glycoprotein B of human cytomegalovirus. Virology **305:**201-209.

109. **Lee, C. P., and M. R. Chen.** 2010. Escape of herpesviruses from the nucleus. Rev Med Virol **20:**214-230.

110. **Leong, K., W. Lee, and A. J. Berk.** 1990. High-level transcription from the adenovirus major late promoter requires downstream binding sites for late-phase-specific factors. J Virol **64:**51-60.

111. **Leopold, P. L., G. Kreitzer, N. Miyazawa, S. Rempel, K. K. Pfister, E. Rodriguez-Boulan, and R. G. Crystal.** 2000. Dynein- and microtubule-mediated translocation of adenovirus serotype 5 occurs after endosomal lysis. Hum Gene Ther **11:**151-165.

112. **Lewis, B. A., and D. Reinberg.** 2003. The mediator coactivator complex: functional and physical roles in transcriptional regulation. J Cell Sci **116:**3667-3675.

113. **Lillie, J. W., and M. R. Green.** 1989. Transcription activation by the adenovirus E1a protein. Nature **338:**39-44.

114. **Liu, F., and M. R. Green.** 1994. Promoter targeting by adenovirus E1a through interaction with different cellular DNA-binding domains. Nature **368:**520-525.

115. **Liu, H., L. Jin, S. B. Koh, I. Atanasov, S. Schein, L. Wu, and Z. H. Zhou.** 2010. Atomic structure of human adenovirus by cryo-EM reveals interactions among protein networks. Science **329:**1038-1043.

116. **Losse, D., R. Lauer, D. Weder, and K. Radsak.** 1982. Actin distribution and synthesis in human fibroblasts infected by cytomegalovirus. Arch Virol **71:**353-359.

117. **Lyman, M. G., and L. W. Enquist.** 2009. Herpesvirus interactions with the host cytoskeleton. J Virol **83:**2058-2066.

118. **Mabit, H., M. Y. Nakano, U. Prank, B. Saam, K. Dohner, B. Sodeik, and U. F. Greber.** 2002. Intact microtubules support adenovirus and herpes simplex virus infections. J Virol **76:**9962-9971.

119. **Mansour, S. L., T. Grodzicker, and R. Tjian.** 1986. Downstream sequences affect transcription initiation from the adenovirus major late promoter. Mol Cell Biol **6:**2684-2694.

120. **Marschall, M., A. Marzi, P. aus dem Siepen, R. Jochmann, M. Kalmer, S. Auerochs, P. Lischka, M. Leis, and T. Stamminger.** 2005. Cellular p32 recruits cytomegalovirus kinase pUL97 to redistribute the nuclear lamina. J Biol Chem **280:**33357-33367.

121. **Martin, K. J., J. W. Lillie, and M. R. Green.** 1990. Evidence for interaction of different eukaryotic transcriptional activators with distinct cellular targets. Nature **346:**147-152.

122. **Masse, M. J., S. Karlin, G. A. Schachtel, and E. S. Mocarski.** 1992. Human cytomegalovirus origin of DNA replication (oriLyt) resides within a highly complex repetitive region. Proc Natl Acad Sci U S A **89:**5246-5250.

123. **McDonagh, S., E. Maidji, H. T. Chang, and L. Pereira.** 2006. Patterns of human cytomegalovirus infection in term placentas: a preliminary analysis. J Clin Virol **35:**210-215.

124. **McNabb, D. S., and R. J. Courtney.** 1992. Analysis of the UL36 open reading frame encoding the large tegument protein (ICP1/2) of herpes simplex virus type 1. J Virol **66:**7581-7584.

125. **Meng, X., P. Webb, Y. F. Yang, M. Shuen, A. F. Yousef, J. D. Baxter, J. S. Mymryk, and P. G. Walfish.** 2005. E1A and a nuclear receptor corepressor splice variant (N-CoRI) are thyroid hormone receptor coactivators that bind in the corepressor mode. Proc Natl Acad Sci U S A **102:**6267-6272.

126. **Meng, X., Y. F. Yang, X. Cao, M. V. Govindan, M. Shuen, A. N. Hollenberg, J. S. Mymryk, and P. G. Walfish.** 2003. Cellular context of coregulator and adaptor proteins regulates human adenovirus 5 early region 1A-dependent gene activation by the thyroid hormone receptor. Mol Endocrinol **17:**1095-1105.

127. **Mercer, S. E., and E. Friedman.** 2006. Mirk/Dyrk1B: a multifunctional dual-specificity kinase involved in growth arrest, differentiation, and cell survival. Cell Biochem Biophys **45:**303-315.

128. **Mettenleiter, T. C.** 2002. Herpesvirus assembly and egress. J Virol **76:**1537-1547.

129. **Miceli, M. V., D. A. Newsome, L. C. Novak, and R. W. Beuerman.** 1989. Cytomegalovirus replication in cultured human retinal pigment epithelial cells. Curr Eye Res **8:**835-839.

130. **Miki, H., Y. Okada, and N. Hirokawa.** 2005. Analysis of the kinesin superfamily: insights into structure and function. Trends Cell Biol **15:**467-476.

131. **Milbradt, J., S. Auerochs, and M. Marschall.** 2007. Cytomegaloviral proteins pUL50 and pUL53 are associated with the nuclear lamina and interact with cellular protein kinase C. J Gen Virol **88:**2642-2650.

132. **Milbradt, J., S. Auerochs, H. Sticht, and M. Marschall.** 2009. Cytomegaloviral proteins that associate with the nuclear lamina: components of a postulated nuclear egress complex. J Gen Virol **90:**579-590.

133. **Milbradt, J., R. Webel, S. Auerochs, H. Sticht, and M. Marschall.** 2010. Novel mode of phosphorylation-triggered reorganization of the nuclear lamina during nuclear egress of human cytomegalovirus. J Biol Chem **285:**13979-13989.

134. **Minton, E. J., C. Tysoe, J. H. Sinclair, and J. G. Sissons.** 1994. Human cytomegalovirus infection of the monocyte/macrophage lineage in bone marrow. J Virol **68:**4017-4021.

135. **Mocarski, E. S., M. N. Prichard, C. S. Tan, and J. M. Brown.** 1997. Reassessing the organization of the UL42-UL43 region of the human cytomegalovirus strain AD169 genome. Virology **239:**169-175.

136. **Mocarski, E. S., T. Shenk, and R. F. Pass.** 2007. Cytomegaloviruses, p. 2701-2772. *In* P. M. H. D. M. Knipe, D. E. Griffin, R. A. Lamb, M. A. Martin, B. Roizman, and S. E. Straus (ed.), Field's Virology, 5th ed. Lippincott Williams *&* Wilkins, Philadelphia, PA.

137. **Moir, R. D., T. P. Spann, and R. D. Goldman.** 1995. The dynamic properties and possible functions of nuclear lamins. Int Rev Cytol **162B:**141-182.

138. **Mondesert, G., and C. Kedinger.** 1991. Cooperation between upstream and downstream elements of the adenovirus major late promoter for maximal late phase-specific transcription. Nucleic Acids Res **19:**3221-3228.

139. **Mondesert, G., C. Tribouley, and C. Kedinger.** 1992. Identification of a novel downstream binding protein implicated in late-phase-specific activation of the adenovirus major late promotor. Nucleic Acids Res **20:**3881-3889.

140. **Montell, C., G. Courtois, C. Eng, and A. Berk.** 1984. Complete transformation by adenovirus 2 requires both E1A proteins. Cell **36:**951-961.

141. **Muranyi, W., J. Haas, M. Wagner, G. Krohne, and U. H. Koszinowski.** 2002. Cytomegalovirus recruitment of cellular kinases to dissolve the nuclear lamina. Science **297:**854-857.

142. **Murphy, E., I. Rigoutsos, T. Shibuya, and T. E. Shenk.** 2003. Reevaluation of human cytomegalovirus coding potential. Proc Natl Acad Sci U S A **100:**13585-13590.

143. **Murphy, E., D. Yu, J. Grimwood, J. Schmutz, M. Dickson, M. A. Jarvis, G. Hahn, J. A. Nelson, R. M. Myers, and T. E. Shenk.** 2003. Coding potential of laboratory and clinical strains of human cytomegalovirus. Proc Natl Acad Sci U S A **100:**14976-14981.

144. **Nakano, M. Y., K. Boucke, M. Suomalainen, R. P. Stidwill, and U. F. Greber.** 2000. The first step of adenovirus type 2 disassembly occurs at the cell surface, independently of endocytosis and escape to the cytosol. J Virol **74:**7085-7095.

145. **Nawaz, Z., and B. W. O'Malley.** 2004. Urban renewal in the nucleus: is protein turnover by proteasomes absolutely required for nuclear receptor-regulated transcription? Mol Endocrinol **18:**493-499.

146. **Nevins, J. R.** 2001. The Rb/E2F pathway and cancer. Hum Mol Genet **10:**699-703.

147. **Nevins, J. R., H. S. Ginsberg, J. M. Blanchard, M. C. Wilson, and J. E. Darnell, Jr.** 1979. Regulation of the primary expression of the early adenovirus transcription units. J Virol **32:**727-733.

148. **Nevins, J. R., G. Leone, J. DeGregori, and L. Jakoi.** 1997. Role of the Rb/E2F pathway in cell growth control. J Cell Physiol **173:**233-236.

149. **Nigg, E. A.** 1992. Assembly and cell cycle dynamics of the nuclear lamina. Semin Cell Biol **3:**245-253.

150. **Nikiforov, M. A., S. Chandriani, J. Park, I. Kotenko, D. Matheos, A. Johnsson, S. B. McMahon, and M. D. Cole.** 2002. TRRAP-dependent and TRRAP-independent transcriptional activation by Myc family oncoproteins. Mol Cell Biol **22:**5054-5063.

151. **Nomura, H., Y. Sawada, and S. Ohtaki.** 1998. Interaction of p27 with E1A and its effect on CDK kinase activity. Biochem Biophys Res Commun **248:**228-234.

152. **O'Connor, M. J., H. Zimmermann, S. Nielsen, H. U. Bernard, and T. Kouzarides.** 1999. Characterization of an E1A-CBP interaction defines a novel transcriptional adapter motif (TRAM) in CBP/p300. J Virol **73:**3574-3581.

153. **Obert, S., R. J. O'Connor, S. Schmid, and P. Hearing.** 1994. The adenovirus E4-6/7 protein transactivates the E2 promoter by inducing dimerization of a heteromeric E2F complex. Mol Cell Biol **14:**1333-1346.

154. **Ogawa-Goto, K., K. Tanaka, W. Gibson, E. Moriishi, Y. Miura, T. Kurata, S. Irie, and T. Sata.** 2003. Microtubule network facilitates nuclear targeting of human cytomegalovirus capsid. J Virol **77:**8541-8547.

155. **Ostapchuk, P., M. E. Anderson, S. Chandrasekhar, and P. Hearing.** 2006. The L4 22-kilodalton protein plays a role in packaging of the adenovirus genome. J Virol **80:**6973-6981.

156. **Ostapchuk, P., J. Yang, E. Auffarth, and P. Hearing.** 2005. Functional interaction of the adenovirus IVa2 protein with adenovirus type 5 packaging sequences. J Virol **79:**2831-2838.

157. **Pardo-Mateos, A., and C. S. Young.** 2004. Adenovirus IVa2 protein plays an important role in transcription from the major late promoter in vivo. Virology **327:**50-59.

158. **Parks, C. L., and T. Shenk.** 1997. Activation of the adenovirus major late promoter by transcription factors MAZ and Sp1. J Virol **71:**9600-9607.

159. **Patrone, M., M. Secchi, E. Bonaparte, G. Milanesi, and A. Gallina.** 2007. Cytomegalovirus UL131-128 products promote gB conformational transition and gB-gH interaction during entry into endothelial cells. J Virol **81:**11479-11488.

160. **Paulus, C., S. Krauss, and M. Nevels.** 2006. A human cytomegalovirus antagonist of type I IFN-dependent signal transducer and activator of transcription signaling. Proc Natl Acad Sci U S A **103:**3840-3845.

161. **Pelka, P., J. N. Ablack, G. J. Fonseca, A. F. Yousef, and J. S. Mymryk.** 2008. Intrinsic structural disorder in adenovirus E1A: a viral molecular hub linking multiple diverse processes. J Virol **82:**7252-7263.

162. **Pelka, P., J. N. Ablack, J. Torchia, A. S. Turnell, R. J. Grand, and J. S. Mymryk.** 2009. Transcriptional control by adenovirus E1A conserved region 3 via p300/CBP. Nucleic Acids Res **37:**1095-1106.

163. **Pelka, P., M. S. Miller, M. Cecchini, A. F. Yousef, D. M. Bowdish, F. Dick, P. Whyte, and J. S. Mymryk.** 2011. Adenovirus E1A Directly Targets the E2F/DP-1 Complex. J Virol **85:**8841-8851.

164. **Penfold, M. E., and E. S. Mocarski.** 1997. Formation of cytomegalovirus DNA replication compartments defined by localization of viral proteins and DNA synthesis. Virology **239:**46-61.

165. **Perez-Romero, P., R. E. Tyler, J. R. Abend, M. Dus, and M. J. Imperiale.** 2005. Analysis of the interaction of the adenovirus L1 52/55-kilodalton and IVa2 proteins with the packaging sequence in vivo and in vitro. J Virol **79:**2366-2374.

166. **Perricaudet, M., G. Akusjarvi, A. Virtanen, and U. Pettersson.** 1979. Structure of two spliced mRNAs from the transforming region of human subgroup C adenoviruses. Nature **281:**694-696.

167. **Peter, M., E. Heitlinger, M. Haner, U. Aebi, and E. A. Nigg.** 1991. Disassembly of in vitro formed lamin head-to-tail polymers by CDC2 kinase. EMBO J **10:**1535-1544.

168. **Pfister, K. K., P. R. Shah, H. Hummerich, A. Russ, J. Cotton, A. A. Annuar, S. M. King, and E. M. Fisher.** 2006. Genetic analysis of the cytoplasmic dynein subunit families. PLoS Genet **2:**e1.

169. **Phelps, W. C., S. Bagchi, J. A. Barnes, P. Raychaudhuri, V. Kraus, K. Munger, P. M. Howley, and J. R. Nevins.** 1991. Analysis of trans activation by human papillomavirus type 16 E7 and adenovirus 12S E1A suggests a common mechanism. J Virol **65:**6922-6930.

170. **Prchla, E., C. Plank, E. Wagner, D. Blaas, and R. Fuchs.** 1995. Virus-mediated release of endosomal content in vitro: different behavior of adenovirus and rhinovirus serotype 2. J Cell Biol **131:**111-123.

171. **Prokocimer, M., M. Davidovich, M. Nissim-Rafinia, N. Wiesel-Motiuk, D. Z. Bar, R. Barkan, E. Meshorer, and Y. Gruenbaum.** 2009. Nuclear lamins: key regulators of nuclear structure and activities. J Cell Mol Med **13:**1059-1085.

172. **Rasti, M., R. J. Grand, A. F. Yousef, M. Shuen, J. S. Mymryk, P. H. Gallimore, and A. S. Turnell.** 2006. Roles for APIS and the 20S proteasome in adenovirus E1A-dependent transcription. EMBO J **25:**2710-2722.

173. **Reddy, V. S., S. K. Natchiar, P. L. Stewart, and G. R. Nemerow.** 2010. Crystal structure of human adenovirus at 3.5 A resolution. Science **329:**1071-1075.

174. **Rekosh, D. M., W. C. Russell, A. J. Bellet, and A. J. Robinson.** 1977. Identification of a protein linked to the ends of adenovirus DNA. Cell **11:**283-295.

175. **Reynolds, A. E., L. Liang, and J. D. Baines.** 2004. Conformational changes in the nuclear lamina induced by herpes simplex virus type 1 require genes U(L)31 and U(L)34. J Virol **78:**5564-5575.

176. **Roberts, B. E., J. S. Miller, D. Kimelman, C. L. Cepko, I. R. Lemischka, and R. C. Mulligan.** 1985. Individual adenovirus type 5 early region 1A gene

products elicit distinct alterations of cellular morphology and gene expression. J Virol **56:**404-413.

177. **Roberts, R. J., K. E. O'Neill, and C. T. Yen.** 1984. DNA sequences from the adenovirus 2 genome. J Biol Chem **259:**13968-13975.

178. **Rosen, L.** 1960. A hemagglutination-inhibition technique for typing adenoviruses. Am J Hyg **71:**120-128.

179. **Rowe, W. P., R. J. Huebner, L. K. Gilmore, R. H. Parrott, and T. G. Ward.** 1953. Isolation of a cytopathogenic agent from human adenoids undergoing spontaneous degeneration in tissue culture. Proc Soc Exp Biol Med **84:**570-573.

180. **Russell, W. C., W. G. Laver, and P. J. Sanderson.** 1968. Internal components of adenovirus. Nature **219:**1127-1130.

181. **Rux, J. J., and R. M. Burnett.** 2004. Adenovirus structure. Hum Gene Ther **15:**1167-1176.

182. **Rux, J. J., and R. M. Burnett.** 2000. Type-specific epitope locations revealed by X-ray crystallographic study of adenovirus type 5 hexon. Mol Ther **1:**18-30.

183. **Ryckman, B. J., M. A. Jarvis, D. D. Drummond, J. A. Nelson, and D. C. Johnson.** 2006. Human cytomegalovirus entry into epithelial and endothelial cells depends on genes UL128 to UL150 and occurs by endocytosis and low-pH fusion. J Virol **80:**710-722.

184. **Ryckman, B. J., B. L. Rainish, M. C. Chase, J. A. Borton, J. A. Nelson, M. A. Jarvis, and D. C. Johnson.** 2008. Characterization of the human cytomegalovirus gH/gL/UL128-131 complex that mediates entry into epithelial and endothelial cells. J Virol **82:**60-70.

185. **Sam, M. D., B. T. Evans, D. M. Coen, and J. M. Hogle.** 2009. Biochemical, biophysical, and mutational analyses of subunit interactions of the human cytomegalovirus nuclear egress complex. J Virol **83:**2996-3006.

186. **Sampaio, K. L., Y. Cavignac, Y. D. Stierhof, and C. Sinzger.** 2005. Human cytomegalovirus labeled with green fluorescent protein for live analysis of intracellular particle movements. J Virol **79:**2754-2767.

187. **San Martin, C., and R. M. Burnett.** 2003. Structural studies on adenoviruses. Curr Top Microbiol Immunol **272:**57-94.

188. **Sanchez, V., K. D. Greis, E. Sztul, and W. J. Britt.** 2000. Accumulation of virion tegument and envelope proteins in a stable cytoplasmic compartment during human cytomegalovirus replication: characterization of a potential site of virus assembly. J Virol **74:**975-986.

189. **Sato, Y., A. Ding, R. A. Heimeier, A. F. Yousef, J. S. Mymryk, P. G. Walfish, and Y. B. Shi.** 2009. The adenoviral E1A protein displaces corepressors and relieves gene repression by unliganded thyroid hormone receptors in vivo. Cell Res **19:**783-792.

190. **Satyanarayana, A., R. A. Greenberg, S. Schaetzlein, J. Buer, K. Masutomi, W. C. Hahn, S. Zimmermann, U. Martens, M. P. Manns, and K. L. Rudolph.** 2004. Mitogen stimulation cooperates with telomere shortening to activate DNA damage responses and senescence signaling. Mol Cell Biol **24:**5459-5474.

191. **Schleiss, M.** 2005. Progress in cytomegalovirus vaccine development. Herpes **12:**66-75.

192. **Scrivano, L., C. Sinzger, H. Nitschko, U. H. Koszinowski, and B. Adler.** 2011. HCMV spread and cell tropism are determined by distinct virus populations. PLoS Pathog **7:**e1001256.

193. **Seto, D., J. Chodosh, J. R. Brister, and M. S. Jones.** 2011. Using the whole-genome sequence to characterize and name human adenoviruses. J Virol **85:**5701-5702.

194. **Severi, B., M. P. Landini, and E. Govoni.** 1988. Human cytomegalovirus morphogenesis: an ultrastructural study of the late cytoplasmic phases. Arch Virol **98:**51-64.

195. **Sha, J., M. K. Ghosh, K. Zhang, and M. L. Harter.** 2010. E1A interacts with two opposing transcriptional pathways to induce quiescent cells into S phase. J Virol **84:**4050-4059.

196. **Shahin, V., W. Hafezi, H. Oberleithner, Y. Ludwig, B. Windoffer, H. Schillers, and J. E. Kuhn.** 2006. The genome of HSV-1 translocates through the nuclear pore as a condensed rod-like structure. J Cell Sci **119:**23-30.

197. **Shaw, A. R., and E. B. Ziff.** 1980. Transcripts from the adenovirus-2 major late promoter yield a single early family of 3' coterminal mRNAs and five late families. Cell **22:**905-916.

198. **Silva, M. C., Q. C. Yu, L. Enquist, and T. Shenk.** 2003. Human cytomegalovirus UL99-encoded pp28 is required for the cytoplasmic envelopment of tegument-associated capsids. J Virol **77:**10594-10605.

199. **Sinzger, C., M. Digel, and G. Jahn.** 2008. Cytomegalovirus cell tropism. Curr Top Microbiol Immunol **325:**63-83.

200. **Sinzger, C., A. Grefte, B. Plachter, A. S. Gouw, T. H. The, and G. Jahn.** 1995. Fibroblasts, epithelial cells, endothelial cells and smooth muscle cells are major

targets of human cytomegalovirus infection in lung and gastrointestinal tissues. J Gen Virol **76 (Pt 4):**741-750.

201.   **Sinzger, C., and G. Jahn.** 1996. Human cytomegalovirus cell tropism and pathogenesis. Intervirology **39:**302-319.

202.   **Sinzger, C., M. Kahl, K. Laib, K. Klingel, P. Rieger, B. Plachter, and G. Jahn.** 2000. Tropism of human cytomegalovirus for endothelial cells is determined by a post-entry step dependent on efficient translocation to the nucleus. J Gen Virol **81:**3021-3035.

203.   **Smart, J. E., and B. W. Stillman.** 1982. Adenovirus terminal protein precursor. Partial amino acid sequence and the site of covalent linkage to virus DNA. J Biol Chem **257:**13499-13506.

204.   **Smith, J. D., and E. de Harven.** 1974. Herpes simplex virus and human cytomegalovirus replication in WI-38 cells. II. An ultrastructural study of viral penetration. J Virol **14:**945-956.

205.   **Soroceanu, L., A. Akhavan, and C. S. Cobbs.** 2008. Platelet-derived growth factor-alpha receptor activation is required for human cytomegalovirus infection. Nature **455:**391-395.

206.   **Spector, D. J., D. N. Halbert, and H. J. Raskas.** 1980. Regulation of integrated adenovirus sequences during adenovirus infection of transformed cells. J Virol **36:**860-871.

207.   **Spindler, K. R., C. Y. Eng, and A. J. Berk.** 1985. An adenovirus early region 1A protein is required for maximal viral DNA replication in growth-arrested human cells. J Virol **53:**742-750.

208.   **Stabel, S., P. Argos, and L. Philipson.** 1985. The release of growth arrest by microinjection of adenovirus E1A DNA. EMBO J **4:**2329-2336.

209.   **Stein, G. H., M. Beeson, and L. Gordon.** 1990. Failure to phosphorylate the retinoblastoma gene product in senescent human fibroblasts. Science **249:**666-669.

210.   **Stein, G. H., and V. Dulic.** 1998. Molecular mechanisms for the senescent cell cycle arrest. J Investig Dermatol Symp Proc **3:**14-18.

211.   **Stein, R. W., M. Corrigan, P. Yaciuk, J. Whelan, and E. Moran.** 1990. Analysis of E1A-mediated growth regulation functions: binding of the 300-kilodalton cellular product correlates with E1A enhancer repression function and DNA synthesis-inducing activity. J Virol **64:**4421-4427.

212.   **Sterner, D. E., and S. L. Berger.** 2000. Acetylation of histones and transcription-related factors. Microbiol Mol Biol Rev **64:**435-459.

213.   **Subramanian, T., M. La Regina, and G. Chinnadurai.** 1989. Enhanced ras oncogene mediated cell transformation and tumorigenesis by adenovirus 2 mutants lacking the C-terminal region of E1a protein. Oncogene **4:**415-420.

214.   **Subramanian, T., S. E. Malstrom, and G. Chinnadurai.** 1991. Requirement of the C-terminal region of adenovirus E1a for cell transformation in cooperation with E1b. Oncogene **6:**1171-1173.

215.   **Suomalainen, M., M. Y. Nakano, S. Keller, K. Boucke, R. P. Stidwill, and U. F. Greber.** 1999. Microtubule-dependent plus- and minus end-directed motilities are competing processes for nuclear targeting of adenovirus. J Cell Biol **144:**657-672.

216.   **Thomas, G. P., and M. B. Mathews.** 1980. DNA replication and the early to late transition in adenovirus infection. Cell **22:**523-533.

217.   **Tihanyi, K., M. Bourbonniere, A. Houde, C. Rancourt, and J. M. Weber.** 1993. Isolation and properties of adenovirus type 2 proteinase. J Biol Chem **268:**1780-1785.

218.   **Tollefson, A. E., A. Scaria, S. K. Saha, and W. S. Wold.** 1992. The 11,600-MW protein encoded by region E3 of adenovirus is expressed early but is greatly amplified at late stages of infection. J Virol **66:**3633-3642.

219.   **Toth, M., W. Doerfler, and T. Shenk.** 1992. Adenovirus DNA replication facilitates binding of the MLTF/USF transcription factor to the viral major late promoter within infected cells. Nucleic Acids Res **20:**5143-5148.

220.   **Trentin, J. J., Y. Yabe, and G. Taylor.** 1962. The quest for human cancer viruses. Science **137:**835-841.

221.   **Trimarchi, J. M., and J. A. Lees.** 2002. Sibling rivalry in the E2F family. Nat Rev Mol Cell Biol **3:**11-20.

222.   **Turnell, A. S., R. J. Grand, C. Gorbea, X. Zhang, W. Wang, J. S. Mymryk, and P. H. Gallimore.** 2000. Regulation of the 26S proteasome by adenovirus E1A. EMBO J **19:**4759-4773.

223.   **Vale, R. D.** 2003. The molecular motor toolbox for intracellular transport. Cell **112:**467-480.

224.   **van Ormondt, H., J. Maat, and R. Dijkema.** 1980. Comparison of nucleotide sequences of the early E1a regions for subgroups A, B and C of human adenoviruses. Gene **12:**63-76.

225. **Varnum, S. M., D. N. Streblow, M. E. Monroe, P. Smith, K. J. Auberry, L. Pasa-Tolic, D. Wang, D. G. Camp, 2nd, K. Rodland, S. Wiley, W. Britt, T. Shenk, R. D. Smith, and J. A. Nelson.** 2004. Identification of proteins in human cytomegalovirus (HCMV) particles: the HCMV proteome. J Virol **78:**10960-10966.

226. **Virtanen, A., and U. Pettersson.** 1983. The molecular structure of the 9S mRNA from early region 1A of adenovirus serotype 2. J Mol Biol **165:**496-499.

227. **Wahlstrom, G. M., B. Vennstrom, and M. B. Bolin.** 1999. The adenovirus E1A protein is a potent coactivator for thyroid hormone receptors. Mol Endocrinol **13:**1119-1129.

228. **Waldman, W. J., J. M. Sneddon, R. E. Stephens, and W. H. Roberts.** 1989. Enhanced endothelial cytopathogenicity induced by a cytomegalovirus strain propagated in endothelial cells. J Med Virol **28:**223-230.

229. **Walters, R. W., P. Freimuth, T. O. Moninger, I. Ganske, J. Zabner, and M. J. Welsh.** 2002. Adenovirus fiber disrupts CAR-mediated intercellular adhesion allowing virus escape. Cell **110:**789-799.

230. **Wang, D., and T. Shenk.** 2005. Human cytomegalovirus virion protein complex required for epithelial and endothelial cell tropism. Proc Natl Acad Sci U S A **102:**18153-18158.

231. **Wang, G., and A. J. Berk.** 2002. In vivo association of adenovirus large E1A protein with the human mediator complex in adenovirus-infected and -transformed cells. J Virol **76:**9186-9193.

232. **Wang, H. G., Y. Rikitake, M. C. Carter, P. Yaciuk, S. E. Abraham, B. Zerler, and E. Moran.** 1993. Identification of specific adenovirus E1A N-terminal residues critical to the binding of cellular proteins and to the control of cell growth. J Virol **67:**476-488.

233. **Wang, X., S. M. Huong, M. L. Chiu, N. Raab-Traub, and E. S. Huang.** 2003. Epidermal growth factor receptor is a cellular receptor for human cytomegalovirus. Nature **424:**456-461.

234. **Weber, J.** 1976. Genetic analysis of adenovirus type 2 III. Temperature sensitivity of processing viral proteins. J Virol **17:**462-471.

235. **Weber, J., and L. Philipson.** 1984. Protein composition of adenovirus nucleoprotein complexes extracted from infected cells. Virology **136:**321-327.

236. **Weber, J. M.** 2003. Adenain, the adenovirus endoprotease (a review). Acta Microbiol Immunol Hung **50:**95-101.

237. **White, E. A., C. J. Del Rosario, R. L. Sanders, and D. H. Spector.** 2007. The IE2 60-kilodalton and 40-kilodalton proteins are dispensable for human cytomegalovirus replication but are required for efficient delayed early and late gene expression and production of infectious virus. J Virol **81:**2573-2583.

238. **Whyte, P., K. J. Buchkovich, J. M. Horowitz, S. H. Friend, M. Raybuck, R. A. Weinberg, and E. Harlow.** 1988. Association between an oncogene and an anti-oncogene: the adenovirus E1A proteins bind to the retinoblastoma gene product. Nature **334:**124-129.

239. **Wickham, T. J., P. Mathias, D. A. Cheresh, and G. R. Nemerow.** 1993. Integrins alpha v beta 3 and alpha v beta 5 promote adenovirus internalization but not virus attachment. Cell **73:**309-319.

240. **Wiebusch, L., J. Asmar, R. Uecker, and C. Hagemeier.** 2003. Human cytomegalovirus immediate-early protein 2 (IE2)-mediated activation of cyclin E is cell-cycle-independent and forces S-phase entry in IE2-arrested cells. J Gen Virol **84:**51-60.

241. **Wiebusch, L., and C. Hagemeier.** 2001. The human cytomegalovirus immediate early 2 protein dissociates cellular DNA synthesis from cyclin-dependent kinase activation. EMBO J **20:**1086-1098.

242. **Wiethoff, C. M., H. Wodrich, L. Gerace, and G. R. Nemerow.** 2005. Adenovirus protein VI mediates membrane disruption following capsid disassembly. J Virol **79:**1992-2000.

243. **Winberg, G., and T. Shenk.** 1984. Dissection of overlapping functions within the adenovirus type 5 E1A gene. EMBO J **3:**1907-1912.

244. **Ying, B., and W. S. Wold.** 2003. Adenovirus ADP protein (E3-11.6K), which is required for efficient cell lysis and virus release, interacts with human MAD2B. Virology **313:**224-234.

245. **Yu, D., M. C. Silva, and T. Shenk.** 2003. Functional map of human cytomegalovirus AD169 defined by global mutational analysis. Proc Natl Acad Sci U S A **100:**12396-12401.

246. **Zamanian, M., and N. B. La Thangue.** 1992. Adenovirus E1a prevents the retinoblastoma gene product from repressing the activity of a cellular transcription factor. EMBO J **11:**2603-2610.

247. **Zerler, B., B. Moran, K. Maruyama, J. Moomaw, T. Grodzicker, and H. E. Ruley.** 1986. Adenovirus E1A coding sequences that enable ras and pmt oncogenes to transform cultured primary cells. Mol Cell Biol **6:**887-899.

248. **Zerler, B., R. J. Roberts, M. B. Mathews, and E. Moran.** 1987. Different functional domains of the adenovirus E1A gene are involved in regulation of host cell cycle products. Mol Cell Biol **7:**821-829.

249. **Zhang, D., M. M. Johnson, C. P. Miller, T. J. Pircher, J. N. Geiger, and D. M. Wojchowski.** 2001. An optimized system for studies of EPO-dependent murine pro-erythroblast development. Exp Hematol **29:**1278-1288.

250. **Zhang, W., and R. Arcos.** 2005. Interaction of the adenovirus major core protein precursor, pVII, with the viral DNA packaging machinery. Virology **334:**194-202.

251. **Zubieta, C., G. Schoehn, J. Chroboczek, and S. Cusack.** 2005. The structure of the human adenovirus 2 penton. Mol Cell **17:**121-135.

Chapter 2

ONSET OF HUMAN CYTOMEGALOVIRUS REPLICATION IN FIBROBLASTS REQUIRES THE PRESENCE OF AN INTACT VIMENTIN CYTOSKELETON

2.1 Introduction

CMV is a ubiquitous herpesvirus that can cause serious disease in immunocompromised individuals (8, 58). Virtually all cell types, with the exception of lymphocytes and polymorphonuclear leukocytes, can support CMV replication in vivo (80), and this remarkably broad tropism is the basis of the numerous clinical manifestations of CMV infection (8, 58). The range of permissive cells in vitro is more limited, with HF and endothelial cells being the most widely used for propagation of clinical isolates. Two extensively studied strains, AD169 and Towne, were generated by serial passage of tissue isolates in HF for the purpose of vaccine development (22, 68). During this process, both strains accumulated numerous genomic changes (11) and lost the ability to grow in cell types other than HF. By contrast, propagation in endothelial cells produced strains with more intact genomes and tropism, such as TB40/E, VR1814, TR, and PH (59, 80).

The viral determinants of endothelial and epithelial cell tropism have recently been mapped to the UL128-UL131A genomic locus (32, 92, 93). Each of the products of the UL128, UL130, and UL131A genes is independently required for tropism and participates in the formation of a complex at the surface of the virion with the viral glycoproteins gH and gL (74, 93), which can also independently associate with gO (45).

The gH/gL/UL128-131A complex appears to be required for entry into endothelial cells by endocytosis, followed by low-pH-dependent fusion of the virus envelope with endosomal membranes (73, 74) although some virus strains expressing the UL128-UL131A genes do not require endosome acidification for capsid release (66, 79).

HF-adapted strains consistently contain mutations in the UL128-131A genes (32). Loss of endothelial cell tropism in AD169 has been associated with a frameshift mutation in the UL131A gene, leading to the production of a truncated protein and to the loss of the gH/gL/UL128-131A complex, but not the gH/gL/gO complex, from the surface of AD169 virions (1, 3, 92). Reestablishment of wild-type UL131A expression in AD169 by repair of the UL131A gene mutation or by *cis*-complementation yielded viruses with restored tropism for endothelial cells but with reduced replication capacities in HF (1, 92). Interestingly, the efficiencies of entry of wild-type and repaired or complemented AD169 viruses were comparable, suggesting that the presence of UL131A did not interfere with the initial steps of infection in HF but negatively affected virion release (1, 92).

The cellular determinants of CMV tropism are numerous and have not been fully identified. Virus entry begins with virion attachment to the ubiquitously expressed heparin sulfate proteoglycans at the cell surface (17), followed by engagement of one or more receptor(s) including the integrin heterodimers α2β1, α6β1, and αVβ3 (23, 39, 94); the platelet-derived growth factor-α receptor (84); or the epidermal growth factor receptor, whose role in CMV entry is still debated (38, 95).

Subsequent delivery of capsids into the cytoplasm requires fusion of the virus envelope with cellular membranes. Release of AD169 capsids in HF occurs mainly by fusion at the plasma membrane at neutral pH although incoming virions have also been found within phagolysosome-like vacuoles (16, 83). Fusion with the plasmalemma appears to be mediated by the gH/gL/gO complex as AD169 virions do not contain the gH/gL/UL128-131A complex, and infectivity of a gO mutant was severely reduced (37). The mechanism used by strain TB40/E to penetrate into HF has not been described but was assumed to be similar to that of AD169 (80) even though TB40/E virions contain both gH/gL/gO and gH/gL/UL128-131A complexes.

Transport of released, de-enveloped capsids toward the nucleus is mediated by cellular microtubules, and treatment of Towne-infected HF with microtubule-depolymerizing agents substantially reduced expression levels of the viral nuclear IE1 (64). Depolymerization of actin microfilaments was also observed in HF as early as 10 to 20 min post-infection with the Towne strain while stress fiber disappearance was evident at 3 to 5 hpi with AD169 (4, 42, 54), suggesting that microfilament rearrangement may be required to facilitate capsid transition through the actin-rich cell cortex.

The role of IF in CMV infection not been studied. In vivo, expression of the IF protein vimentin is specific to cells of mesenchymal origin like HF and endothelial cells (12). Although the phenotype of vimentin$^{-/-}$ (vim$^-$) mice appears to be mild (15), vimentin-null cells display numerous defects including fragmentation of the Golgi apparatus (26),

development of nuclear invaginations in some instances (76), and reduced formation of lipid droplets, glycolipids, and autophagosomes (29, 52, 87). Vimentin IF interact with integrins α2β1, α6β4, and αVβ3 at the cell surface and participate in recycling of integrin-containing endocytic vesicles (40, 41). They also accompany endocytic vesicles during their perinuclear accumulation (34), regulate endosome acidification by binding to the adaptor complex AP-3 (86), control lysosome distribution into the cytoplasm (87), and promote directional mobility of cellular vesicles (69). The vimentin cytoskeleton is tightly associated with the nuclear lamina (10) and was shown to anchor the nucleus within the cell, to mediate force transfer from the cell periphery to the nucleus, and to bind to repetitive DNA sequences as well as to supercoiled DNA and histones in the nuclear matrix (56, 89, 90). Microtubules and vimentin IF form close connections in HF (30). Drug-induced disassembly of the microtubule network alters IF synthesis and organization, leading to the collapse of vimentin IF into perinuclear aggregates (2, 25, 30, 70). By contrast, coiling of IF after injection of antivimentin antibodies has no effect on the structure of microtubules (28, 46, 53), indicating that the interaction between vimentin IF and microtubules is functionally unidirectional.

In this work, we sought to assess the role of the vimentin cytoskeleton in CMV entry. We hypothesized that vimentin association with integrins at the cell surface, with endosomes and microtubules in the cytoplasm, and with the lamina and matrix in the nucleus facilitates viral binding and penetration, capsid transport toward the nucleus, and nuclear deposition of the viral genome.

We found that, akin to microtubules, vimentin IF do not depolymerize during entry of either AD169 or TB40/E. In comparison to AD169, onset of TB40/E infection in HF was delayed, and the proportion of infected cells was reduced. Virus entry was negatively affected by the disruption of vimentin networks after exposure to acrylamide (ACR), by IF bundling in cells from patients with giant axonal neuropathy (GAN), and by the absence of vimentin IF in vim⁻ mouse embryo fibroblasts (MEF). In vim⁻ cells, the efficiency of particles trafficking toward the nucleus appeared significantly lower than in vimentin$^{+/+}$ (vim$^+$) cells, and in each instance the negative effects were more pronounced in TB40/E-infected cells than in AD169-infected cells. These data show that vimentin is required for efficient entry of CMV into HF and that the EC-tropic strain TB40/E is more reliant on the presence and integrity of vimentin IF than the HF-adapted strain AD169.

2.2   Materials and Methods

2.2.1   Cells and virus

Primary foreskin HF (a gift from E. S. Mocarski, Atlanta, GA) were propagated in Dulbecco's modified Eagle medium (DMEM) supplemented with 10% fetal clone serum III (HyClone), 4 mM 4-(2-hydroxyethyl)-1-piperazineethanesulfonic acid (HEPES), 1 mM sodium pyruvate, and 100 U/ml penicillin and 100 µg/ml streptomycin (all from Gibco Invitrogen Corp. [completeDMEM]) and were used between passages 17 and 27 postisolation. Normal dermal HF (MCH070 cells) and dermal HF from a patient with GAN (WG0321cells) were obtained from the Repository for Mutant Human Cell Strains at Montreal Children's Hospital and were propagated as described above with the

addition of 10% fetal bovine serum (HyClone). To induce vimentin IF bundling, cells were cultured in medium lacking serum for 4 days. Vim$^+$ (MFT-6) and vim$^-$ (MFT-16) immortalized MEF (a gift of R. Evans, Aurora, CO) were propagated as described for foreskin HF. Human CMV strains AD169*var*ATCC and TB40/E were kind gifts from E. S. Mocarski and were originally obtained from the ATCC and C. Sinzger (Tübingen, Germany), respectively. Propagation and purification of both strains were performed as described previously (35). Virus titers were determined by plaque assay on HF monolayers in 12-well tissue culture plates. Five different stocks of TB40/E and five of AD169 were used for the experiments described. The identity of each strain was verified by PCR amplification of AD169 and TB40/E genomic extracts with primers mapping to the UL150 gene.

2.2.2   Cell infection

For analysis of microtubules, microfilaments, and vimentin IF structure, HF were plated at a density of 5×10^4 cells/cm^2 in 24-well plates with coverslips 1 day prior to infection with AD169 or TB40/E at a multiplicity of infection (MOI) of 5. Mock-infected samples were exposed to culture medium alone. Cells were harvested at 5 and 30 min (min) post-infection and at 1, 2, and 4 hpi. For expression analyses of IE1 and IE2, HF were plated as above and infected with AD169 or TB40/E at an MOI of 1 or 5 at confluence (3 days post-seeding). After adsorption for 1 h, cells were washed twice and incubated in fresh DMEM until 2, 4, 8, 24, 48, 72, and 96 hpi. Endpoint titers of cell-free virus were determined by plaque assay on confluent HF by serial dilution of supernatants from HF infected with AD169 or TB40/E at an MOI of 1 and collected at 24, 48, 72, 96, 120, 144,

and 168 hpi. MCH070 and WG0321 cells were seeded in serum-free DMEM at a density

of 5×10^4 cells/cm^2 in 24-well plates with coverslips 4 days prior to infection with

AD169 or TB40/E at an MOI of 1 or 10. After adsorption for 1 h, cells were washed

twice and incubated in fresh DMEM until 4, 8, and 24 hpi. For IE1/IE2 expression

analyses, vim$^+$ and vim$^-$ MEF were seeded at a density of 7.7×10^4 cells/well in 24-well

plates with coverslips 1 day prior to infection with AD169 or TB40/E at an MOI of 1 or

10. After adsorption for 1 h, cells were washed twice and incubated in fresh DMEM until

4, 8, and 24 hpi. For pp150 staining analyses, vim$^+$ and vim$^-$ MEF were prechilled on ice

for 20 min before exposure to AD169 or TB40/E virions (MOI of 3) for 1 h on ice. Cells

were then transferred to 37°C for 1 h, washed three times with culture medium, and

further incubated for 4 and 8 h.

2.2.3   ACR treatment of HF

Confluent HF cultures were exposed for 2, 4, 6, and 8 h to a 5 mM ACR solution made

by diluting ACR/bis-ACR solution (30% [wt/vol]; Bio-Rad, Hercules, CA) in culture

medium. Uninfected cells were harvested immediately after ACR incubation or after

ACR removal, washing, and incubation in fresh medium for 4 h. For infection with

AD169 or TB40/E at an MOI of 1 or 5, ACR-pretreated cells were washed, exposed to

each virus for 1 h, washed again, and collected at 4 hpi.

2.2.4   Antibodies and immunoflourescence staining analysis

Cells were fixed, permeabilized, and blocked as described previously (36) before

incubation with monoclonal antibodies anti-human vimentin (1:200; V9; Santa Cruz

Biotechnology, Santa Cruz, CA), anti-α-tubulin (1:100; B-5-1-2; Sigma, St. Louis, MO), anti-pp150 (1:400; originally from W. Britt, Birmingham, AL), or anti-IE1/IE2 (1:500; fluorescein isothiocyanate-conjugated MAb810F; Chemicon, Temecula, CA) for 1 h at room temperature (RT). Samples were then washed in phosphate-buffered saline (PBS)– 0.05% Tween-20 and incubated with Alexa Fluor 594-conjugated anti-mouse immunoglobulin G (1:100; Molecular Probes, Eugene, OR) for 1 h at RT. For dual stainings, fixed cells were incubated with a primary antibody and with the Alexa Fluor 594-conjugated goat anti-mouse antibody, blocked with normal mouse immunoglobulin G (1:100; Caltag, Burlingame, CA), and finally stained for IE1/IE2 with MAb810F. Microfilaments were stained with a 1:100 dilution in PBS of Alexa Fluor 568-conjugated phalloidin (Molecular Probes, Eugene, OR), and nuclei were labeled with a 0.2 mg/ml dilution of Hoechst 33342 (Molecular Probes, Eugene, OR) in PBS for 3 min at RT. Coverslips were mounted in 90% glycerol–10% PBS containing 2.5 g/liter of 1, 4 diazabicyclo-(2, 2, 2)-octane (DABCO; Alfa Aesar, Pelham, NH) and analyzed on a Zeiss Axioskop 2 magneto-optical trap fluorescence microscope equipped with a Qimaging Retiga 1300 coded monochrome 12-bit camera. Images were collected and pseudo-colored using Northern Eclipse, version 7.0, software. Confocal images were acquired on a Zeiss LSM 510 META ConfoCor2 laser-scanning confocal microscope equipped with Zeiss LSM 510 META image processing software.

2.3 Results

2.3.1 Virus entry does not alter vimentin IF structure

To determine whether the integrity of vimentin IF can impact viral entry, foreskin HF infected with AD169 or TB40/E were harvested at 5 and 30 min and at 1, 2, and 4 hpi; cells were stained with anti-vimentin and anti-IE1/IE2 antibodies and analyzed by fluorescence microscopy (Fig. 2-1 and data not shown). In HF infected with AD169 at an MOI of 5, nuclear IE1/IE2 staining was observed in about 10% of the cells as early as at 2 hpi (Fig. 2-1R), indicating that, by this time, AD169 entry had been successfully completed, with the nuclear deposition of the viral genome and the onset of viral gene synthesis. By contrast, IE1/IE2 expression was not detected in TB40/E-infected cultures until 4 hpi (data not shown).

In mock-infected cells, vimentin filaments formed a dense, web-like network stretching in all directions toward the cell periphery and forming a border around the nucleus (Fig. 2-1A to D). Cells infected with AD169 (Fig. 2-1E to X) or TB40/E (data not shown) exhibited a staining pattern virtually identical to that of mock-infected cells at each of the times tested, suggesting that vimentin IF did not undergo substantial modifications during the initial phase of infection. At later times (24, 72, and 96 hpi), infected cells became rounded and enlarged. Despite these morphological changes, the vimentin perinuclear border and cytoplasmic network remained intact (data not shown).

Parallel sets of samples were also stained for α-tubulin and for actin to determine the effects of viral entry on the structure of microtubules and microfilaments. In AD169 or TB40/E-infected cells, no microtubule disassembly was observed from 5 min to 4 hpi (data not shown), consistent with the role of microtubules in facilitating capsid movement toward the nucleus (64). During infection with AD169, microfilament depolymerisation and stress fiber disappearance occurred in 2.6% ± 5% and 35% ± 20% of IE1/IE2-
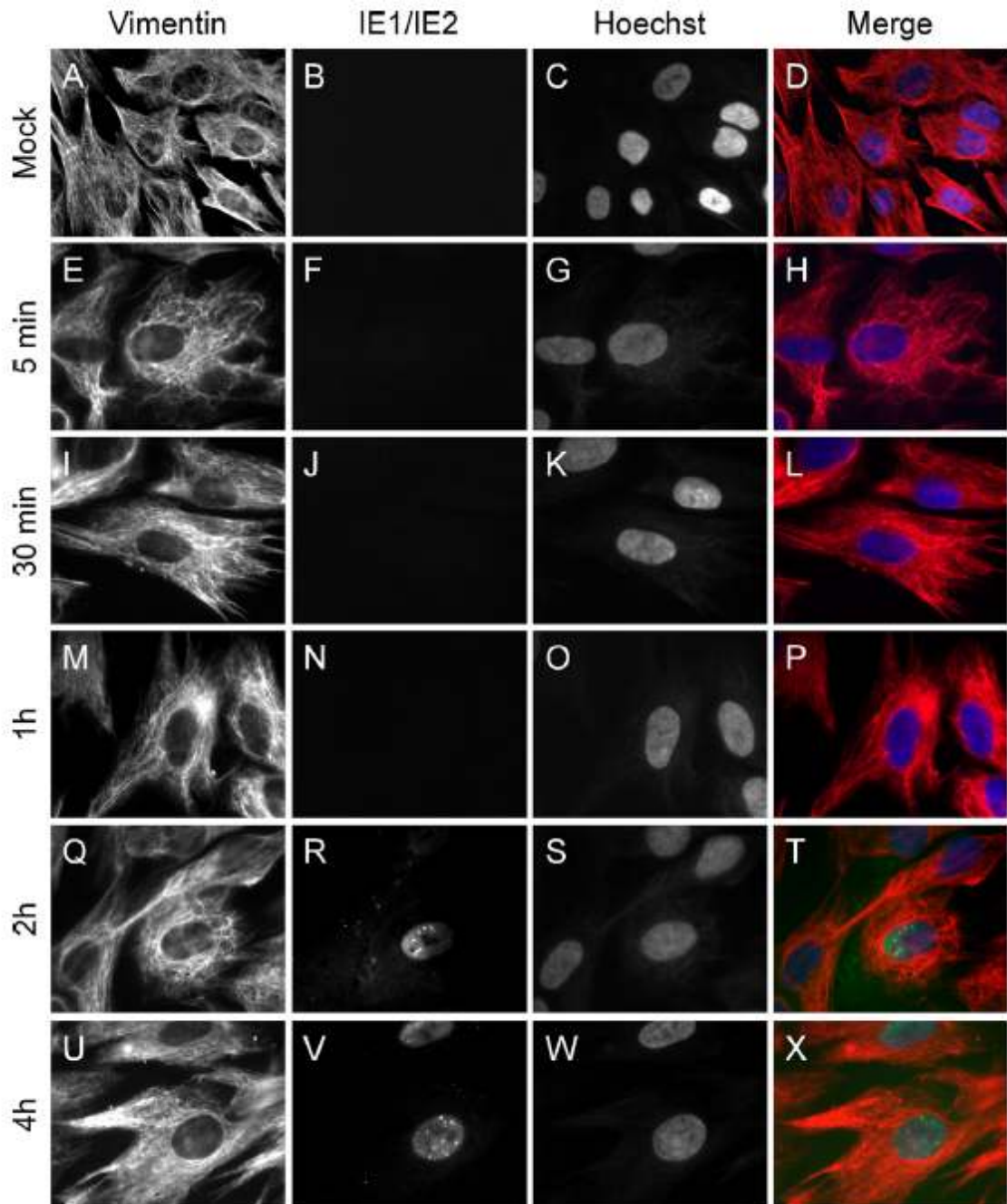
FIG. 2-1. Organization of the vimentin cytoskeleton during entry of AD169 in HF. Mock-infected (A to D) or AD169-infected (MOI of 5; E to X) HF harvested at 5 or 30 min post-infection and at 1, 2, or 4 hpi were stained with a monoclonal anti-vimentin antibody followed by an Alexa Fluor 594-conjugated goat anti-mouse antibody (red) and a fluorescein isothiocyanate-conjugated anti-IE1/IE2 antibody (green). Nuclear DNA was stained with Hoechst 33342 (blue). Merged images are shown in panels on the right. Original magnification was 400× for panels A to D and 100 for panels E to X.

expressing cells at 2 and 4 hpi, respectively. Interestingly, development of this phenotype occurred later and to a lower extent in TB40/E-infected HF, with 5% ± 5% and 7.6% ± 5% of IE1/IE2-positive cells displaying loss of stress fibers at 4 and 8 hpi, respectively. Together, these results indicate that microtubules and vimentin IF remain structurally intact throughout the initial steps of infection with both strains, suggesting that the integrity of both networks may be required during virus entry. Moreover, onset of replication and microfilament disassembly in TB40/E-infected HF occurred approximately 2 h later than in AD169-infected cells, indicating a potential delay in the initiation of TB40/E infection in HF.

2.3.2   AD169 and TB40/E kinetics of infection in HF are different

To directly compare the growth kinetics of AD169 and TB40/E in HF, confluent cell monolayers were infected in parallel with AD169 or TB40/E at an MOI of 1 or 5. Cells were harvested at 2, 4, 8, 24, 48, 72, and 96 hpi, and IE1/IE2 expression was monitored by immunofluorescence staining analysis. Cell supernatants were also collected at 24, 48, 72, 96, 120, 144, and 168 hpi, and the amount of cell-free virus released during infection was quantified by plaque assay. IE1/IE2 expression was detected in 16% ± 5% (MOI of 1) and in 7.4% ± 3% (MOI of 5) of AD169-infected HF at 2 hpi, with the percentage of positive cells increasing with time up to 89% ± 8% (MOI of 1) and 97% ± 2% (MOI of 5) at 96 hpi (Fig. 2-2A and B). By contrast, IE1/IE2 expression was not detected at 2 hpi in TB40/E-infected HF (Fig. 2-2A and B) while at 4 hpi, approximately 10% of infected cells
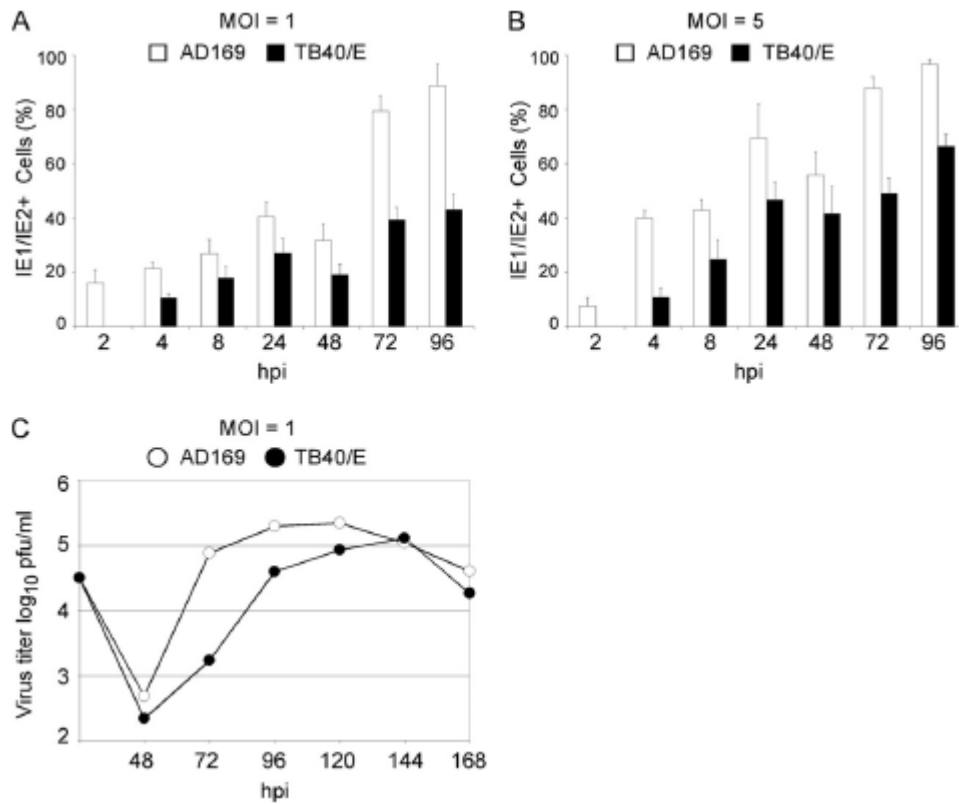
FIG. 2-2. AD169 and TB40/E infection time course in HF. Cells and supernatants from cultures infected with AD169 or TB40/E at an MOI of 1 (A and C) or 5 (B) were collected at the indicated times postinfection. (A and B) Cells were stained for IE1/IE2, and the percentage of expressing cells was calculated. Means and standard deviations of the percentage values of IE1/IE2-positive cells scored in five separate fields per sample in one representative experiment are shown. (C) Amount of cell-free virus released in supernatants of AD169- and TB40/E-infected HF as quantified by plaque assay.

displayed nuclear staining at either MOI. From 4 hpi onwards, the percentage of TB40/E infected cells increased with time at a rate comparable to that of AD169-infected cells, so that a 1.5- to 2-fold difference in the proportion of AD169- and TB40/E-positive cells was maintained at each time, irrespective of the MOI used.

Consistent with this difference in the number of infected cells, the amount of cell-free virus released in the supernatant of TB40/E-infected cultures was about 100-fold lower than that released by AD169-infected cells at 72 hpi and about fivefold lower at 96 hpi. At later times, yields became similar, mostly because of the drop in the AD169 virus production (Fig. 2-2C). These data indicate that the onset of TB40/E infection in HF is delayed compared to AD169 and that the initial difference in the proportion of infected cells is maintained with time. Consequently, TB40/E-infected cells also released smaller amounts of newly formed particles over time.

2.3.3   Pretreatment of HF with ACR inhibits the onset of infection

To determine whether the integrity of the vimentin cytoskeleton is required to facilitate the onset of viral infection, HF were treated with a 5 mM ACR solution for 2, 4, 6, or 8 h prior to infection with either AD169 or TB40/E. ACR is a neurotoxin that has been extensively used to disrupt the organization of IF in neurons and in other cells types (2, 20, 21, 33, 75). ACR treatment of HF induced cell rounding and contraction, accompanied by the aggregation of vimentin IF in elongated bundles extending into the cells' retraction fibers (Fig. 2-3A to E) (2, 20) and by the appearance of invaginations or folds in the nuclear envelope (Fig. 2-3F). Consistent with literature reports (20, 47), actin

stress fiber disassembly but no microtubule depolymerisation was detected in ACR-treated cells (data not shown). As the emergence of nuclear folds has been described to occur in some vimentin null cells, in cells expressing vimentin mutants or containing thick IF bundles, and in ACR-treated neurons (33, 43, 76, 78), we used the percentage of cells with nuclear invaginations as an estimate of the extent of IF disruption. As expected, an exposure time-dependent increase in percentage values was observed, from 1.5% ± 1% after 2 h to 32% ± 7% after 8 h of continual treatment (Fig. 2-3G). The number of cells displaying nuclear folding became even larger after replacement of ACR with fresh medium for 4 h (Fig. 2-3G), while incubation in fresh medium for 24 h led to the complete reestablishment of the vimentin IF network and to the disappearance of nuclear invaginations (data not shown), underscoring the reversible nature of ACR-induced changes (2). ACR treatment also did not trigger widespread cell death, as the proportion of cells displaying apoptotic nuclei never increased above 2% (Fig. 2-3H).

HF pretreated with ACR were infected with AD169 at an MOI of 1 or 5, and the percentage of cells with nuclear invaginations or with apoptotic nuclei at 4 hpi was determined. The extent of nuclear folding in samples infected at either MOI was similar to that of uninfected cells treated with ACR and subsequently incubated for 4 h in fresh medium (Fig. 2-3, compare panels I and G), suggesting that infection had no effect on the formation of nuclear invaginations. By contrast, a slightly higher fraction of dead cells was found after infection of ACR-treated cells, with the highest value (4.2% ± 3%) observed after 8 h of pretreatment and infection at an MOI of 5 (Fig. 2-3J).

The proportion of AD169-infected, untreated cells expressing IE1/IE2 was 28% ± 8% at an MOI of 1 and 57% ± 14% at an MOI of 5 (Fig. 2-4A). ACR pretreatment led to a marked decline in the proportion of IE1/IE2-positive cells. The extent of this decline was dependent on the length of the pretreatment period, with a maximum reduction, relative to untreated samples, of 12-fold (MOI of 1) and 14-fold (MOI of 5) in cells pretreated for 8 h.

The percentage of untreated HF expressing IE1/IE2 after infection with TB40/E was 11% ± 2% at an MOI of 1 and 13% ± 0.2% at an MOI of 5. In cells pretreated with ACR for 6 h, the proportion of IE1/IE2-positive cells had dropped to 0.6% ± 0.9% (19-fold reduction; MOI of 1) and 1.2% ± 1.1% (11-fold reduction; MOI of 5) while in cells pretreated with ACR for 8 h, no IE1/IE2 expression was detected (Fig. 2-4B). Thus, pretreatment of HF with ACR significantly inhibited the onset of both AD169 and TB40/E replication.

To assess the reversibility of inhibition, HF were either left untreated or were pretreated with ACR for 4 h prior to ACR removal and exposure to AD169 or TB40/E at an MOI of 1. Removal of the virus inoculum was followed by extensive washing of cells to remove unbound particles and by incubation in fresh medium for 4, 18, and 24 hpi. At 4 hpi, the percentage of IE1/IE2- expressing cells in the pretreated samples was approximately 5-fold (AD169) and 3.5-fold (TB40/E) lower than that of untreated cells at the same time

FIG. 2-3. Effects of ACR pretreatment and AD169 infection on IF organization and nuclear morphology in HF. (A to F) Fluorescence microscopy analysis of vimentin IF organization in untreated HF (A) and in HF exposed to a 5 mM solution of ACR for 2 (B), 4 (C), 6 (D), or 8 h (E) prior to staining with antivimentin antibodies. (F) Confocal microscopy image of lamin B-stained cell nuclei after 6 h of ACR pretreatment. (G and H) Percentage of cells with nuclear invaginations (G) or with nuclear outlines consistent with apoptosis (H) in HF monolayers harvested immediately after ACR treatment for the indicated times (white bars) or harvested after ACR removal and incubation of cells in fresh medium for 4 h (black bars). (I and J) Percentage of cells with nuclear invaginations (I) or with apoptotic nuclei (J) in HF monolayers harvested after ACR treatment for the indicated times and AD169 infection at an MOI of 1 (white bars) or 5 (black bars) for 4 h. Mean and standard deviation values from three independent experiments are shown.
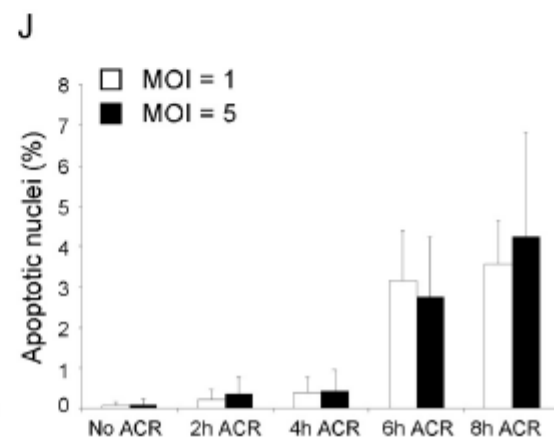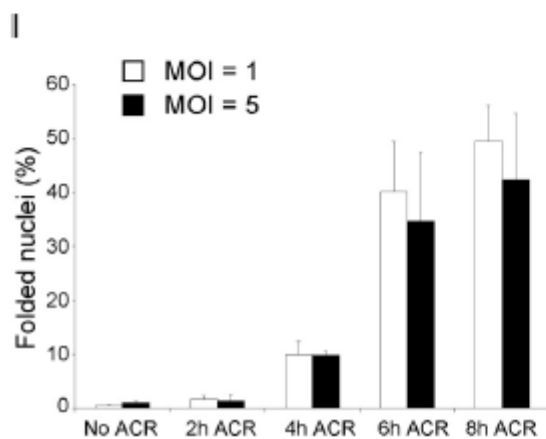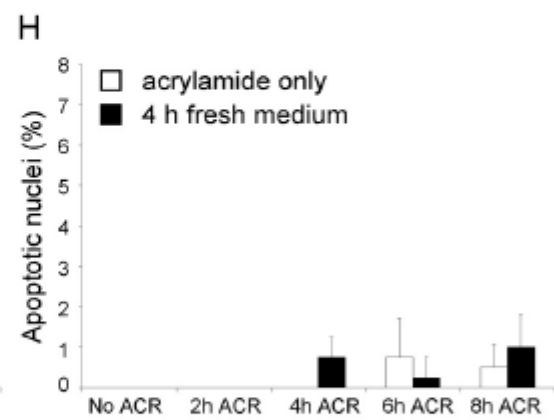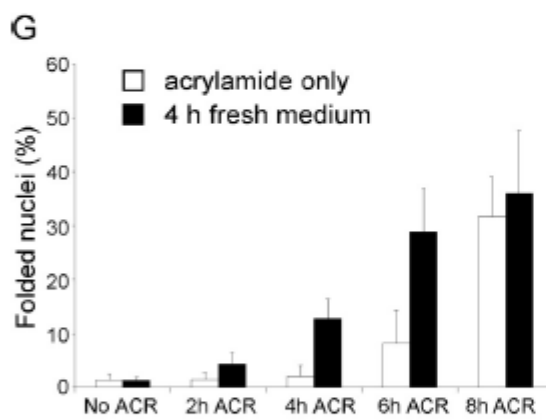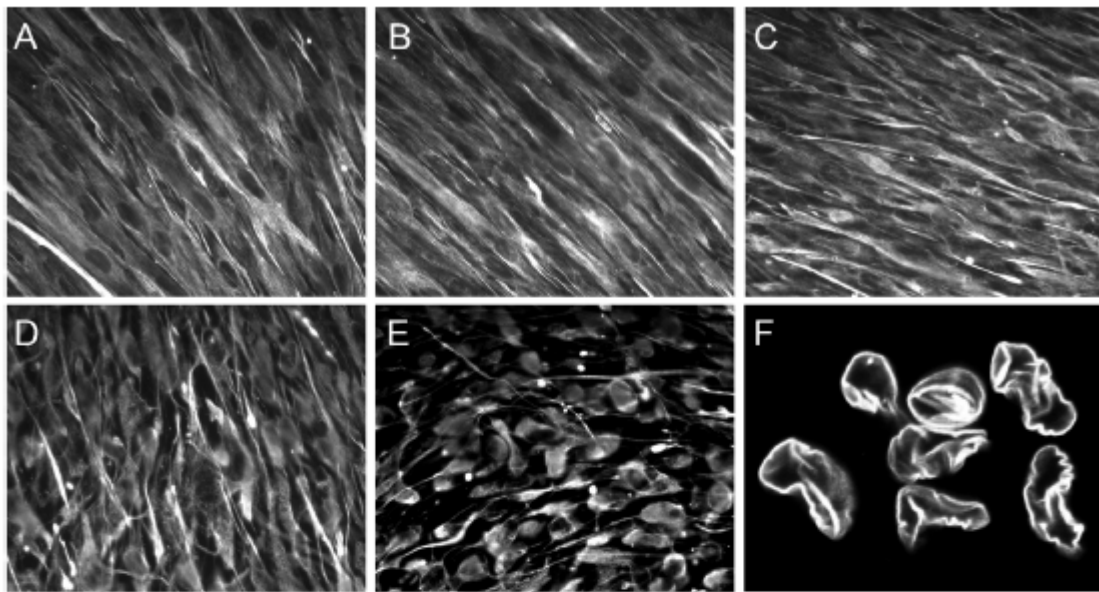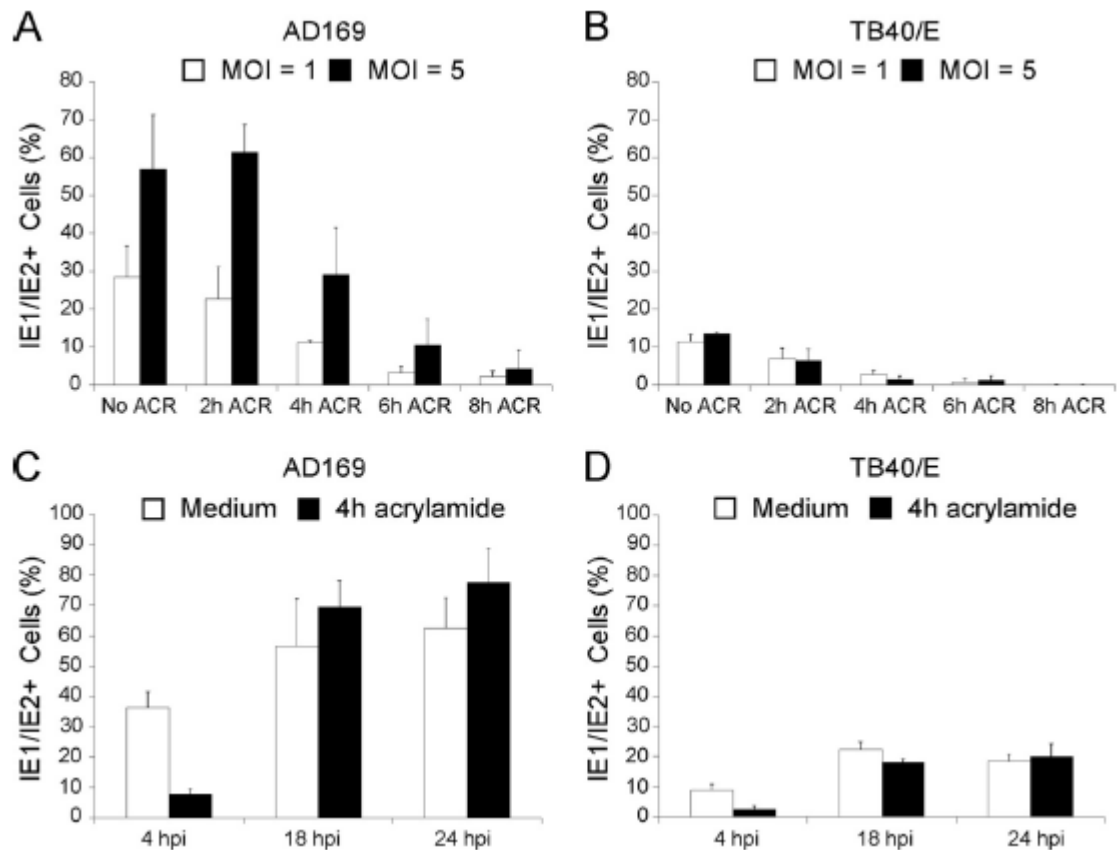
FIG. 2-4. Impact of ACR pretreatment on AD169 and TB40/E infection efficiency. (A and B) Percentage of IE1/IE2-expressing HF either untreated (No ACR) or after exposure to a 5 mM solution of ACR for 2, 4, 6, or 8 h prior to infection with AD169 or TB40/E at an MOI of 1 or 5 for 4 h. (C and D) Percentage of IE1/IE2-expressing HF left untreated (white bars) or treated with a 5 mM solution of ACR for 4 h (black bars) prior to infection with AD169 or TB40/E at an MOI of 1. Mean and standard deviation values from three (A and C) and two (B and D) independent experiments are shown.

point (Fig. 2-4C and D). This result was expected, as the vimentin cytoskeleton remains largely disorganized at 4 h after ACR removal (Fig. 2-3G). However, at 18 and 24 hpi the proportion of IE1/IE2-positive nuclei in ACR-pretreated cells was similar or greater than that of their untreated counterparts, indicating that the block in progression of the infection was removed after the reestablishment of a normal vimentin cytoskeleton.

2.3.4 Vimentin bundling in HF from GAN patients reduces the efficiency of infection

In addition to IF aggregation, ACR treatment of HF also caused stress fiber disassembly (data not shown) and the development of nuclear invaginations (Fig. 2-3F) and was reported to inhibit protein synthesis (2). Each of these effects might contribute to the observed decrease in the percentage of infected cells. To assess the effects of vimentin IF disruption on viral entry using a different system, we compared the efficiency of onset of AD169 and TB40/E infection in dermal HF harvested from patients with GAN (WG0321 cells) and from healthy control subjects (MCH070 cells).

GAN is a neurodegenerative disorder characterized by bundling of IF in neurons and in other cell types, including HF (67, 96). This phenotype can be conditionally induced in vitro by exposing HF from GAN patients to low-serum conditions (48, 51). Serum starvation for a period of 4 days induced vimentin bundling in 88.8% ± 2.9% of WG0321 cells but did not affect the IF network of MCH070 cells (Fig. 2-5A to F). IF alteration in WG0321 cells was phenotypically different from that occurring in ACR-treated HF, with the appearance of dense, spherical bundles of vimentin IF in specific areas of the cell and

with peripheral filaments and nuclear contacts remaining unperturbed in the majority of the cells. In addition, retraction fibers, nuclear invaginations, and microfilament or microtubule depolymerisation were not observed (Fig. 2-5D to F and data not shown). Serum-starved WG0321 and MCH070 cells were infected with either AD169 or TB40/E at an MOI of 1 or 10, and the percentage of IE1/IE2-positive cells at 4, 8, and 24 hpi was determined. At 4 hpi, 55% ± 16% (MOI of 1) and 78% ± 12% (MOI of 10) of AD169-infected MCH070 cells showed IE1/IE2 expression (Fig. 2-5G, H, I, and K). These percentages were slightly higher than those observed at 4 hpi in HF, likely on account of the greater degree of quiescence reached by MCH070 cells after serum starvation. At the same time point, a 3-fold (MOI of 1) and a 1.2-fold (MOI of 10) reduction in the percentage of IE1/IE2-positive nuclei was observed in WG0321 cells (Fig. 2-5I and K). By contrast, at 8 and 24 hpi, WG0321 and MCH070 cell populations contained equal proportions of IE1/IE2-expressing cells at each MOI. These data suggest that vimentin bundling in WG0321 cells may be detrimental to the onset of AD169 replication and that this effect is both MOI and time dependent: smaller differences are observed between the two cell populations after infection at an MOI of 10, and no differences are observed at later time points postinfection.

No IE1/IE2-positive nuclei were detected at 4 hpi in TB40/E-infected WG0321 or MCH070 cells at either MOI (Fig. 2-5J and L). At 8 and 24 hpi, however, both WG0321 and MCH070 cells expressed IE1/IE2, indicating that initiation of TB40/E replication was delayed but not abrogated. Similar to the situation in HF (Fig. 2-2A and B), infection of MCH070 with TB40/E yielded approximately 30 to 40% fewer IE1/IE2-positive cells

than infection with AD169 at 8 and 24 hpi and at both MOIs, indicating that efficient initiation of TB40/E infection is impaired in HF, regardless of their origin (foreskin or dermis) and of the presence (HF) or absence (MCH070) of serum in the culture medium.

A 1.8-fold reduction in the proportion of IE1/IE2-positive nuclei was observed at 8 h after TB40/E infection of WG0321 cells compared to MCH070 cells, irrespective of the MOI used (Fig. 2-5J and L). At 24 hpi, the extent of this reduction appeared to decrease slightly to 1.65-fold (MOI of 1) and 1.5-fold (MOI of 10), but was not eliminated as it was for AD169-infected WG0321 cells.

Combined, these data indicate that the presence of vimentin bundles can directly or indirectly impair the efficient onset of both AD169 and TB40/E replication. In contrast to infection with AD169, the degree of impairment of TB40/E infection was MOI independent, and the defect could not be corrected with time.

FIG. 2-5. Structure of vimentin IF and expression of viral IE1/IE2 proteins in WG0321 and WG0321 dermal fibroblasts. (A to F) Serum-starved dermal fibroblasts from healthy donors (MCH070) and from patients with GAN (WG0321) were stained for vimentin and with Hoechst 33342. Merged images are shown as indicated. (G and H) Serum-starved MCH070 (G) and WG0321 (H) dermal fibroblasts were infected with AD169 at an MOI of 10 for 4 h prior to staining for vimentin (green) and for IE1/IE2 (red). (I to L) Percentage of serum-starved MCH070 (white bars) and WG0321 (black bars) cells expressing IE1/IE2 after infection with AD169 (I and K) or TB40/E (J and L) at an MOI of 1 or 10. Mean and standard deviation values from three (I, K, and L) and two (J) independent experiments are shown. ND, not detected.

84
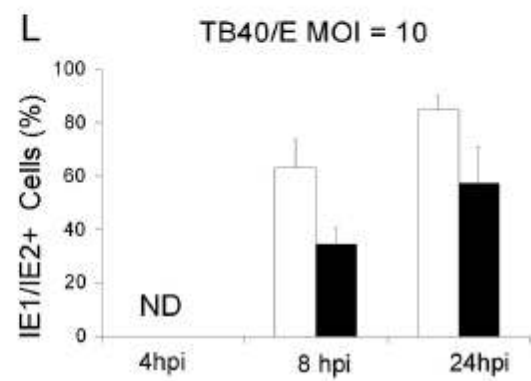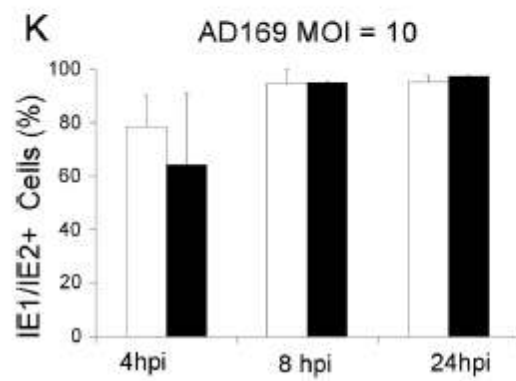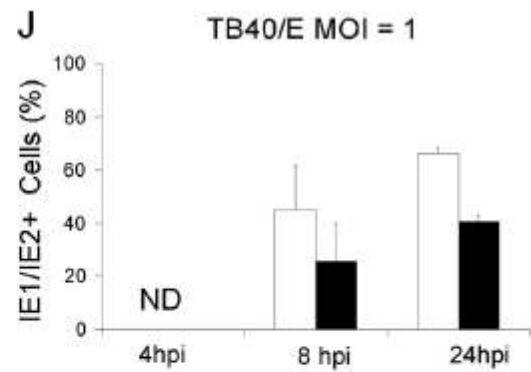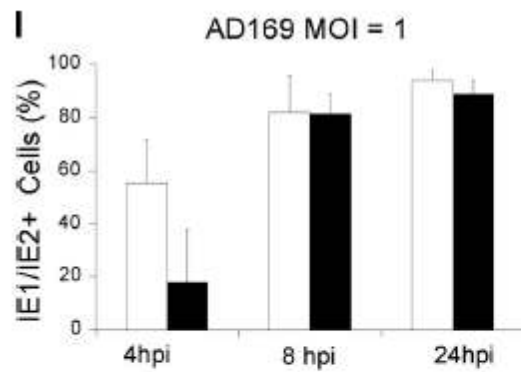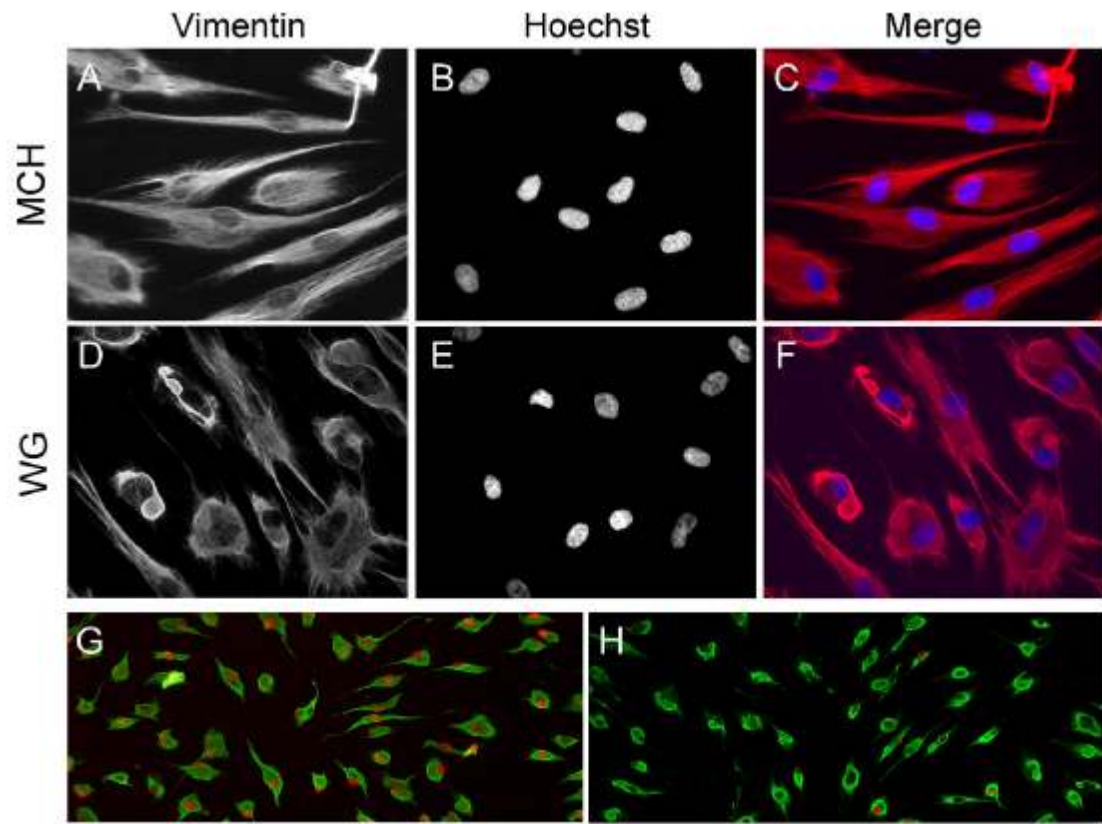
2.3.5   Absence of vimentin impairs the onset of infection

To further investigate the role of vimentin on virus entry, immortalized vim$^+$ and vim$^-$ MEF were infected with AD169 or TB40/E at an MOI of 1 or 10, and the proportion of IE1/IE2-positive cells at 4, 8, and 24 hpi was determined. MEF do not support human CMV replication but allow normal entry events to proceed (49, 50), with the block in infection occurring after IE gene expression. Consistent with literature data, IE1/IE2 expression was observed in MEF infected with either strain (Fig. 2-6), but the percentages of IE1/IE2-positive cells were lower than those found in HF or MCH070 cell populations, possibly as a result of the reduced degree of quiescence reached by immortalized cells compared to primary HF. While the proportion of AD169-infected vim$^+$ MEF remained unchanged over time, a sudden increase in the number of TB40/E-infected vim$^+$ MEF was observed between 8 and 24 hpi at each MOI.

At all times tested and at both MOIs, the percentage of IE1/IE2-expressing vim$^-$ MEF infected with AD169 was markedly lower than that observed in vim$^+$ MEF (Fig. 2-6 A and C). The largest differences were recorded during infection at an MOI of 1, with fivefold, fourfold, and threefold reductions at 4, 8, and 24 hpi, respectively. At an MOI of 10, differences appeared to be slightly reduced, to an average of 2.3-fold. Interestingly, while the proportion of IE1/IE2-positive, vim$^+$ cells remained fairly constant (Fig. 2-6A and C,), the percentage of IE1/IE2-positive, vim$^-$ cells appeared to slowly increase with time at both MOIs (Fig. 2-6A and C), suggesting that the onset of AD169 infection in vim$^-$ cells was delayed but not abrogated.
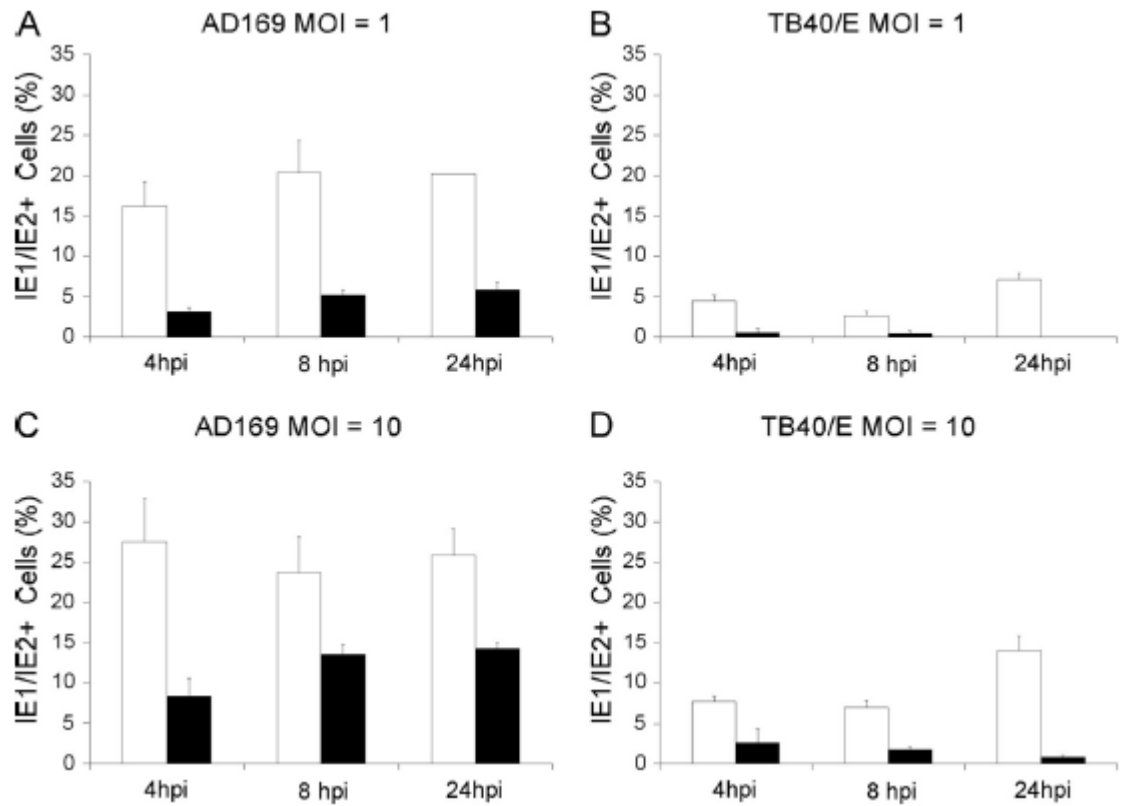
FIG. 2-6. Viral IE1/IE2 gene expression in vim$^+$ and vim$^-$ MEF. Percentage of vim$^+$ (white bars) and vim$^-$ (black bars) MEF expressing IE1/IE2 after infection with AD169 (A and C) or TB40/E (B and D) at an MOI of 1 or 10. Mean and standard deviation values from two independent experiments are shown.

Similar to what was observed in HF, the proportion of TB40/E-infected vim$^+$ cells at either MOI was about three- to fourfold lower than that of AD169-infected vim$^-$ cells (Fig. 2-6, compare A to B and C to D). In addition, the absence of vimentin appeared to have a larger impact on the onset of TB40/E infection, with 7- to 9-fold and 3- to 17-fold reductions in the percentages of IE1/IE2-positive vim$^-$ cells observed at an MOI of 1 and 10, respectively (Fig. 2-6B and D). Finally, and contrary to infection with AD169, the percentages of IE1/IE2-positive vim$^-$ cells appeared to steadily decrease with time during TB40/E infection at both MOIs, an indication of abortive infection.

Together, these data show that the presence of vimentin is required for the efficient start of both AD169 and TB40/E replication. While onset of AD169 infection in vim$^-$ cells is initially delayed, it appears to recover with time. By contrast, TB40/E infection becomes abortive, suggesting a larger degree of reliance on vimentin for the initial stages of TB40/E infection.

2.3.6   Vimentin is required for proper viral particle trafficking

To assess whether vimentin affected intracellular capsid transport, virion localization was tracked by staining AD169- or TB40/E-infected vim$^+$ and vim$^-$ MEF for pp150, a tegument phosphoprotein that remains strongly associated with capsids during entry and that has been used as capsid marker in other studies (64, 81). At 1 hpi with AD169, the pp150 signal was found predominantly at the cell surface and within the cytoplasm of vim$^+$ and vim$^-$ cells (Fig. 2-7A and B), and no obvious differences were found between

cell types in the total numbers of particles per cell at 1 and 4 hpi. By 8 hpi, only few vim$^+$ cells still contained particles while the pp150 signal was clearly evident in the cytoplasm of several vim$^-$ cells (Fig. 2-7C and D). The number of pp150-positive, vim$^+$ cells seemed to decline with time much more rapidly than the number of pp150-positive, vim$^-$ cells, suggesting that capsid disassembly and concomitant loss of the pp150 signal might occur more rapidly in the presence of vimentin. To quantify this result, the percentage of pp150-positive vim$^+$ and vim$^-$ MEF was determined after infection with AD169 or TB40/E at an MOI of 3 in synchronized infections. After virus adsorption at 4°C for 1 h, cultures were shifted at 37°C for 1 h to allow for penetration to occur, then washed, and further incubated for 4 and 8 h. The proportions of pp150-positive cells after virus adsorption and penetration were virtually identical in all samples (Fig. 2-7E), indicating that the absence of vimentin did not affect binding of either strain. After 4 h at 37°C, however, the percentage of pp150-positive vim$^+$ cells infected with AD169 was dramatically lower than that of vim$^-$ cells (Fig. 2-7E). By 8 h, a slight additional decrease in the percentage of particle-containing cells was observed in vim$^-$ cells (Fig. 2-7E). In TB40/E-infected cultures, the proportions of virion-containing vim$^+$ and vim$^-$ cells after 1 h at 37°C were almost identical, and no decrease relative to the percentage of pp150-positive cells after virus adsorption for 1 h at 4°C was observed (Fig. 7E). This situation remained unchanged in vim$^-$ MEF until the 8-h time point, when a decrease in the percentage of cells with particles was registered. By contrast, vim$^+$ cultures were characterized by a more gradual decrease in pp150-positive cells over time. Thus, the rate of pp150 signal loss in AD169-infected, vim$^+$ cells was significantly faster than that in TB40/E-infected, vim$^+$ cells, suggesting that AD169 virions may be reaching the nucleus

more rapidly than TB40/E virions. To assess if this was indeed the case, the proportion of pp150-positive virions localizing at the cell surface, in the cytoplasm, or in close proximity to the nucleus of infected cells at 1 h posttransfer at 37°C was calculated. In vim$^+$ cells infected with AD169, particles were equally distributed between the cytoplasm and the nucleus while in vim$^-$ cells, virions accumulated in the cytoplasm (Fig. 2-7F). The majority of virus particles were also found in the cytoplasm of vim$^+$ and vim$^-$ cells infected with TB40/E, supporting the hypothesis of a slower rate of intracellular movement of TB40/E virions than of AD169 virions. In vim$^-$ cells, a slightly higher proportion of TB40/E particles were also observed at the cell periphery, suggesting that penetration of TB40/E capsids may also be delayed by the absence of vimentin.

2.4   Discussion

During entry, all viruses interact with components of the cellular cytoskeleton to reach their appropriate intracellular sites of replication (71). The role of microfilaments and microtubules in mediating transport of viral particles has been well established for several viruses, including other herpesviruses (31, 55, 71). Although vimentin IF lack polarity and do not directly participate in intracellular cargo movements, they are dynamically integrated with microfilaments and microtubules and are important for infection with a variety of viruses. Expression of vimentin at the cell surface allows for binding and internalization of porcine reproductive and respiratory syndrome virus (44) while its association with capsid components of the human immunodeficiency virus type 1 (88), Theiler's murine encephalomyelitis virus (62), and adenovirus type 2 (5) assists with virus entry. Vimentin was shown to promote assembly of African swine fever virus, frog

virus 3, and vaccinia virus by forming protective cage-like structures around the sites of virion production (61, 72, 85), to enhance egress of bluetongue virus particles via interactions with the outer capsid protein VP2 (18), and to be required for Junin virus replication at a stage subsequent to entry but preceding viral protein synthesis (7). A specific role for vimentin in entry of herpesviruses has not been described. Here, we show that vimentin IF are likely to play a role during entry of two CMV strains with different tropisms and that their degree of dependency on an intact vimentin cytoskeleton correlates with the extent of tropism, possibly as a result of different entry mechanisms. Like all herpesviruses, CMV replicates in the nucleus and requires virions to be actively transferred from the cell membrane to the nuclear envelope at the start of infection. Entry can occur by direct penetration across the plasma membrane or by macropinocytosis, depending on the cell type and the virus strain (16, 79, 83). Both mechanisms require fusion of the virus envelope with cellular lipid bilayers, and the subsequent transport of capsids along cellular microtubules, whose structural integrity is maintained during entry. Consistent with data from Arcangeletti et al. (4), our results show that the vimentin cytoskeleton is not disassembled during the initial steps of CMV infection, suggesting that maintenance of an intact IF network may be necessary for entry. Vimentin disruption and reorganization are induced early during infection with a variety of viruses including reovirus (77), respiratory syncytial virus (27), frog virus 3 (60), Thelier's murine encephalomyelitis virus (62), vaccinia virus (24), and adenovirus types 2, 5, 4, and 9 (6). By contrast, IF connections are preserved in cells infected with herpes simplex virus type 1 (HSV-1) (63), equine herpes virus type 1 (91) and adenovirus types 3, 7, and 12, whose particles are predominantly found within phagosomes (6), indicating that the requirement

FIG. 2-7. Detection of virus particles in vim$^+$ and vim$^-$ MEF. (A to D) Confocal immunofluorescence images of AD169-infected MEF stained for pp150 at 1 and 8 hpi. The pp150 signal is depicted in red while the green signal emanates from cellular autofluorescence. (E) Percentage of AD169- and TB40/E-infected vim$^+$ and vim$^-$ MEF containing pp150-positive particles immediately after adsorption (black bars) and at three different times postpenetration (dark gray, light gray, and white bars; times are indicated at the top of the panel). A minimum of 110 cells were counted for each sample. Mean and standard deviation values from separate cell fields in one representative experiment (out of three) are shown. (F) Proportion of pp150-positive particles localizing at the cell surface, in the cytoplasm, or at the nucleus in vim$^+$ and vim$^-$ MEF infected with AD169 or TB40/E at 1 h postpenetration. Mean and standard deviation of values from eight different cells per sample are shown. AD, AD169; TB, TB40/E.
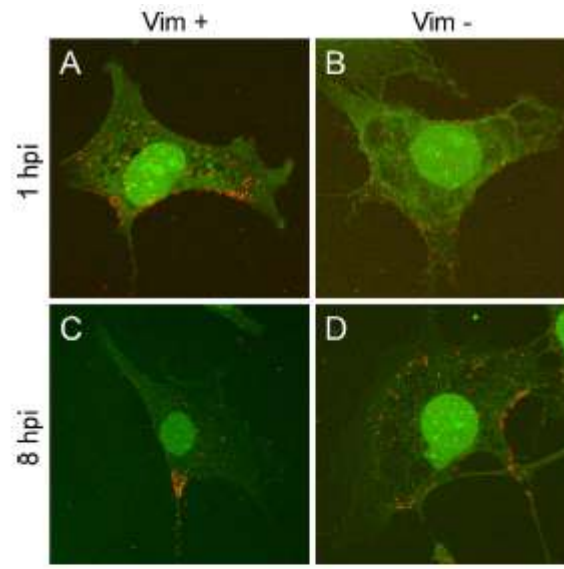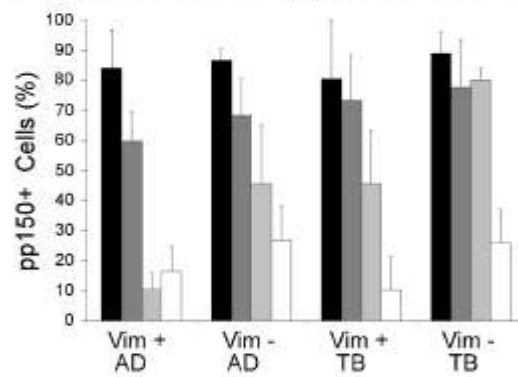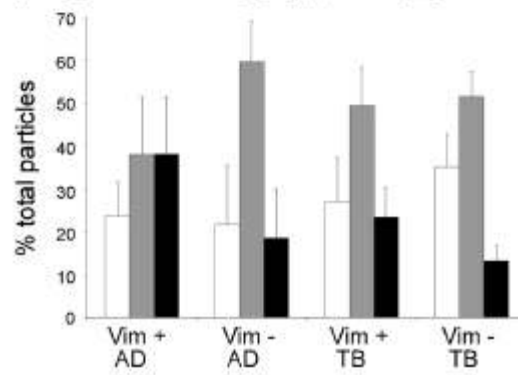
for an intact IF cytoskeleton may be shared among different herpesviruses and may be relevant for entry via intracellular vesicles.

In contrast to IF, microfilament disassembly was evident by 2 hpi with AD169 and by 4 hpi with TB40/E. Binding of some herpesviruses to the cell surface triggers rapid reorganization of the actin cytoskeleton (55), and actin depolymerization close to viral particles was observed upon fusion of the Towne envelope with the plasma membrane (42). Microfilament disassembly appeared to be beneficial for the onset of Towne and AD169 infection (4, 42) as it likely facilitated virion transit across the actin-rich cell cortex. By contrast, treatment with actin depolymerizing drugs inhibited uptake of HSV-1 particles in cells where entry by phagocytosis dominated over fusion at the plasma membrane (14), pointing at a possible requirement for intact microfilaments to support myosin VI-mediated transport of endocytic vesicles toward the cell center (9). Thus, the difference we observed between AD169 and TB40/E in the timing of microfilament depolymerization may potentially reflect two different mechanisms of entry of each strain into HF, with fusion at the plasma membrane followed by immediate actin disassembly being predominant for AD169 and endocytosis accompanied by delayed microfilament reorganization being more common for TB40/E. AD169 virions contain the gH/gL/gO complex, which mediates entry by fusion with the plasma membrane, but lack the gH/gL/UL128-131A complex, which is required for entry by endocytosis (73, 74). By contrast, TB40/E virions contain both gH/gL/gO and gH/gL/UL128-131A complexes endowing TB40/E virions with the potential to enter HF either by fusion at the cell surface, by endocytosis, or by a combination of both mechanisms.

Onset of TB40/E infection was delayed by approximately 2 h relative to infection with AD169, and this resulted in a similar delay throughout the time course of infection, with the proportion of IE1/IE2-positive cells in TB40/E-infected monolayers remaining lower than that in AD169- infected cells at each time and irrespective of the MOI used (Fig. 2-2A and B). These differences are likely to be due to slower and less efficient transport of TB40/E particles, especially if TB40/E entry mechanisms require the generation and intracellular movement of vesicles. Fusion of AD169 virions at the plasma membrane may allow capsids to associate with microtubules in a rapid and efficient manner while escape of TB40/E capsids from endosomes may require longer times. Although the intracellular content of AD169 and TB40/E DNA in HF was reported to be

similar at 1.5 hpi (81), HF internalization of radiolabeled AD169 particles was found to be more efficient than that of the clinical strain TR (73). The delay in TB40/E infection onset was also reflected by the lower levels of cell-free virus produced by infected cells at 72, 96, and 120 hpi although by 144 and 168 hpi AD169 and TB40/E yields had equalized (Fig. 2-2C). To our knowledge, this is the first report directly comparing growth of AD169 and TB40/E in HF. A 10-fold reduction in cell-free virus yields relative to AD169 has been described for another clinical strain, VR1814 (1), while repair or complementation of the UL131A gene mutation in AD169 reduced virus production in HF (1, 92). It is thus conceivable that expression of UL131A might be detrimental for efficient TB40/E production in HF, and additional functions encoded by genes mutated during the process of AD169 adaptation to growth in HF may also contribute to the phenotype we observed.

Previous studies have shown that drug-mediated disassembly of microtubules inhibits onset of infection by CMV (64), HSV-1 (63), and other viruses (31, 57, 71). Microtubules and IF are closely connected; hence, chemical disruption of microtubule networks also invariably leads to changes in the organization of IF, complicating the separation of each system's contribution. To dissect the role of vimentin IF during CMV entry, we determined the efficiency of onset of AD169 and TB40/E infection in fibroblasts with disrupted or absent IF.

ACR has been widely used to selectively and reversibly disrupt vimentin IF without altering microtubule structures (2, 65, 75) and has been employed in studies addressing the role of IF in Junin, bluetongue, and dengue virus replication (7, 13, 18). Treatment of HF with ACR prior to infection with AD169 or TB40/E resulted in an exposure time-dependent decrease in the percentage of infected cells (Fig. 2-4A and B), suggesting that the integrity of vimentin IF is required for CMV entry. Changes in cell and nuclear morphology and ACR-induced inhibition of protein synthesis may also have contributed to reduce infection rates while the concomitant disassembly of actin stress fibers may have affected the onset of TB40/E, but not of AD169 infection, as microfilament disassembly facilitates entry of AD169 virions (4). By contrast, cell death was not considered to be a significant factor as the percentage of cells with apoptotic nuclei remained consistently low (Fig. 2-3H and J), and removal of ACR allowed for resumption of infection (Fig. 2-4C and D). Intriguingly, infection recovery after ACR removal suggests that viral particles are still capable of entering cells with disrupted

vimentin IF. Perhaps in the absence of an extended vimentin cytoskeleton, virions remain trapped in the cytoplasm or become unable to deposit the viral genome in nuclei with membrane invaginations. Restoration of a proper IF cytoskeleton accompanied by the disappearance of nuclear folding may then allow for viral particle trafficking and nuclear genome deposition to resume.

To establish the role of vimentin IF during CMV infection in a setting that did not involve exposure to pharmacological agents, IF bundling was induced in fibroblasts from GAN patients by serum starvation. The phenotype of IF in GAN HF cultures was less uniform than that in ACR-treated cultures, with some cells showing more prominent bundling than others and with bundles localizing in distinct areas of each cell, leaving the rest of the IF network fairly intact (Fig. 2-5F). Inhibition of AD169 infection in this system appeared to be temporary and MOI dependent, which suggests that particles could circumvent the obstacle represented by accumulated IF when given enough time or when present in large amounts. By contrast, TB40/E infection was severely impacted, and the percentage of infected cells did not substantially increase with time or at higher MOIs. These results point again at possible differences in AD169 and TB40/E entry mechanisms. As retrograde transport of endocytic vesicles is severely impaired in neurons from GAN-null mice (19), it is tempting to speculate that transport of CMV particles toward the nucleus may be preferentially delayed in GAN HF if capsids are contained within endosomes rather than free in the cytoplasm following penetration at the cell surface. A block in the endocytic route of infection is also less likely to be overcome

by raising the MOI as the speed and direction of vesicle movements would still remain the limiting factors even in the presence of numerous particles.

Both AD169 and TB40/E were able to infect MEF cells (Fig. 2-6), but as was observed with HF cultures, the efficiency of onset of TB40/E infection in MEF was lower than that of AD169, pointing at a possible conservation of entry mechanisms between human and mouse HF. While the proportion of AD169- infected vim$^+$ MEF remained stable from 4 to 24 hpi, an increase in the percentage of TB40/E-infected cells was observed at 24 hpi at both MOIs. Intriguingly, the number of vim$^+$ MEF containing AD169 particles decreased very rapidly after penetration and remained stable at later times while the reduction in the number of TB40/E-positive cells occurred much more gradually (Fig. 2-7). Combined, these results suggest that entry of AD169 is more rapid and efficient than that of TB40/E, with prompt capsid trafficking and nuclear genome translocation occurring in the majority of AD169-infected cells. By contrast, cytoplasmic movement of TB40/E virions is lengthier, and, perhaps as a result of this delay, the percentage of cells expressing IE1/IE2 increases only at later times in infection. Initiation of infection with both strains in vim$^-$ MEF is dramatically hampered, particularly at low MOIs, demonstrating that this protein is required for infection. Intriguingly, although the absence of vimentin seemed to only reduce the speed of AD169 particle translocation, it effectively blocked progression of TB40/E virions. Consequently, the proportion of AD169-infected vim$^-$ cells still increased over time while TB40/E infection became abortive, perhaps as a result of virion degradation in the cytoplasm. Viral DNA was

indeed reported to be eliminated from the cytoplasm of endothelial cells as a consequence of failures in particle transport toward the nucleus and in nuclear genome deposition (82).

In summary, the efficiency of onset of CMV infection depends on the presence and integrity of the vimentin cytoskeleton, which may facilitate virus entry at different steps. As the proportions of vim$^+$ and vim$^-$ pp150-positive cells were similar, a role for vimentin as a CMV receptor at the cell surface is unlikely (Fig. 2-8, step a). Likewise, participation of IF in uncoating of clathrin from endocytic vesicles (86) is not expected to impact CMV entry (Fig. 2-8, step b), as clathrin-coated endosomes are too small to accommodate CMV virions (79). By contrast, vimentin could promote capsid binding to microtubules after entry at the plasma membrane (Fig. 2-8, step c), enhance internalization of endocytic vesicles carrying virions bound to integrins (Fig. 2-8, step d), or allow for rapid AP-3-mediated acidification of endosomes and concomitant intracytoplasmic release of endocytosed virions (Fig. 2-8, step e). Finally, vimentin interactions with the nuclear lamina (10) and with cellular DNA (89, 90) may increase the speed of viral genome translocation across the nuclear envelope and of IE gene transcription (Fig. 2-8, step f). Additional work will be needed to pinpoint the exact steps during viral entry that require vimentin assistance. Based on the differences we observed between AD169 and TB40/E, these will likely depend on the mechanisms of virus entry and will require the engagement of different virion components encoded by each strain.
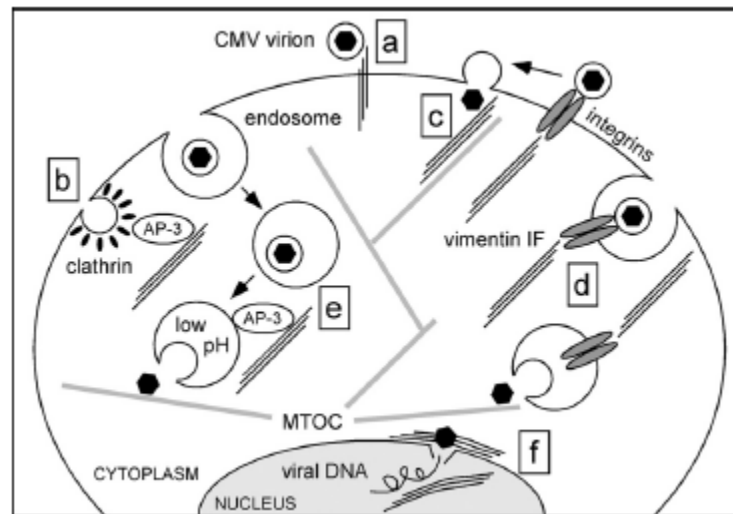
FIG. 2-8. Hypothetical steps during CMV entry requiring vimentin assistance for efficient completion. Vimentin IF and microtubules are shown as three parallel thin lines and as thick gray lines, respectively. Black hexagons enclosed in a circle depict enveloped virions while isolated black hexagons represent virus capsids. Steps are as follows: (a) vimentin IF acting as receptors for CMV virions at the surface, (b) AP-3-mediated involvement of vimentin IF in internalization of clathrin-coated endosomes, (c) enhancement of capsid attachment and movement along microtubules via vimentin IF, (d) internalization of integrin-bound virions under the control of vimentin IF, (e) AP-3-mediated involvement of vimentin IF in endosome acidification and cytoplasmic release of capsids, and (f) facilitation of nuclear genome deposition and of gene transcription onset by nuclear lamina- and matrix-associated vimentin. MTOC, microtubule organizing center.

2.5   References

1. **Adler, B., L. Scrivano, Z. Ruzcics, B. Rupp, C. Sinzger, and U. Koszinowski.** 2006. Role of human cytomegalovirus UL131A in cell type-specific virus entry and release. J. Gen. Virol. **87:**2451–2460.

2. **Aggeler, J., and K. Seely.** 1990. Cytoskeletal dynamics in rabbit synovial fibroblasts. I. Effects of acrylamide on intermediate filaments and microfilaments. Cell Motil. Cytoskeleton **16:**110–120.

3. **Akter, P., C. Cunningham, B. P. McSharry, A. Dolan, C. Addison, D. J. Dargan, A. F. Hassan-Walker, V. C. Emery, P. D. Griffiths, G. W. Wilkinson, and A. J. Davison.** 2003. Two novel spliced genes in human cytomegalovirus. J. Gen. Virol. **84:**1117–1122.

4. **Arcangeletti, M. C., F. Pinardi, M. C. Medici, E. Pilotti, F. De Conto, F. Ferraglia, M. P. Landini, C. Chezzi, and G. Dettori.** 2000. Cytoskeleton involvement during human cytomegalovirus replicative cycle in human embryo fibroblasts. New Microbiol. **23:**241–256.

5. **Belin, M. T., and P. Boulanger.** 1985. Cytoskeletal proteins associated with intracytoplasmic human adenovirus at an early stage of infection. Exp. Cell Res. **160:**356–370.

6. **Belin, M. T., and P. Boulanger.** 1987. Processing of vimentin occurs during the early stages of adenovirus infection. J. Virol. **61:**2559–2566.

7. **Bhattacharya, B., R. J. Noad, and P. Roy.** 2007. Interaction between Bluetongue virus outer capsid protein VP2 and vimentin is necessary for virus egress. Virol. J. **4:**7.

8. **Britt, W.** 2008. Manifestations of human cytomegalovirus infection: proposed mechanisms of acute and chronic disease. Curr. Top. Microbiol. Immunol. **325:**417–470.

9. **Buss, F., G. Spudich, and J. Kendrick-Jones.** 2004. Myosin VI: cellular functions and motor properties. Annu. Rev. Cell Dev. Biol. **20:**649–676.

10. **Capco, D. G., K. M. Wan, and S. Penman.** 1982. The nuclear matrix: three-dimensional architecture and protein composition. Cell **29:**847–858.

11. **Cha, T. A., E. Tom, G. W. Kemble, G. M. Duke, E. S. Mocarski, and R. R. Spaete.** 1996. Human cytomegalovirus clinical isolates carry at least 19 genes not found in laboratory strains. J. Virol. **70:**78–83.

12. **Chang, L., and R. D. Goldman.** 2004. Intermediate filaments mediate cytoskeletal crosstalk. Nat. Rev. Mol. Cell Biol. **5:**601–613.

13. **Chen, W., N. Gao, J. L. Wang, Y. P. Tian, Z. T. Chen, and J. An.** 2008. Vimentin is required for dengue virus serotype 2 infection but microtubules are not necessary for this process. Arch. Virol. **153:**1777–1781.

14. **Clement, C., V. Tiwari, P. M. Scanlan, T. Valyi-Nagy, B. Y. Yue, and D. Shukla.** 2006. A novel role for phagocytosis-like uptake in herpes simplex virus entry. J. Cell Biol. **174:**1009–1021.

15. **Colucci-Guyon, E., M. M. Portier, I. Dunia, D. Paulin, S. Pournin, and C. Babinet.** 1994. Mice lacking vimentin develop and reproduce without an obvious phenotype. Cell **79:**679–694.

16. **Compton, T., R. R. Nepomuceno, and D. M. Nowlin.** 1992. Human cytomegalovirus penetrates host cells by pH-independent fusion at the cell surface. Virology **191:**387–395.

17. **Compton, T., D. M. Nowlin, and N. R. Cooper.** 1993. Initiation of human cytomegalovirus infection requires initial interaction with cell surface heparin sulfate. Virology **193:**834–841.

18. **Cordo, S. M., and N. A. Candurra.** 2003. Intermediate filament integrity is required for Junin virus replication. Virus Res. **97:**47–55.

19. **Ding, J., E. Allen, W. Wang, A. Valle, C. Wu, T. Nardine, B. Cui, J. Yi, A. Taylor, N. L. Jeon, S. Chu, Y. So, H. Vogel, R. Tolwani, W. Mobley, and Y. Yang.** 2006. Gene targeting of GAN in mouse causes a toxic accumulation of microtubule-associated protein 8 and impaired retrograde axonal transport. Hum. Mol. Genet. **15:**1451–1463.

20. **Durham, H. D., S. D. Pena, and S. Carpenter.** 1983. The neurotoxins 2,5-hexanedione and acrylamide promote aggregation of intermediate filaments in cultured fibroblasts. Muscle Nerve **6:**631–637.

21. **Eckert, B. S.** 1985. Alteration of intermediate filament distribution in PtK1 cells by acrylamide. Eur. J. Cell Biol. **37:**169–174.

22. **Elek, S. D., and H. Stern.** 1974. Development of a vaccine against mental retardation caused by cytomegalovirus infection in utero. Lancet **1:**1–5.

23. **Feire, A. L., H. Koss, and T. Compton.** 2004. Cellular integrins function as entry receptors for human cytomegalovirus via a highly conserved disintegrin-like domain. Proc. Natl. Acad. Sci. USA **101:**15470–15475.

24. **Ferreira, L. R., N. Moussatche, and V. Moura Neto.** 1994. Rearrangement of intermediate filament network of BHK-21 cells infected with vaccinia virus. Arch. Virol. **138:**273–285.

25. **Franke, W. W., E. Schmid, M. Osborn, and K. Weber.** 1978. Different intermediate-sized filaments distinguished by immunofluorescence microscopy. Proc. Natl. Acad. Sci. USA **75:**5034–5038.

26. **Gao, Y., and E. Sztul.** 2001. A novel interaction of the Golgi complex with the vimentin intermediate filament cytoskeleton. J. Cell Biol. **152:**877–894.

27. **Garcia-Barreno, B., J. L. Jorcano, T. Aukenbauer, C. Lopez-Galindez, and J. A. Melero.** 1988. Participation of cytoskeletal intermediate filaments in the infectious cycle of human respiratory syncytial virus (RSV). Virus Res. **9:**307–321.

28. **Gawlitta, W., M. Osborn, and K. Weber.** 1981. Coiling of intermediate filaments induced by microinjection of a vimentin-specific antibody does not interfere with locomotion and mitosis. Eur. J. Cell Biol. **26:**83–90.

29. **Gillard, B. K., R. Clement, E. Colucci-Guyon, C. Babinet, G. Schwarzmann, T. Taki, T. Kasama, and D. M. Marcus.** 1998. Decreased synthesis of glycosphingolipids in cells lacking vimentin intermediate filaments. Exp. Cell Res. **242:**561–572.

30. **Goldman, R. D.** 1971. The role of three cytoplasmic fibers in BHK-21 cell motility. I. Microtubules and the effects of colchicine. J. Cell Biol. **51:**752–762.

31. **Greber, U. F., and M. Way.** 2006. A superhighway to virus infection. Cell **124:**741–754.

32. **Hahn, G., M. G. Revello, M. Patrone, E. Percivalle, G. Campanini, A. Sarasini, M. Wagner, A. Gallina, G. Milanesi, U. Koszinowski, F. Baldanti, and G. Gerna.** 2004. Human cytomegalovirus UL131-128 genes are indispensable for virus growth in endothelial cells and virus transfer to leukocytes. J. Virol. **78:**10023–10033.

33. **Hay, M., and U. De Boni.** 1991. Chromatin motion in neuronal interphase nuclei: changes induced by disruption of intermediate filaments. Cell Motil. Cytoskeleton. **18:**63–75.

34. **Herman, B., and D. F. Albertini.** 1982. The intracellular movement of endocytic vesicles in cultured granulosa cells. Cell Motil. **2:**583–597.

35. **Hertel, L., V. G. Lacaille, H. Strobl, E. D. Mellins, and E. S. Mocarski.** 2003. Susceptibility of immature and mature Langerhans cell-type dendritic cells to infection and immunomodulation by human cytomegalovirus. J. Virol. **77:** 7563–7574.

36. **Hertel, L., and E. S. Mocarski.** 2004. Global analysis of host cell gene expression late during cytomegalovirus infection reveals extensive dysregulation of cell cycle gene expression and induction of pseudomitosis independent of US28 function. J. Virol. **78:**11988–12011.

37. **Hobom, U., W. Brune, M. Messerle, G. Hahn, and U. H. Koszinowski.** 2000. Fast screening procedures for random transposon libraries of cloned herpesvirus genomes: mutational analysis of human cytomegalovirus envelope glycoprotein genes. J. Virol. **74:**7720–7729.

38. **Isaacson, M. K., A. L. Feire, and T. Compton.** 2007. Epidermal growth factor receptor is not required for human cytomegalovirus entry or signaling. J. Virol. **81:**6241–6247.

39. **Isaacson, M. K., L. K. Juckem, and T. Compton.** 2008. Virus entry and innate immune activation. Curr. Top. Microbiol. Immunol. **325:**85–100.

40. **Ivaska, J., H. M. Pallari, J. Nevo, and J. E. Eriksson.** 2007. Novel functions of vimentin in cell adhesion, migration, and signaling. Exp. Cell Res. **313:** 2050–2062.

41. **Ivaska, J., K. Vuoriluoto, T. Huovinen, I. Izawa, M. Inagaki, and P. J. Parker.** 2005. PKε-mediated phosphorylation of vimentin controls integrin recycling and motility. EMBO J. **24:**3834–3845.

42. **Jones, N. L., J. C. Lewis, and B. A. Kilpatrick.** 1986. Cytoskeletal disruption during human cytomegalovirus infection of human lung fibroblasts. Eur. J. Cell Biol. **41:**304–312.

43. **Kamei, H.** 1994. Relationship of nuclear invaginations to perinuclear rings composed of intermediate filaments in MIA PaCa-2 and some other cells. Cell Struct. Funct. **19:**123–132.

44. **Kim, J. K., A. M. Fahad, K. Shanmukhappa, and S. Kapil.** 2006. Defining the cellular target(s) of porcine reproductive and respiratory syndrome virus blocking monoclonal antibody 7G10. J. Virol. **80:**689–696.

45. **Kinzler, E. R., R. N. Theiler, and T. Compton.** 2002. Expression and reconstitution of the gH/gL/gO complex of human cytomegalovirus. J. Clin. Virol. **25**(Suppl. 2)**:**S87–S95.

46. **Klymkowsky, M. W.** 1981. Intermediate filaments in 3T3 cells collapse after intracellular injection of a monoclonal anti-intermediate filament antibody. Nature **291:**249–251.

47. **Klymkowsky, M. W.** 1988. Metabolic inhibitors and intermediate filament organization in human fibroblasts. Exp. Cell Res. **174:**282–290.

48. **Klymkowsky, M. W., and D. J. Plummer.** 1985. Giant axonal neuropathy: a conditional mutation affecting cytoskeletal organization. J. Cell Biol. **100:** 245–250.

49. **LaFemina, R. L., and G. S. Hayward.** 1988. Differences in cell-type-specific blocks to immediate early gene expression and DNA replication of human, simian and murine cytomegalovirus. J. Gen. Virol. **69:**355–374.

50. **LaFemina, R. L., and G. S. Hayward.** 1983. Replicative forms of human cytomegalovirus DNA with joined termini are found in permissively infected human cells but not in non- permissive Balb/c-3T3 mouse cells. J. Gen. Virol. **64:**373–389.

51. **Leung, C. L., Y. Pang, C. Shu, D. Goryunov, and R. K. Liem.** 2007. Alterations in lipid metabolism gene expression and abnormal lipid accumulation in fibroblast explants from giant axonal neuropathy patients. BMC Genet. **8:**6.

52. **Lieber, J. G., and R. M. Evans.** 1996. Disruption of the vimentin intermediate filament system during adipose conversion of 3T3-L1 cells inhibits lipid droplet accumulation. J. Cell Sci. **109:**3047–3058.

53. **Lin, J. J., and J. R. Feramisco.** 1981. Disruption of the in vivo distribution of the intermediate filaments in fibroblasts through the microinjection of a specific monoclonal antibody. Cell **24:**185–193.

54. **Losse, D., R. Lauer, D. Weder, and K. Radsak.** 1982. Actin distribution and synthesis in human fibroblasts infected by cytomegalovirus. Arch. Virol. **71:**353–359.

55. **Lyman, M. G., and L. W. Enquist.** 2009. Herpesvirus interactions with the host cytoskeleton. J. Virol. **83:**2058–2066.

56. **Maniotis, A. J., C. S. Chen, and D. E. Ingber.** 1997. Demonstration of mechanical connections between integrins, cytoskeletal filaments, and nucleoplasm that stabilize nuclear structure. Proc. Natl. Acad. Sci. USA **94:**849–854.

57. **Marsh, M., and A. Helenius.** 2006. Virus entry: open sesame. Cell **124:**729–740.

58. **Mocarski, E. S., T. Shenk, and R. F. Pass.** 2007. Cytomegaloviruses, p.2701–2772. *In* D. M. Knipe, P. M. Howley, D. E. Griffin, R. A. Lamb, M. A. Martin, B. Roizman, and S. E. Straus (ed.), Fields virology, 5th ed. Lippincott Williams & Wilkins, Philadelphia, PA.

59. **Murphy, E., and T. Shenk.** 2008. Human cytomegalovirus genome. Curr. Top. Microbiol. Immunol. **325:**1–19.

60. **Murti, K. G., and R. Goorha.** 1983. Interaction of frog virus-3 with the cytoskeleton. I. Altered organization of microtubules, intermediate filaments, and microfilaments. J. Cell Biol. **96:**1248–1257.

61. **Murti, K. G., R. Goorha, and M. W. Klymkowsky.** 1988. A functional role for intermediate filaments in the formation of frog virus 3 assembly sites. Virology **162:**264–269.

62. **Nedellec, P., P. Vicart, C. Laurent-Winter, C. Martinat, M. C. Prevost, and M. Brahic.** 1998. Interaction of Theiler's virus with intermediate filaments of infected cells. J. Virol. **72:**9553–9560.

63. **Norrild, B., V. P. Lehto, and I. Virtanen.** 1986. Organization of cytoskeleton elements during herpes simplex virus type 1 infection of human fibroblasts: an immunofluorescence study. J. Gen. Virol. **67:**97–105.

64. **Ogawa-Goto, K., K. Tanaka, W. Gibson, E. Moriishi, Y. Miura, T. Kurata, S. Irie, and T. Sata.** 2003. Microtubule network facilitates nuclear targeting of human cytomegalovirus capsid. J. Virol. **77:**8541–8547.

65. **Olink-Coux, M., M. Huesca, and K. Scherrer.** 1992. Specific types of prosomes are associated to subnetworks of the intermediate filaments in PtK1 cells. Eur. J. Cell Biol. **59:**148–159.

66. **Patrone, M., M. Secchi, E. Bonaparte, G. Milanesi, and A. Gallina.** 2007. Cytomegalovirus UL131-128 products promote gB conformational transition and gB-gH interaction during entry into endothelial cells. J. Virol. **81:**11479–11488.

67. **Pena, S. D.** 1981. Giant axonal neuropathy: intermediate filament aggregates in cultured skin fibroblasts. Neurology **31:**1470–1473.

68. **Plotkin, S. A., T. Furukawa, N. Zygraich, and C. Huygelen.** 1975. Candidate cytomegalovirus strain for human vaccination. Infect. Immun. **12:**521–527.

69. **Potokar, M., M. Kreft, L. Li, J. Daniel Andersson, T. Pangrsic, H. H. Chowdhury, M. Pekny, and R. Zorec.** 2007. Cytoskeleton and vesicle mobility in astrocytes. Traffic **8:**12–20.

70. **Prahlad, V., M. Yoon, R. D. Moir, R. D. Vale, and R. D. Goldman.** 1998. Rapid movements of vimentin on microtubule tracks: kinesin-dependent assembly of intermediate filament networks. J. Cell Biol. **143:**159–170.

71. **Radtke, K., K. Dohner, and B. Sodeik.** 2006. Viral interactions with the cytoskeleton: a hitchhiker's guide to the cell. Cell Microbiol. **8:**387–400.

72. **Risco, C., J. R. Rodriguez, C. Lopez-Iglesias, J. L. Carrascosa, M. Esteban, and D. Rodriguez.** 2002. Endoplasmic reticulum-Golgi intermediate compartment membranes and vimentin filaments participate in vaccinia virus assembly. J. Virol. **76:**1839–1855.

73. **Ryckman, B. J., M. A. Jarvis, D. D. Drummond, J. A. Nelson, and D. C. Johnson.** 2006. Human cytomegalovirus entry into epithelial and endothelial cells depends on genes UL128 to UL150 and occurs by endocytosis and low-pH fusion. J. Virol. **80:**710–722.

74. **Ryckman, B. J., B. L. Rainish, M. C. Chase, J. A. Borton, J. A. Nelson, M. A. Jarvis, and D. C. Johnson.** 2008. Characterization of the human cytomegalovirus gH/gL/UL128-131 complex that mediates entry into epithelial and endothelial cells. J. Virol. **82:**60–70.

75. **Sager, P. R.** 1989. Cytoskeletal effects of acrylamide and 2,5-hexanedione: selective aggregation of vimentin filaments. Toxicol. Appl. Pharmacol. **97:**141–155.

76. **Sarria, A. J., J. G. Lieber, S. K. Nordeen, and R. M. Evans.** 1994. The presence or absence of a vimentin-type intermediate filament network affects the shape of the nucleus in human SW-13 cells. J. Cell Sci. **107:**1593–1607.

77. **Sharpe, A. H., L. B. Chen, and B. N. Fields.** 1982. The interaction of mammalian reoviruses with the cytoskeleton of monkey kidney CV-1 cells. Virology **120:**399–411.

78. **Shoeman, R. L., C. Huttermann, R. Hartig, and P. Traub.** 2001. Aminoterminal polypeptides of vimentin are responsible for the changes in nuclear architecture associated with human immunodeficiency virus type 1 protease activity in tissue culture cells. Mol. Biol. Cell **12:**143–154.

79. **Sinzger, C.** 2008. Entry route of HCMV into endothelial cells. J. Clin. Virol. **41:**174–179.

80. **Sinzger, C., M. Digel, and G. Jahn.** 2008. Cytomegalovirus cell tropism. Curr. Top. Microbiol. Immunol. **325:**63–83.

81. **Sinzger, C., M. Kahl, K. Laib, K. Klingel, P. Rieger, B. Plachter, and G. Jahn.** 2000. Tropism of human cytomegalovirus for endothelial cells is determined by a post-entry step dependent on efficient translocation to the nucleus. J. Gen. Virol. **81:**3021–3035.

82. **Slobbe-van Drunen, M. E., A. T. Hendrickx, R. C. Vossen, E. J. Speel, M. C. van Dam-Mieras, and C. A. Bruggeman.** 1998. Nuclear import as a barrier to infection of human umbilical vein endothelial cells by human cytomegalovirus strain AD169. Virus Res. **56:**149–156.

83. **Smith, J. D., and E. de Harven.** 1974. Herpes simplex virus and human cytomegalovirus replication in WI-38 cells. II. An ultrastructural study of viral penetration. J. Virol. **14:**945–956.

84. **Soroceanu, L., A. Akhavan, and C. S. Cobbs.** 2008. Platelet-derived growth factor-alpha receptor activation is required for human cytomegalovirus infection. Nature **455:**391–395.

85. **Stefanovic, S., M. Windsor, K. I. Nagata, M. Inagaki, and T. Wileman.** 2005. Vimentin rearrangement during African swine fever virus infection involves retrograde transport along microtubules and phosphorylation of vimentin by calcium calmodulin kinase II. J. Virol. **79:**11766–11775.

86. **Styers, M. L., A. P. Kowalczyk, and V. Faundez.** 2005. Intermediate filaments and vesicular membrane traffic: the odd couple's first dance? Traffic **6:**359–365.

87. **Styers, M. L., G. Salazar, R. Love, A. A. Peden, A. P. Kowalczyk, and V. Faundez.** 2004. The endo-lysosomal sorting machinery interacts with the intermediate filament cytoskeleton. Mol. Biol. Cell **15:**5369–5382.

88. **Thomas, E. K., R. J. Connelly, S. Pennathur, L. Dubrovsky, O. K. Haffar, and M. I. Bukrinsky.** 1996. Anti-idiotypic antibody to the V3 domain of gp120 binds to vimentin: a possible role of intermediate filaments in the early steps of HIV-1 infection cycle.Viral Immunol. **9:**73–87.

89. **Tolstonog, G. V., E. Mothes, R. L. Shoeman, and P. Traub.** 2001. Isolation of SDS-stable complexes of the intermediate filament protein vimentin with repetitive, mobile, nuclear matrix attachment region, and mitochondrial DNA sequence elements from cultured mouse and human fibroblasts. DNA Cell Biol. **20:**531–554.

90. **Traub, P.** 1995. Intermediate filaments and gene regulation. Physiol. Chem. Phys Med. NMR **27:**377–400.

91. **Walter, I., and N. Nowotny.** 1999. Equine herpes virus type 1 (EHV-1) infection induces alterations in the cytoskeleton of Vero cells but not apoptosis. Arch. Virol. **144:**1827–1836.

92. **Wang, D., and T. Shenk.** 2005. Human cytomegalovirus UL131 open reading frame is required for epithelial cell tropism. J. Virol. **79:**10330–10338.

93. **Wang, D., and T. Shenk.** 2005. Human cytomegalovirus virion protein complex required for epithelial and endothelial cell tropism. Proc. Natl. Acad. Sci. USA **102:**18153–18158.

94. **Wang, X., D. Y. Huang, S. M. Huong, and E. S. Huang.** 2005. Integrin αvβ3 is a coreceptor for human cytomegalovirus. Nat. Med. **11:**515–521.

95. **Wang, X., S. M. Huong, M. L. Chiu, N. Raab-Traub, and E. S. Huang.** 2003. Epidermal growth factor receptor is a cellular receptor for human cytomegalovirus. Nature **424:**456–461.

96. **Yang, Y., E. Allen, J. Ding, and W. Wang.** 2007. Giant axonal neuropathy. Cell Mol. Life Sci. **64:**601–609.

Chapter 3

CHARACTERIZATION OF THE 55 RESIDUE E1A PROTEIN ENCODED BY SPECIES C HUMAN ADENOVIRUS

3.1 Introduction

HAdV belong to the family *Adenoviridae*. These viruses have been isolated from vertebrates ranging from fish to humans. The first human adenoviruses were isolated in 1953 by independent groups searching for etiological agents responsible for acute respiratory infections (19, 48). However, it was not until 1962, when Trentin and colleagues discovered that HAdV-12 could cause tumors when injected into newborn hamsters, that interest in the field exploded (56). This was the first demonstration of a human virus that could cause cancer. Subsequent to that seminal observation, HAdV has been used extensively to study fundamental biological processes ranging from regulation of the cell cycle to mRNA splicing.

Later studies would reveal that genes encoded at the leftmost end of the HAdV genome were responsible for its oncogenic capacity. E1A of HAdV type 2/5 encodes 5 proteins of 289, 243, 217, 171 and 55 R (Fig. 3-1A). These proteins are generated by differential splicing of a single mRNA species. At the earliest stages of infection, E1A transcription is controlled by a constitutive enhancer and expression of the largest two isoforms dominates, with the smaller three isoforms accumulating later (42, 55). While the largest two proteins have been studied extensively, no specific functions have been assigned to the smallest three isoforms. The 289R and 243R E1A products are extensively phosphorylated and these modifications are important for regulation of E1A function (11,

29, 62). E1A is sufficient to immortalize primary rodent cells when expressed alone (20), and can transform these cells in cooperation with a second oncogene, such as E1B (14) or activated *Ras* (49). During infection, the major functions of E1A include inducing the host cell to enter S-phase and activating the transcription of downstream viral genes (4). These functions of E1A are essential for efficient replication of HAdV (23, 52).

E1A does not exhibit DNA binding activity, and its ability to activate transcription is mediated by its interaction with variety of cellular transcription factors and regulatory proteins (39). 289R E1A activates transcription from early viral promoters as well as wild-type, although 243R can also perform this function to a lesser degree (33-35, 46, 67). This difference in the ability to activate expression of viral genes is largely attributed to CR3 which is present in 289R E1A, but absent in 243R E1A. By itself, CR3 functions as a potent activation domain when fused to a Gal4 DNA-binding domain (31). Its ability to activate transcription is dependent upon its association with the mediator complex via direct interaction with MED23 (1, 7, 13, 30, 60). Interactions of CR3 with other cellular proteins, including TATA box-binding protein (TBP) (27), the proteosome component S8 (45) and the acetyltransferase p300/CBP (40-41) also play an important role in CR3-mediated transcriptional activation. Transcription from the E2 early promoter represents a special case as it is induced in a specific, and indirect manner via 243R E1A-mediated activation of the E2F family of transcription factors. The 243R E1A protein binds pRb, thereby facilitating the release of E2Fs. Free E2Fs then bind to inverted sites located within the E2 promoter to activate transcription (3, 25-26, 43, 71). The major late promoter, which controls expression of the viral structural proteins, is active at a low level at early times post-infection and expression increases several hundred fold at late

times (51). Binding of E1A to Sp1 and MAZ transcription factors contributes to this activation, but does not account for the delayed kinetics of expression from this promoter (38).

Recruitment of APIS to early viral promoters by E1A enhances transcription of early viral genes (45). The HAdV-5 289R and 243R E1A proteins and the HAdV-12 266R and 235R proteins can be immunoprecipitated with proteasomes (15). Amino acids 4-25 mediate binding of E1A to members of the 19S regulatory components of the proteasome, human hSug1 (S8) and S4. Binding inhibits the ATPase activity of this subunit which correlates with decreased proteasome activity (57). S8 is also recruited by CR3 to enhance transcription of early viral genes. Interestingly, the 20S proteasome is also recruited to CR3 independently of APIS and the 26S proteasome. E1A, S8 and the 20S proteasome are found on early gene promoters and sequences during infection and thus, may be important in transcriptional initiation and elongation. In addition, inhibition of proteasome activity represses E1A-dependent transcriptional activation, further supporting the importance of this interaction during infection (45).

Despite the fact that no specific functions have been assigned to the smallest three E1A proteins, the 55R isoform constitutes a particularly interesting case. Its function has remained elusive despite the initial discovery of its mRNA species over 30 years ago (5). This may be attributed, at least in part, to the fact that no existing E1A Abs are able to recognize the 55R product. While 55R shares the first 26 amino acids encoded by exon 1 with the other E1A proteins, reconstitution of the splice junction linking exon 1 and exon 2 results in a frameshift relative to the other isoforms which results in a unique C-

terminal amino acid sequence (10, 47, 59). The 55R mRNA species accumulates preferentially at late times post-infection and seems to require replication of the viral genome, since 55R mRNA species are only detected in HAdV-infected human HEK293, and not in mock infected cells despite the integration of genomic E1A and constitutive expression of 289R and 243R E1A in this cell line (8, 53-54, 59, 66). These properties suggest that in addition to possibly binding targets which are known to interact with the extreme N-terminus of the larger E1A isoforms, 55R E1A may also interact with unique targets via its novel C-terminus region. Due to the late kinetics of 55R E1A expression, these interactions may play important roles during the latest stages of HAdV infection.

Here, we characterize an antibody which specifically recognizes the 55R E1A protein encoded by HAdV-2. This antibody can be used for detection of HAdV-2 55R E1A by western blot, indirect immunofluorescence and immunoprecipitation. We report for the first time a series of phenotypic and functional properties associated with 55R E1A. It is primarily localized to the nucleus and is sufficient to promote virus growth in growth-arrested IMR-90 fibroblasts. This may be due, in part, to the ability of 55R E1A to activate transcription of viral genes with kinetics and magnitudes that are unique in comparison to genomic E1A. Finally, we demonstrate that 55R E1A interacts with S8, a member of the APIS complex, but not with S4. This is the first reported cellular target of 55R E1A. Knockdown of S8 was detrimental to virus replication, suggesting that this interaction is functionally important during infection.

3.2 Materials and Methods

3.2.1 Cells and viruses

HEK293, HEK293T, HT1080, A549 and IMR-90 cells were originally obtained from the American type culture collection (ATCC). dl309 (expresses all E1A proteins) (23), dl312 (does not express any E1A proteins) (23), dl520 (does not express 289R E1A) (16), dl521 (expresses only 55R E1A) (16), pm975 (does not express 243R E1A) (34) and HAdV-2 have all been described previously. JM17-55R was constructed cloning the 55R E1A coding sequence into pXC-Myc+ which had been digested with EcoRI and SalI to remove the myc epitope tag. Recombinant virus was rescued by transfecting 5 µg of the new plasmid, pXC-55R HAdV-2 E1A, into HEK293 cells along with 10 µg of pJM17 using a 1:14 DNA-to-Superfect (Qiagen) ratio. Virus was then plaque purified and screened by sequencing of viral DNA. All cells were propagated in DMEM (Wisent) supplemented with 10 % heat-inactivated FBS, 100U/ml penicillin and 100 µg/ml streptomycin (all from Gibco). All viruses were grown on either HEK293 or A549 and were purified using cesium chloride gradient, as described previously (68).

3.2.2 Cell transfections and infections

To analyze the kinetics of 55R E1A mRNA and protein expression, A549 cells were infected with HAdV-2 at an MOI of 1. Samples were collected at 24, 48, 72, 96 and 120 hpi to analyze the kinetics of E1A mRNA expression. For analysis of protein expression, samples were collected at 6, 24, 48 and 72 hpi.

For virus replication assays, IMR-90 cells were seeded in 6-well dishes and were growth arrested by contact inhibition for 3 days after reaching confluency. For single-virus infections, cells were infected with either dl309, pm975, dl520, dl521 or dl312 at an MOI of 5 and were then incubated at 37° C, 5 % CO_2 for 1 h to permit adsorption. Cells were

washed 5 times with PBS and were re-incubated with fresh medium. For growth assays, supernatants were collected at 4, 48 and 120 hpi and the titre of cell-free virus was assessed by plaque assay on HEK293 cells. For analysis of viral gene expression, cells were collected at 24, 48, 72, 96, 120 and 144 hpi. Virus co-infection replication assays were performed in a similar manner, with growth arrested IMR-90 cells being infected with either pm975 + dl521, pm975 + dl312, dl520 + dl521 or dl520 + dl312 at an MOI of 5 per virus.

For transfections, HT1080 and HEK293T cells were seeded on glass coverslips at a density of 5×10^4 cells/cm^2 one day prior to transfection with Superfect (Qiagen) according to manufacturer's guidelines.

siRNA knockdown of S8 was performed in A549 seeded at 5×10^4 cells/cm^2 using siLentFect^{TM} (Bio-Rad) transfection reagent and 10 nM PMSC5 Silencer® Select siRNA (Ambion). A second set of cells were treated with siRNA Control #2 (Ambion). Following a 12 h incubation, cells were infected with either dl521 or dl312. Supernatants were collected at 24 and 96 hpi and virus yield was determined by plaque assay on HEK293 cells.

3.2.3   mRNA isolation and qRT-PCR

Total RNA was isolated using TRIzol reagent (Invitrogen) and was subjected to first strand cDNA synthesis using Superscript II reverse transcriptase (Invitrogen) and a mixture of random hexamers and oligo(dT)$_{20,}$ according to manufacturer's instructions. qRT-PCR was performed using EXPRESS SYBR GreenER qPCR supermix (Invitrogen) on a Bio-Rad iQ5 iCycler according to manufacturer's guidelines. E1B 2.2 kb, E3A, E4

orf6/7 (45), E2 (2) and hexon (24) were amplified using primers described previously. GAPDH was amplified using the forward primer CCTGGCCAAGGTCATCCATGAC and the reverse primer TGTCATACCAGGAAATGAGCTTG. Conventional RT-PCR was performed using PCR-EZ D-PCR Master Mix (Bio Basic Inc.). E1A species were amplified using the forward primer CCACGGAGGTGTTATTACCG and the reverse primer TCAGGATAGCAGGCACCAAT. 55R E1A was detected using the forward primer AATGAATTCTTGGACCAGCTGATCGAAGAGG and reverse primer GATCCTTATGGCCTGGGGCGTTTACAGCTCAAG.

3.2.4 Plasmid construction

pLE-9S and pEGFP-N1 were kind gifts of E. Moran and J. Torchia, respectively. All ligations were performed using T4 Ligase (NEB) according manufacturer's instructions. To construct pCANmycEGFP-55R, HAdV-2 55R-EGFP was cut out of pEGFP-55R using NcoI and XbaI. Overhangs were filled in using the Klenow fragment from *E. coli* DNA polymerase I (NEB) and the insert was ligated into the BamHI site of pCANmyc that had also been blunted using the Klenow fragment. pEGFP-N1-9S was constructed by PCR of HAdV-2 55R E1A from pCANmycEGFP-55R using the forward primer ATCTCGAGATGAGACATATTAT, which contains a BamHI restriction site and the reverse primer GTGGATCCTTGGATAGCAGG, which contains an XhoI restriction site. The insert and vector (pEGFP-N1) were each digested with BamHI and XhoI and were then ligated together. pCANmyc-55R was constructed by cloning 55R hAdV-2 E1A in-frame with the N-terminal myc tag of pCANmyc. GST-55R/53R E1A fusions were made by cloning the 55R E1A proteins from HAdV-2 and HAdV-5, as well as the 53R E1A

protein of HAdV-12 into the EcoRI/SalI sites of pGEX 4T1. PCNA4-HA-S8 and PCNA4-HA-S4 have been described previously (45).

3.2.5 Generation of anti-55R E1A Abs

Polyclonal rabbits Abs were generated against a peptide corresponding to the unique C-terminal region of HAdV-2 55R E1A: KYG-43-NRSLQDLPGVLNWCLLS-55. The peptide was coupled to keyhole limpet hemocyanin (KLH) using bis-diazobenzidine. 5 mg of peptide was conjugated to 5 mg of KLH. The KLH-peptide conjugate was injected subcutaneously into female New Zealand White rabbits. Each rabbit was injected at four sites with 100 ug at each site. Before injecting, the KLH-peptide conjugate was emulsified with Freund's Complete Adjuvant for the initial inoculation and with Freund's Incomplete Adjuvant for subsequent injections. The rabbits were injected at three week intervals and test bleeds were taken 10 days following the preceding injection.

Antibody reacting against the peptide was affinity purified using a peptide column that was prepared by conjugating 5 mg of peptide to 6 mls bed volume of Affi-gel 10 (BioRad) via hydroxysuccinimide linkage. The serum was diluted two-fold in Tris-buffered saline (TBS) and then passed twice over the affinity column. The column was washed and then eluted with 100 uM glycine, pH 2.2 and the eluted antibody was dialysed against TBS. The antibody was initially tested against sequential dilutions of the peptide spotted onto nitrocellulose. The rabbits underwent a total of eight injections.

3.2.6 Protein purification

pGEX4T1-HAdV-2-55R, pGEX4T1-HAdV-5-55R and pGEX4T1-HAdV-12 53R were expressed in E. coli RIL (Stratagene) and were purified using standard methods.

3.2.7   Immunoprecipitation, GST-pulldown and immunoblot analysis

For immunoprecipitation experiments, HEK293T or A549 were lysed in NP-40 lysis buffer (0.5 % NP-40, 50 mM Tris pH 7.8, 150mM NaCl) supplemented with protease inhibitor cocktail (Sigma). One microgram of anti-GFP mAb (Clontech) was used for immunoprecipitation of EGFP-55R in combination with 125 µl of 10 % protein A-sepharose resin (Sigma) from 0.5 mg of cell lysate. Samples were agitated for 1 h at 4 °C. Beads were washed five times with lysis buffer and samples were boiled in 1x lithium dodecyl sulfate (LDS) sample buffer for 5 min. Samples were separated on a sodium dodecyl sulfate polyacrylamide gel electrophoresis (SDS-PAGE) and were transferred onto a polyvinylidene difluoride (PVDF) membrane (GE Healthcare). Membranes were blocked in 5 % nonfat milk in 1x Tris-buffered saline with 0.1 % Tween-20.

For western blots, cells were lysed in NP-40 lysis buffer and were then boiled in sample buffer and treated as described above. Membranes were stripped by heating in a 2 M glycine buffer, pH 2.2 with 0.5 % SDS. Ponceau staining was performed according to standard protocols.

GST pulldowns were performed using 0.25 µg of GST-55R E1A and 0.5 mg of lysate from HEK293T or A549 cells that had been transfected with constructs expressing HA-S8, HA-S4 or were left untransfected. Samples were agitated for 1 h at 4 °C with 12.5 µl of glutathione sepharose 50 % slurry and were then treated as described for immunoprecipitation experiments. HA-S8 and HA-S4 were detected using rat anti-HA mAb (1:2000, 3F10, Roche). EGFP was detected using anti-GFP mAb (1:2000,

Clontech). 55R E1A was detected using custom rabbit polyclonal anti-HAdV-2 55R E1A antibodies (1 µg/ml).

Secondary antibodies used included goat anti-mouse IgG (1:200 000, Jackson Labs), goat anti-rabbit IgG (1:200 000, Jackson Labs) and goat anti-rat IgG (1:20 000, Pierce); all were conjugated to horseradish peroxidase. Membranes were incubated with ECL+ substrate (GE Healthcare) for 1 min prior to exposures.

3.2.8 Immunofluorescence microscopy

All cells were seeded on coverslips in 24-well tissue culture dishes and were fixed in 3.7 % paraformaldehyde (Fisher) for 30 min at room temperature. After washing in PBS, cells were permeabilized on ice using 0.2 % Triton X-100 (Biobasic) for 20 min. Coverslips were transferred to humidity chambers and were blocked using 10 % FBS in PBS (blocking buffer, BB) for 30 min at room temperature. Cells were incubated at room temperature for 1 h with anti-55R E1A rabbit polyclonal Abs (1:50), anti-E1A mAb M73 hybridoma supernatant (neat) and/or anti-myc (9E10 hybridoma supernatant, neat) primary Abs. After washing 3x with BB, cells were incubated for another hour at room temperature with with Alexa Fluor® 546 goat anti-mouse IgG, Alexa Fluor® 594 goat anti-rabbit IgG and/or Alexa Fluor® 488 goat anti-mouse IgG (all from Molecular Probes). Finally, cells were washed 3x with PBS and nuclei were labeled with 0.2 mg/ml Hoechst 33342 (Molecular Probes) for 3 min at room temperature. Cells were washed three more times and coverslips were then mounted on glass microscope slides using mounting media consisting of 90 % glycerol (Biobasic), 10 % PBS and 2.5 g/litre 1,4-diazabicyclo(2,2,2)octane (DABCO, Alfa Aesar). Imaging was performed using a Zeiss

Axioskop 2 magneto-optical trap fluorescence microscope equipped with a QImaging Retiga 1300-coded monochrome 12-bit camera. Images were captured and pseudocolored using Northern Eclipse version 7.0 software. Confocal images were acquired using a Zeiss LSM 510 META confocal laser scanning microscope equipped with Zeiss Zen imaging software for analysis.

3.3 Results

3.3.1 Characterization of anti-55R E1A polyclonal Abs

Despite discovery of the putative 55R E1A product of species C HAdV over 30 years ago, the protein itself has never been detected or systematically characterized in the context of infection. This is due, in part, to the fact that none of the existing Abs which recognize various epitopes of E1A from species C HAdV are able to detect the 55R isoform. To address this issue, we generated rabbit polyclonal antibodies which specifically recognize the 55R E1A species of subgroup C HAdV.

A peptide was synthesized corresponding to residues 43-55 of the unique C-terminal region of HAdV-2 (KYG-43-NRSLQDLPGVLNWCLLS-55). This peptide was coupled to keyhole limpet hemocyanin and was used to immunize rabbits. Antibodies were affinity purified from rabbit serum and specificity was demonstrated by dot blot assay using the immunizing peptide (data not shown). In order to determine the breadth of specificity of the affinity purified Abs, a western blot was performed against purified GST-55R E1A from HAdV-2 and HAdV-5, as well as the equivalent 53R E1A isoform of HAdV-12. Interestingly, the antibody demonstrated exquisite specificity for 55R E1A from HAdV-2, but was unable to detect the 55R E1A protein from HAdV-5 (Fig. 3-1C),

a closely related species C HAdV with only 3 non-identical amino acids located in the C-terminus of the protein (Fig. 3-1B). The Abs were also unable to recognize the 53R E1A protein of HAdV-12, a more divergent species A HAdV, or GST alone (Fig. 3-1C).

We next sought to determine whether the Abs could be used to immunoprecipitate HAdV-2 55R E1A. To do this, lysates were prepared from HEK293T cells expressing EGFP-55R E1A, EGFP alone or from mock transfected cells. Lysates were then incubated with polyclonal anti-55R E1A Abs along with protein A-sepharose beads. After washing the beads thoroughly and boiling them with LDS sample buffer, proteins were separated by SDS-PAGE and were transferred to a PDVF membrane. A band corresponding to the molecular weight (MW) of EGFP-55R E1A appeared only in the sample from EGFP-55R E1A-expressing cells when the membrane was probed with anti-55R E1A polyclonal antibodies or anti-GFP mAb (Fig. 3-1D). Thus, the polyclonal anti-55R E1A Abs can likely recognize both native and denatured HAdV-2 55R E1A.

Finally, we aimed to determine whether our anti-55R E1A Abs could be used to study the subcellular localization of 55R E1A by indirect immunofluorescence. HT1080 cells were either mock transfected (data not shown) or were transfected with a construct which expressed myc-55R. 24 h post-transfection, cells were fixed and stained using anti-55R E1A and anti-myc followed by Alexa Fluor® 594 goat anti-rabbit IgG or Alexa Fluor® 488 goat anti-mouse IgG. Samples were analyzed by confocal microscopy and colocalization of signal was observed only in cells expressing myc-55R E1A (Fig. 3-1E), demonstrating that the Ab could also be used for determination of the subcellular
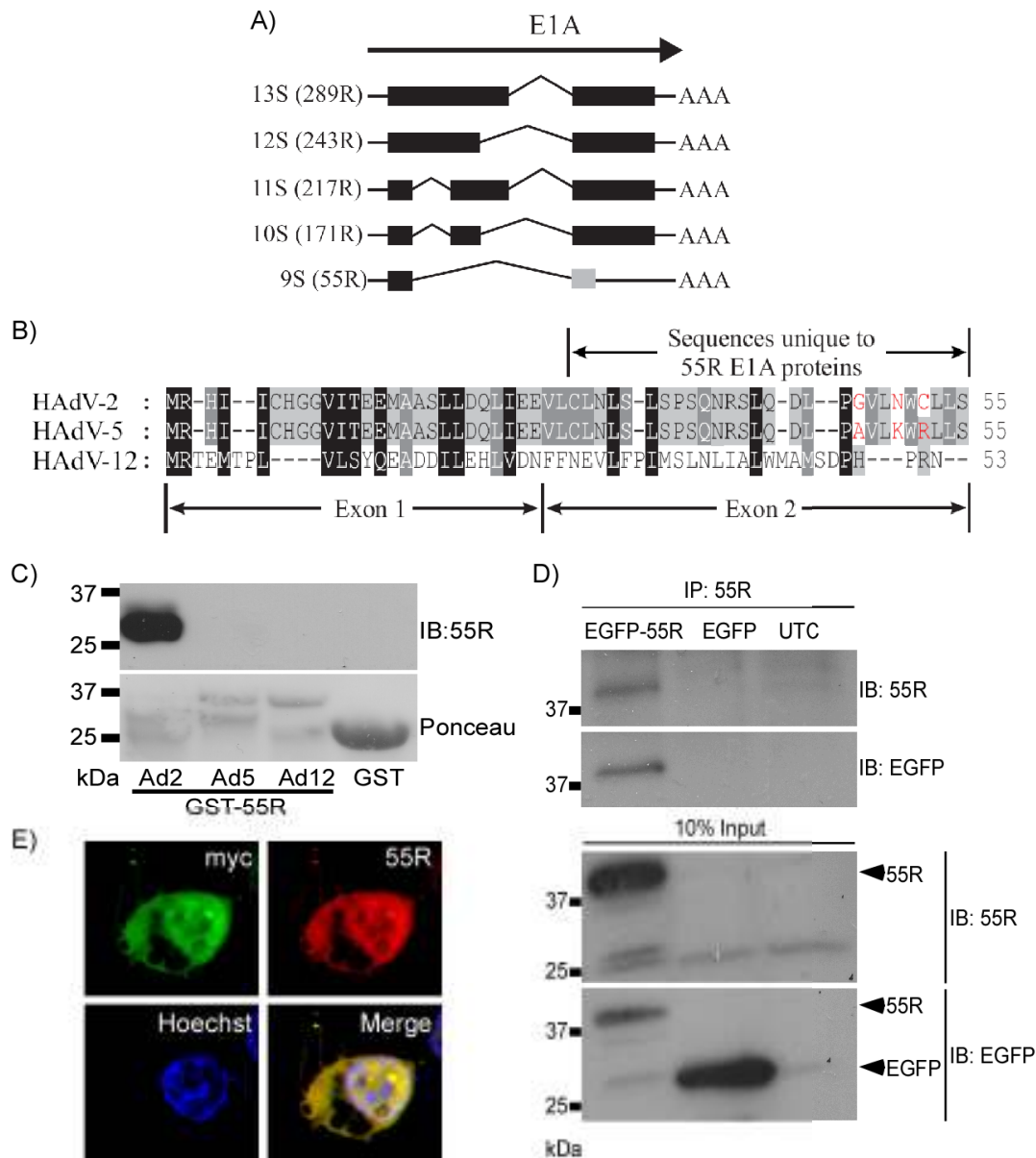
FIG. 3-1. Characterization of 55R E1A polyclonal antibodies. A) Graphical depiction of the mRNA species generated by splicing of the primary E1A transcript. B) Amino acid sequence comparison of the proteins encoded by the 9S mRNA species of HAdV-2, HAdV-5 and HAdV-12. Amino acids which differ between HAdV-2 and HAdV-5 are denoted in red. C) Western blot of GST-purified 55R E1A (or 53R E1A, in the case of HAdV-12) using our custom rabbit polyclonal anti-55R E1A Abs. D) EGFP-55R E1A was immunoprecipitated from HT1080 cells using custom rabbit polyclonal anti-55R E1A Abs. e) Indirect immunofluorescence images of HT1080 cell expressing myc-55R E1A, stained with an anti-myc Ab and anti-55R E1A polyclonal Abs. Nuclei were stained with Hoechst 33342.

localization of 55R E1A. 55R E1A could be found in both the nucleus and cytoplasm of these cells, similar to what has been described for the larger E1A isoforms (12, 28).

3.3.2   55R E1A is Expressed at Late Times Post-Infection and is Localized Mainly to the Nucleus

Although several studies have reported the kinetics of 55R E1A expression at the mRNA level, the expression kinetics of the protein itself have never been investigated (8, 53-54, 58-59, 66). Indeed, prior to this study, the 55R E1A protein has never been detected in the context of infection. To examine the relationship between 55R E1A mRNA expression and expression of the 55R E1A protein, A549 cells were infected with HAdV-2 at an MOI of 1. Kinetics of E1A mRNA expression were first examined by RT-PCR in order to verify the results of earlier studies under our specific experimental conditions. Expression of 13S and 12S mRNA could be detected at 24 hpi and increased from 48 to 96 hpi. Expression of 11S and 10S mRNA was detectable from 48 to 120 hpi, with maximal expression at 96 hpi. The 9S E1A mRNA species could also be detected from 48-120 hpi, with maximal expression occurring at 96 hpi (Fig. 3-2A). The reduced abundance of all mRNA species at 120 hpi is likely due to both cell death (which was observed at this stage of infection) as well as the end of one round of viral replication and the beginning of a second round of infection in previously uninfected cells. These results closely matched those found in previously published reports (58-59).

Next, we analyzed samples prepared in parallel for expression of E1A proteins by immunofluorescence microscopy. Using the M73 antibody, which recognizes the C-terminal region encoded by exon 2 of all E1A products except 55R E1A, expression of E1A protein could begin to be detected as early as 6 hpi. This increased up to 24 hpi and

then stayed relatively consistent. Conversely, expression of 55R E1A could be detected only faintly and in very few cells starting at 24 hpi, with expression increasing up to 72 hpi (Fig. 3-2B). These results are consistent with 55R E1A expression occurring primarily at late times post-infection, as suggested by the kinetics of 9S mRNA species. Importantly, this is the first time that 55R E1A has been detected in the context of viral infection. Interestingly, 55R E1A seems to be localized mainly in the nucleus, similar to the larger E1A isoforms, despite the fact that it lacks the nuclear localization signal present in these proteins (Fig. 3-2B). These results show for the first time that like the 9S E1A mRNA, 55R E1A protein is expressed preferentially at late times post-infection and appears to be present mainly in the nucleus of infected cells.

3.3.3   55R E1A activates expression of viral genes

Given the kinetics of 55R E1A expression and its localization in the nucleus, we sought to assess whether, akin to the largest E1A isoforms, 55R E1A could transactivate viral genes. To accomplish this, we performed a qRT-PCR assay on growth-arrested IMR-90 cells infected with dl309, JM17-55R, dl521 and dl312 using primers which recognize transcripts expressed from selected viral promoters (2, 24, 45). RNA was extracted from contact inhibited IMR-90 fibroblasts which had been infected with the viruses mentioned above for 24, 48, 72, 96,
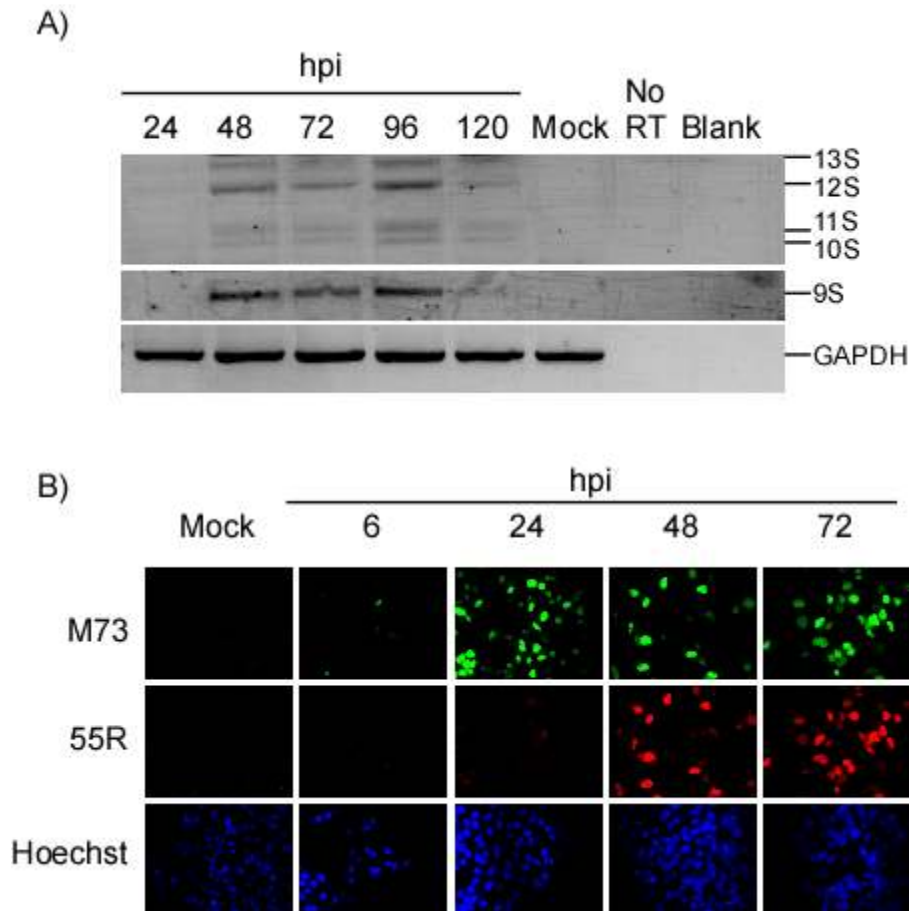
FIG. 3-2. Determination of 55R E1A mRNA and protein expression kinetics in A549 cells. A549 cells were infected with HAdV-2 at an MOI of 1. A) Cells were collected at 24, 48, 72, 96 or 120 hpi for RT-PCR analysis of each E1A mRNA species. GAPDH was also analyzed as a loading control. B) Cells were grown on coverslips and were collected and fixed at 6, 24, 48 and 72 hpi. The larger E1A isoforms were labeled with the monoclonal E1A Ab M73, while 55R E1A was labeled with custom rabbit polyclonal anti-55R E1A Abs. Nuclei were stained with Hoechst 33342.

120 or 144 hpi. All samples were normalized internally to GAPDH and viral gene expression was compared to that observed for dl312-infected samples.

dl309, which expresses all E1A isoforms, induced expression of E1B approximately 10,000-fold relative to dl312 at 24 hpi. The level of transactivation induced by dl309 reached a maximum of approximately 317 000-fold by 120 hpi. In comparison, JM17-55R, which constitutively expresses only 55R E1A, resulted in only a 52-fold induction of E1B expression relative to dl312 24 hpi, with no appreciable increase as the infection progressed. In correlation with the expected expression kinetics of 55R E1A, the levels of E1B steadily increased during dl521 infection (harbors genomic E1A and splices only 55R E1A) up to a maximum of 165-fold at 72 hpi (Fig. 3-3A). Thus, 55R E1A is able to induce expression of E1B to a modest extent when compared to wild-type E1A. In addition, the maximal degree of induction remains consistent whether 55R E1A is expressed constitutively from cDNA or requires splicing of the primary E1A transcript.

The E2A transcript was induced later and to much lower levels compared to E1B during dl309 infection. This was expected based on the indirect mode of E2 promoter activation by E1A (3, 25-26, 43, 71). At 72 hpi, E2A was induced approximately 5-fold compared to dl312 infection. This level of induction remained relatively consistent until 144 hpi. During infection with viruses expressing 55R E1A only, E2A levels did not reliably increase above those observed in dl312 until 144 hpi and even then expression only reached 2- to 4-fold above background (Fig. 3-3B).

Levels of E3A expression during dl309 infection ranged from approximately 26 000-fold at 24 hpi to 1.2-million fold at 48 hpi. Induction of E3A expression was much more

modest during infection with 55R E1A-expressing viruses. At 24 hpi, E3A was induced only 2- and 10-fold by JM17-55R and dl521, respectively. Maximum E3A induction reached 4000-fold at 96 hpi during dl521 infection and 2900-fold at 120 hpi during JM17-55R infection. Again, both the kinetics and magnitude of E3A expression differed during infection with 55R E1A-expressing viruses when compared to dl309, expressing wildtype E1A (Fig. 3-3C).

Unlike E3A, which was induced to much higher levels at 24 hpi by wildtype E1A virus than those expressing only 55R E1A, E4orf6/7 levels were comparable among all three viruses tested at this time point and were around 50-fold higher than those observed during dl312 infection. In this case, the kinetics of transcript expression were also similar among all three viruses and peaked at 120 hpi, although by this point transcript levels in dl309-infected cells were over three logs higher than those observed in cells infected with JM17-55R or dl521 (Fig. 3-3D).

Finally, transactivation of the MLP was read out by assessing the levels of hexon mRNA expression induced by each virus. During dl309 infection, hexon transcript levels progressively increased from 46-fold above dl312 at 24 hpi to a maximum of 424 000-fold above dl312 at 120 hpi. In comparison, hexon was induced only 7-fold by JM17-55R at 24 hpi, and not at all by dl521. By 96 hpi, dl521 had reached its maximum degree of hexon expression at 24 000-fold greater than dl312, while induction by JM17-55R reached a plateau of 800- to 900-fold at 96 and 120 hpi, respectively (Fig. 3-3E).
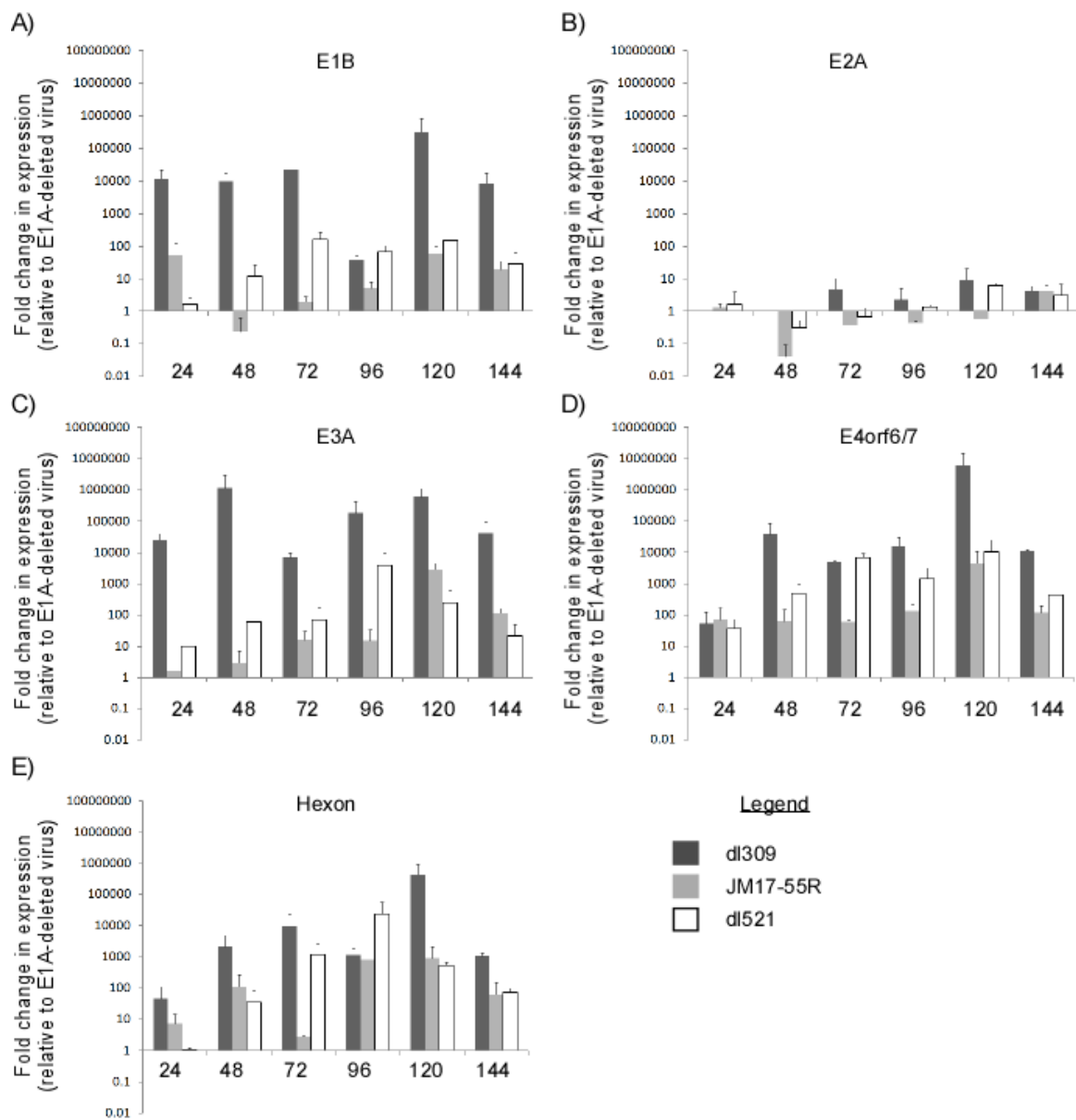
FIG. 3-3. Transactivation of viral genes by 55R E1A. A-E) Contact-inhibited primary IMR-90 fibroblasts were infected with dl309, JM17-55R, dl521 or dl312 at an MOI of 5. Cells were collected at 24, 48, 72, 96 or 120 hpi. Samples were subjected to qRT-PCR analysis using primers specific to transcripts controlled by various HAdV promoters including A) E1B, B) E2A, C) E3A, D) E4orf6/7 or E) Hexon. All samples were normalized internally to GAPDH and then to the levels of gene expression observed in dl312-infected cells using the $\Delta\Delta C_T$ method.

Taken together, these results show that 55R E1A is able to transactivate the expression of viral genes. This was true in the case of both dl521, which contains genomic E1A but splices only the 9S product, and of JM17-55R, which carries 55R cDNA in an E1A-deleted background. In each case, the levels of viral gene expression observed were distinct (and usually several log-fold lower at peak expression) from that of virus harboring wildtype E1A, as were the kinetics of gene expression. The ability of 55R E1A to transactivate viral genes is particularly interesting in light of the fact that 55R E1A does not contain any of the CRs present in the larger E1A isoforms. Further elucidation of the mechanism through which 55R accomplishes this feat will be of great interest.

3.3.4   55R E1A is sufficient to promote replication of HAdV in Contact-Inhibited IMR-90 fibroblasts

The observation that 55R E1A was able to transactivate expression of viral genes led us to investigate whether this E1A isoform could also promote virus growth when expressed alone in an E1A-deleted virus background. Contact-inhibited IMR-90 cells were infected with dl309, pm975, dl520, JM17-55R, dl521 or dl312 at an MOI of 5. Supernatants were collected at 4, 48 and 120 hpi and the yield of cell-free virus was assessed by plaque assay on HEK293 cells. In samples collected at 4 hpi, no more than 40 plaque-forming units (pfu/ml) were ever present and there was no significant difference between dl312 and the viruses expressing various E1A proteins. Since growth was measured as fold-change relative to dl312 (E1A-deleted virus), this demonstrated that washing of cells 1 h after adsorption efficiently removed residual virus particles and ensured that virus yield at later times was due to *de novo* virus replication (data not shown).

As expected, dl309 grew best on the contact-inhibited IMR-90 fibroblasts, followed by pm975. To our surprise, JM17-55R produced approximately 7-fold more virus than dl520 at 48 hpi, while at 120 hpi this trend was reversed, with dl520 producing about 14-fold more virus than JM17-55R. dl521 grew to titres which closely resembled those reached by dl520 at both 48 and 120 hpi. Most importantly, viruses expressing only 55R E1A consistently exhibited a 30- to 2800-fold growth advantage compared to E1A-deleted virus, demonstrating that on its own, 55R E1A was sufficient to promote replication of HAdV in contact-inhibited IMR-90 (Fig. 3-4A). Therefore, not only can 55R E1A transactivate expression of viral genes, it is also sufficient to promote viral replication.

Due to the genetic organization of genomic E1A, it was not possible to construct a virus that lacks expression of only 55R E1A without inducing mutations in the other E1A isoforms. Such a strategy runs the serious risk of confounding the interpretation of results gathered from this type of approach due to the large numbers of proteins with which E1A interacts. Nevertheless, it was important to evaluate the impact of 55R E1A on virus growth in the context of the two major E1A isoforms, 289R and 243R. To accomplish this, we made use of a co-infection model, whereby growth arrested IMR-90 fibroblasts were infected with either pm975 or dl520, in combination with either dl521 or the E1A-deleted dl312. Cells were infected with each virus at an MOI of 5, for a total MOI of 10. In combination with a virus expressing 289R E1A (pm975), co-infection with dl521 only moderately improved virus yield compared to co-infection with dl312. However, co-infection of dl521 with a virus expressing only 243R E1A (dl520) resulted in 1-log growth increase relative to co-infection with dl312 at 48 hpi. This improved to a 2-log increase by 120 hpi (Fig. 3-4B). It is important to note that both pm975 and dl520 can, on

their own, produce 55R E1A. Thus, these results suggest that in combination with 289R E1A, endogenous levels of 55R E1A are sufficient to maximize virus replication in contact-inhibited IMR-90. However, in the context of 243R E1A, additional 55R E1A provided by co-infection with dl521 has a growth-promoting effect which implies a unique mechanism for the replication-promoting phenotype exhibited by 55R E1A.
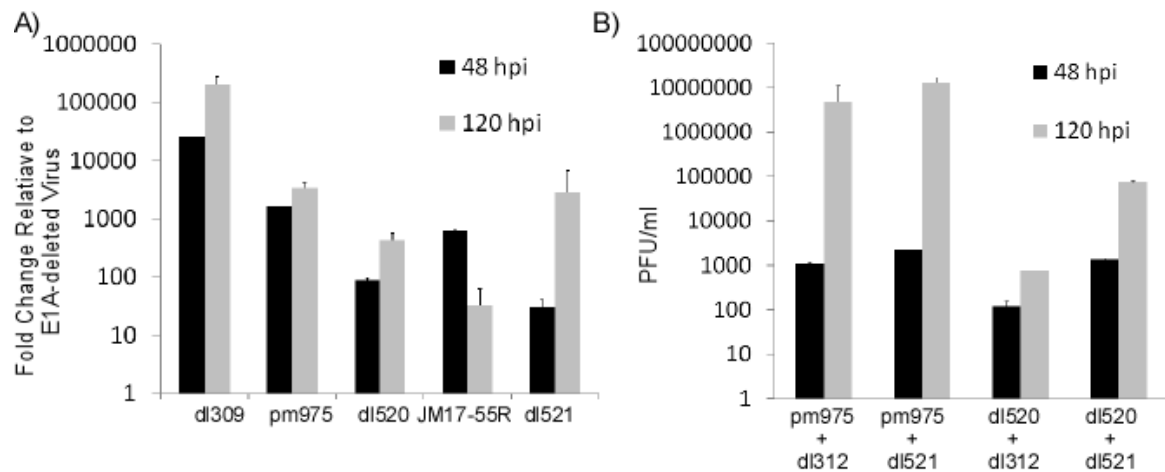
FIG. 3-4. Replication of viruses expressing 55R E1A in contact-inhibited IMR-90 cells. A) Contact-inhibited primary IMR-90 cells were infected with dl309, pm975, dl520, JM17-55R, dl521 or dl312 at an MOI of 5. Supernatants were collected at 4, 48 or 120 hpi and cell-free virus titres were determined by serial dilution on HEK293 cells. B) Contact-inhibited primary IMR-90 fibroblasts were infected with pm975 and dl312, pm975 and dl521, dl520 and dl312 or dl520 and dl521. Supernatants were collected at 4, 48 and 120 hpi and the titres of cell-free virus were assayed as described in A).

3.3.5   55R interacts with the S8 component of the 19S regulatory proteasome

Interaction of the major E1A isoforms with the APIS complex has been demonstrated previously and is known to be important in the ability of E1A to enhance transcription of early genes (45). Binding of E1A to the S4 and S8 components of APIS was initially mapped to amino acids 4-25 on the E1A protein (57). Later studies would show that S8 could also be recruited by CR3 (45). In light of the fact that 55R E1A shares homology to the larger E1A isoforms in its first 28 amino acids, we sought to determine whether it too could interact with components of APIS and whether this interaction was important for its ability to enhance virus replication.

To determine whether 55R E1A could interact with S4 and/or S8, A549 cells were transfected with a construct expressing either HA-S4, HA-S8 or were mock transfected as a control. Lysates from these cells were incubated with GST-purified HAdV-2 55R E1A which was pulled down with glutathione sepharose beads. Quite interestingly, we observed an interaction of GST-55R E1A with HA-S8, but not with HA-S4 (Fig. 3-5A). To confirm whether this interaction occurred in a more natural setting, we also cotransfected A549 cells with constructs expressing 55R-GFP or GFP alone with constructs expressing HA-S8. Indeed, 55R-GFP was able to pull down HA-S8, whereas GFP alone could not (Fig. 3-5B).

To determine whether this interaction had functional consequences in the context of virus replication, we knocked down endogenous S8 in A549 cells using validated siRNA directed against S8. We infected cells with either dl312 or dl521 and normalized dl521 growth to that observed using dl312 in cells treated with siRNA directed against S8

(siS8) or a scrambled siRNA control. This allowed us to control for any non-specific effects of S8 knockdown on virus growth. Interestingly, at 48 hpi dl521 growth in cells treated with siS8 was reduced 2-fold compared to cells treated with control siRNA (Fig. 3-5C). This led us to conclude that the interaction of 55R E1A with S8 is functionally important in the ability of 55R E1A to promote virus replication. While the specific mechanism for the replication-promoting phenotype of the 55R E1A-S8 interaction remains to be elucidated, it is likely that it is important in the ability of 55R E1A to transactivate viral genes, analogous to the larger E1A isoforms.

3.4   Discussion

Despite discovery of the 9S mRNA species over 30 years ago, the protein that it encodes, as well as the function of that protein has remained completely elusive. Early studies successfully demonstrated that the 9S mRNA product is processed preferentially at late times post-infection, and that this shift in splice site preference seems to require viral DNA replication (8, 53-54, 59, 66). Unfortunately, the kinetics of 55R E1A protein expression could not be assessed at that time. To our knowledge, none of the abundant E1A-directed Abs generated since that time have been able to specifically detect the 55R E1A protein. This limitation has severely hampered efforts to biochemically and functionally characterize this E1A species.

To address this important issue, we generated polyclonal rabbit Abs against a peptide corresponding to amino acids 43-55 of the unique C-terminal region of the 55R E1A protein from HAdV-2. We demonstrated that these Abs specifically recognized GST-purified 55R E1A from HAdV-2, but not from the closely related HAdV-5 55R E1A or
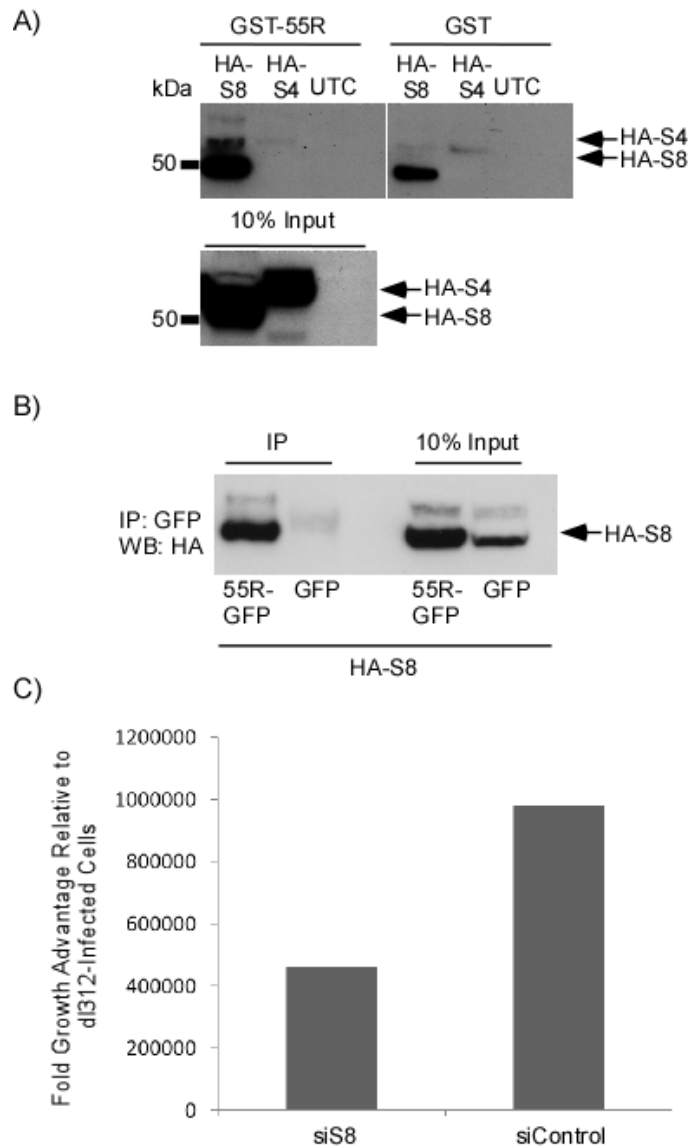
FIG. 3-5. Interaction and consequences of 55R E1A interaction with the APIS component S8. A) Lysates were prepared from A549 cells transiently transfected with constructs expressing either HA-S8 or HA-S4. Lysates were incubated with GST-purified 55R E1A and complexes were pulled down using glutathione sepharose beads. Membrane was probed with anti-HA (3F10). B) Lysates were prepared from A549 cells transiently transfected with constructs expressing HA-S8 and either 55R-GFP or GFP alone. Complexes were immunopreciptated using rabbit polyclonal anti-55R Abs and Protein A sepharose beads. Membrane was probed with anti-HA (3F10). C) A549 cells were treated with scrambled siRNA or siRNA directed against S8. These cells were infected with either dl521 or dl312 and supernatants were collected 48 hpi. Virus titres were determined by serial dilution of supernatants on HEK293cells.

the equivalent, but more distantly-related 53R E1A protein encoded by HAdV-12 (Fig. 3-1C). The utility of these Abs was demonstrated in western blot, immunoprecipitation and indirect immunofluorescence assays (Fig. 3-1C-E). We are convinced that the development of this extremely valuable tool will aid in the further study of the HAdV-2 55R E1A protein, especially given the breadth of assays for which it is useful.

We next set out to finally reconcile earlier studies which have described the kinetics of 9S mRNA expression with the kinetics of 55R E1A protein expression. In agreement with earlier studies performed on other cell lines, 9S mRNA expression was observed at late times post-infection of A549 cells (48-96 hpi, Fig. 3-2A) (58-59). Co-staining of the larger E1A isoforms and 55R E1A yielded two interesting and important findings. Firstly, the kinetics of 55R E1A protein expression match nicely with the kinetics of 9S mRNA expression that we observed in A549 cells. Secondly, 55R E1A was found to localize primarily to the nucleus, similar to the larger E1A isoforms, despite the fact that it lacks the NLS present in the larger proteins (Fig. 3-2B). The ability of 55R E1A to enter the nucleus may be explained by the fact that molecules less than 40 kDa in size are able to pass relatively freely through the NPC (61). 55R E1A falls well below this limit, with a predicted MW of approximately 6 kDa. Once in the nucleus, 55R E1A is likely enriched and retained there by binding to cellular partners also present in the nucleus.

The localization of E1A in the nucleus led us to investigate whether, akin to the larger E1A isoforms, 55R E1A had any role in transactivation of viral genes. This is one of the two major functions of E1A, the other of course being the induction of S-phase. Early studies have yielded some peripheral observations regarding the effects (or lack thereof)

of 55R E1A on the host cell, but none have examined the role of 55R E1A on viral replication directly. For example, dl521 was not able to transform either cloned rat embryo fibroblasts or baby rat kidney cells (16). This is not surprising given that it lacks several regions known to be essential for transformation by the larger E1A proteins. In addition, the 289R and 243R E1A isoforms have long been known to cause the *cyt* and *deg* phenotypes (later recognized to be apoptosis) in the absence of E1B 19K. Conversely, virus expressing 55R E1A in the absence of E1B 19K failed to produce this phenotype (64). E1A-induced apoptosis has been attributed to the ability of E1A to bind p300 and pRb, key regulators of E2F1-induced apoptosis (44). The regions required for binding of these factors are missing from the 55R E1A isoform. Similar work examining the role of E1B 19K in regulating early gene expression hinted at some interesting properties of a virus carrying 9S cDNA in an E1A-deleted background. Namely, while E1B 19K repressed viral gene expression in HeLa cells infected with 13S and 12S cDNA viruses, it had a stimulatory effect on early gene expression in cells infected with a 9S cDNA virus (63-64). While the particular reasons for this phenotype remain unclear, they led us to wonder whether 55R E1A could also transactivate viral gene expression in contact-inhibited, primary IMR-90 cells.

Indeed, our studies showed that viruses expressing only 55R E1A were sufficient to transactivate expression of both early and late viral genes. While the kinetics and magnitude of this transactivation varied from gene-to-gene, as expected, the maximal levels of expression induced were consistently lower than virus expressing wildtype E1A (Fig. 3-3). The transactivating properties of 289R and 243R E1A have been studied quite extensively. The difference in phenotypes induced by 289R and 243R E1A have been

attributed to the presence of CR3 in the 289R protein, which itself serves as a potent transcriptional activation domain (31). As mentioned earlier, the ability of CR3 to activate transcription relies heavily on its association with MED23, a component of the mediator complex (1, 7, 13, 30, 60). CR1, 2 and 4 are then responsible for many of the properties exhibited by 243R E1A, including those common to 289R E1A, through mediating interactions with a variety of cellular factors including: pRb (21, 32, 65), p300/CBP (37, 69), TRRAP (9), BS69 (17, 22), UBC9 (18, 70) and CtBP (6, 50). As 55R E1A does not contain any of the CRs, the mechanism through which it is able to transactivate viral genes remains of great interest. This may be mediated in part through interactions with proteins known to bind within the first 28 amino acids of E1A which are conserved in 55R. In addition, it is highly probable that 55R E1A interacts with novel partners through its unique 27 C-terminal amino acids. This region is predicted to be unstructured and does not contain any easily recognizable domains which would help predict binding partners or function. An in-depth, systematic characterization of this region will be the focus of intense future studies.

While the ability of 55R E1A to stimulate expression of viral genes in contact-inhibited IMR-90 cells was highly interesting, it did not guarantee that the virus could replicate productively under these conditions. It is known that E1A-deleted viruses can undergo low level replication in transformed cell lines. However, E1A-null viruses replicate extremely poorly in primary, growth arrested cells unless infected at extremely high MOIs (36). Therefore, we assessed the replication of HAdVs expressing various combinations of E1A proteins in growth-arrested, primary IMR-90 cells infected at an MOI of 5. In all cases, replication was normalized to that observed during infection with

dl312 (an E1A-null virus) such that any growth above this level could be attributed to a replication-promoting role for the respective E1A protein(s) carried by each virus. As expected, dl309 harboring wildtype genomic E1A replicated to the highest titres at both 48 and 120 hpi. This was followed by pm975, which expresses 289R, but not 243R E1A. dl520, which expresses 243R E1A, but not 289R E1A, grew approximately 2- to 3-logs better than dl312-infected virus at 48 and 120 hpi, respectively. Surprisingly, JM17-55R carrying 9S cDNA in an E1A-deleted background, and dl521 grew to equivalent, and in some cases, higher titres than dl520 (Fig. 3-4A). Again, this was unexpected given the lack of CRs present in 55R E1A and coupled with the observation that it does not have the potent transforming effects on cells of its larger counterparts (16). The differences observed in the growth of JM17-55R and dl521 likely reflect both the expression level and kinetics of 55R E1A. While both viruses express 55R E1A under the control of the E1 promoter, it is expressed constitutively by JM17-55R and must be spliced from genomic E1A during infection with dl521.

During natural infection, 55R E1A is not expressed alone, but in the context of the other E1A isoforms. Therefore, it was important for us to examine the effect of 55R E1A on virus replication in the presence of the larger E1A proteins. Co-infection experiments revealed that infection of cells with pm975 and dl521 did not enhance virus replication beyond that observed in cells infected with pm975 and dl312. This suggests that the endogenous levels of 55R E1A produced by pm975 are sufficient to maximize virus replication in combination with 289R E1A. However, co-infection of cells with dl520 and dl521 enhanced virus titres 1- to 2-logs relative to cells infected with dl520 and dl312 at 48 and 120 hpi, respectively. These results indicate that in the context of 243R E1A,

addition of exogenous 55R E1A can enhance virus replication (Fig. 3-4B). This observation is especially intriguing given that 243R E1A causes only low levels of viral gene transactivation on its own, while 289R can by itself activate viral gene expression to wildtype levels (34, 67). Together, these observations lend even more strength to the evidence that 55R E1A directly and actively transactivates expression of viral genes, which promotes productive virus replication.

Finally, we determined that like 289R and 243R E1A, 55R E1A was able to bind S8, a regulatory component of the 26S proteasome and member of the APIS complex. This is the first reported cellular binding partner of 55R E1A (Fig. 3-5A, B). The binding site for S8 was originally mapped to residues 4-25 of E1A (57). These residues are conserved in the 55R E1A isoform. S4, another member of APIS, was also found to bind residues 4-25 of E1A. Notably, 55R E1A does not appear to bind this APIS subunit (57). The reason for this selectivity is unclear but may a result of an inhibitory effect exerted by the C-terminus of 55R E1A on the binding of S4. Alternatively, binding to S4 may be promoted by regions of the larger E1A proteins not present in 55R E1A.

Further studies determined that S8 can also bind to CR3. CR3 could recruit S8 to early viral promoters which in turn stimulated the transactivation activity of CR3. On the other hand, inhibition of proteasome function was detrimental to the ability of CR3 to transactivate viral genes. Unfortunately, the result of proteasome inhibition on virus growth was not evaluated (45). Despite the fact that 55R E1A does not contain CR3, we hypothesized that its interaction with S8 might have a similar functional outcome and that this outcome should impact virus replication if important. Knockdown of S8 reduced

growth of dl521 2-fold by 48 hpi in A549 cells (Fig. 3-5C). Since growth was normalized to dl312, this effect could be fully attributed to the effect of S8 knockdown on the function of 55R E1A. Therefore, in addition to identifying the first binding partner of 55R E1A, we have also determined that this interaction is important for its transactivating and growth promoting activities.

In summary, we have developed the first Abs capable of specifically recognizing the 55R E1A isoform of HAdV-2. These antibodies could be used for detection of 55R E1A by western blot, immunoprecipitation and indirect immunofluorescence. This is the first report describing the kinetics of 55R E1A protein expression, which was done in parallel with the expression kinetics of 9S mRNA. We have discovered that like the larger E1A isoforms, 55R E1A is localized predominantly in the nucleus of host cells, despite the fact that it lacks the NLS present in the larger E1A proteins. 55R E1A was able to transactivate viral genes in contact-inhibited IMR-90 cells, and was sufficient to promote replication of the virus in these same cells. We have identified the first binding partner of 55R E1A in S8, a component of APIS. This interaction is presumed to occur through amino acids 4-25, also present in the larger E1A proteins. Interestingly, 55R E1A demonstrates a unique specificity in this regard, and does not bind to S4, which was also shown to interact with the larger E1A isoforms through amino acids 4-25. Knockdown of S8 had a detrimental effect of growth of dl521, a virus which expresses only the 55R E1A isoform. Therefore, this interaction is likely to be important in mediating the transactivating and replication-promoting properties of 55R E1A. We believe that this study represents an extremely important contribution to the E1A field and in the understanding of AdV biology in general. This is the first report to observe and

functionally characterize 55R E1A since its discovery over 30 years ago. Further studies focused on unraveling the mechanism of 55R E1A-mediated viral gene transactivation and of its growth promoting properties will be important in understanding novel mechanisms controlling viral gene regulation. In addition, identification of putative binding partners of the unique C-terminal region of 55R E1A is likely to enhance our understanding of the interactions of HAdV with host cells, and more specifically, the E1A-mediated events that are important at late times post-infection.

3.5   References

1. **Ablack, J. N., P. Pelka, A. F. Yousef, A. S. Turnell, R. J. Grand, and J. S. Mymryk.** 2010. Comparison of E1A CR3-dependent transcriptional activation across six different human adenovirus subgroups. J Virol **84:**12771-12781.

2. **Abou El Hassan, M. A., S. R. Braam, and F. A. Kruyt.** 2006. A real-time RT-PCR assay for the quantitative determination of adenoviral gene expression in tumor cells. J Virol Methods **133:**53-61.

3. **Bagchi, S., P. Raychaudhuri, and J. R. Nevins.** 1990. Adenovirus E1A proteins can dissociate heteromeric complexes involving the E2F transcription factor: a novel mechanism for E1A trans-activation. Cell **62:**659-669.

4. **Berk, A. J.** 2007. Adenoviridae, p. 2355-2394. *In* D. M. Knipe (ed.), Field's Virology, 5th ed. Lippincott Williams & Wilkins, Philadelphia, PA.

5. **Berk, A. J., and P. A. Sharp.** 1978. Structure of the adenovirus 2 early mRNAs. Cell **14:**695-711.

6. **Boyd, J. M., T. Subramanian, U. Schaeper, M. La Regina, S. Bayley, and G. Chinnadurai.** 1993. A region in the C-terminus of adenovirus 2/5 E1a protein is required for association with a cellular phosphoprotein and important for the negative modulation of T24-ras mediated transformation, tumorigenesis and metastasis. EMBO J **12:**469-478.

7. **Boyer, T. G., M. E. Martin, E. Lees, R. P. Ricciardi, and A. J. Berk.** 1999. Mammalian Srb/Mediator complex is targeted by adenovirus E1A protein. Nature **399:**276-279.

8. **Chow, L. T., T. R. Broker, and J. B. Lewis.** 1979. Complex splicing patterns of RNAs from the early regions of adenovirus-2. J Mol Biol **134:**265-303.

9. **Deleu, L., S. Shellard, K. Alevizopoulos, B. Amati, and H. Land.** 2001. Recruitment of TRRAP required for oncogenic transformation by E1A. Oncogene **20:**8270-8275.

10. **Dijkema, R., B. M. Dekker, H. van Ormondt, A. de Waard, J. Maat, and H. W. Boyer.** 1980. Gene organization of the transforming region of weakly oncogenic adenovirus type 7: the E1a region. Gene **12:**287-299.

11. **Dumont, D. J., and P. E. Branton.** 1992. Phosphorylation of adenovirus E1A proteins by the p34cdc2 protein kinase. Virology **189:**111-120.

12. **Ferguson, B., B. Krippl, O. Andrisani, N. Jones, H. Westphal, and M. Rosenberg.** 1985. E1A 13S and 12S mRNA products made in Escherichia coli both function as nucleus-localized transcription activators but do not directly bind DNA. Mol Cell Biol **5:**2653-2661.

13. **Gold, M. O., J. P. Tassan, E. A. Nigg, A. P. Rice, and C. H. Herrmann.** 1996. Viral transactivators E1A and VP16 interact with a large complex that is associated with CTD kinase activity and contains CDK8. Nucleic Acids Res **24:**3771-3777.

14. **Graham, F. L., A. J. van der Eb, and H. L. Heijneker.** 1974. Size and location of the transforming region in human adenovirus type 5 DNA. Nature **251:**687-691.

15. **Grand, R. J., A. S. Turnell, G. G. Mason, W. Wang, A. E. Milner, J. S. Mymryk, S. M. Rookes, A. J. Rivett, and P. H. Gallimore.** 1999. Adenovirus early region 1A protein binds to mammalian SUG1-a regulatory component of the proteasome. Oncogene **18:**449-458.

16. **Haley, K. P., J. Overhauser, L. E. Babiss, H. S. Ginsberg, and N. C. Jones.** 1984. Transformation properties of type 5 adenovirus mutants that differentially express the E1A gene products. Proc Natl Acad Sci U S A **81:**5734-5738.

17. **Hateboer, G., A. Gennissen, Y. F. Ramos, R. M. Kerkhoven, V. Sonntag-Buck, H. G. Stunnenberg, and R. Bernards.** 1995. BS69, a novel adenovirus E1A-associated protein that inhibits E1A transactivation. EMBO J **14:**3159-3169.

18. **Hateboer, G., E. M. Hijmans, J. B. Nooij, S. Schlenker, S. Jentsch, and R. Bernards.** 1996. mUBC9, a novel adenovirus E1A-interacting protein that complements a yeast cell cycle defect. J Biol Chem **271:**25906-25911.

19. **Hilleman, M. R., and J. H. Werner.** 1954. Recovery of new agent from patients with acute respiratory illness. Proc Soc Exp Biol Med **85:**183-188.

20. **Houweling, A., P. J. van den Elsen, and A. J. van der Eb.** 1980. Partial transformation of primary rat cells by the leftmost 4.5% fragment of adenovirus 5 DNA. Virology **105:**537-550.

21. **Ikeda, M. A., and J. R. Nevins.** 1993. Identification of distinct roles for separate E1A domains in disruption of E2F complexes. Mol Cell Biol **13:**7029-7035.

22. **Isobe, T., C. Uchida, T. Hattori, K. Kitagawa, T. Oda, and M. Kitagawa.** 2006. Ubiquitin-dependent degradation of adenovirus E1A protein is inhibited by BS69. Biochem Biophys Res Commun **339:**367-374.

23. **Jones, N., and T. Shenk.** 1979. An adenovirus type 5 early gene function regulates expression of other early viral genes. Proc Natl Acad Sci U S A **76:**3665-3669.

24. **Jothikumar, N., T. L. Cromeans, V. R. Hill, X. Lu, M. D. Sobsey, and D. D. Erdman.** 2005. Quantitative real-time PCR assays for detection of human adenoviruses and identification of serotypes 40 and 41. Appl Environ Microbiol **71:**3131-3136.

25. **Kovesdi, I., R. Reichel, and J. R. Nevins.** 1986. E1A transcription induction: enhanced binding of a factor to upstream promoter sequences. Science **231:**719-722.

26. **Kovesdi, I., R. Reichel, and J. R. Nevins.** 1986. Identification of a cellular transcription factor involved in E1A trans-activation. Cell **45:**219-228.

27. **Lee, W. S., C. C. Kao, G. O. Bryant, X. Liu, and A. J. Berk.** 1991. Adenovirus E1A activation domain binds the basic repeat in the TATA box transcription factor. Cell **67:**365-376.

28. **Lyons, R. H., B. Q. Ferguson, and M. Rosenberg.** 1987. Pentapeptide nuclear localization signal in adenovirus E1a. Mol Cell Biol **7:**2451-2456.

29. **Mal, A., A. Piotrkowski, and M. L. Harter.** 1996. Cyclin-dependent kinases phosphorylate the adenovirus E1A protein, enhancing its ability to bind pRb and disrupt pRb-E2F complexes. J Virol **70:**2911-2921.

30. **Malik, S., and R. G. Roeder.** 2005. Dynamic regulation of pol II transcription by the mammalian Mediator complex. Trends Biochem Sci **30:**256-263.

31. **Martin, K. J., J. W. Lillie, and M. R. Green.** 1990. Evidence for interaction of different eukaryotic transcriptional activators with distinct cellular targets. Nature **346:**147-152.

32. **Mittnacht, S., J. A. Lees, D. Desai, E. Harlow, D. O. Morgan, and R. A. Weinberg.** 1994. Distinct sub-populations of the retinoblastoma protein show a distinct pattern of phosphorylation. EMBO J **13:**118-127.

33. **Montell, C., G. Courtois, C. Eng, and A. Berk.** 1984. Complete transformation by adenovirus 2 requires both E1A proteins. Cell **36:**951-961.

34. **Montell, C., E. F. Fisher, M. H. Caruthers, and A. J. Berk.** 1982. Resolving the functions of overlapping viral genes by site-specific mutagenesis at a mRNA splice site. Nature **295:**380-384.

35. **Moran, E., B. Zerler, T. M. Harrison, and M. B. Mathews.** 1986. Identification of separate domains in the adenovirus E1A gene for immortalization activity and the activation of virus early genes. Mol Cell Biol **6:**3470-3480.

36. **Nevins, J. R.** 1981. Mechanism of activation of early viral transcription by the adenovirus E1A gene product. Cell **26:**213-220.

37. **O'Connor, M. J., H. Zimmermann, S. Nielsen, H. U. Bernard, and T. Kouzarides.** 1999. Characterization of an E1A-CBP interaction defines a novel transcriptional adapter motif (TRAM) in CBP/p300. J Virol **73:**3574-3581.

38. **Parks, C. L., and T. Shenk.** 1997. Activation of the adenovirus major late promoter by transcription factors MAZ and Sp1. J Virol **71:**9600-9607.

39. **Pelka, P., J. N. Ablack, G. J. Fonseca, A. F. Yousef, and J. S. Mymryk.** 2008. Intrinsic structural disorder in adenovirus E1A: a viral molecular hub linking multiple diverse processes. J Virol **82:**7252-7263.

40. **Pelka, P., J. N. Ablack, M. Shuen, A. F. Yousef, M. Rasti, R. J. Grand, A. S. Turnell, and J. S. Mymryk.** 2009. Identification of a second independent binding site for the pCAF acetyltransferase in adenovirus E1A. Virology **391:**90-98.

41. **Pelka, P., J. N. Ablack, J. Torchia, A. S. Turnell, R. J. Grand, and J. S. Mymryk.** 2009. Transcriptional control by adenovirus E1A conserved region 3 via p300/CBP. Nucleic Acids Res **37:**1095-1106.

42. **Perricaudet, M., G. Akusjarvi, A. Virtanen, and U. Pettersson.** 1979. Structure of two spliced mRNAs from the transforming region of human subgroup C adenoviruses. Nature **281:**694-696.

43. **Phelps, W. C., S. Bagchi, J. A. Barnes, P. Raychaudhuri, V. Kraus, K. Munger, P. M. Howley, and J. R. Nevins.** 1991. Analysis of trans activation by human papillomavirus type 16 E7 and adenovirus 12S E1A suggests a common mechanism. J Virol **65:**6922-6930.

44. **Putzer, B. M., T. Stiewe, K. Parssanedjad, S. Rega, and H. Esche.** 2000. E1A is sufficient by itself to induce apoptosis independent of p53 and other adenoviral gene products. Cell Death Differ **7:**177-188.

45. **Rasti, M., R. J. Grand, A. F. Yousef, M. Shuen, J. S. Mymryk, P. H. Gallimore, and A. S. Turnell.** 2006. Roles for APIS and the 20S proteasome in adenovirus E1A-dependent transcription. EMBO J **25:**2710-2722.

46. **Ricciardi, R. P., R. L. Jones, C. L. Cepko, P. A. Sharp, and B. E. Roberts.** 1981. Expression of early adenovirus genes requires a viral encoded acidic polypeptide. Proc Natl Acad Sci U S A **78:**6121-6125.

47. **Roberts, B. E., J. S. Miller, D. Kimelman, C. L. Cepko, I. R. Lemischka, and R. C. Mulligan.** 1985. Individual adenovirus type 5 early region 1A gene products elicit distinct alterations of cellular morphology and gene expression. J Virol **56:**404-413.

48. **Rowe, W. P., R. J. Huebner, L. K. Gilmore, R. H. Parrott, and T. G. Ward.** 1953. Isolation of a cytopathogenic agent from human adenoids undergoing spontaneous degeneration in tissue culture. Proc Soc Exp Biol Med **84:**570-573.

49. **Ruley, H. E.** 1983. Adenovirus early region 1A enables viral and cellular transforming genes to transform primary cells in culture. Nature **304:**602-606.

50. **Schaeper, U., J. M. Boyd, S. Verma, E. Uhlmann, T. Subramanian, and G. Chinnadurai.** 1995. Molecular cloning and characterization of a cellular phosphoprotein that interacts with a conserved C-terminal domain of adenovirus E1A involved in negative modulation of oncogenic transformation. Proc Natl Acad Sci U S A **92:**10467-10471.

51. **Shaw, A. R., and E. B. Ziff.** 1980. Transcripts from the adenovirus-2 major late promoter yield a single early family of 3' coterminal mRNAs and five late families. Cell **22:**905-916.

52. **Shenk, T., N. Jones, W. Colby, and D. Fowlkes.** 1980. Functional analysis of adenovirus-5 host-range deletion mutants defective for transformation of rat embryo cells. Cold Spring Harb Symp Quant Biol **44 Pt 1:**367-375.

53. **Spector, D. J., D. N. Halbert, and H. J. Raskas.** 1980. Regulation of integrated adenovirus sequences during adenovirus infection of transformed cells. J Virol **36:**860-871.

54. **Spector, D. J., M. McGrogan, and H. J. Raskas.** 1978. Regulation of the appearance of cytoplasmic RNAs from region 1 of the adenovirus 2 genome. J Mol Biol **126:**395-414.

55. **Stephens, C., and E. Harlow.** 1987. Differential splicing yields novel adenovirus 5 E1A mRNAs that encode 30 kd and 35 kd proteins. EMBO J **6:**2027-2035.

56. **Trentin, J. J., Y. Yabe, and G. Taylor.** 1962. The quest for human cancer viruses. Science **137:**835-841.

57. **Turnell, A. S., R. J. Grand, C. Gorbea, X. Zhang, W. Wang, J. S. Mymryk, and P. H. Gallimore.** 2000. Regulation of the 26S proteasome by adenovirus E1A. EMBO J **19:**4759-4773.

58. **Ulfendahl, P. J., S. Linder, J. P. Kreivi, K. Nordqvist, C. Sevensson, H. Hultberg, and G. Akusjarvi.** 1987. A novel adenovirus-2 E1A mRNA encoding a protein with transcription activation properties. EMBO J **6:**2037-2044.

59. **Virtanen, A., and U. Pettersson.** 1983. The molecular structure of the 9S mRNA from early region 1A of adenovirus serotype 2. J Mol Biol **165:**496-499.

60. **Wang, G., and A. J. Berk.** 2002. In vivo association of adenovirus large E1A protein with the human mediator complex in adenovirus-infected and -transformed cells. J Virol **76:**9186-9193.

61. **Wente, S. R., and M. P. Rout.** 2010. The nuclear pore complex and nuclear transport. Cold Spring Harb Perspect Biol **2:**a000562.

62. **Whalen, S. G., R. C. Marcellus, A. Whalen, N. G. Ahn, R. P. Ricciardi, and P. E. Branton.** 1997. Phosphorylation within the transactivation domain of adenovirus E1A protein by mitogen-activated protein kinase regulates expression of early region 4. J Virol **71:**3545-3553.

63. **White, E., A. Denton, and B. Stillman.** 1988. Role of the adenovirus E1B 19,000-dalton tumor antigen in regulating early gene expression. J Virol **62:**3445-3454.

64. **White, E., and B. Stillman.** 1987. Expression of adenovirus E1B mutant phenotypes is dependent on the host cell and on synthesis of E1A proteins. J Virol **61:**426-435.

65. **Whyte, P., K. J. Buchkovich, J. M. Horowitz, S. H. Friend, M. Raybuck, R. A. Weinberg, and E. Harlow.** 1988. Association between an oncogene and an anti-oncogene: the adenovirus E1A proteins bind to the retinoblastoma gene product. Nature **334:**124-129.

66. **Wilson, M. C., and J. E. Darnell, Jr.** 1981. Control of messenger RNA concentration by differential cytoplasmic half-life. Adenovirus messenger RNAs from transcription units 1A and 1B. J Mol Biol **148:**231-251.

67. **Winberg, G., and T. Shenk.** 1984. Dissection of overlapping functions within the adenovirus type 5 E1A gene. EMBO J **3:**1907-1912.

68. **Wold, W. S. a. T.** 2007. Adenovirus Methods and Protocols: Adenoviruses, ad vectors, quantitation and animal models. Humana Press, Totawa, NJ.

69. **Wong, H. K., and E. B. Ziff.** 1994. Complementary functions of E1a conserved region 1 cooperate with conserved region 3 to activate adenovirus serotype 5 early promoters. J Virol **68:**4910-4920.

70. **Yousef, A. F., G. J. Fonseca, P. Pelka, J. N. Ablack, C. Walsh, F. A. Dick, D. P. Bazett-Jones, G. S. Shaw, and J. S. Mymryk.** 2010. Identification of a molecular recognition feature in the E1A oncoprotein that binds the SUMO conjugase UBC9 and likely interferes with polySUMOylation. Oncogene **29:**4693-4704.

71. **Zamanian, M., and N. B. La Thangue.** 1992. Adenovirus E1a prevents the retinoblastoma gene product from repressing the activity of a cellular transcription factor. EMBO J **11:**2603-2610.

Chapter 4

RASCAL IS A NEW HUMAN CYTOMEGALOVIRUS-ENCODED PROTEIN THAT LOCALIZES TO THE NUCLEAR LAMINA AND IN CYTOPLASMIC VESICLES AT LATE TIMES POST-INFECTION

4.1 Introduction

CMV is a highly prevalent betaherpesvirus that can cause severe multiorgan disease in immunocompromised individuals (45). The ability of this virus to infect an exceptionally wide variety of different cell types substantially contributes to pathogenesis (5, 68). CMV tropism is largely determined by a finely tuned interplay between cellular and viral factors, many of which act at the earliest stages of infection (30, 68). We recently showed that the cellular protein vimentin is required for efficient onset of infection in primary human foreskin fibroblasts (HF). Interestingly, the degree of reliance on the presence and integrity of vimentin intermediate filaments is dependent on the virus strain, with the broadly tropic strain TB40/E being more negatively affected than the HF-adapted, attenuated strain AD169 (44).

Serial passage of clinical isolates in HF or in EC has produced strains with different tropisms. The attenuated strains AD169 and Towne were developed as vaccine candidates by propagation in HF for more than 50 (AD169) and 125 (Towne) serial passages (19, 53, 61). During this process, both strains, compared to clinical isolates, accumulated multiple mutations and genomic deletions, resulting in the loss of more than 19 ORFs (8). The number of serial passages in HF of another commonly used strain, Toledo, has been more moderate (19, 54, 58). This, however, did not prevent the

emergence of numerous genomic mutations, including the inversion of a 15-kb fragment (8, 16, 56). As a consequence of these changes, productive infections by AD169, Towne, and Toledo are largely restricted to HF. In contrast, propagation of clinical isolates in EC has yielded a series of strains with more-intact genomes and broader tropisms, such as TB40/E, VHL/E, and FIX (VR1814) (25, 60, 71). These strains retain the ability to grow in a wider variety of cell types, including EC, epithelial cells, and DC, in addition to HF (23, 28, 59, 60, 68).

The UL128, UL130, and UL131A gene products were recently identified as essential mediators of CMV infection of EC and epithelial cells (26, 72, 73) and of virus transfer from infected EC to monocyte-derived DC (23). Each of these proteins is independently required for the broader tropisms of EC-propagated CMV isolates (63, 64), and the presence of mutations affecting their functionality has been directly linked to the inability of AD169, Towne, and Toledo to initiate productive infections in EC and epithelial cells (26, 72, 73). We have shown that mature Langerhans-type DC differentiated in vitro from CD34$^+$ hematopoietic progenitor cells are highly permissive to direct infection with TB40/E or VHL/E, with 48 to 72% of cells in culture expressing the viral immediate-early genes IE1 and IE2 at 48 hpi (28). In contrast, only 2 to 5% and 0% of mature Langerhans cells were IE1/IE2 positive after exposure to Towne and Toledo, respectively. However, productive infection was detected in 12 to 17% of cells infected with AD169, despite the fact that this strain lacks expression of the UL131A gene as a consequence of a frameshift mutation (26). These results suggested the existence of additional viral genes with products involved in mediating tropisms for specific cell types, such as DC. To identify possible candidates, we compared the amino acid

sequence of each ORF found in the genome of TB40-BAC4, a sequenced clone of the TB40/E strain in a bacterial artificial chromosome (BAC) (GenBank accession number EF999921) (69), to the sequence of each ORF found in AD169 and AD169- BAC (accession numbers X17403 and AC146999) (10, 49), Towne and Towne-BAC (accession numbers FJ616285, AC146851, and AY315197) (17, 18, 49), and Toledo-BAC (accession number AC146905) (49). The product of a putative ORF, originally identified by Murphy et al. and named c-ORF29 (49), was considered of particular interest because the amino acid sequence of the putative protein encoded by Toledo and Towne was extended by 79 residues compared to the putative protein encoded by TB40/E and AD169. This led to our speculation that that the extended version might result in a nonfunctional version of the c-ORF29-encoded protein. We thus focused our studies on the products of this ORF.

Here, we show for the first time that CMV c-ORF29 encodes a protein expressed at early to late times postinfection and localizes to the nuclear rim in peculiar invaginations of the nuclear lamina and in cytoplasmic vesicular structures at late times p.i. Based on this localization pattern, we named this gene product nuclear rim-associated cytomegaloviral protein, or RASCAL. Surprisingly, no difference was observed in the distributions of RASCAL during infection of HF with TB40/E or Towne, suggesting that the intracellular trafficking of this protein is not affected by the presence of the additional residues at the C terminus of RASCAL from strain Towne (RASCAL$_{Towne}$). Ectopic expression of RASCAL in human embryo kidney 293T (HEK293T) cells further revealed that this protein requires the presence of the NEC member UL50 to reach the nuclear rim, while coimmunoprecipitation (co-IP) assays provided evidence for the existence of an

interaction between RASCAL and UL50. These findings suggest that RASCAL may be a new component of the NEC with possible roles in remodeling the nuclear lamina during nucleocapsid egress from the nucleus.

4.2   Materials & Methods

4.2.1   *In silico* analysis

RASCAL amino acid sequences were analyzed using the following programs: ClustalW2 (32), NetPhosK (4), NetNGlyc (http://www.cbs.dtu.dk/services/NetNGlyc/), SignalP3.0 (2), Kyte-Doolittle hydropathy plot (31), TMpred (http://www.ch.embnet.org/software/TMPRED_form.html), TopPred II (11), dense alignment surface (DAS) (13), ESLpred (3), HSLpred (22), TargetP1.1(20), and SubLoc v1.0 (29).

4.2.2   Cells and virus

 HF and HEK293T cells were gifts of E. S. Mocarski, Emory University, Atlanta, GA, and were propagated in Dulbecco's modified Eagle medium supplemented with 10% fetal clone serum III (HyClone), 100 U/ml penicillin, 100 μg/ml streptomycin, 4 mM HEPES, and 1 mM sodium pyruvate(all from Gibco Invitrogen Corp.). HF were used between passages 17 and 27 postisolation. Human CMV strains AD169varATCC and TB40/E and the green fluorescent protein (GFP)-tagged derivative of TownevarRIT3, Towne/GFP-IE2 (J. Xu, D. Formankova, and E. S. Mocarski, unpublished), were originally obtained from the American Type Culture Collection, from C. Sinzger

(Tübingen, Germany), and from E. S. Mocarski (Emory University, Atlanta, GA), respectively. Propagation and purification of all strains were performed as previously described (28).

4.2.3 HF infection and cell transfection

HF were plated at a density of 5×10^4 cells/cm^2 3 days prior to exposure to AD169, TB40/E, or Towne/GFP-IE2 at a multiplicity of infection (MOI) of 3 or 5. Mock-infected samples were exposed to culture medium alone. After virus adsorption at 37°C in 5% CO2 for 1 h, the inoculum was removed, and cells were washed three times with medium prior to incubation in fresh medium until they were harvested at different times p.i. For phosphonoformic acid (PFA) treatment, HF were exposed to Towne/GFP-IE2 (MOI of 3) for 1 h at 37°C, washed, and further incubated in fresh culture medium containing 300 µg/ml of PFA (Sigma, St. Louis, MO). HEK293T cell transfection was performed using PolyFect (Qiagen) as per the manufacturer's guidelines.

4.2.4 mRNA isolation and RT-PCR

mRNA was isolated from mock-, TB40/E-, or Towne/GFP-IE2-infected HF using the µMACS mRNA isolation kit (Miltenyi Biotec, Bergisch Gladbach, Germany). First-strand cDNA synthesis was performed using SuperScript III reverse transcriptase according to the manufacturer's guidelines (Gibco Invitrogen Corp.). c-ORF29 TB40/E was amplified with the forward primer GCGGATCCTAATGGGGGAACGCC (labeled a > in Fig. 2A,top) and the reverse primer GTGGATCCAGAGATGCGGAAAAGCC (labeled <b in Fig. 2A, top), c-ORF29 Towne was amplified with the forward primer

GCGGATCCTAATGGGGGAACGCC (labeled a > in Fig. 2A, top) and the reverse primer CCTCGAGAAAAGCACGCAAGC (labeled <c in Fig. 2A, top), vimentin was amplified with the forward primer CGGATCCATGTCCACCAG and the reverse primer CGAATTCTTCAAGGTCAT, UL99 was amplified with the forward primer CGGATCCATGGGTGGCGAACTCT and the reverse primer GGATATCTGAAAGGACAAGGGGGCG, and β-actin cDNA was amplified with the forward primer GGTCATCACCATTGGCAATGAGCGG and the reverse primer GGACTCGTCATACTCCTGCTTGCTG.

4.2.5   Plasmid construction

L-RASCAL$_{TB40/E}$ (where the prefix "L" stands for LNCX) was generated by excising GFP from LNCX-GFP (LGFP) (36) using EcoRI and EcoRV and by replacing it with the RASCALTB40/E sequence amplified by PCR using a forward primer containing the EcoRI restriction site (GGAATTCATGGGGGAACGCCGTGTG) and a reverse primer containing the RASCALTB40/E stop codon and the EcoRV restriction site (GCGATATCTTAAGATGCGGAAAAGCCA). L-RASCAL$_{TB40/E-GFP}$ was generated by cloning RASCALTB40/E, lacking its stop codon, in frame with the N terminus of GFP using the EcoRI and BamHI restriction sites present in LGFP. The forward primer used to make L-RASCALTB40/E-GFP was the same as that used to make L-RASCAL$_{TB40/E}$. The reverse primer (GTGGATCCAGAGATGCGGAAAAGCC) contained a BamHI restriction site and was designed to remove the RASCAL stop codon. Hemagglutinin-tagged LNCX UL50 (LNCX UL50-HA) was generated by amplifying the UL50 sequence from cDNA populations derived from AD169-infected HF using the forward

primer AGAATTCATGGAGATGAACAAGGTT, containing an EcoRI restriction site, and the reverse primer TTTTGTCGACTCAAGCGTAATCTGGAACATCGTATGGGTAGTCGCGGTGTGCG GAG, containing the HA tag nucleotide sequence. This PCR product was cloned into the pSC-B vector (Stratagene, La Jolla, CA) and subsequently excised using EcoRI before being ligated into the EcoRI restriction site of LNCX (43). FLAG- tagged L-UL53 (L-UL53-FLAG) was created by amplifying the UL53 sequence from cDNA populations derived from TB40/E-infected HF using the forward primer AGAATTCATGTCTAGCGTGAGCG, containing the EcoRI restriction site, and the reverse primer TTTTGTCGACTCACTTGTCATCGTCGTCCTTGTAGTCAGGCGCACGAATGCTG TTGA, containing the FLAG tag nucleotide sequence and the SalI restriction site. The UL53-FLAG PCR product was ligated into the EcoRI and SalI sites of LGFP after excision of the GFP coding sequence.

4.2.6   Generation of anti-RASCAL Abs

Polyclonal rabbit antibodies (Abs) were raised by ProSci Inc. (Poway, CA) against the RASCAL peptide YAPFDSHRRHVSELRGHRD conjugated to the keyhole limpet hemocyanin. Abs were affinity purified and were provided at a final concentration of 1.7 mg/ml.

4.2.7   Immunoblot analysis

Cell pellets from mock-, TB40/E-, or Towne/GFP-IE2-infected HF and from HEK293T cells nontransfected or transiently transfected with L-RASCAL$_{TB40/E-GFP}$ or with L-RASCAL$_{TB40/E}$ were resuspended in 3% sodium dodecyl sulfate (SDS) lysis buffer containing 125 mM Tris-HCl (pH 6.8), 3% SDS, 10 mM dithiothreitol, 0.4 mM phenylmethylsulfonyl fluoride, and complete EDTA-free protease inhibitor cocktail (Roche). Cell lysates were boiled at 100°C for 5 min, and cell debris were eliminated by centrifugation at 16,100 × g for 3 min. Protein concentrations were determined with the DC protein assay kit (Bio-Rad). Protein extracts were then separated by electrophoresis on a 15% SDS-polyacrylamide gel and transferred to polyvinylidene difluoride membranes. Membranes were blocked overnight at 4°C in blocking buffer containing 10 mM Tris-Cl (pH 7.5), 100 mM NaCl, 5% milk powder, 0.1% Tween 20 prior to incubation with rabbit anti-RASCAL Abs (1:1,000) or with mouse anti-HA Abs (1:1,000) for 1 h at room temperature (RT). Membranes were rinsed in wash buffer (10 mM Tris-Cl [pH 8.0], 150 mM NaCl, and 0.05% Tween 20) and were incubated with horseradish peroxidase-conjugated goat anti-rabbit IgG (1:4,000; Vector Laboratories) or goat anti-mouse IgG (1:5,000; Vector Laboratories) for 1 h at RT. For reprobing, membranes were incubated in 62.5 mM Tris-Cl (pH 6.8), 100 mM β-mercaptoethanol, and 2% SDS at 50°C for 30 min, rinsed with phosphate-buffered saline (PBS) containing 0.1% Tween 20, blocked overnight at 4°C, and incubated with preimmune rabbit serum (1:1,000) followed by horseradish peroxidase-conjugated goat anti-rabbit IgG (1:4,000), both for 1

h at RT. Signal was developed by enhanced chemiluminescence (ECL plus kit; GE Healthcare).

4.2.8   Co-immunoprecipitation assays

HEK293T cells were transfected with LNCX (control) or were cotransfected with L-RASCAL$_{TB40/E}$ and LNCX UL50-HA at a 1:3 molar ratio or with LNCX UL50-HA and L-UL53-FLAG at a 1:1 molar ratio in T25 flasks. At 24 h posttransfection, cells were harvested in 500 μl of co-IP buffer containing 50 mM Tris-HCl (pH 8), 100 mM NaCl, 5 mM EDTA, 0.5% NP-40, 1 mM phenylmethylsulfonyl fluoride, and complete EDTA-free protease inhibitor cocktail (Roche) prior to the addition of 5 μg of mouse monoclonal anti-HA Abs (Invitrogen) or of polyclonal anti-RASCAL Abs for 2 h at 4°C under rotation. Extracts were incubated with 100 μl of protein A-Sepharose bead slurry (Sigma) for 2 h at 4°C, pelleted, washed in lysis buffer containing 200 mM NaCl, and subjected to immunoblot analysis as described above.

4.2.9   Immunofluorescence staining analysis

Cells were fixed in 3.7% paraformaldehyde (Fisher Chemicals, Fairlawn, NJ) for 30 min at RT, permeabilized in 0.2% Triton X-100 (USB Corporation, Cleveland, OH) for 20 min on ice, and blocked in 100% horse serum (HS; PML Microbiologicals, Wilsonville, OR) for 30 min at RT. Cells were then incubated with rabbit polyclonal anti-RASCAL Abs (1:500) alone or in combination with monoclonal Abs directed against the FLAG tag (1:1,000; clone M2; Sigma, St. Louis, MO), the HA tag (1:500; Invitrogen), IE1/IE2 (1:500; fluorescein isothiocyanate [FITC]-conjugated MAb810F; Chemicon, Temecula,

CA), lamin B (1:50; Santa Cruz Biotechnology, Santa Cruz, CA), or lamin A/C (1:50; Santa Cruz Biotechnology, Santa Cruz, CA). Samples were washed in PBS-0.05% Tween 20 prior to incubation with Alexa Fluor 594-conjugated goat anti-rabbit IgG Abs (1:500; Molecular Probes, Eugene, OR) alone or in combination with FITC-conjugated goat anti-mouse IgG Abs (1:100; Invitrogen, Carlsbad, CA). For control stainings, cells were incubated with preimmune sera diluted 1:500 in 100% HS. For dual staining of cells expressing UL50-HA and UL53-FLAG, samples were incubated with mouse monoclonal anti-FLAG Abs and rabbit polyclonal anti-HA Abs (1:500; Zymed), followed by FITC-conjugated goat anti-mouse IgG Abs and Alexa Fluor 594-conjugated goat anti-rabbit IgG Abs. All Abs were diluted in 100% HS and were incubated on samples for 1 h at RT. Nuclei were labeled with Hoechst 33342 (0.2 mg/ml; Molecular Probes, Eugene, OR) for 3 min at RT and were mounted in 90% glycerol-10% PBS containing 2.5 g/liter of 1,4-diazabicyclo(2,2,2)octane (DABCO; Alfa Aesar, Pelham, NH). Samples were analyzed on a Zeiss Axioskop2 magneto-optical trap fluorescence microscope equipped with a QImaging Retiga 1300-coded monochrome 12-bit camera. Images were captured and pseudocolored using Northern Eclipse version 7.0 software. Confocal images were acquired on a Zeiss LSM 510 META ConfoCor2 confocal laser scanning microscope equipped with Zeiss LSM 510 META image processing software.

4.3   Results

4.3.1   Identification of the ORF encoding RASCAL and *in silico* analysis of the predicted amino acid sequence

The genomic region of TB40-BAC4 corresponding to nucleotides 9100 to 11200 was screened for the presence of ORFs with the potential to encode proteins of at least 80 amino acids (aa) and containing a 5'ATG codon. One ORF of 294 nucleotides encoding a putative protein of 97 aa was found. As described for c-ORF29 (48, 49), the sequence of this ORF was located on the negative strand of the genome (nucleotides 9855 to 10148 in TB40-BAC4) and partially overlapped (206 nucleotides) the 5' end of the US17 gene (Fig. 1A, left). An ortholog of this ORF was found in the Towne-BAC genome, spanning nucleotides 199167 to 199697 (in GenBank accession no. AY315197) and overlapping the 5' end of the US17 gene by 442 nucleotides (Fig. 4-1A, right). In contrast to what was previously reported for c-ORF29 (48, 49), however, searches of the nonredundant nucleotide collection databases using the BLASTN algorithm failed to reveal the presence of a full-length c-ORF29 ortholog in the genome of chimpanzee CMV. A ClustalW2 global alignment of the predicted amino acid sequence of c-ORF29 from strain TB40-BAC4 (RASCAL$_{TB40/E}$) with sequences from 13 other human CMV strains showed that RASCAL is highly conserved and that not only strains Towne and Toledo, but also two new CMV strains, HAN20 and HAN38, carry a longer version of this protein, containing 79 additional amino acids (Fig. 4-1B). No significant homology

between either isoform of RASCAL and proteins of cellular or viral origin was detected in extensive searches of multiple amino acid sequence databases.

Two potential phosphorylation sites with scores greater than 80% were identified in RASCAL$_{TB40/E}$ by the NetPhosK software, one of which was specific for protein kinase C (PKC) at Thr 48 and the other for protein kinase A (PKA) at Ser 65. One additional site for PKA was found in the longer version of the protein at Ser 103 (Fig. 4-1B). A single potential N-glycosylation site was detected by the NetNGlyc software at residue Asn 17 (Fig. 4-1B). However, the SignalP3.0 algorithm failed to predict the presence of a signal sequence at the N terminus of RASCAL, suggesting that this protein may not be recognized by the glycosylation machinery *in vivo*.

A Kyte-Doolittle hydropathy plot of RASCAL$_{TB40/E}$ revealed the presence of two regions of at least 17 aa with overall hydrophobicity values greater than 1, one located at the N terminus (aa 6 to 24) and the other at the C terminus (aa 79 to 97) (Fig. 4-1C, left, shaded boxes). Both were predicted to contain a transmembrane domain (TMD) by three protein topology prediction algorithms, TMpred, TopPred II, and DAS. The amino acid sequences of these putative TMDs are highly conserved in all strains (Fig. 4-1B, black lines). Although strains Merlin, JP, and HAN13 carry a single amino acid replacement of Leu 12 with Ile, HAN38 carries a Leu 13-to-Ser substitution, and 3301 carries a Val 6-to-Met substitution, none of these changes altered the outcome of the predictions. Two additional hydrophobic regions consisting of more than 17 aa were detected in RASCAL$_{Towne}$ (Fig. 4-1C, right, boxes with dashed borders), but neither was predicted to be a TMD by all three software programs.

4.3.2 RASCAL expression in infected and transfected cells

To determine if c-ORF29 was expressed during infection, we performed reverse transcriptase-PCR (RT-PCR) analyses of mRNA extracts from mock-, TB40/E-, or Towne/GFP-IE2-infected HF using the primers schematically depicted in the top panel of Fig. 4-2A. A single product of approximately 300 nucleotides was detected in extracts from TB40/E-infected cells amplified with primers a > and < b (Fig. 4-2A, bottom). Mock-infected samples and control reaction mixtures lacking the cDNA template were negative (Fig. 4-2A, bottom, and data not shown). Although the sequence of primer < c is complementary to nucleotides 9621 to 9624 of the TB40/E genome, no product was obtained when the same extracts were amplified with primers a > and < c (not shown), suggesting that no transcript spanning the region between these primers was produced in cells infected with TB40/E. In contrast, a single product of about 550 nucleotides was observed in extracts from Towne/GFP-IE2-infected cells amplified using primers a > and < c (not shown). Sequence analysis of this PCR product confirmed the presence of a T-to-C mutation at position 292, resulting in the conversion of a TAA stop codon into a CAA codon coding for the amino acid Gln. RT-PCR analyses of mRNA extracts from HF infected with TB40/E in the presence of PFA revealed that c-ORF29 expression was reduced, but not completely abrogated, in the absence of viral DNA replication (Fig. 4-2B). In contrast, no expression of the true late gene UL99 was detected in PFA-treated cells (Fig. 4-2B). Together, these data indicate that c-ORF29 is transcribed with early-late kinetics during infection and confirm that the Towne strain carries a longer version of this ORF.

To determine if c-ORF29 did encode a protein, affinity-purified, polyclonal rabbit Abs were raised against residues 21 to 39 of the predicted RASCAL$_{TB40/E}$ amino acid sequence. The specificities of these Abs were tested using Western blot analyses of protein extracts from HEK293T cells transiently transfected with expression plasmids encoding RASCAL$_{TB40/E}$ only or RASCAL$_{TB40/E}$ fused to the N terminus of the GFP amino acid sequence (RASCAL$_{TB40/E-GFP}$). Two proteins with expected molecular masses of approximately 11 kDa (Fig. 4-2C, asterisk) and 38 kDa (Fig. 4-2C, arrowhead) were detected in extracts from cells transfected with expression plasmids encoding RASCAL$_{TB40/E}$ and RASCAL$_{TB40/E-GFP}$, respectively. These proteins were not recognized by the anti-RASCAL Abs in extracts from nontransfected cells (Fig. 4-2C) or by the preimmune serum (not shown). Moreover, the 38-kDa protein was also specifically detected in membranes reprobed with anti-GFP monoclonal Abs (not shown), indicating that this polypeptide did contain both the RASCAL and the GFP epitopes. Two additional bands of 15 and 20 kDa were observed in extracts from both transfected and nontransfected cells and were considered to be cellular proteins nonspecifically recognized by the anti-RASCAL Abs. Finally, two products with molecular masses of less than 15 kDa were observed exclusively in cells expressing RASCALTB40/E-GFP, suggesting that they might correspond to degradation products of the fusion protein.

To assess if RASCAL was expressed in CMV-infected cells, protein extracts from mock-, TB40/E-, and Towne/GFP-IE2-infected HF were separated by SDS-polyacrylamide gel electrophoresis (PAGE). The same membrane was probed with anti-RASCAL Abs and, after being stripped, with preimmune serum. A single band of approximately 11 kDa was detected in extracts from TB40/E-infected HF and in extracts from HEK293T cells

expressing RASCAL$_{TB40/E}$, used as the control (Fig. 4-2D, left, asterisks). This band was not detected in samples from mock- and Towne/GFP-IE2-infected cells. In addition, two proteins with molecular masses larger than 15 kDa but smaller than 20 kDa were observed exclusively in extracts from Towne/GFP-IE2-infected HF (Fig. 4-2D, left). While the larger protein (Fig. 4-2D, left, square) is likely to correspond to RASCAL$_{Towne}$ (predicted molecular mass, 19.4 kDa), the smaller protein remains uncharacterized. None of these bands, including the nonspecific protein of approximately 15 kDa recognized by the anti-RASCAL Abs in HF and HEK293T cell extracts, was detected by the preimmune serum (Fig. 4-2D, right).

4.3.3   RASCAL localizes at the nuclear envelope and in cytoplasmic vesicular structures during infection

To establish the subcellular localization of RASCAL during infection, mock-, AD169-, TB40/E-, and Towne/GFP-IE2-infected HF (MOI of 5) were harvested at 24, 48, 72, 96, 120, and 144 hpi. Cells were stained with the preimmune serum or with the affinity-purified anti-RASCAL Abs and with FITC- conjugated anti-IE1/IE2 Abs. Nuclei were stained with Hoechst 33342. No signal was observed in mock-infected cells (Fig. 4-3A to C), indicating that no cellular proteins were recognized nonspecifically by the anti-RASCAL Abs in immunofluorescence staining assays. Similarly, staining of infected cells with the preimmune serum did not yield any specific signal (not shown). At 24 hpi, RASCAL fluorescence was barely detectable (not shown). By 48 hpi, a prominent cytoplasmic signal was observed in infected cells, with a punctuate pattern more densely concentrated around the nucleus (Fig. 4-3D to F). At 72 hpi, RASCAL accumulation in a perinuclear ring was clearly detectable in a large proportion of cells (Fig. 4-3G to I,

arrow), and by 96 hpi most of the RASCAL signal emanated from the nuclear rim, with very little diffuse fluorescence remaining in the cytoplasm (Fig. 4-3J to L). In some cells, RASCAL appeared to also concentrate in cytoplasmic vesicular compartments distributed from the nuclear envelope to the cell surface (Fig. 4-3J to L, asterisk). At 96 hpi and, more prominently, at 120 hpi, RASCAL fluorescence appeared to originate almost exclusively from peculiar structures likely located on the nuclear envelope and characterized by a central "knot" with rod-like extensions (Fig. 4-3M to O, arrowheads). These nuclear envelopes and the cytoplasmic structures became clearly visible at 144 hpi (Fig. 4-3P to R), at a time when few or no perinuclear rings were still detectable. The same staining pattern was observed in AD169- and TB40/E-infected cells (not shown), indicating that the presence of the 79 additional amino acids in RASCAL$_{Towne}$ did not interfere with its localization.

To determine if the RASCAL protein was produced in the absence of viral DNA replication, HF were infected with Towne/GFP-IE2 (MOI of 3) in the presence or absence of PFA. Cells were harvested at 24, 48, 72, 96, 120, and 144 hpi and stained for RASCAL and for IE1/IE2. As expected, intranuclear accumulation of IE1/IE2 at the sites of viral genome replication (52) was observed exclusively in untreated HF (Fig. 4-4B and D). In these cells, RASCAL expression was detected starting from 24 hpi, and signal accumulated at the nuclear rim, on the nuclear envelope, and in cytoplasmic vesicles at late times p.i. (Fig. 4-4A and C). In contrast, no RASCAL-specific signal was detected in PFA-treated cells at each time p.i. (Fig. 4-4E and G and data not shown), suggesting that expression of the RASCAL protein was reduced to levels below detection in the absence of viral DNA replication.

FIG. 4-1. Genomic location of the c-ORF29 gene and in silico analysis of the RASCAL amino acid sequence. (A) Schematic map of the TB40-BAC4 (GenBank accession no. EF999921) and of the Towne-BAC (accession no. AY315197) genomic regions corresponding to nucleotides 9200 to 10200 (TB40/E) and 198750 to 199750 (Towne). The black horizontal line depicts the viral genome, with vertical lines positioned every 500 nucleotides. ORFs are represented by arrows pointing in the direction of transcription. (B) ClustalW2 alignment of RASCAL amino acid sequences from 14 human CMV strains. Viral genome accession numbers are as follows: TB40-BAC, EF999921; PH-BAC, AC146904; TR-BAC, AC146906; FIX-BAC, AC146907; 3157, GQ221974; 3301, GQ466044; HAN13, GQ221973; JP, GQ221975; Merlin, AY44689; AD169, X17403; HAN38, GQ396662; HAN20, GQ396663; Toledo-BAC, AC146905; and Towne-BAC, AC146851. Dots and dashes indicate identical and absent amino acids, respectively. The asterisks mark the specific amino acid predicted to be phosphorylated by PKA or PKC or to be N glycosylated (N-glyc). The black lines underscore the putative TMDs. (C) Kyte-Doolittle (K-D) hydropathy plot of RASCAL$_{TB40/E}$ and RASCAL$_{Towne}$ amino acid sequences, performed using a window size of 9 aa. The shaded boxes include the stretch of amino acids corresponding to the putative TMDs, while the boxes with the dashed borders include the two additional hydrophobic regions of more than 17 aa detected in RASCAL$_{Towne}$.
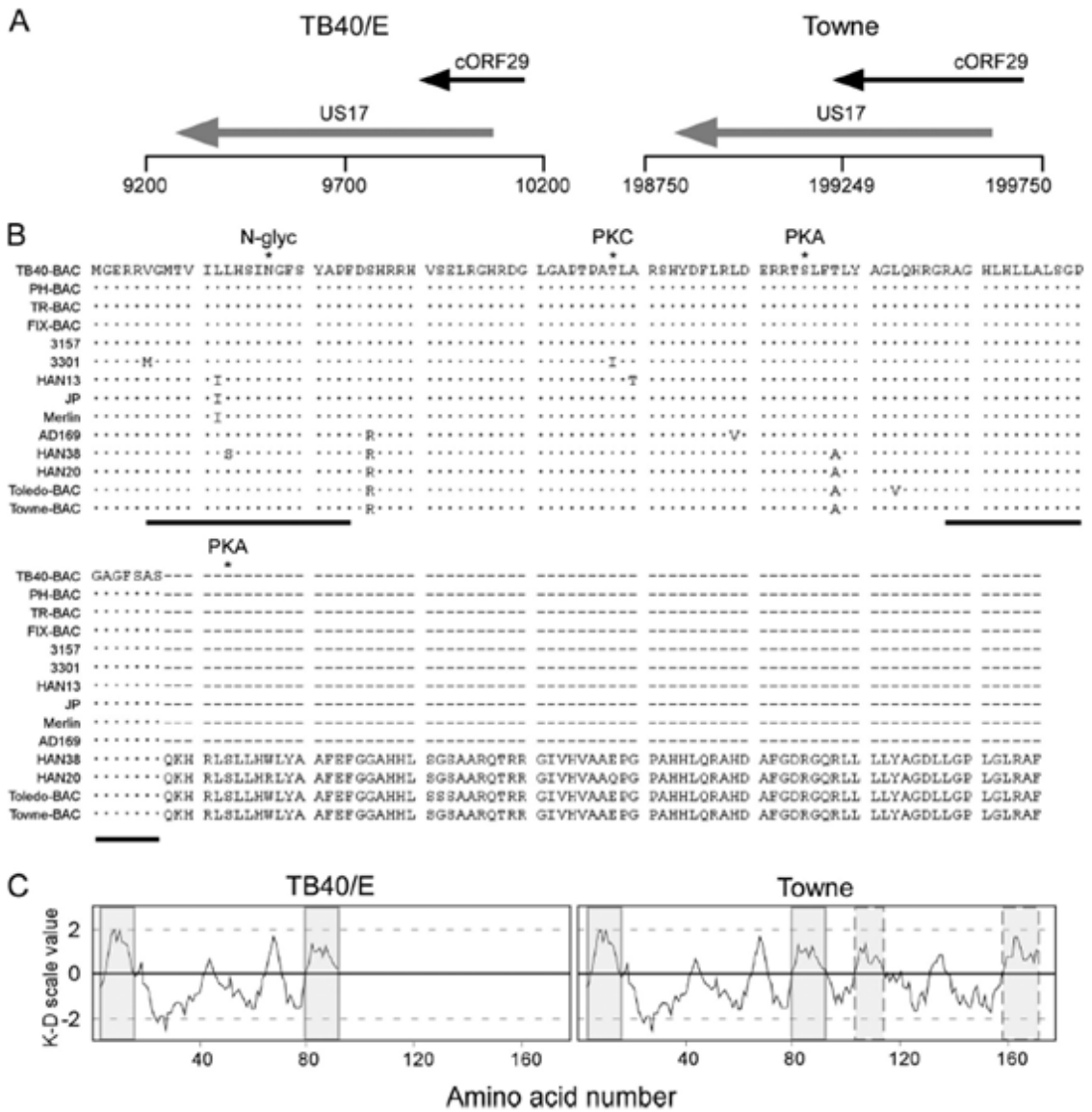
4.3.4 RASCAL and lamin B colocalize at the nuclear lamina and in cytoplasmic vesicular structures

To establish the subcellular localization of RASCAL during infection, mock-, AD169-, TB40/E-, and Towne/GFP-IE2-infected HF (MOI of 5) were harvested at 24, 48, 72, 96, 120, and 144 hpi. Cells were stained with the preimmune serum or with the affinity-purified anti-RASCAL Abs and with FITC-conjugated anti-IE1/IE2 Abs. Nuclei were highlighted with Hoechst 33342. No signal was observed in mock-infected cells (Fig. 4-3A to C), indicating that no cellular proteins were recognized nonspecifically by the anti-RASCAL Abs in immunofluorescence staining assays. Similarly, staining of infected cells with the preimmune serum did not yield any specific signal (not shown). At 24 hpi, RASCAL fluorescence was barely detectable (not shown). By 48 hpi, a prominent cytoplasmic signal was observed in infected cells, with a punctuate pattern more densely concentrated around the nucleus (Fig. 4-3D to F). At 72 hpi, RASCAL accumulation in a perinuclear ring was clearly detectable in a large proportion of cells (Fig. 4-3G to I, arrow), and by 96 hpi most of the RASCAL signal emanated from the nuclear rim, with very little diffuse fluorescence remaining in the cytoplasm (Fig. 4-3J to L). In some cells, RASCAL appeared to also concentrate in cytoplasmic vesicular compartments distributed from the nuclear envelope to the cell surface (Fig. 4-3J to L, asterisk). At 96 hpi and, more prominently, at 120 hpi, RASCAL fluorescence appeared to originate almost exclusively from peculiar structures likely located on the nuclear envelope and characterized by a central "knot" with rod-like extensions (Fig. 4-3M to O, arrowheads). These nuclear envelopes and the cytoplasmic structures became clearly visible at 144 hpi

(Fig. 4-3P to R), at a time when few or no perinuclear rings were still detectable. The same staining pattern was observed in AD169- and TB40/E-infected cells (not shown), indicating that the presence of the 79 additional amino acids in RASCAL$_{Towne}$ did not interfere with its localization.

To determine if the RASCAL protein was produced in the absence of viral DNA replication, HF were infected with Towne/GFP-IE2 (MOI of 3) in the presence or absence of PFA. Cells were harvested at 24, 48, 72, 96, 120, and 144 hpi and stained for RASCAL and for IE1/IE2. As expected, intranuclear accumulation of IE1/IE2 at the sites of viral genome replication (52) was observed exclusively in untreated HF (Fig. 4-4B and D). In these cells, RASCAL expression was detected starting from 24 hpi, and signal accumulated at the nuclear rim, on the nuclear envelope, and in cytoplasmic vesicles at late times p.i. (Fig. 4-4A and C). In contrast, no RASCAL-specific signal was detected in PFA-treated cells at each time p.i. (Fig. 4-4E and G and data not shown), suggesting that expression of the RASCAL protein was reduced to levels below detection in the absence of viral DNA replication.

4.3.5 RASCAL interacts with UL50 and requires its presence to gather at the nuclear lamina

At early times p.i. (48 hpi), RASCAL localizes mainly in a cytoplasmic punctuate pattern (Fig. 4-3D to F). Relocalization to the nuclear rim occurs only later in infection (72 hpi [Fig. 4-3G to I]), at a time when both UL50 and UL53 are abundantly expressed and gathered at the NEC. This suggested that RASCAL might require the presence of other NEC components to reach the nuclear lamina. To test if, akin to UL53, RASCAL relocalization to the nuclear lamina was mediated by UL50, three expression plasmids

were constructed, one containing RASCAL$_{TB40/E}$, one containing a C-terminal FLAG-tagged version of UL53 (UL53-FLAG), and one containing a C-terminal HA-tagged version of UL50 (UL50-HA), as described previously (14, 40). HEK293T cells transfected with one of these constructs were stained with rabbit anti-RASCAL Abs and with mouse anti-HA or mouse anti-FLAG Abs. No signal was detected in cells expressing UL50-HA or UL53-FLAG after being stained with anti-RASCAL Abs (Fig. 4-7B and D), indicating that these Abs did not cross-react with either protein. As previously shown (7, 41, 42), UL50-HA localized at the nuclear lamina and in cytoplasmic vesicular structures (Fig. 4-7A), while UL53-FLAG was predominantly nuclear, with some cytoplasmic dotted staining (Fig. 4-7C). When expressed in the

FIG. 4-2. RASCAL expression in infected and transfected cells. (A, top) Schematic depiction of the primers used to amplify c-ORF29 by RT-PCR from TB40/E- or Towne/GFP-IE2-infected HF. The > and < symbols depict the direction of polymerization. The sequence of primer a > is complementary to nucleotides 1 to 13 of c-ORF29$_{TB40/E}$ and of c-ORF29$_{Towne}$, the sequence of primer < b is complementary to nucleotides 277 to 291 of c-ORF29$_{TB40/E}$ and of c-ORF29$_{Towne}$ and to nucleotides 189 to 203 of US17, while the sequence of primer < c is complementary to nucleotides 515 to 528 of c-ORF29Towne and nucleotides 427 to 440 of US17. (Bottom) RT-PCR analysis of c-ORF29 transcription in mock or TB40/E-infected HF at the indicated times p.i., using primers a > and < b. Amplification of vimentin's cDNA was used as the PCR control. (B) RT-PCR analysis of c-ORF29 and of UL99 transcription in HF infected with TB40/E in the presence (+) or absence (-) of PFA (300 μg/ml). Amplification of β-actin's cDNA was used as the PCR control. (C) Immunoblot analysis results of RASCAL$_{TB40/E}$ expression in protein extracts from HEK293T cells nontransfected or transfected with expression plasmids encoding RASCAL$_{TB40/E-GFP}$ or RASCAL$_{TB40/E}$. The blot was incubated with an anti-RASCAL polyclonal Ab as described in Materials and Methods. Expected molecular masses were 10.6 kDa for RASCAL$_{TB40/E}$ and 37.6 kDa for RASCAL$_{TB40/E-GFP}$. Asterisk, RASCAL$_{TB40/E}$; arrowhead, RASCAL$_{TB40/E-GFP}$. (D) Immunoblot analysis of RASCAL expression in protein extracts from mock-, TB40/E-, or Towne/GFP-IE2-infected HF and in HEK293T cells expressing RASCAL$_{TB40/E}$. The same membrane was incubated first with an anti-RASCAL polyclonal Ab (left) and subsequently with the preimmune serum (right) as described in Materials and Methods. Expected molecular masses were 10.6 kDa for RASCALTB40/E and 19.4 kDa for RASCALTowne. Asterisk, RASCAL$_{TB40/E}$; square, RASCAL$_{Towne}$.
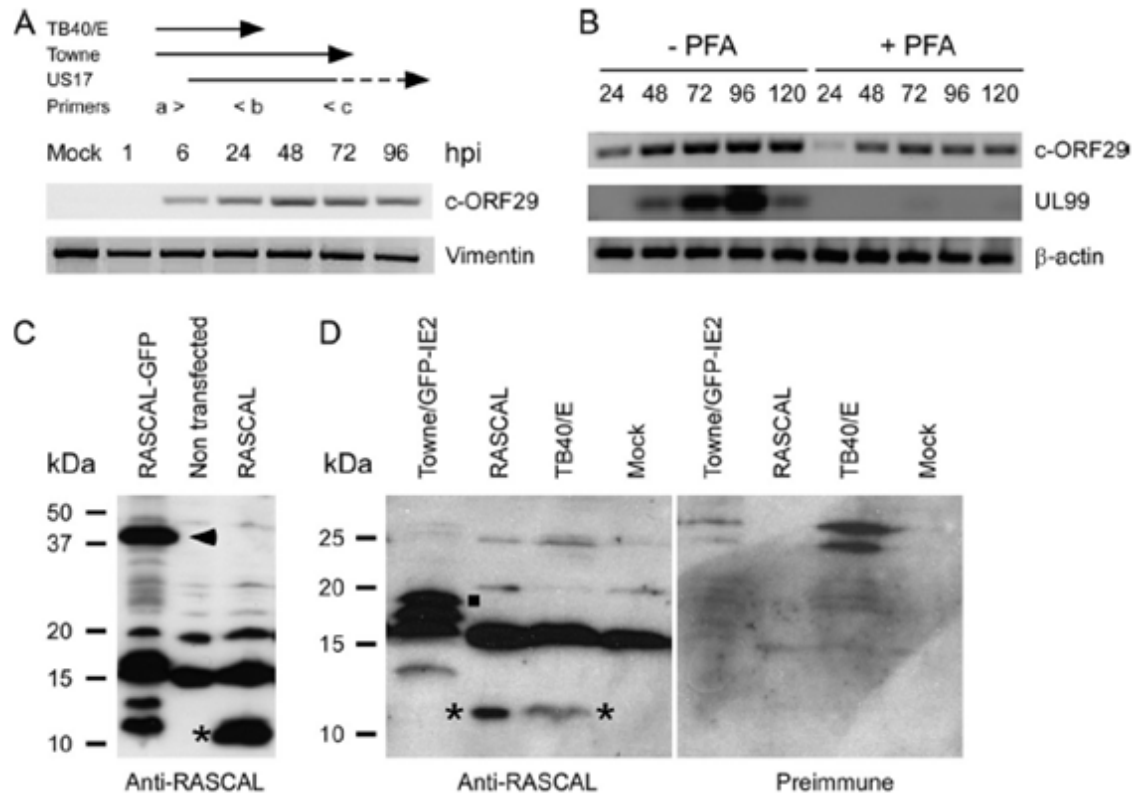
FIG. 4-3. RASCAL intracellular localization. Mock-infected (A to C) or Towne/GFP-IE2-infected HF (MOI of 5) (D to R) were harvested at the indicated times p.i. and were stained with affinity-purified rabbit anti-RASCAL polyclonal Abs followed by Alexa Fluor 594-conjugated goat anti-rabbit Abs. The signal emitted from the GFP-IE2 protein was further amplified with FITC-conjugated anti-IE1/IE2 Abs, and nuclear DNA was stained with Hoechst 33342. The arrows point at RASCAL accumulation at the nuclear rim, the arrowheads indicate the peculiar structures observed on the nuclear surface at late times p.i., and the asterisks mark the locations of the cytoplasmic RASCAL-positive vesicles. Original magnification, 400×.

RASCAL IE1/IE2 Hoechst

Mock A B C

48 hpi D E F

72 hpi G H I

96 hpi J K L

120 hpi M N O

144 hpi P Q R
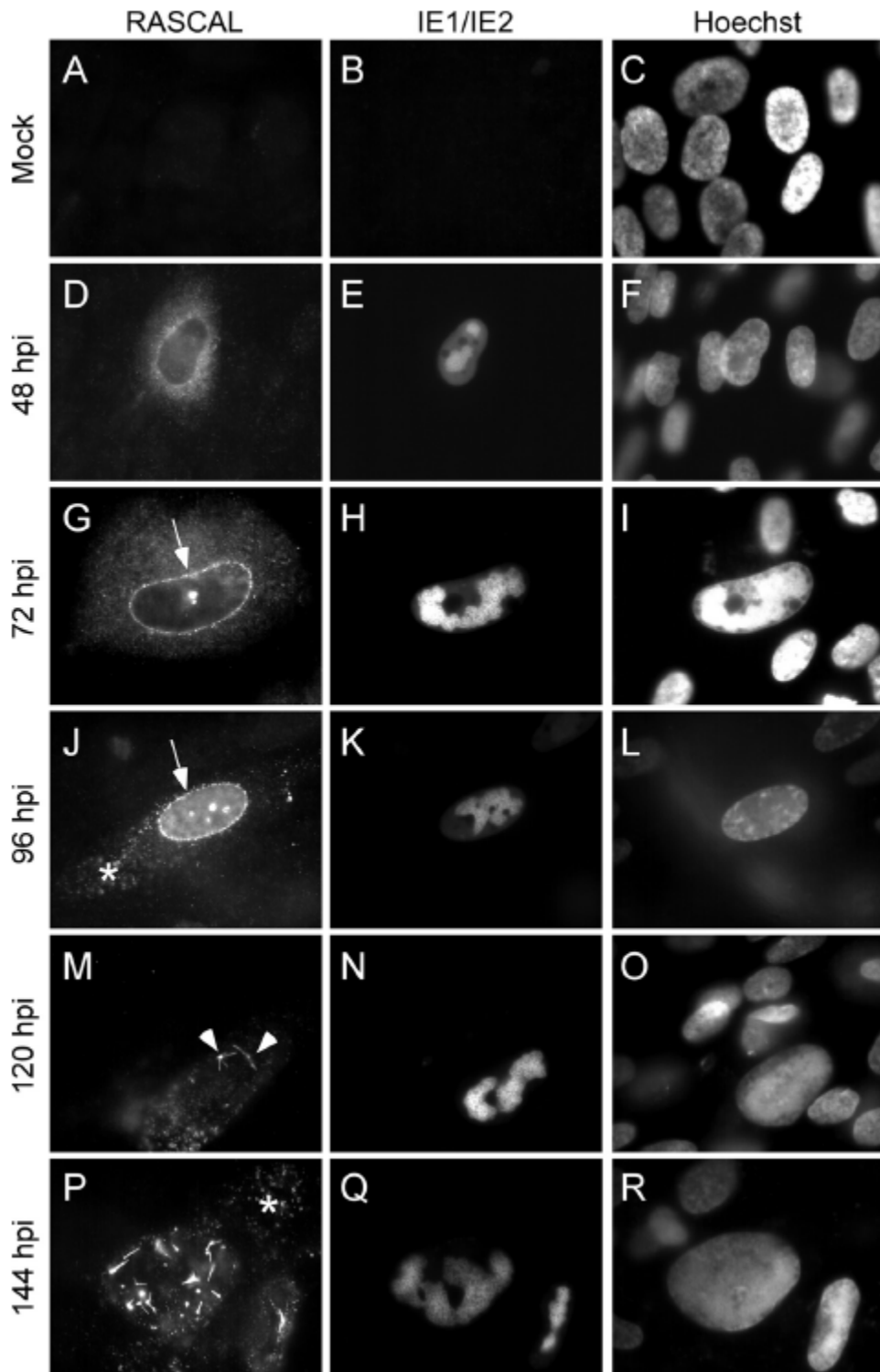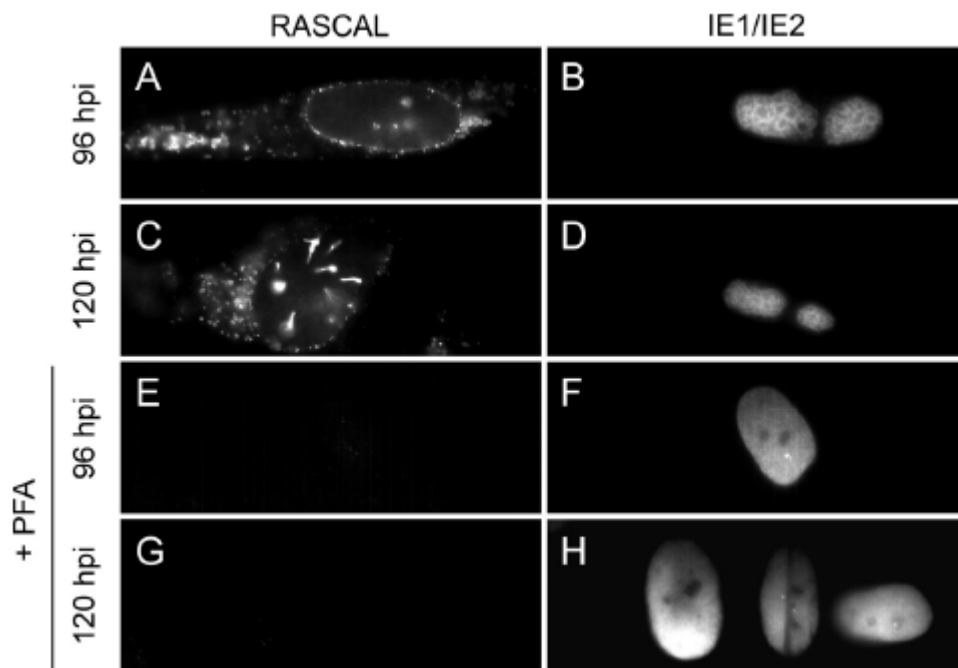
FIG. 4-4. RASCAL expression in the absence of viral DNA synthesis. HF infected with Towne/GFP-IE2 (MOI of 3) in the presence or absence of PFA (300 μg/ml) were harvested at the indicated times p.i. and stained with affinity-purified rabbit anti-RASCAL polyclonal Abs followed by Alexa Fluor 594-conjugated goat anti-rabbit Abs and FITC-conjugated anti IE1/IE2 Abs. Original magnification, 400×.

absence of CMV infection, RASCAL$_{TB40/E}$ did not accumulate at the nuclear rim but displayed a punctuate cytoplasmic staining similar, although not completely identical, to that observed in infected HF at 48 and 72 hpi (compare Fig. 4-7E to Fig. 4-3D and G). Coexpression of UL50-HA and UL53-FLAG induced the relocalization of UL53-FLAG to the endoplasmic reticulum and to the nuclear rim (Fig. 4-7F to H), as expected (7, 40). Expression of RASCAL$_{TB40/E}$ in the presence of UL53-FLAG did not modify the localization of either protein (Fig. 4-7I to K), while coexpression of RASCAL$_{TB40/E}$ and UL50-HA triggered the accumulation of RASCAL$_{TB40/E}$ in a UL50-positive, perinuclear region (Fig. 4-7L to N). These data indicate that the presence of UL50, but not of UL53, is required to mediate RASCAL$_{TB40/E}$ tethering to the nuclear rim and suggest that RASCAL$_{TB40/E}$ may interact with UL50. Expression of RASCAL$_{TB40/E}$ in the presence of both UL50-HA and UL53-FLAG did not change the localization pattern of either RASCAL$_{TB40/E}$ or UL53, and both proteins still accumulated at the nuclear lamina together with UL50 (not shown), suggesting that UL50 may bind to RASCAL$_{TB40/E}$ and UL53 via two different interaction domains. To investigate if RASCAL did indeed interact with UL50, protein extracts from HEK293T cells transfected with LNCX or cotransfected with L-RASCAL$_{TB40/E}$ and LNCX UL50-HA were subjected to co-IP using anti-HA or anti-RASCAL Abs. As a control, extracts from HEK293T cells transfected with LNCX or cotransfected with LNCX UL50-HA and L-UL53-FLAG were subjected to co-IP using anti-HA Abs. As expected (7, 40, 41, 65), UL53-FLAG did coimmunoprecipitate with UL50-HA (Fig. 4-8A, lane 4), while no signal was observed in immunoprecipitates from control cells (Fig. 4-8A, lane 3). Specific bands of about 44 kDa (UL50-HA) and 10 kDa (RASCAL) were detected in cell lysates (Fig. 4-8B, left,
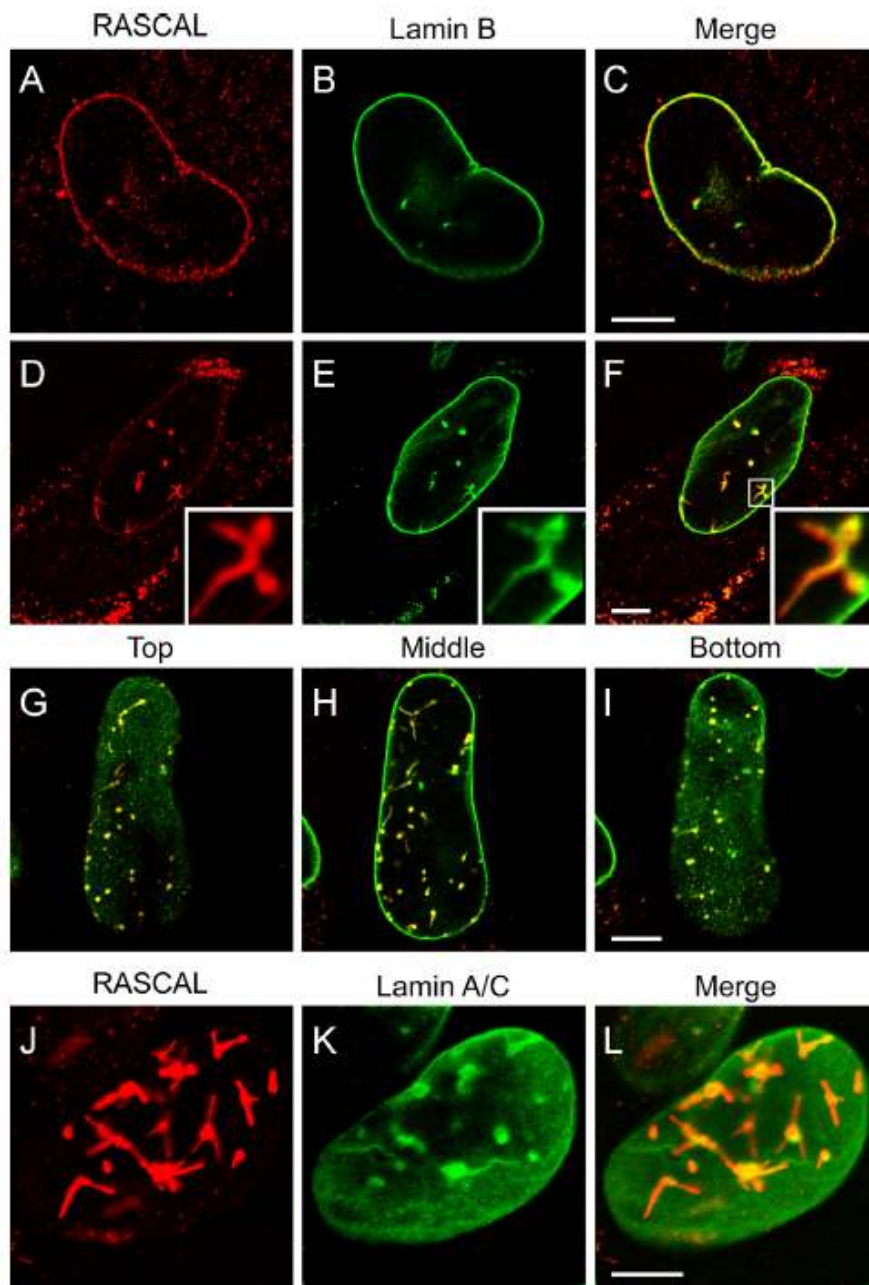
FIG. 4-5. RASCAL colocalization with lamin B and with lamin A/C at the nuclear envelopes of infected cells. Confocal images of TB40/E infected HF (MOI of 5) harvested at 72 hpi (A to C) or 96 hpi (D to L) and stained with affinity-purified rabbit anti-RASCAL polyclonal Abs followed by Alexa Fluor 594-conjugated goat anti-rabbit Abs (red), with monoclonal anti-lamin B Abs followed by FITC-conjugated anti-mouse Abs (green), or with monoclonal anti-lamin A/C Abs (K-L) followed by FITC-conjugated anti-mouse Abs (green). Consecutive confocal planes were images to show the extent of invaginations through the nucleus (G-I). Bar size, 10 μm.
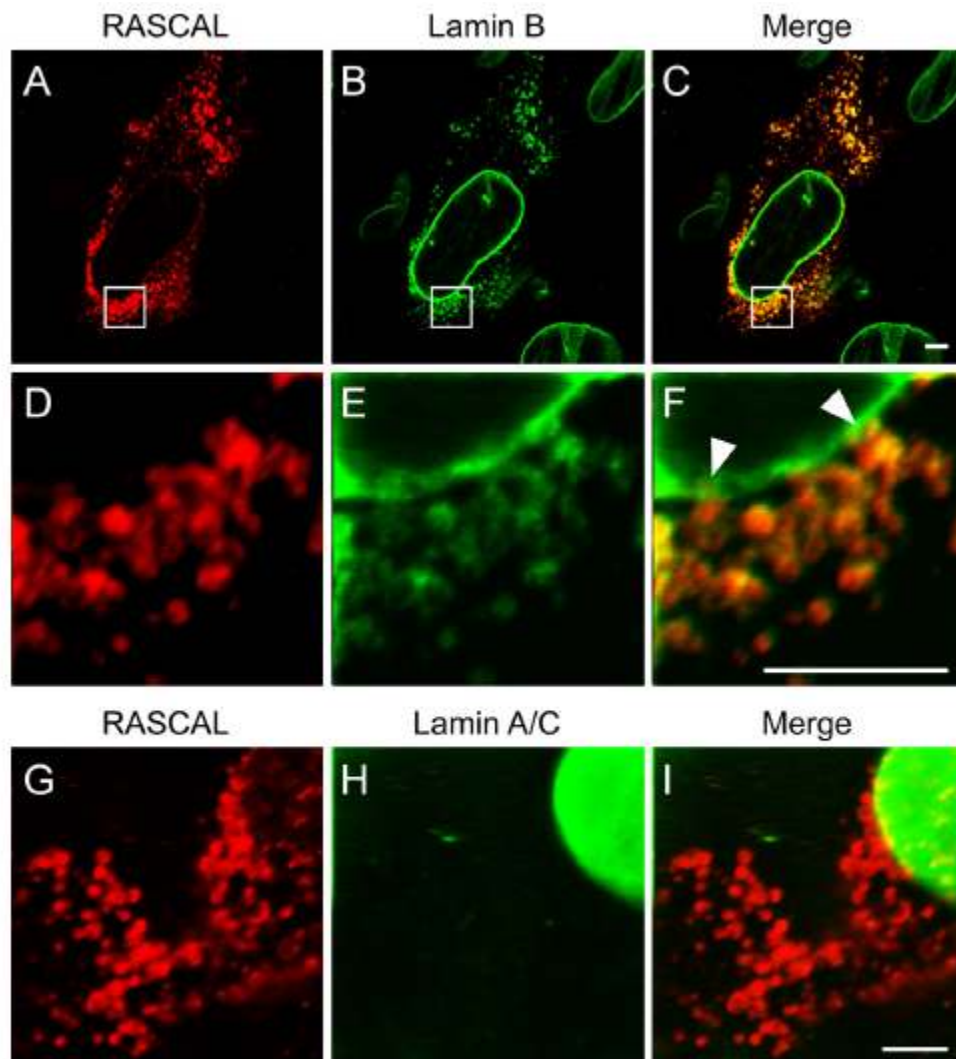
FIG. 4-6. RASCAL colocalization with lamin B but not lamin A/C in cytoplasmic vesicles. Confocal images of TB40/E-infected HF (MOI of 5) harvested at 96 hpi and stained with affinity-purified rabbit anti-RASCAL polyclonal Abs followed by Alexa Fluor 594-conjugated goat anti-rabbit Abs (red), with monoclonal anti-lamin B Abs followed by FITC-conjugated anti-mouse Abs (green) (A to F), or with monoclonal anti-lamin A/C Abs followed by FITC-conjugated anti-mouse Abs (green) (G to I). The area magnified in panels D to F is framed by a square box in panels A to C. Arrowheads indicate the points of close contact between the cytoplasmic vesicles and the nuclear lamina. Bar size, 5 μm.

lane 10) and in immunoprecipitates (Fig. 4-8B, left, lane 8, and right, lane 14) from L-RASCAL$_{TB40/E}$- and LNCX UL50-HA cotransfected cells, irrespective of whether anti-HA or anti- RASCAL Abs were used as immunoprecipitating reagents. No bands were detected in extracts from control cells (Fig. 4-8B, left, lanes 5, 6, and 9, and right, lanes 11 and 12). Together, these data indicate that RASCAL and UL50 can be found in the same complex and suggest that RASCAL is likely to be a new NEC member.

4.4 Discussion

In this report, we show that the putative CMV gene c-ORF29 encodes a protein, RASCAL, displaying a dual localization to the nuclear lamina and to cytoplasmic vesicles at late times during infection. Accumulation of RASCAL at the nuclear lamina requires the presence of UL50. The interaction of these two proteins suggests that RASCAL is likely to be a new component of the NEC. The occurrence of lamin B-positive vesicular structures in the cytoplasm of infected cells at late times p.i. has been previously reported (42, 47, 66), but the nature and function of these vesicles has not yet been determined. The presence of RASCAL and lamin B within these structures suggests that they may originate from the nuclear envelope. We thus speculate that RASCAL may play a role in facilitating the transition of nucleocapsids across the nuclear envelope and may have additional functions in promoting virion maturation and trafficking toward the plasma membrane.

Akin to all herpesviruses, CMV genome replication and encapsidation occur in the nuclei of host cells (45). Release of newly assembled nucleocapsids into the cytoplasm

necessarily entails crossing of the nuclear envelope, in a process presumed to involve an initial envelopment of nucleocapsids by budding through the INM, followed by a de-envelopment step as virions traverse the outer nuclear membrane (ONM) (34, 37, 38, 50, 67). The INM is structurally supported by the nuclear lamina, a dense fibrillar network composed of A- and B-type lamins and their partners (57). Localized destabilization of this structure is required for virions to gain access to the INM and is mediated by components of the NEC, a multiprotein complex composed of the viral proteins UL50, UL53, and UL97 and of the cellular proteins p32, LBR, and PKC (41). UL50 is a key mediator of the NEC formation and directly interacts with UL53, p32, and PKC (41). Recruitment of UL53 and PKC to the nuclear lamina is strictly dependent on the presence of UL50, while p32 can reach this location also via interactions with LBR (7, 40, 41). UL50 also acts to enhance the accumulation at the NEC of the viral kinase UL97, although UL97 recruitment is largely mediated by binding to p32 (35).

Similar to UL53 and PKC, RASCAL localization to the nuclear rim is dependent on UL50 (Fig. 4-7L to N). RASCAL and UL50 could also be coimmunoprecipitated (Fig. 4-8B), indicating the existence of direct or indirect interactions between the two proteins. Thus, RASCAL may either be a new UL50 binding partner or may be recruited to the NEC via interactions with PKC and/or p32.

Both RASCAL and UL53 were able to reach the nuclear lamina when coexpressed in the presence of UL50 (not shown), indicating a lack of competition between these two proteins for binding to UL50. Thus, if the RASCAL-to-UL50 link is direct, two distinct binding domains must exist on the surface of UL50, one for RASCAL and one for UL53.

Although our data do not exclude the possibility of an interaction between RASCAL and UL53, complete overlap of signals emanating from each of these proteins was not observed in the cytoplasm of cotransfected cells, and expression of UL53-FLAG did not result in the relocation of RASCAL to the nucleus (Fig. 4-7I to K). We thus believe that the formation of RASCAL-UL53 complexes is unlikely to occur.

Quite interestingly, no differences were observed in the intracellular localization of $RASCAL_{TB40/E}$ and $RASCAL_{Towne}$ during infection, despite the fact that the RASCAL version encoded by Towne is substantially longer than that encoded by TB40/E (Fig. 4-1 and 2). As both proteins accumulate at the NEC, the domains required for this localization must be located within the first 97 aa of RASCAL, while the presence of the 79 additional amino acids in $RASCAL_{Towne}$ does not contribute to, or interfere with, the recruitment process. We thus speculate that the two proteins, although similarly localized, will prove to be functionally different and that these differences will be dependent on their ability to interact with specific cellular and/or viral proteins in addition to the components of the NEC. Studies are currently in progress to identify the exact domains required for the tethering of $RASCAL_{TB40/E}$ and $RASCAL_{Towne}$ to the nuclear lamina and to isolate the potential binding partners of each protein.

Extensive overlap of the RASCAL and lamin B signals was observed at the nuclear rim and in intranuclear invaginations of the INM in TB40/E-, Towne/GFP-IE2-, or AD169-infected HF (Fig. 4-5A to I and data not shown). Substantial infoldings of the INM have been described in a number of ultrastructural studies of CMV-infected cells, and the presence of UL50, UL53, and UL97 at these sites was documented by immunoelectron

and immunofluorescence microscopy (6, 7, 14, 24, 35, 50, 62, 67). These invaginations were shown to be sites of nucleocapsid budding across the INM and were proposed to enhance the efficiency of virion egress from the nucleus by increasing the surface area of the INM and by acting as channels for the unhindered transport of primary enveloped virions toward the ONM (6). Confocal microscopy imaging of cells stained for RASCAL and lamin B clearly showed that both these proteins are located at sites found deep within the nuclear volume (Fig. 4-5D to I). In contrast, lamin A/C colocalization with RASCAL was less prominently in the nuclear invaginations and more evident at the openings of the INM channels (Fig. 4-5J to L). Although these staining pattern differences could potentially be due to some variation in the binding efficiency of each Ab, it is also conceivable that they might reflect functional differences between the two types of lamins (57). Together, these results strongly suggest that RASCAL is associated with the INM and provide further support to the hypothesis that RASCAL is a new component of the NEC.

Although expression of UL50 and UL53 was reported to be sufficient for the remodeling of the nuclear lamina and for the formation of INM invaginations in COS7 cells (7), the presence of nuclear foldings was not observed in HeLa (40) or in HEK293T (Fig. 4-7F to H) cells coexpressing these proteins. Expression of RASCAL$_{TB40/E}$ in the presence of UL53 (Fig. 4-7I to K), UL50 (Fig. 4-7L to N), or both (not shown) also did not induce the formation of INM folds, indicating that RASCAL expression on its own, or in conjunction with UL50 and UL53, is not sufficient to trigger the development of these structures. These data suggest that the generation of INM invaginations in the absence of infection may be cell type dependent and may be affected by the intracellular content and

FIG. 4-7. Localization of UL50-HA, UL53-FLAG, and RASCALTB40/E in transfected cells. (A to D) Confocal images of HEK293T transiently transfected with expression plasmids encoding UL50-HA (A and B) or UL53-FLAG (C and D) and stained with mouse anti-HA Ab (A), mouse anti-FLAG Abs (C), or affinity-purified rabbit anti-RASCAL polyclonal Abs (B and D) followed by FITC-conjugated goat anti-mouse Abs (green) or Alexa Fluor 594-conjugated goat anti-rabbit Abs. (E to M) Confocal images of HEK293T coexpressing UL50-HA and UL53-FLAG (E to F), UL53-FLAG and RASCAL$_{TB40/E}$ (H to J), or UL50-HA and RASCAL$_{TB40/E}$ (K to M). Cells were stained with rabbit anti-HA and mouse anti-FLAG Abs followed by Alexa Fluor 594 goat anti-rabbit Abs (green) and FITC-conjugated goat anti-mouse Abs (red) (E to G), with mouse anti-FLAG and rabbit anti-RASCAL Abs followed by FITC-conjugated goat anti-mouse Abs (green) and Alexa Fluor 594-conjugated goat anti-rabbit Ab (red) (H to J), or with mouse anti-HA and rabbit anti-RASCAL Abs followed by FITC-conjugated goat anti-mouse Abs (green) and Alexa Fluor 594-conjugated goat anti-rabbit Abs (red) (K to M). Bar size, 10 μm.

184

Single transfection
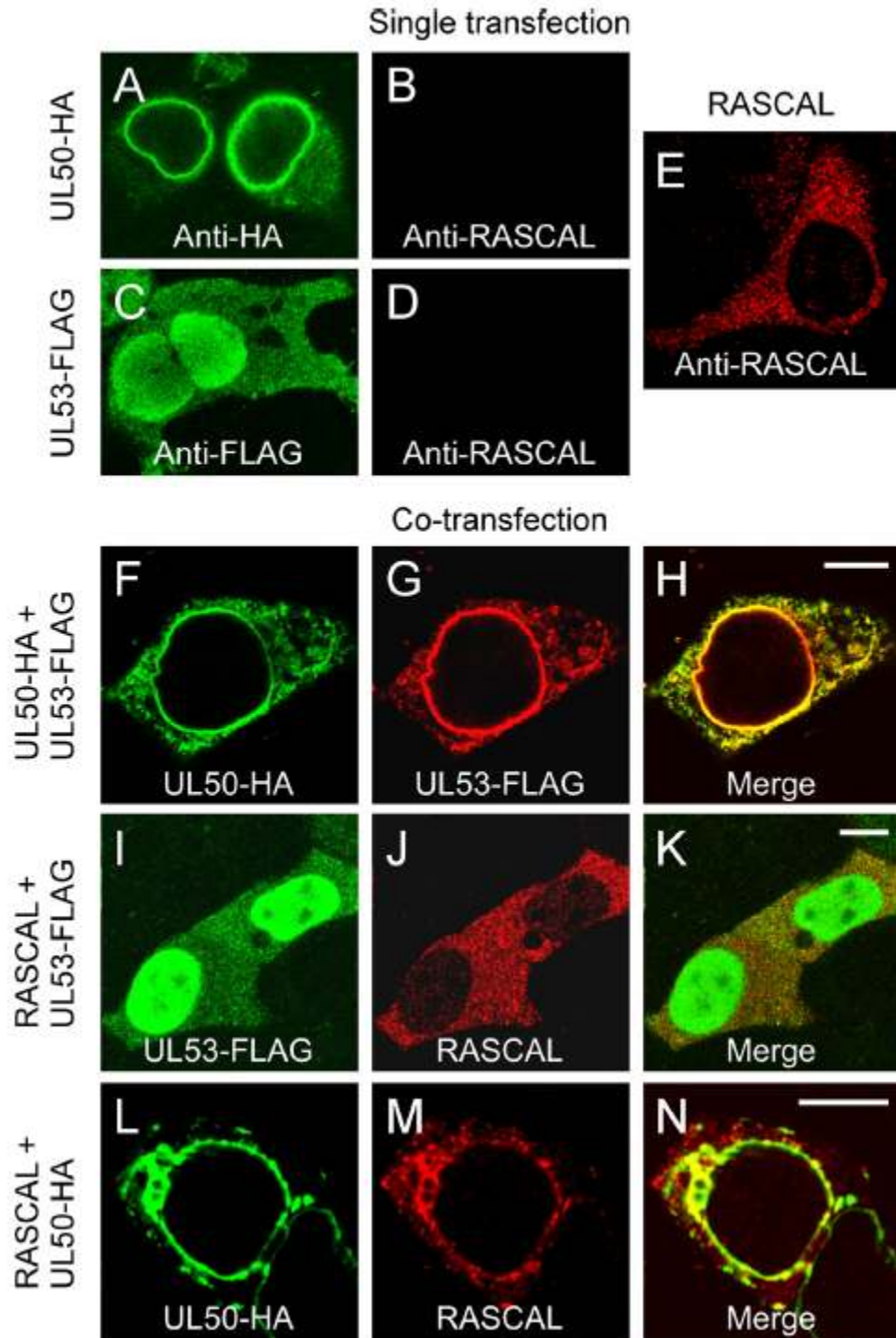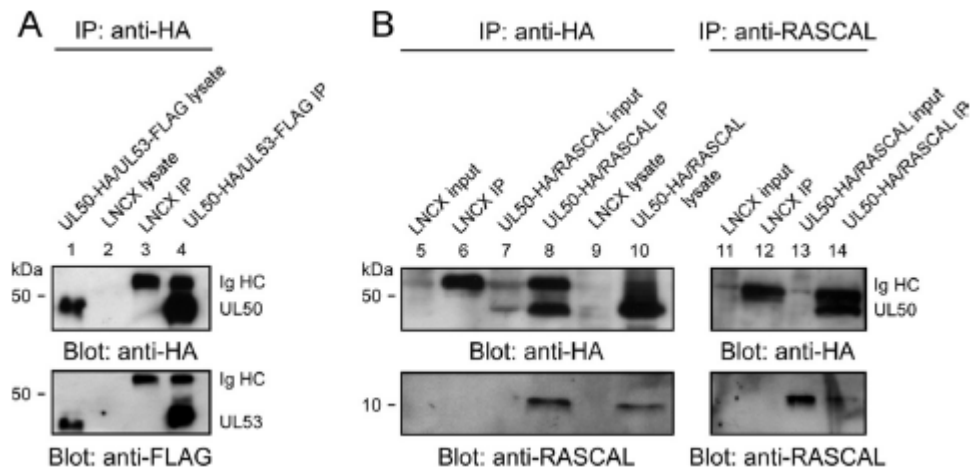
Co-transfection

FIG. 4-8. Determination of RASCAL's interaction with UL50 by co-IP. (A) Immunoblot analysis of protein extracts from HEK293T cells transiently transfected with LNCX or cotransfected with L-RASCALTB40/E and LNCX UL50-HA. Proteins were denatured in 3% SDS lysis buffer (lysate) or were subjected to co-IP with anti-HA Abs (left) or with anti-RASCAL Abs (right) prior to separation on 10% (UL50-HA) or 15% (RASCAL$_{TB40/E}$) SDS-PAGE gels. An aliquot corresponding to 2% of the original co-IP buffer volume was loaded onto the gels as the input control (input). Membranes were probed with anti-HA (1:500) or anti-RASCAL (1:1,000) Abs. (B) Immunoblot analysis of protein extracts from HEK293T cells transiently transfected with LNCX or cotransfected with LNCX UL50-HA and L-UL53-FLAG. Proteins were denatured in 3% SDS lysis buffer (lysate) or were subjected to co-IP with anti-HA Abs, prior to separation on 10% SDS-PAGE gels. Membranes were probed with anti-HA (1:500) or anti-FLAG (1:500) Abs. Expected molecular masses were 43.9 kDa for UL50-HA, 10.6 kDa for RASCAL$_{TB40/E}$, and 43.3 kDa for UL53-FLAG.

availability of PKC, a kinase whose activity is required to enhance the disassembly of the nuclear lamina during mitosis (12) and during egress of herpes simplex virus type 1 (HSV-1) and of murine and human CMV (33, 40, 46, 47, 51). In addition to PKC, the viral kinase UL97 is recruited to the nuclear lamina (35) and substantially contributes to its phosphorylation-mediated dissolution (27, 35, 41, 42, 55). The presence of these two kinases at the NEC fostered the speculation that they might phosphorylate specific NEC components. Although no significant posttranslational modification was detected for UL53 in infected HF (14), phosphorylation of both UL50 and UL53 was reported to occur after in vivo labeling of transfected cells with 33P (40), and phosphorylation of UL50 was shown to be mediated by PKC (40).

We did not observe substantial changes in the SDS-PAGE mobility of RASCAL$_{TB40/E}$ from either infected or transfected cells (Fig. 4-2C and D), despite the predicted presence of potential phosphorylation sites for both PKC and PKA (Fig. 4-1B). Protein phosphorylation, however, has been reported to increase, decrease, or leave unaffected the apparent molecular weights of proteins separated on SDS-PAGE gels. It is thus conceivable that both RASCAL$_{TB40/E}$ and RASCAL$_{Towne}$ might indeed be phosphorylated. The potential presence of this modification might explain the appearance of a faster-migrating band in protein extracts from Towne-infected cells (Fig. 4-2D), particularly considering that the amino acid sequence of RASCAL$_{Towne}$ is predicted to contain two additional phosphorylation sites compared to that of RASCAL$_{TB40/E}$. Further analyses are in progress to clarify this issue. While expression of UL53 was reported to occur with late kinetics (14), c-ORF29 transcription was observed starting from 6 hpi (Fig. 4-2A), and its protein product was detected at low levels starting from 24 hpi, with signal intensities

markedly increasing at later times (Fig. 4-3). These data suggest that RASCAL accumulation in infected cells may begin before synthesis of UL53 and, possibly, of UL50, while RASCAL gathering at the nuclear rim occurs exclusively at late times p.i., when both UL50 and UL53 are present within the NEC. c-ORF29 transcription was reduced, but not completely abolished, in the absence of viral DNA replication (Fig. 4-2B), while signal from the protein product of c-ORF29 became completely undetectable by immunofluorescence staining analysis of PFA-treated cells (Fig. 4-4). These results suggest that, as with the synthesis of another NEC component, UL97, RASCAL is expressed with early-late kinetics, requiring viral DNA replication for maximum expression (39).

As previously mentioned, the c-ORF29 and US17 nucleotide sequences partially overlap. Although the kinetics of US17 gene expression have not been studied in detail, the presence of early transcripts hybridizing to the US17 gene region was detected in microarray studies of viral gene expression in Towne-infected HF (9). Interestingly, however, synthesis of the US17 protein was observed starting from 72 hpi and was entirely inhibited by treatment with PFA (15). These data suggest that, although both the US17 and c-ORF29 genes are located on the negative strand of the genome and have partially overlapping sequences, their transcription may be controlled by different promoters.

While expression of both UL50 and UL53 is absolutely necessary for the production of viral progeny from infected cells (18, 74), growth of two distinct US17 deletion mutant viruses in HF was not impaired (18, 74). As the c-ORF29 and US17 nucleotide sequences

extensively overlap, it is likely that deletion of c-ORF29 will also not lead to dramatic reductions in mutant virus yields, at least in HF. Although the absence of RASCAL expression might still affect the efficiency of virion egress in HF, we expect that more dramatic effects may be observed in cell types other than HF.

Substantial overlap of the RASCAL and lamin B, but not lamin A/C, signals was observed in cytoplasmic vesicles distributed from the nucleus to the cytoplasm of infected HF at late times p.i. (Fig. 4-3J, M, and P, 4-4A and C, and 4-6A to F). Although the existence of similar vesicles has been mentioned in previous analyses of human- or murine-CMV-infected cells stained for lamin B (47, 66), their origin and nature has not yet been established and is the subject of ongoing investigations. Our confocal microscopy images indicate that they are likely to originate from the nuclear envelope (Fig. 4-6), an assumption further reinforced by the fact that they do appear to contain lamin B. It is currently unclear, however, whether they consist of a single or of a double membrane and if they are derived from the INM, the ONM, or both. As these structures have been noticed before in cells expressing exogenous UL50 (7), it is possible that they may contain additional NEC components and possibly even nucleocapsids. If so, they may constitute a completely novel, alternative route of virion maturation and transport from the nucleus to the cell surface. Alternatively, they may represent sites of viral particle degradation, similar to the nuclear envelope-derived, four-layered structures described in the cytoplasm of HSV-1-infected HF (1), which were recently shown to be autophagosomes (21).

The presence of RASCAL at these sites raises the intriguing possibility that RASCAL might remain associated with virions during egress, possibly becoming a tegument component. UL50 was reported to be an envelope glycoprotein in proteomic analyses of the CMV particles (70), and UL53 was shown by immunoelectron microscopy to be a tegument protein (14), although this localization was not confirmed by the proteomic study (70). It is thus conceivable that RASCAL may accompany newly formed nucleocapsids during their journey from the nucleus to the periphery, perhaps by triggering the formation of nucleus-derived vesicles. If so, RASCAL may indeed function as a new determinant of viral tropism by enhancing virion egress from specific cell types or, if included in the tegument, by promoting entry of viral particles into uninfected cells.

4.5   References

1. **Alexander, D. E., S. L. Ward, N. Mizushima, B. Levine, and D. A. Leib.** 2007. Analysis of the role of autophagy in replication of herpes simplex virus in cell culture. J. Virol. **81**:12128–12134.

2. **Bendtsen, J. D., H. Nielsen, G. von Heijne, and S. Brunak.** 2004. Improved prediction of signal peptides: SignalP 3.0. J. Mol. Biol. **340**:783–795.

3. **Bhasin, M., and G. P. S. Raghava.** 2004. ESLpred: SVM-based method for subcellular localization of eukaryotic proteins using dipeptide composition and PSI-BLAST. Nucleic Acids Res. **32**:W414–W419.

4. **Blom, N., T. Sicheritz-Ponten, R. Gupta, S. Gammeltoft, and S. Brunak**. 2004. Prediction of post- translational glycosylation and phosphorylation of proteins from the amino acid sequence. Proteomics **4**:1633–1649.

5. **Britt, W**. 2008. Manifestations of human cytomegalovirus infection: proposed mechanisms of acute and chronic disease. Curr. Top. Microbiol. Immunol. **325**:417–470.

6. **Buser, C., P. Walther, T. Mertens, and D. Michel.** 2007. Cytomegalovirus primary envelopment occurs at large infoldings of the inner nuclear membrane. J. Virol. **81**:3042–3048.

7. **Camozzi, D., S. Pignatelli, C. Valvo, G. Lattanzi, C. Capanni, P. Dal Monte, and M. P. Landini.** 2008. Remodelling of the nuclear lamina during human cytomegalovirus infection: role of the viral proteins pUL50 and pUL53. J. Gen. Virol. **89**:731–740.

8. **Cha, T. A., E. Tom, G. W. Kemble, G. M. Duke, E. S. Mocarski, and R. R. Spaete.** 1996. Human cytomegalovirus clinical isolates carry at least 19 genes not found in laboratory strains. J. Virol. **70**:78–83.

9. **Chambers, J., A. Angulo, D. Amaratunga, H. Guo, Y. Jiang, J. S. Wan, A. Bittner, K. Frueh, M. R. Jackson, P. A. Peterson, M. G. Erlander, and P. Ghazal.** 1999. DNA microarrays of the complex human cytomegalovirus genome: profiling kinetic class with drug sensitivity of viral gene expression. J. Virol. **73**:5757–5766.

10. **Chee, M. S., A. T. Bankier, S. Beck, R. Bohni, C. M. Brown, R. Cerny, T. Horsnell, C. A. Hutchison III, T. Kouzarides, J. A. Martignetti,** *et al.* 1990. Analysis of the protein-coding content of the sequence of human cytomegalovirus strain AD169. Curr. Top. Microbiol. Immunol. **154**:125–169.

11. **Claros, M. G., and G. von Heijne**. 1994. TopPred II: an improved software for membrane protein structure predictions. Comput. Appl. Biosci. **10**:685–686.

12. **Collas, P., L. Thompson, A. P. Fields, D. L. Poccia, and J. C. Courvalin**. 1997. Protein kinase C-mediated interphase lamin B phosphorylation and solubilization. J. Biol. Chem. **272**:21274–21280.

13. **Cserzo, M., E. Wallin, I. Simon, G. von Heijne, and A. Elofsson**. 1997. Prediction of transmembrane alpha-helices in prokaryotic membrane proteins: the dense alignment surface method. Protein Eng. **10**:673–676.

14. **Dal Monte, P., S. Pignatelli, N. Zini, N. M. Maraldi, E. Perret, M. C. Prevost, and M. P. Landini.** 2002. Analysis of intracellular and intraviral localization of the human cytomegalovirus UL53 protein. J. Gen. Virol. **83**:1005–1012.

15. **Das, S., Y. Skomorovska-Prokvolit, F.-Z. Wang, and P. E. Pellett**. 2006. Infection-dependent nuclear localization of US17, a member of the US12 family of human cytomegalovirus-encoded seven-transmembrane proteins. J. Virol. **80**:1191–1203.

16. **Davison, A. J., A. Dolan, P. Akter, C. Addison, D. J. Dargan, D. J. Alcendor, D. J. McGeoch, and G. S. Hayward.** 2003. The human cytomegalovirus genome revisited: comparison with the chimpanzee cytomegalovirus genome. J. Gen. Virol. **84**:17–28.

17. **Dolan, A., C. Cunningham, R. D. Hector, A. F. Hassan-Walker, L. Lee, C. Addison, D. J. Dargan, D. J. McGeoch, D. Gatherer, V. C. Emery, P. D. Griffiths, C. Sinzger, B. P. McSharry, G. W. Wilkinson, and A. J. Davison.** 2004. Genetic content of wild-type human cytomegalovirus. J. Gen. Virol. **85**:1301–1312.

18. **Dunn, W., C. Chou, H. Li, R. Hai, D. Patterson, V. Stolc, H. Zhu, and F. Liu.** 2003. Functional profiling of a human cytomegalovirus genome. Proc. Natl. Acad. Sci. U. S. A. **100**:14223–14228.

19. **Elek, S. D., and H. Stern**. 1974. Development of a vaccine against mental retardation caused by cytomegalovirus infection in utero. Lancet **1**:1–5.

20. **Emanuelsson, O., H. Nielsen, S. Brunak, and G. von Heijne.** 2000. Predicting subcellular localization of proteins based on their N-terminal amino acid sequence. J. Mol. Biol. **300**:1005–1016.

21. **English, L., M. Chemali, and M. Desjardins**. 2009. Nuclear membrane-derived autophagy, a novel process that participates in the presentation of endogenous viral antigens during HSV-1 infection. Autophagy **5**:1026–1029.

22. **Garg, A., M. Bhasin, and G. P. S. Raghava**. 2005. Support vector machine-based method for subcellular localization of human proteins using amino acid compositions, their order, and similarity search. J. Biol. Chem. **280**: 14427–14432.

23. **Gerna, G., E. Percivalle, D. Lilleri, L. Lozza, C. Fornara, G. Hahn, F. Baldanti, and M. G. Revello.** 2005. Dendritic-cell infection by human cytomegalovirus is restricted to strains carrying functional UL131-128 genes and mediates efficient viral antigen presentation to CD8 T cells. J. Gen. Virol. **86**:275–284.

24. **Gilloteaux, J., and M. R. Nassiri**. 2000. Human bone marrow fibroblasts infected by cytomegalovirus: ultrastructural observations. J. Submicrosc. Cytol. Pathol. **32**:17–45.

25. **Hahn, G., H. Khan, F. Baldanti, U. H. Koszinowski, M. G. Revello, and G. Gerna.** 2002. The human cytomegalovirus ribonucleotide reductase homolog UL45 is dispensable for growth in endothelial cells, as determined by a BAC-cloned clinical isolate of human cytomegalovirus with preserved wildtype characteristics. J. Virol. **76**:9551–9555.

26. **Hahn, G., M. G. Revello, M. Patrone, E. Percivalle, G. Campanini, A. Sarasini, M. Wagner, A. Gallina, G. Milanesi, U. Koszinowski, F. Baldanti, and G. Gerna.** 2004. Human cytomegalovirus UL131-128 genes are indispensable for virus growth in endothelial cells and virus transfer to leukocytes. J. Virol. **78**:10023–10033.

27. **Hamirally, S., J. P. Kamil, Y. M. Ndassa-Colday, A. J. Lin, W. J. Jahng, M. C. Baek, S. Noton, L. A. Silva, M. Simpson-Holley, D. M. Knipe, D. E. Golan, J. A. Marto, and D. M. Coen.** 2009. Viral mimicry of cdc2/cyclindependent kinase 1 mediates disruption of nuclear lamina during human cytomegalovirus nuclear egress. PLoS Pathog. **5**:e1000275.

28. **Hertel, L., V. G. Lacaille, H. Strobl, E. D. Mellins, and E. S. Mocarski.** 2003. Susceptibility of immature and mature Langerhans cell-type dendritic cells to infection and immunomodulation by human cytomegalovirus. J. Virol. **77**: 7563–7574.

29. **Hua, S. J., and Z. R. Sun.** 2001. Support vector machine approach for protein subcellular localization prediction. Bioinformatics **17**:721–728.

30. **Isaacson, M. K., L. K. Juckem, and T. Compton.** 2008. Virus entry and innate immune activation. Curr. Top. Microbiol. Immunol. **325**:85–100.

31. **Kyte, J., and R. F. Doolittle.** 1982. A simple method for displaying the hydropathic character of a protein. J. Mol. Biol. **157**:105–132.

32. **Larkin, M. A., G. Blackshields, N. P. Brown, R. Chenna, P. A. McGettigan, H. McWilliam, F. Valentin, I. M. Wallace, A. Wilm, R. Lopez, J. D. Thompson, T. J. Gibson, and D. G. Higgins.** 2007. Clustal W and clustal X version 2.0. Bioinformatics **23**:2947–2948.

33**. Leach, N., S. L. Bjerke, D. K. Christensen, J. M. Bouchard, F. Mou, R. Park, J. Baines, T. Haraguchi, and R. J. Roller.** 2007. Emerin is hyperphosphorylated and redistributed in herpes simplex virus type 1-infected cells in a manner dependent on both UL34 and US3. J. Virol. **81**:10792–10803.

34. **Lee, C. P., and M. R. Chen**. 2010. Escape of herpesviruses from the nucleus. Rev. Med. Virol. [Epub ahead of print.] doi:10.1002/rmv.643.

35. **Marschall, M., A. Marzi, P. aus dem Siepen, R. Jochmann, M. Kalmer, S. Auerochs, P. Lischka, M. Leis, and T. Stamminger.** 2005. Cellular p32 recruits cytomegalovirus kinase pUL97 to redistribute the nuclear lamina. J. Biol. Chem. **280**:33357–33367.

36. **McCormick, A. L., C. D. Meiering, G. B. Smith, and E. S. Mocarski.** 2005. Mitochondrial cell death suppressors carried by human and murine cytomegalovirus confer resistance to proteasome inhibitor-induced apoptosis. J. Virol. **79**:12205–12217.

37. **Mettenleiter, T. C.** 2002. Herpesvirus assembly and egress. J. Virol. **76**:1537–1547.

38. **Mettenleiter, T. C., B. G. Klupp, and H. Granzow**. 2009. Herpesvirus assembly: an update. Virus Res. **143**:222–234.

39. **Michel, D., I. Pavic, A. Zimmermann, E. Haupt, K. Wunderlich, M. Heuschmid, and T. Mertens.** 1996. The UL97 gene product of human cytomegalovirus is an early-late protein with a nuclear localization but is not a nucleoside kinase. J. Virol. **70**:6340–6346.

40. **Milbradt, J., S. Auerochs, and M. Marschall**. 2007. Cytomegaloviral proteins pUL50 and pUL53 are associated with the nuclear lamina and interact with cellular protein kinase C. J. Gen. Virol. **88**:2642–2650.

41. **Milbradt, J., S. Auerochs, H. Sticht, and M. Marschall**. 2009. Cytomegaloviral proteins that associate with the nuclear lamina: components of a postulated nuclear egress complex. J. Gen. Virol. **90**:579–590.

42. **Milbradt, J., R. Webel, S. Auerochs, H. Sticht, and M. Marschall.** 2010. Novel mode of phosphorylation-triggered reorganization of the nuclear lamina during nuclear egress of human cytomegalovirus. J. Biol. Chem. [Epub ahead of print.] doi:10.1074/jbc.M109.063628.

43**. Miller, A. D., and G. J. Rosman.** 1989. Improved retroviral vectors for gene transfer and expression. Biotechniques **7**:980–990.

44. **Miller, M., and L. Hertel**. 2009. Onset of human cytomegalovirus replication in fibroblasts requires the presence of an intact vimentin cytoskeleton. J. Virol. **83**:7015–7028.

45. **Mocarski, E. S., T. Shenk, and R. F. Pass.** 2007. Cytomegaloviruses, p. 2701–2772. In A. P. M. Howley and D. M. Knipe (ed.), Fields virology. Lippincott Williams & Wilkins, Philadelphia, PA.

46. **Morris, J. B., H. Hofemeister, and P. O'Hare.** 2007. Herpes simplex virus infection induces phosphorylation and delocalization of emerin, a key inner nuclear membrane protein. J. Virol. **81**:4429–4437.

47. **Muranyi, W., J. Haas, M. Wagner, G. Krohne, and U. H. Koszinowski.** 2002. Cytomegalovirus recruitment of cellular kinases to dissolve the nuclear lamina. Science **297**:854–857.

48. **Murphy, E., and T. Shenk.** 2008. Human cytomegalovirus genome. Curr. Top. Microbiol. Immunol. **325**:1–19.

49. **Murphy, E., D. Yu, J. Grimwood, J. Schmutz, M. Dickson, M. A. Jarvis, G. Hahn, J. A. Nelson, R. M. Myers, and T. E. Shenk.** 2003. Coding potential of laboratory and clinical strains of human cytomegalovirus. Proc. Natl. Acad. Sci. U. S. A. **100**:14976–14981.

50. **Papadimitriou, J. M., G. R. Shellam, and T. A. Robertson.** 1984. An ultrastructural investigation of cytomegalovirus replication in murine hepatocytes. J. Gen. Virol. **65**(Pt. 11):1979–1990.

51. **Park, R., and J. D. Baines.** 2006. Herpes simplex virus type 1 infection induces activation and recruitment of protein kinase C to the nuclear membrane and increased phosphorylation of lamin B. J. Virol. **80**:494–504.

52. **Penfold, M. E., and E. S. Mocarski.** 1997. Formation of cytomegalovirus DNA replication compartments defined by localization of viral proteins and DNA synthesis. Virology **239**:46–61.

53. **Plotkin, S. A., T. Furukawa, N. Zygraich, and C. Huygelen**. 1975. Candidate cytomegalovirus strain for human vaccination. Infect. Immun. **12**:521–527.

54. **Plotkin, S. A., S. E. Starr, H. M. Friedman, E. Gonczol, and R. E. Weibel**. 1989. Protective effects of Towne cytomegalovirus vaccine against low-passage cytomegalovirus administered as a challenge. J. Infect. Dis. **159**:860–865.

55. **Prichard, M. N.** 2009. Function of human cytomegalovirus UL97 kinase in viral infection and its inhibition by maribavir. Rev. Med. Virol. **19**:215–229.

56. **Prichard, M. N., M. E. Penfold, G. M. Duke, R. R. Spaete, and G. W. Kemble.** 2001. A review of genetic differences between limited and extensively passaged human cytomegalovirus strains. Rev. Med. Virol. **11**:191–200.

57**. Prokocimer, M., M. Davidovich, M. Nissim-Rafinia, N. Wiesel-Motiuk, D. Bar, R. Barkan, E. Meshorer, and Y. Gruenbaum.** 2009. Nuclear lamins: key regulators of nuclear structure and activities. J. Cell. Mol. Med. [Epub ahead of print.] doi:10.1111/j.1582–4934.2008.00676.x.

58. **Quinnan, G. V., Jr., M. Delery, A. H. Rook, W. R. Frederick, J. S. Epstein, J. F. Manischewitz, L. Jackson, K. M. Ramsey, K. Mittal, S. A. Plotkin,** *et al.* 1984. Comparative virulence and immunogenicity of the Towne strain and a nonattenuated strain of cytomegalovirus. Ann. Intern. Med. **101**:478–483.

59. **Revello, M. G., D. Lilleri, M. Zavattoni, M. Stronati, L. Bollani, J. M. Middeldorp, and G. Gerna.** 2001. Human cytomegalovirus immediate-early messenger RNA in blood of pregnant women with primary infection and of congenitally infected newborns. J. Infect. Dis. **184**:1078–1081.

60. **Riegler, S., H. Hebart, H. Einsele, P. Brossart, G. Jahn, and C. Sinzger.** 2000. Monocyte-derived dendritic cells are permissive to the complete replicative cycle of human cytomegalovirus. J. Gen. Virol. **81**:393–399.

61. **Rowe, W. P., J. W. Hartley, S. Waterman, H. C. Turner, and R. J. Huebner.** 1956. Cytopathogenic agent resembling human salivary gland virus recovered from tissue cultures of human adenoids. Proc. Soc. Exp. Biol. Med. **92**:418–424.

62. **Ruebner, B. H., K. Miyai, R. J. Slusser, P. Wedemeyer, and D. N. Medearis, Jr.** 1964. Mouse cytomegalovirus infection. An electron microscopic study of hepatic parenchymal cells. Am. J. Pathol. **44**:799–821.

63. **Ryckman, B. J., M. A. Jarvis, D. D. Drummond, J. A. Nelson, and D. C. Johnson.** 2006. Human cytomegalovirus entry into epithelial and endothelial cells depends on genes UL128 to UL150 and occurs by endocytosis and low-pH fusion. J. Virol. **80**:710–722.

64. **Ryckman, B. J., B. L. Rainish, M. C. Chase, J. A. Borton, J. A. Nelson, M. A. Jarvis, and D. C. Johnson.** 2008. Characterization of the human cytomegalovirus gH/gL/UL128-131 complex that mediates entry into epithelial and endothelial cells. J. Virol. **82**:60–70.

65. **Sam, M. D., B. T. Evans, D. M. Coen, and J. M. Hogle.** 2009. Biochemical, biophysical, and mutational analyses of subunit interactions of the human cytomegalovirus nuclear egress complex. J. Virol. **83**:2996–3006.

66**. Sanchez, V., P. C. Angeletti, J. A. Engler, and W. J. Britt.** 1998. Localization of human cytomegalovirus structural proteins to the nuclear matrix of infected human fibroblasts. J. Virol. 72:3321–3329.

67**. Severi, B., M. P. Landini, and E. Govoni**. 1988. Human cytomegalovirus morphogenesis: an ultrastructural study of the late cytoplasmic phases. Arch. Virol. 98:51–64.

68. **Sinzger, C., M. Digel, and G. Jahn**. 2008. Cytomegalovirus cell tropism. Curr.Top. Microbiol. Immunol. 325:63–83.

69**. Sinzger, C., G. Hahn, M. Digel, R. Katona, K. L. Sampaio, M. Messerle, H. Hengel, U. Koszinowski, W. Brune, and B. Adler.** 2008. Cloning and sequencing of a highly productive, endotheliotropic virus strain derived from human cytomegalovirus TB40/E. J. Gen. Virol. 89:359–368.

70**. Varnum, S. M., D. N. Streblow, M. E. Monroe, P. Smith, K. J. Auberry, L. Pasa-Tolic, D. Wang, D. G. Camp II, K. Rodland, S. Wiley, W. Britt, T. Shenk, R. D. Smith, and J. A. Nelson.** 2004. Identification of proteins in human cytomegalovirus (HCMV) particles: the HCMV proteome. J. Virol. 78:10960–10966.

71. **Waldman, W. J., W. H. Roberts, D. H. Davis, M. V. Williams, D. D. Sedmak, and R. E. Stephens.** 1991. Preservation of natural endothelial cytopathogenicity of cytomegalovirus by propagation in endothelial cells. Arch. Virol. 117:143–164.

72. **Wang, D., and T. Shenk.** 2005. Human cytomegalovirus UL131 open reading frame is required for epithelial cell tropism. J. Virol. 79:10330–10338.

73. **Wang, D., and T. Shenk.** 2005. Human cytomegalovirus virion protein complex required for epithelial and endothelial cell tropism. Proc. Natl. Acad. Sci. U. S. A. 102:18153–18158.

74**. Yu, D., M. C. Silva, and T. Shenk.** 2003. Functional map of human cytomegalovirus AD169 defined by global mutational analysis. Proc. Natl. Acad. Sci. U. S. A. 100:12396–12401.

Chapter 5

GENERAL DISCUSSION

"Every honest researcher I know admits he's just a professional amateur. He's doing whatever he's doing for the first time. That makes him an amateur. He has the sense to know that he's going to have a lot of trouble, so that makes him professional."

-Charles Franklin Kettering (1876-1958) U.S. Engineer and Inventor

5.1   Thesis Summary and Significance of Research

Despite their amazing biological diversity, all viruses face at least three common obstacles: they must enter host cells, express their genes and replicate, and finally, exit the host cell so that the cycle of infection can continue. While the breadth of strategies employed by viruses to accomplish each of these feats is striking, so too are the commonalities exhibited by many viruses that are otherwise quite phylogenetically distinct. The study of these fundamental processes not only teaches us much about our virus of particular interest, but also of the basic biological pathways in general.

Herein, I have described studies focusing on each of these three common processes. In Chapter 2, I have shown that vimentin, an IF protein, is required for the efficient onset of CMV infection. We found that vimentin remains stable during entry of CMV strains AD169 and TB40/E (Fig. 2-1). Virus entry was hampered in HF treated with the vimentin-disrupting agent, ACR (Fig. 2-4), and in cells harvested from patients with GAN, a genetic disorder which causes vimentin bundling (Fig. 2-5). Finally, virus entry was also negatively affected during infection of vim$^-$ MEFs (Fig. 2-6). In these cells, virus particle trafficking towards the nucleus appeared much less efficient than in vim$^+$ MEFs

(Fig. 2-7). In each case, the EC-tropic strain TB40/E exhibited a greater reliance on vimentin during entry than the fibroblast-adapted strain, AD169. These observations may indicate that these two strains, which were previously thought to enter HF in a similar manner, actually employ different modes of entry in this cell type. Further, these studies highlight a potentially important and previously underappreciated role for IFs during entry of CMV, and possibly other herpesviruses.

In Chapter 3, I have shifted models and focused on the 55R E1A protein of species C HAdV. This protein is encoded by the 9S mRNA species and is the smallest of all the E1A isoforms. While the mRNA encoding this protein was discovered over 30 years ago, the lack of an Ab which specifically recognizes 55R E1A has precluded more detailed biochemical and functional characterization to this point. To address this issue, we generated rabbit polyclonal Abs against the unique C-terminal amino acid sequence of HAdV-2. I have demonstrated that these Abs can be used to detect HAdV-2 55R E1A by western blot, immunoprecipitation and by indirect immunofluorescence (Fig. 3-1). I have confirmed that like 9S mRNA, 55R E1A is expressed at late times post-infection and that the protein is localized primarily to the nucleus (Fig. 3-2). Using several mutant and recombinant viruses, I have shown that 55R E1A is capable of transactivating the expression of viral genes in primary, contact-inhibited IMR-90 cells (Fig. 3-3). This promoted virus replication, as viruses expressing only the 55R E1A isoform were able to replicate productively and to titres several log-fold greater than E1A null virus in these same cells (Fig. 3-4). I have also identified the first binding partner of 55R E1A in S8 (Fig. 3-5A, B). S8 is a component of APIS, a regulatory subunit of the 26S proteasome. Knockdown of S8 reduced the infectious yield of a virus which expresses only the 55R

E1A isoform, indicating that this interaction is important for the replication-promoting properties of 55R E1A (Fig. 3-5C). These studies are the first to detect and functionally characterize the 55R E1A isoform. The identification of the transactivating and growth-promoting capacities of this protein are intriguing observations that are likely to spawn a new field of E1A research.

Studies described in Chapter 4 again focus on CMV, and in particular, on a novel CMV-encoded protein which we have dubbed RASCAL. RASCAL is encoded by c-ORF29, which is located within the U_S segment of the CMV genome. Interestingly, the RASCAL protein encoded by CMV strains Towne and Toledo is extended by 79 residues, giving the protein a total size of 177 amino acids, compared to the 98 amino acid protein encoded by strains TB40/E and AD169 (Fig. 4-1B). However, the phenotypes that we observed did not seem to be affected by this extension. RASCAL is expressed with early-late kinetics (Fig. 4-2A, B) and localizes to the nuclear rim and in deep intranuclear invaginations at late times post-infection (Fig. 4-3, 4-5). This localization was dependent on the NEC component pUL50 (Fig. 4-7). Co-immunoprecipitation experiments revealed an interaction between RASCAL and pUL50, suggesting that RASCAL is likely a new viral component of the CMV NEC (Fig. 4-8). Intriguingly, RASCAL was also found in small membranous, lamin B-positive vesicles that appeared to emanate from the nucleus at late times post-infection (Fig. 4-6). In the future, it will be interesting to determine whether these unique structures play an active role in viral egress. It will also be important to dissect the particular mechanism through which RASCAL may aide in the egress of CMV.

Taken together, these studies represent focused investigations of three critical stages in viral replication: entry, gene regulation and egress. In addition to gaining valuable knowledge regarding the biology's of CMV and HAdV, these studies have also yielded insights into more basic and general biological principles. The study of processes so fundamental to virus replication always provide the enticing opportunity to identify targets for therapeutic intervention. While it is unclear whether the particular proteins and pathways described herein represent viable therapeutic targets, contextualization of the relative contributions of these phenomena to the process of viral replication as a whole will surely aide in the rational design of compounds that have the potential to improve human health on a global scale.

5.2 Requirement for an Intact Vimentin IF Network to Facilitate Efficient Onset of CMV Infection

Although virus entry may seem like a relatively discreet and straightforward matter of penetrating the cell membrane, it is in fact a complex, multifactorial process that relies on the exploitation of many cellular pathways. After binding to and penetrating the cell membrane, CMV capsids associate the microtubule network where they are presumably transported by dynein motor proteins toward the MTOC (36). While the MTOC is located in close proximity to the nucleus (generally within 1.5 μm in the case of fibroblasts, and even larger distances in other cell types, such as neurons), how capsids make their way from the MTOC to NPCs where nuclear deposition of the viral genome occurs remains poorly understood (49). These distances are 10-80 fold larger than the diameter of the capsid itself (19). The size of CMV capsids coupled with the density of the cytoplasmic

environment make passive diffusion an unlikely explanation for this process (28, 54). Together, these observations would suggest that the virus has evolved a more efficient mechanism to facilitate this process. In addition, studies which have investigated the role of microtubules in CMV transport have used methods that also result in the disruption of IFs, confounding the interpretation of their results (36).

The impact of microtubules and microfilaments on the entry of herpesviruses has been appreciated for some time (28). However, the contributions of IFs during this process have largely been ignored. This is likely due, in large part, to the fact the IFs are unique among the three classes of cytoskeletal proteins in that they lack polarity and associated motor proteins (15). Despite this perceived deficiency, they do possess many other properties that could be considered important in the context of viral infection. IFs are responsible for providing mechanical support for the cell, maintaining the shape and positioning of the nucleus, and organelle targeting, among other functions (13). Finally, the IF network stretches from the plasma membrane (and in some cell types, from the cell surface) to the nucleus, thereby providing multiple opportunities for exploitation during viral entry.

Early observations outlining the dynamics of microtubule and microfilament polymerization during CMV infection led us to first investigate that status of the IF network from viral penetration to expression of IE genes. We found that, akin to microtubules, the vimentin IF network remains stable from binding to expression of IE genes (Fig. 2-1) (36). Given the differential regulation of the other cytoskeletal components, we hypothesized that maintenance of vimentin stability might be

functionally important during CMV entry in HF. We also observed that in comparison to infection with AD169, onset of TB40/E infection as measured by IE gene expression was substantially delayed in HF. This delay was maintained throughout virus replication up to 144 hpi, at which time titres of AD169 and TB40/E equalized (Fig. 2-2). AD169 entry in HF occurs predominantly through direct fusion at the plasma membrane (9, 53). This seems to be mediated by the gH/gL/gO glycoprotein complex present on AD169 virions (21). Historically, entry of TB40/E into HF has been assumed to occur through the same mechanism, despite the fact that in addition to the gH/gL/gO complex expressed by AD169, TB40/E is also capable of expressing gH/gL/UL128-131A. This complex seems to be required for endothelial and epithelial cell tropism (17, 60-61). Strains expressing UL128-131A have been observed to enter endothelial cells by endocytosis, followed by fusion of the viral envelope with the endosomal membrane, which may or may not require low pH (39, 46-47, 51). Considered in the context of the delayed kinetics of TB40/E entry in HF relative to AD169 observed in our study, it is tempting to speculate that TB40/E may also enter HF by endocytosis, or by a combination of endocytosis and direct fusion, depending on the viral glycoprotein - cellular receptor complex that is primarily engaged upon binding. More detailed studies will be necessary to delineate the precise pathway(s) through which TB40/E enters HF. Understanding these processes in detail is of great importance, especially considering the attractiveness of targeting entry in the rational design of anti-viral therapeutics.

To determine if the stability of the vimentin IF network was indeed important during the onset of CMV infection, we treated HF with ACR, a vimentin IF-disrupting agent, prior to infection with strains AD169 or TB40/E. ACR treatment induced aggregation of

vimentin into bundles which were most dense along the cell's retraction fibers. Vimentin aggregation was accompanied by rounding of the cell and a morphological change of the nuclei, characterized primarily by folds and invaginations of the nuclear membrane (Fig. 2-3A-F). As reported in the literature, this treatment left the microtubule network intact, thereby allowing us to assess the role of vimentin IF network directly (2, 37, 48). ACR treatment had an exposure time-dependent inhibitory effect on infection with either AD169 or TB40/E. As expected, the overall proportion of cells infected with TB40/E was lower than that of AD169, consistent with the delay in onset of TB40/E infection of HF observed earlier (Fig. 2-4A, B). Importantly, the effect of ACR treatment on the onset of infection could be overcome at later times post-infection (Fig. 2-4C, D). This was attributed to the reversibility of ACR treatment on the structure of the vimentin cytoskeleton and also gave us confidence that ACR did not have a direct effect on the CMV particles themselves.

Given the potentially pleiotropic effects of ACR on the cell, we felt that it was important to validate our results in other model systems. We were able to exploit fibroblasts from patients with GAN, a neurodegenerative disorder caused in part, by bundling of IFs (42, 66). In HF, this phenotype could be conditionally induced by growing cells from GAN patients in low serum conditions (23). Of particular interest to us, the vimentin abnormalities caused by serum starvation of fibroblasts from GAN patients were distinct from those caused by ACR treatment. GAN fibroblasts exhibited local regions of spherical vimentin bundling, while the structure of vimentin IFs in other parts of the cell remained structurally intact (Fig. 2-5A-H). Infection of these cells with AD169 at an MOI of 1 delayed onset of infection at 4 hpi, but this delay was overcome at 8 and 24 hpi.

Infection at an MOI of 10 reduced the impact of vimentin bundling in GAN HF on AD169 infection. In comparison, we could not detect IE1/IE2 expression in GAN fibroblasts or normal dermal fibroblasts infected with TB40/E at 4 hpi. This delay relative to AD169 infection was thus consistent in fibroblasts regardless of their origin. At 8 and 24 hpi we observed significantly reduced levels at IE1/IE2 expression in fibroblasts from GAN patients infected with TB40/E at an MOI of 1. This reduction was not appreciably reduced when cells were infected at an MOI of 10 (Fig. 2-5I-L).

Together with the results gathered during infection of ACR-treated HF, the GAN model continued to suggest that an intact vimentin cytoskeleton was crucial for the efficient onset of CMV infection. In the context of AD169 infection, vimentin bundling in GAN fibroblasts caused a delay in the onset of infection that could be overcome by both time and MOI. Based on these results, we speculated that vimentin IFs may be important in the proper trafficking of CMV particles to the nucleus. At low MOIs, particles which encountered these bundles would be temporarily impeded. However, at higher MOIs the probability that one or more particles could travel from the cell periphery to the nucleus in a regions where the structure of vimentin IFs remained intact would be greatly improved. Additionally, vimentin bundling in GAN fibroblasts did not result in the severe distortions in nuclear morphology induced by ACR treatment. This reduced the possibility that widespread nuclear instability simply abrogated the ability of viral particles to dock at or translocate their genomes through NPCs. TB40/E was more negatively affected by vimentin bundling than AD169 further suggesteing that these two strains may enter fibroblasts using different mechanisms.

As a final validation that the vimentin IF network is important during onset of CMV infection, we compared the efficiency of infection with AD169 or TB40/E in vim$^+$ or vim$^-$ MEFs. While MEFs do not support productive human CMV infection, the restriction event occurs after expression of IE genes (24-25). Therefore, these cells represented an excellent system through which to study the impact of vimentin on CMV entry. Vim$^-$ MEFs displayed a significantly reduced proportion of IE1/IE2-expressing cells than vim$^+$ MEFs infected with AD169 or TB40/E. The proportion of vim$^+$ MEFs infected with AD169 remained consistent over time and at both tested MOIs. However, the proportion of vim$^-$ MEFs expressing IE1/IE2 moderately increased with time, indicating that the absence of vimentin delayed onset of infection, rather than inhibiting it altogether (Fig. 2-6A, C).

Contrary to the steady proportion of vim$^+$ cells observed at all times during AD169 infection, we observed a sharp rise in the proportion of vim$^+$ cells expressing IE1/IE2 during TB40/E infection between 8 and 24 hpi. In contrast, the number of IE1/IE2-expressing vim$^-$ cells slowly decreased over time. The decrease was not due to the proliferation of uninfected cells, and thus seems to represent abortive infection (Fig. 2-6B, D). In agreement with our earlier observations, TB40/E was again more negatively affected by the absence of vimentin than was AD169. The consistency with which this phenotype was observed serves as strong evidence that these two strains utilize distinct entry pathways in fibroblasts.

To identify the stage at which the absence of vimentin impairs the onset of CMV infection, we tracked individual viral particles stained with an antibody specific for the

capsid-associated tegument protein pp150 during the early stages of infection of vim$^+$ and vim$^-$ MEFs (Fig. 2-7). This protein is known to remain associated with the capsid until disassembly following nuclear deposition of the viral genome (36, 52). There was no difference in the number of pp150+ cells exposed to either strain of virus for 1 h at 4°C. This indicated that vimentin does not affect binding of either AD169 or TB40/E. After transfer of cells to 37°C for 1h, the proportion of pp150+ cells remained consistent among all samples. However, by 4 hpi a sharp decrease was observed in the proportion of pp150+ vim$^+$ cells infected with AD169 relative to pp150+ vim$^-$ cells treated in the same way. This trend was also observed 8 hpi, although the overall number of pp150+ cells steadily decreased. TB40/E infection produced similar results, however the differences between pp150+ vim$^+$ and pp150+ vim$^-$ cells was less pronounced at 4 hpi (Fig. 2-7E). Since pp150 remains associated with the capsid throughout entry, loss of signal is likely to represent degradation subsequent to disassembly of the capsid after nuclear deposition of the viral genome. Taken together, these results suggest that vimentin IFs increase the efficiency of this process at a step subsequent to binding.

To more precisely determine the fate of viral particles in vim$^+$ and vim$^-$ MEFs, we monitored their localization 1 h after transfer to 37°C, at a time wherein the number of pp150+ cells had been determined to be equal among all treatment groups (Fig. 2-7F). Interestingly, we found that there was a general decrease in the proportion of particles localized at the nucleus in vim$^-$ MEFs infected with either AD169 or TB40/E. In the case of AD169, the was accompanied by a concomitant increase in the proportion of particles maintained in the cytoplasm, while TB40/E particles appeared to be retained mainly at the cell periphery (Fig. 2-7A-D). This again led us to conclude that an intact vimentin

cytoskeleton is important for the efficient onset of CMV infection and that it is likely to play a role subsequent to virus binding, potentially during trafficking of particles towards the nucleus.

In summary, we have investigated a previously unappreciated aspect of CMV entry in fibroblasts. We have shown that TB40/E exhibits a consistent delay in the onset of infection in fibroblasts relative to AD169. Our results demonstrate that both the fibroblast-adapted strain AD169, and the EC-tropic strain TB40/E rely on an intact vimentin cytoskeleton during onset of infection in fibroblasts. The structure of vimentin IFs remain unchanged during entry of both CMV strains in fibroblasts, akin to microtubules. Disruption of the vimentin IF network using the chemical agent acrylamide, vimentin bundling in fibroblasts harvested from patients with GAN, and the absence of vimentin in vim⁻ MEFs all had a negative effect on the efficiency of CMV infection. TB40/E consistently exhibited a greater degree of reliance on vimentin IFs than did AD169. Coupled with the delay in onset of infection observed for TB40/E and its retention at the periphery of vim⁻ MEFs, we speculate that TB40/E may enter fibroblasts through a mechanism other than direct fusion at the plasma membrane. The presence of the gH/gL/UL128-131A glycoprotein complex on TB40/E particles offers the possibility that strains expressing this complex are also capable of entering fibroblasts through an endocytic pathway, similar to that observed in endothelial and epithelial cells. Given recent advances in dissecting the multitude of possible endocytic routes of entry exploited by enveloped virus, careful future studies will be needed to understand the specific cellular processes involved (22). The apparent defect in viral particle trafficking observed during infection of vim⁻ MEFs suggested that vimentin IFs are likely to play a role in the

trafficking of AD169 and TB40/E virions post-penetration. Again, retention of TB40/E virions at the periphery of vim⁻ cells may imply that vimentin is also important during penetration of this strain. These dual roles for vimentin during TB40/E entry may account for the greater degree of reliance on vimentin IFs displayed by TB40/E in the various systems explored herein.

Future studies should focus on elucidating the processes through which TB40/E enters fibroblasts. This is likely to be an important point especially as it relates to the development of entry-inhibitor anti-viral therapeutics. In addition, dissecting the specific role assumed by vimentin during the onset of CMV infection will be important in enhancing our understanding of the IF network during CMV entry. It is possible, perhaps even likely, that these same mechanisms are involved in the onset of infection with other types of herpesviruses. Finally, it would be of particular interest to determine whether IF types expressed by other cells function in a way that is analogous to vimentin during CMV entry. Epidemiological data relating the susceptibility of patients with disorders which affect IFs to CMV infection would be especially interesting in this regard.

5.3   A Transactivating and Growth-Promoting Role for 55R E1A During HAdV Infection

It is amazing that despite over three decades of intense study, there remains much to be learned about the many functions of E1A during HAdV infection. This speaks to the amazing complexity and importance of regulating the expression of both viral and cellular genes during the course of infection. While the majority of studies have focused on the products of the 13S and 12S mRNA species, little to nothing is known about the

specific functions of the the product of the 9S mRNA species. The 9S E1A mRNA produced by species C HAdV encodes a 55R protein. Unlike the products of the 11S and 10S E1A which do not contain any novel sequences relative to the 13S product, splicing of 9S E1A causes a frameshift which results in 27 unique C-terminal residues (12, 44, 59). This is not the only property that makes 55R E1A unique relative to all other isoforms, it also accumulates preferentially at late times post-infection and seems to require replication of viral DNA to do so efficiently (8, 55-56, 59, 65). A major barrier to the direct study of 55R E1A function has been the lack of an Ab which specifically recognizes this E1A isoform. Therefore, we set out to generate such and Ab and subsequently perform an initial characterization of 55R E1A encoded by species C HAdV.

Anti-55R E1A polyclonal Abs were generated in rabbits using a peptide immunogen corresponding to residues 43-55 of 55R E1A from HAdV-2 coupled to keyhole limpet hemocyanin. These Abs were affinity-purified and using purified recombinant protein and we were able to show that they are exquisitely specific for the detection of 55R E1A from HAdV-2 (Fig. 3-1C). The Abs could also be used to detect HAdV-2 55R E1A by indirect immunofluorescence and to immunoprecipitate 55R E1A (Fig. 3-1D, E). We were pleased that this new reagent could be used for all of the applications tested and are confident that it will be a useful tool for future studies focused on elucidating the functions of 55R E1A.

As mentioned previously, earlier studies have reported that the 9S E1A mRNA species is expressed with late kinetics and seems to require viral DNA replication (8, 55-56, 59,

65). However, the lack of an Ab which recognizes 55R E1A has precluded an analysis of the kinetics of protein expression until now. In agreement with previous reports, we found that 9S mRNA was expressed at late times post-infection in A549 cells (58-59). Protein expression matched these results closely. The larger E1A isoforms could be detected starting at 6 hpi and expression increased up to 24 hpi. In contrast, 55R E1A could be detected only weakly at 24 hpi and expression increased up to 72 hpi (Fig. 3-2). This was the first time that endogenous 55R E1A has ever been detected. Of particular interest was the observation that during infection, 55R E1A appears to be located predominantly in the nucleus of host cells (Fig. 3-2B). 55R E1A lacks the NLS present in the larger E1A isoforms, however, at a predicted MW of only 6 kDa it falls well below the approximately 40 kDa exclusion size mediated by the NPC (63). Once in the nucleus, 55R E1A may be retained through binding to other factors also present in the nucleus, resulting in the apparent enrichment observed by immunofluorescence analysis.

The localization of 55R E1A in the nucleus led us to question whether 55R E1A played any role in regulation of viral gene expression. Along with helping push host cells into the S-phase of the cell division cycle, this is one of the major functions of E1A, especially the 289R protein (3). We found that compared to dl312 (an E1A-null virus), viruses expressing only the 55R E1A isoform from either cDNA (JM17-55R) or from mutated genomic DNA (dl521), transactivated the expression of all viral genes tested to at least a limited extent. As expected, the maximal level of transactivation achieved by viruses expressing only 55R E1A was consistently lower than those observed during dl309 infection (Fig. 3-3). 289R E1A, which is expressed during dl309 infection, contains CR3, a potent transactivating domain. This activity is mediated through interactions with

a variety of cellular proteins, including MED23 (a component of the mediator complex), TBP, p300/CBP and S8 (1, 4, 16, 26, 29, 40-41, 43, 62). 55R E1A lacks this region as well as all of the other CRs. In fact, it shares only it's first 29 amino acids with the other E1A isoforms. Unlike HAdV-12, these 29 amino acids encoded by HAdV-2 do not seem to possess a transactivation function (27). This would suggest that the transactivating properties of 55R E1A are mediated, at least in part, by the novel C-terminal domain found within this protein. Potential binding partners of this region remain completely unexplored and represent an exciting new field of research. Identifying these putative factors will help in elucidating the mechanism through which 55R E1A transactivates viral gene expression and may uncover as yet undiscovered functions. Given the kinetics of expression, it is tempting to speculate that 55R E1A may preferentially induce viral and cellular genes that are important at the later stages of HAdV infection. In support of this, hexon was one of the most strongly-induced transcripts by viruses which expressed only the 55R E1A isoform (Fig. 3-3E). E4orf6/7 transcription was also potently stimulated by viruses expressing 55R E1A. This protein is known to dimerize with free E2Fs, which increases their affinity to stimulate transcription of the viral E2 promoter (10, 31, 35). Since processing of the 9S transcript seems to rely on viral DNA replication, this may serve as a positive feedback loop at late times post-infection to ensure that the viral genome is replicated to appropriate levels and that 55R E1A is expressed efficiently.

While we have shown that 55R E1A is capable of transactivating the expression of viral genes, it does not appear to be sufficient to transform primary rodent cells in cooperation with E1B, nor does it share the pro-apoptotic properties of 289R E1A (18, 64). This led us to question whether 55R E1A could, in addition to transactivating the expression of

viral genes, promote productive replication of HAdV in contact-inhibited, primary IMR-90 fibroblasts. To assess this, contact inhibited IMR-90 cells were infected with a variety of viruses capable of expressing multiple combinations of E1A isoforms, including both JM17-55R and dl521, which express only 55R E1A. Replication assays were performed and titres for each virus were normalized to those gathered from infections with dl312, an E1A-null virus. As expected, virus expressing wildtype E1A grew to the highest titres, followed by a virus which expresses 289R, but not 243R E1A. Viruses expressing only 55R E1A consistently replicated to titres over one log-fold greater than E1A-null virus. To our surprise, replication of JM17-55R at 48 hpi and dl521 and 120 hpi exceeded that of dl520, a virus which expresses 243R E1A, but not the 289R protein (Fig. 3-4A). These results demonstrate that the 55R E1A can not only stimulate expression of viral genes, but can also promote productive viral replication to a substantial degree in an E1A-null background.

Studying the effect of the 55R E1A isoform in isolation provided a controlled environment through which we were able to dissect the functions of that particular E1A isoform without confounding influences from the other E1A proteins. However, during infection 55R E1A is expressed in the context of the other E1A isoforms, and therefore determining the contribution of 55R E1A to HAdV replication in the context of the other E1A isoforms was important. To do this, we performed co-infections experiments whereby contact-inhibited IMR-90 cells were infected with either a 289R E1A-expressing virus (pm975) or a 243R E1A-expressing virus (dl520) and either dl521 (55R E1A only) or dl312 (E1A null). In combination with pm975, dl521 co-infection did not increase viral titres above those observed during co-infection with dl312. In contrast,

dl521 increased viral titres 1- and 2-log-fold at 48 and 120 hpi, respectively, in combination with dl520 (Fig. 3-4B). Since both pm975 and dl520 are capable of expressing 55R E1A on their own, these results indicate that endogenous levels of 55R E1A are sufficient to maximize the replication potential of HAdV in combination with 289R E1A. However, when 289R E1A is not expressed, as is the case during dl520 infection, providing additional 55R E1A can further enhance viral replication. These results agree well with our earlier observation that both JM17-55R and dl521 are capable of replicating to titres greater than those of dl520 in contact-inhibited IMR-90 cells.

Given that 55R E1A shares its first 29 amino acids with the larger E1A proteins, we hypothesized that cellular partners which interact with this region may also be important for the function of 55R E1A. Based on our finding that 55R E1A was able to transactivate expression of viral genes, we focused our attention on S4 and S8. These two proteins are components of APIS, the regulatory component of the 26S proteasome. Both have been shown to interact with E1A residues 4-25 (57). Later, S8 was also shown to interact with CR3 and could be recruited to HAdV early gene promoters (43). Most interesting in the context of our work, was the observation that inhibition of proteasome activity had an inhibitory effect on the ability of E1A to transactivate viral genes (43). However, the effect of proteasome inhibition on viral replication was not directly tested. We found that 55R E1A interacted well with S8 in both GST pulldown and immunoprecipitation assays. Surprisingly, we did not detect an interaction with S4 (Fig. 3-5A). These results would suggest that 55R E1A interacts with S8 selectively, and that either the C-terminus of 55R E1A had an inhibitory effect on the S4 interaction, or that regions present in the larger E1A isoforms but absent from the 55R isoform stabilize the

interaction. We hypothesized that if the interaction of 55R E1A with S8 played an important role in its ability to transactivate viral gene expression, knockdown of S8 should have an impact on the ability of a virus expressing only 55R E1A to replicate. Indeed, we found that knockdown of S8 in A549 cells reduced viral titres by 2-fold 48 hpi (Fig. 3-5C). This strongly suggests that the interaction with S8 plays an important role in the replication-promoting properties of 55R E1A. Not only does the S8 interaction provide some insight into the mechanism through which 55R E1A accomplishes its functions, it is also the first reported binding partner of 55R E1A.

In the future, it will be of great interest to determine additional binding partners of 55R E1A, specifically those which bind the unique C-terminal region of the protein. Identifying these interactions and elucidating their functional consequences will provide additional insight into a severely understudied area of HAdV biology - the function of the 55R E1A protein.

5.4   RASCAL, a Potential New Member of the CMV NEC

The nuclear egress of CMV nucleocapsids is a complex process that requires the formation of a multiprotein complex consisting of both viral and cellular factors. While several members of this complex have recently been identified, it is highly likely that additional factors are also involved. CMV, like other herpesviruses, contains a very large genome by virus standards and thus, many ORFs have yet to be characterized. Several studies in the past have demonstrated that serial passage of clinical isolates on HF leads to the mutation or deletion of ORFs which are responsible for maintaining the broad cell tropism exhibited during natural infection (7, 17, 60-61). While the loss of epithelial and

endothelial cell tropism has been mapped to mutations in the UL128-131A gene locus, AD169, a fibroblast-adapted CMV strain which contains a frameshift mutation leading to a non-functional UL131A product, remains able to infect mature Langerhans cells (17, 20, 60-61). This suggests that other, as of yet uncharacterized ORFs, may help mediate CMV tropism for specific cell types. In an attempt to identify these factors, we compared each ORF present in TB40/E-BAC4 to the corresponding ORFs from five other common CMV strains. A recently identified putative ORF, originally called c-ORF29, was of particular interest as the putative protein encoded by CMV strains Towne and Toledo was 75 amino acids longer than the corresponding protein encoded by AD169 and TB40/E (34). Thus, we set out to characterize the role of this putative protein during CMV infection, and to compare the two variants of the protein to one another.

In silico analysis of both short and long RASCAL sequence revealed the presence of putative transmembrane domains at the N- and C-termini of the short RASCAL isoform. Two additional regions of high hydrophobicity were identified in the long RASCAL isoform, but neither were reliably predicted to be a transmembrane domain. The protein was also predicted to contain PKC and PKA phosphorylation sites (Fig. 4-1B, C). These predictions were particularly insightful in light of the fact that RASCAL was found to localize at the nuclear membrane and to interact with components of the CMV NEC, which contains PKC and is known to rely on extensive phosphorylation events to remodel the nuclear lamina. In the future it will be interesting to determine whether RASCAL is indeed phosphorylated, and whether phosphorylation is important in regulating its function.

To ensure that c-ORF29 actually produced a transcript, we performed RT-PCR analysis on HF that had been infected with either TB40/E or Towne/GFP-IE2. In each case we observed a band corresponding to the predicted size of the respective c-ORF29 isoform. Sequencing confirmed that a T-to-C transition had occurred at position 292 of RASCAL$_{Towne}$ that resulted in the conversion of a TAA stop codon into a CAA codon, which codes for Gln. To determine the kinetics of c-ORF29 expression, HF were treated with PFA, a compound that inhibits viral DNA replication by interfering with UL44 - the viral DNA polymerase processivity subunit, or were left untreated. These cells were then infected with TB40/E and samples were collected at multiple times post-infection for RT-PCR analysis of c-ORF29 expression. PFA treatment diminished, but did not completely abolish c-ORF29 expression, indicating that it is expressed with early-late kinetics (Fig. 4-2A, B). Interestingly, despite the incomplete inhibition of c-ORF29 mRNA expression, PFA treatment of HF was subsequently found to reduce RASCAL protein levels below detectable levels (Fig. 4-4). These experiments were performed using rabbit polyclonal Abs generated using a peptide corresponding to residues 21 to 39 of RASCAL$_{TB40/E}$. This antibody was able to recognize RASCAL isoforms encoded by both TB40/E and Towne/GFP-IE2 (Fig. 4-2C, D).

In order to narrow down the potential function of RASCAL during infection, we sought to determine its subcellular localization during infection. To this end, HF were infected with either Towne/GFP-IE2 (Fig. 4-3), AD169 or TB40/E, and samples were collected and stained at multiple times post-infection. RASCAL expression was clearly detectable starting at 48 hpi, with punctate cytoplasmic staining and enrichment around the nucleus (Fig. 4-3). As infection progressed, enrichment at the nuclear membrane continued and

RASCAL could be found co-localizing with lamin B in deep intranuclear invaginations (Fig. 4-3, 4-5). These structures were reminiscent of those previously reported during immunofluorescence and ultrastructural studies of CMV infection. The invaginations were subsequently found to occur at late times post-infection and to contain UL50, UL53 and UL97, central components of the CMV NEC (5-6, 11, 14, 30, 38, 45, 50). In these regions, the nuclear lamina has been reported to be dissolved and the INM seems to stretch down to areas which are dense with CMV nucleocapsids. Indeed, capsids can be seen budding into these structures, and therefore, they are thought to be regions of primary envelopment (5).

Strikingly, at late stages of infection RASCAL was also observed in lamin B-positive vesicles that appeared to be derived from the nuclear envelope and stretched throughout the body of the cell (Fig. 4-6). These structures were induced during infection by CMV strains encoding either the large or small RASCAL isoforms. The size of these structures, coupled with their distance from the nuclear envelope raises the intriguing possibility that they may undergo active retrograde transport. Whether these structures contain CMV virions or other viral components remains to be seen. Closer examination of the contents contained within these structures will be of great interest in future studies, as will examining their potential role in the CMV replication cycle.

Due to the kinetics of RASCAL accumulation at the nucleus, we questioned whether other viral factors might be required to mediate its localization. Indeed, pUL50 and its homologs are known to be required for the proper localization of pUL53 (and its homologs) during assembly of the NEC (32-33). Exogenous expression of RASCAL in

HEK293T cells revealed that when expressed alone, RASCAL does not become enriched at the nuclear rim. However, co-expression of RASCAL with UL50-HA, but not UL53-FLAG was sufficient to induce accumulation of RASCAL at the nuclear envelope (Fig. 4-7). The association of RASCAL with pUL50 was also confirmed by immunoprecipitation (Fig. 4-8). Interestingly, contrary to results obtained using COS7 cells, expression of RASCAL, UL50 and UL53 either alone or in combination with one another were insufficient to induce the invaginations of the INM observed during infection (6). This suggests that functioning of the NEC may, in some cases, be cell-type dependent.

It was surprising that at no point in our study did we observe a functional difference between the long and short RASCAL proteins. This leaves us to hypothesize that differences in the function of these two isoforms might be quite subtle and/or context-dependent. We did not directly compare the two RASCAL isoforms in the context of measuring efficiency of viral egress. Therefore, it is possible that differences may exist at that level. It is also possible that the elongated RASCAL isoform may have additional functions only in particular cell types, potentially by interacting with specific viral or cellular NEC components required in only these cells.

In the future, it will be important to carefully map all of the binding partners of RASCAL so that its relative contribution to the NEC can be determined. It will also be interesting to determine whether, and in what contexts, the long and short isforms of RASCAL function differently. The RASCAL- and lamin B-positive vesicles observed at late times post-infection are especially intriguing, as they may constitute a previously unknown

pathway that contributes to CMV egress. In conclusion, we have identified novel CMV protein that exhibits interesting nuclear and vesicular localization at late times post-infection. This protein appears to exist in complex with pUL50, and requires pUL50 for its enrichment at the nuclear rim. Together, these results suggests that RASCAL may be a novel viral component of the CMV NEC.

5.5 Concluding Remarks

" Science is facts; just as houses are made of stone, so is science made of facts; but a pile of stones is not a house, and a collection of facts is not necessarily science."
-*Jules Henri Ponticaré (1854-1912) French Mathematician*

This work has described studies concerned with exploring three processes essential in the replication cycle of all viruses: entry, gene regulation and egress. Considered in isolation, each chapter seems to focus on the investigation of a fixed process, applicable to one particular virus. Even such stepwise contributions to our understanding of viral biology should not be overlooked. We have, after all, not only described a function for two previously unstudied viral proteins and identified a novel cellular factor important during CMV entry, but in doing so, have also catalyzed new fields for future investigation. It is this contextualization of observations and the spawning of new ideas that underlie the very nature of science, and differentiate it from a collection of meaningless facts. Considered together, the studies described herein tell a much more important story about the very nature of infection and the many processes which even the simplest of viruses must accomplish in order to replicate productively. It is in considering these broader truths that we are able to extract the truly immeasurable contribution of scientific inquiry to society. We should not forget the privilege that we experience being in a position to

make such contributions, nor the responsibility that such a privilege entails. Each of these studies has built on years of research describing either the importance of the cytoskeleton during virus entry, the pleiotropic functions of E1A during HAdV infection, or the mechanism of CMV nuclear egress and composition of the CMV NEC. Our contributions to these areas have improved the current state of knowledge underlying three fundamental viral processes. We are confident that this work will now serve as the foundation of future studies that will continue to expand our understanding of the natural world, and that directly or indirectly, they will play a key role in a much larger body of biomedical knowledge that continually catalyzes the improvement of human health.

5.6   References

1.   **Ablack, J. N., P. Pelka, A. F. Yousef, A. S. Turnell, R. J. Grand, and J. S. Mymryk.** 2010. Comparison of E1A CR3-dependent transcriptional activation across six different human adenovirus subgroups. J Virol **84:**12771-12781.

2.   **Aggeler, J.** 1990. Cytoskeletal dynamics in rabbit synovial fibroblasts: II. Reformation of stress fibers in cells rounded by treatment with collagenase-inducing agents. Cell Motil Cytoskeleton **16:**121-132.

3.   **Berk, A. J.** 2007. Adenoviridae, p. 2355-2394. *In* D. M. Knipe (ed.), Field's Virology, 5th ed. Lippincott Williams & Wilkins, Philadelphia, PA.

4.   **Boyer, T. G., M. E. Martin, E. Lees, R. P. Ricciardi, and A. J. Berk.** 1999. Mammalian Srb/Mediator complex is targeted by adenovirus E1A protein. Nature **399:**276-279.

5.   **Buser, C., P. Walther, T. Mertens, and D. Michel.** 2007. Cytomegalovirus primary envelopment occurs at large infoldings of the inner nuclear membrane. J Virol **81:**3042-3048.

6.   **Camozzi, D., S. Pignatelli, C. Valvo, G. Lattanzi, C. Capanni, P. Dal Monte, and M. P. Landini.** 2008. Remodelling of the nuclear lamina during human cytomegalovirus infection: role of the viral proteins pUL50 and pUL53. J Gen Virol **89:**731-740.

7. **Cha, T. A., E. Tom, G. W. Kemble, G. M. Duke, E. S. Mocarski, and R. R. Spaete.** 1996. Human cytomegalovirus clinical isolates carry at least 19 genes not found in laboratory strains. J Virol **70:**78-83.

8. **Chow, L. T., T. R. Broker, and J. B. Lewis.** 1979. Complex splicing patterns of RNAs from the early regions of adenovirus-2. J Mol Biol **134:**265-303.

9. **Compton, T., R. R. Nepomuceno, and D. M. Nowlin.** 1992. Human cytomegalovirus penetrates host cells by pH-independent fusion at the cell surface. Virology **191:**387-395.

10. **Cress, W. D., and J. R. Nevins.** 1994. Interacting domains of E2F1, DP1, and the adenovirus E4 protein. J Virol **68:**4213-4219.

11. **Dal Monte, P., S. Pignatelli, N. Zini, N. M. Maraldi, E. Perret, M. C. Prevost, and M. P. Landini.** 2002. Analysis of intracellular and intraviral localization of the human cytomegalovirus UL53 protein. J Gen Virol **83:**1005-1012.

12. **Dijkema, R., B. M. Dekker, H. van Ormondt, A. de Waard, J. Maat, and H. W. Boyer.** 1980. Gene organization of the transforming region of weakly oncogenic adenovirus type 7: the E1a region. Gene **12:**287-299.

13. **Eriksson, J. E., T. Dechat, B. Grin, B. Helfand, M. Mendez, H. M. Pallari, and R. D. Goldman.** 2009. Introducing intermediate filaments: from discovery to disease. J Clin Invest **119:**1763-1771.

14. **Gilloteaux, J., and M. R. Nassiri.** 2000. Human bone marrow fibroblasts infected by cytomegalovirus: ultrastructural observations. J Submicrosc Cytol Pathol **32:**17-45.

15. **Godsel, L. M., R. P. Hobbs, and K. J. Green.** 2008. Intermediate filament assembly: dynamics to disease. Trends Cell Biol **18:**28-37.

16. **Gold, M. O., J. P. Tassan, E. A. Nigg, A. P. Rice, and C. H. Herrmann.** 1996. Viral transactivators E1A and VP16 interact with a large complex that is associated with CTD kinase activity and contains CDK8. Nucleic Acids Res **24:**3771-3777.

17. **Hahn, G., M. G. Revello, M. Patrone, E. Percivalle, G. Campanini, A. Sarasini, M. Wagner, A. Gallina, G. Milanesi, U. Koszinowski, F. Baldanti, and G. Gerna.** 2004. Human cytomegalovirus UL131-128 genes are indispensable for virus growth in endothelial cells and virus transfer to leukocytes. J Virol **78:**10023-10033.

18. **Haley, K. P., J. Overhauser, L. E. Babiss, H. S. Ginsberg, and N. C. Jones.** 1984. Transformation properties of type 5 adenovirus mutants that differentially express the E1A gene products. Proc Natl Acad Sci U S A **81:**5734-5738.

19. **Hertel, L.** 2011. Herpesviruses and intermediate filaments: Close encounters with the third type. Viruses **3:**1015-1040.

20. **Hertel, L., V. G. Lacaille, H. Strobl, E. D. Mellins, and E. S. Mocarski.** 2003. Susceptibility of immature and mature Langerhans cell-type dendritic cells to infection and immunomodulation by human cytomegalovirus. J Virol **77:**7563-7574.

21. **Hobom, U., W. Brune, M. Messerle, G. Hahn, and U. H. Koszinowski.** 2000. Fast screening procedures for random transposon libraries of cloned herpesvirus genomes: mutational analysis of human cytomegalovirus envelope glycoprotein genes. J Virol **74:**7720-7729.

22. **Klasse, P. J., R. Bron, and M. Marsh.** 1998. Mechanisms of enveloped virus entry into animal cells. Adv Drug Deliv Rev **34:**65-91.

23. **Klymkowsky, M. W., and D. J. Plummer.** 1985. Giant axonal neuropathy: a conditional mutation affecting cytoskeletal organization. J Cell Biol **100:**245-250.

24. **Lafemina, R. L., and G. S. Hayward.** 1988. Differences in cell-type-specific blocks to immediate early gene expression and DNA replication of human, simian and murine cytomegalovirus. J Gen Virol **69 (Pt 2):**355-374.

25. **LaFemina, R. L., and G. S. Hayward.** 1983. Replicative forms of human cytomegalovirus DNA with joined termini are found in permissively infected human cells but not in non-permissive Balb/c-3T3 mouse cells. J Gen Virol **64 (Pt 2):**373-389.

26. **Lee, W. S., C. C. Kao, G. O. Bryant, X. Liu, and A. J. Berk.** 1991. Adenovirus E1A activation domain binds the basic repeat in the TATA box transcription factor. Cell **67:**365-376.

27. **Lipinski, K. S., G. Kroner-Lux, H. Esche, and D. Brockmann.** 1997. The E1A N terminus (aa 1-29) of the highly oncogenic adenovirus type 12 harbours a trans-activation function not detectable in the non-oncogenic serotype 2. J Gen Virol **78 (Pt 2):**413-421.

28. **Lyman, M. G., and L. W. Enquist.** 2009. Herpesvirus interactions with the host cytoskeleton. J Virol **83:**2058-2066.

29. **Malik, S., and R. G. Roeder.** 2005. Dynamic regulation of pol II transcription by the mammalian Mediator complex. Trends Biochem Sci **30:**256-263.

30. **Marschall, M., A. Marzi, P. aus dem Siepen, R. Jochmann, M. Kalmer, S. Auerochs, P. Lischka, M. Leis, and T. Stamminger.** 2005. Cellular p32 recruits cytomegalovirus kinase pUL97 to redistribute the nuclear lamina. J Biol Chem **280:**33357-33367.

31. **Marton, M. J., S. B. Baim, D. A. Ornelles, and T. Shenk.** 1990. The adenovirus E4 17-kilodalton protein complexes with the cellular transcription factor E2F, altering its DNA-binding properties and stimulating E1A-independent accumulation of E2 mRNA. J Virol **64:**2345-2359.

32. **Milbradt, J., S. Auerochs, and M. Marschall.** 2007. Cytomegaloviral proteins pUL50 and pUL53 are associated with the nuclear lamina and interact with cellular protein kinase C. J Gen Virol **88:**2642-2650.

33. **Muranyi, W., J. Haas, M. Wagner, G. Krohne, and U. H. Koszinowski.** 2002. Cytomegalovirus recruitment of cellular kinases to dissolve the nuclear lamina. Science **297:**854-857.

34. **Murphy, E., I. Rigoutsos, T. Shibuya, and T. E. Shenk.** 2003. Reevaluation of human cytomegalovirus coding potential. Proc Natl Acad Sci U S A **100:**13585-13590.

35. **Obert, S., R. J. O'Connor, S. Schmid, and P. Hearing.** 1994. The adenovirus E4-6/7 protein transactivates the E2 promoter by inducing dimerization of a heteromeric E2F complex. Mol Cell Biol **14:**1333-1346.

36. **Ogawa-Goto, K., K. Tanaka, W. Gibson, E. Moriishi, Y. Miura, T. Kurata, S. Irie, and T. Sata.** 2003. Microtubule network facilitates nuclear targeting of human cytomegalovirus capsid. J Virol **77:**8541-8547.

37. **Olink-Coux, M., M. Huesca, and K. Scherrer.** 1992. Specific types of prosomes are associated to subnetworks of the intermediate filaments in PtK1 cells. Eur J Cell Biol **59:**148-159.

38. **Papadimitriou, J. M., G. R. Shellam, and T. A. Robertson.** 1984. An ultrastructural investigation of cytomegalovirus replication in murine hepatocytes. J Gen Virol **65 (Pt 11):**1979-1990.

39. **Patrone, M., M. Secchi, E. Bonaparte, G. Milanesi, and A. Gallina.** 2007. Cytomegalovirus UL131-128 products promote gB conformational transition and gB-gH interaction during entry into endothelial cells. J Virol **81:**11479-11488.

40. **Pelka, P., J. N. Ablack, M. Shuen, A. F. Yousef, M. Rasti, R. J. Grand, A. S. Turnell, and J. S. Mymryk.** 2009. Identification of a second independent binding site for the pCAF acetyltransferase in adenovirus E1A. Virology **391:**90-98.

41. **Pelka, P., J. N. Ablack, J. Torchia, A. S. Turnell, R. J. Grand, and J. S. Mymryk.** 2009. Transcriptional control by adenovirus E1A conserved region 3 via p300/CBP. Nucleic Acids Res **37:**1095-1106.

42. **Pena, S. D.** 1981. Giant axonal neuropathy: intermediate filament aggregates in cultured skin fibroblasts. Neurology **31:**1470-1473.

43. **Rasti, M., R. J. Grand, A. F. Yousef, M. Shuen, J. S. Mymryk, P. H. Gallimore, and A. S. Turnell.** 2006. Roles for APIS and the 20S proteasome in adenovirus E1A-dependent transcription. EMBO J **25:**2710-2722.

44. **Roberts, B. E., J. S. Miller, D. Kimelman, C. L. Cepko, I. R. Lemischka, and R. C. Mulligan.** 1985. Individual adenovirus type 5 early region 1A gene products elicit distinct alterations of cellular morphology and gene expression. J Virol **56:**404-413.

45. **Ruebner, B. H., K. Miyai, R. J. Slusser, P. Wedemeyer, and D. N. Medearis, Jr.** 1964. Mouse Cytomegalovirus Infection. An Electron Microscopic Study of Hepatic Parenchymal Cells. Am J Pathol **44:**799-821.

46. **Ryckman, B. J., M. A. Jarvis, D. D. Drummond, J. A. Nelson, and D. C. Johnson.** 2006. Human cytomegalovirus entry into epithelial and endothelial cells depends on genes UL128 to UL150 and occurs by endocytosis and low-pH fusion. J Virol **80:**710-722.

47. **Ryckman, B. J., B. L. Rainish, M. C. Chase, J. A. Borton, J. A. Nelson, M. A. Jarvis, and D. C. Johnson.** 2008. Characterization of the human cytomegalovirus gH/gL/UL128-131 complex that mediates entry into epithelial and endothelial cells. J Virol **82:**60-70.

48. **Sager, P. R.** 1989. Cytoskeletal effects of acrylamide and 2,5-hexanedione: selective aggregation of vimentin filaments. Toxicol Appl Pharmacol **97:**141-155.

49. **Salpingidou, G., A. Smertenko, I. Hausmanowa-Petrucewicz, P. J. Hussey, and C. J. Hutchison.** 2007. A novel role for the nuclear membrane protein emerin in association of the centrosome to the outer nuclear membrane. J Cell Biol **178:**897-904.

50. **Severi, B., M. P. Landini, and E. Govoni.** 1988. Human cytomegalovirus morphogenesis: an ultrastructural study of the late cytoplasmic phases. Arch Virol **98:**51-64.

51. **Sinzger, C., M. Digel, and G. Jahn.** 2008. Cytomegalovirus cell tropism. Curr Top Microbiol Immunol **325:**63-83.

52. **Sinzger, C., M. Kahl, K. Laib, K. Klingel, P. Rieger, B. Plachter, and G. Jahn.** 2000. Tropism of human cytomegalovirus for endothelial cells is determined by a post-entry step dependent on efficient translocation to the nucleus. J Gen Virol **81:**3021-3035.

53. **Smith, J. D., and E. de Harven.** 1974. Herpes simplex virus and human cytomegalovirus replication in WI-38 cells. II. An ultrastructural study of viral penetration. J Virol **14:**945-956.

54. **Sodeik, B.** 2000. Mechanisms of viral transport in the cytoplasm. Trends Microbiol **8:**465-472.

55. **Spector, D. J., D. N. Halbert, and H. J. Raskas.** 1980. Regulation of integrated adenovirus sequences during adenovirus infection of transformed cells. J Virol **36:**860-871.

56. **Spector, D. J., M. McGrogan, and H. J. Raskas.** 1978. Regulation of the appearance of cytoplasmic RNAs from region 1 of the adenovirus 2 genome. J Mol Biol **126:**395-414.

57. **Turnell, A. S., R. J. Grand, C. Gorbea, X. Zhang, W. Wang, J. S. Mymryk, and P. H. Gallimore.** 2000. Regulation of the 26S proteasome by adenovirus E1A. EMBO J **19:**4759-4773.

58. **Ulfendahl, P. J., S. Linder, J. P. Kreivi, K. Nordqvist, C. Sevensson, H. Hultberg, and G. Akusjarvi.** 1987. A novel adenovirus-2 E1A mRNA encoding a protein with transcription activation properties. EMBO J **6:**2037-2044.

59. **Virtanen, A., and U. Pettersson.** 1983. The molecular structure of the 9S mRNA from early region 1A of adenovirus serotype 2. J Mol Biol **165:**496-499.

60. **Wang, D., and T. Shenk.** 2005. Human cytomegalovirus UL131 open reading frame is required for epithelial cell tropism. J Virol **79:**10330-10338.

61. **Wang, D., and T. Shenk.** 2005. Human cytomegalovirus virion protein complex required for epithelial and endothelial cell tropism. Proc Natl Acad Sci U S A **102:**18153-18158.

62. **Wang, G., and A. J. Berk.** 2002. In vivo association of adenovirus large E1A protein with the human mediator complex in adenovirus-infected and -transformed cells. J Virol **76:**9186-9193.

63. **Wente, S. R., and M. P. Rout.** 2010. The nuclear pore complex and nuclear transport. Cold Spring Harb Perspect Biol **2:**a000562.

64. **White, E., and B. Stillman.** 1987. Expression of adenovirus E1B mutant phenotypes is dependent on the host cell and on synthesis of E1A proteins. J Virol **61:**426-435.

65. **Wilson, M. C., and J. E. Darnell, Jr.** 1981. Control of messenger RNA concentration by differential cytoplasmic half-life. Adenovirus messenger RNAs from transcription units 1A and 1B. J Mol Biol **148:**231-251.

66.   **Yang, Y., E. Allen, J. Ding, and W. Wang.** 2007. Giant axonal neuropathy. Cell Mol Life Sci **64:**601-609.

CURRICULUM VITAE

Matthew S. Miller, B.M.Sc. (Hon.)

Education

2007-2011, The University of Western Ontario
- Ph.D. Candidate-Department of Microbiology and Immunology (Supervisor: Dr. J.S. Mymryk)

2003-2007, The University of Western Ontario
- Bachelor of Medical Sciences [B.M.Sc. (Hon.)]-Honors Specialization in Microbiology and Immunology

2000-2003, Nicholson Catholic College, Belleville, Ontario, Canada

1999-2000, St. Theresa Catholic Secondary School, Belleville, Ontario, Canada

Publications

An Unhealthy Relationship: Viral Manipulation of the Nuclear Receptor Superfamily. **Matthew S. Miller** and Joe S. Mymryk. 2011. Future Microbiol. *In Press*

Adenovirus E1A directly targets the DP-1/E2F complex. Peter Pelka, **Matthew S. Miller**, Matthew Checchini, Ahmed Fayed Yousef, Dawn M. Bowdish, Fred Dick, Peter Whyte and Joe S. Mymryk. 2011. J Virol. Jun 29. [Epub ahead of print]

RASCAL is a new human cytomegalovirus-encoded protein localizing to the nuclear lamina and in cytoplasmic vesicles at late times post-infection. **Matthew S. Miller,** Leesa Pennell, Wendy E. Furlong, Marc Geadah and Laura Hertel. 2010. J. Virol. **84:**6483-6496.

Onset of human cytomegalovirus replication in fibroblasts requires the presence of an intact vimentin cytoskeleton. **Matthew S. Miller** and Laura Hertel. 2009. J. Virol. **83:**7015-1728.

Human cytomegalovirus US9 protein contains an N-terminal signal sequence and a C-terminal mitochondrial localization domain, and does not alter cellular sensitivity to apoptosis. Lana Mandic, **Matthew S. Miller**, Corinne Coulter, Brian Munshaw and Laura Hertel. 2009. J. Gen. Virol. **90**:1172-1182.

Sumitted Manuscripts

Characterization of the 55 Residue Protein Encoded by the 9S mRNA of Species C Adenovirus. **Matthew S. Miller**, Peter Pelka, Michael Cohen, Jenna Kelly, Peter Whyte and Joe S. Mymryk. 2011.

<u>Conference Presentations</u>

*Award-winning presentation (see 'Research Awards and Accomplishments' section for details)

2011 - Molecular Biology of DNA Tumor Viruses Conference, Trieste, Italy
- Oral Presentation - A Forgotten Frontier: Characterization of the Human Adenovirus Species C 55R E1A Protein

*2010 – Infection and Immunity Research Forum, The University of Western Ontario
- Poster - Functional studies of the human adenovirus subgroup C 55R E1A protein

2010-Molecular Biology of DNA Tumor Viruses Conference, The University of Wisconsin, Madison, WI
- Poster - Functional studies of the human adenovirus subgroup C 55R E1A protein

2009-Infection and Immunity Research Forum, The University of Western Ontario
- Oral Presentation – RASCAL, a novel human cytomegalovirus-encoded component of the nuclear egress complex

*2009-International Herpesvirus Workshop, Cornell University, Ithaca, NY
- Oral Presentation - Efficient onset of human cytomegalovirus replication in fibroblasts requires the presence of an intact vimentin cytoskeleton

*2009- Margaret Moffat Research Day, The University of Western Ontario
- Poster - Efficient onset of human cytomegalovirus replication in fibroblasts requires the presence of an intact vimentin cytoskeleton

*2008- Infection and Immunity Research Forum, The University of Western Ontario
- Oral Presentation – Efficient onset of human cytomegalovirus replication in fibroblasts requires the presence of an intact vimentin cytoskeleton

2008- American Society for Virology Annual Conference, Cornell University
- Poster - Human cytomegalovirus entry in host cells: A role for vimentin?

2008- Margaret Moffat Research Day, The University of Western Ontario
- Poster – Human cytomegalovirus entry in host cells: A role for vimentin?

*2007- Infection and Immunity Research Forum, The University of Western Ontario
- Poster – Human cytomegalovirus entry in host cells: A role for vimentin?

<u>Invited Lectures</u>

2011 - A Forgotten Frontier: Characterization of the Human Adenovirus 55 Residue E1A Protein. Seminar in acceptance of the John A. Thomas Award
Location: The University of Western Ontario, London, Ontario.

2010 – Introduction to Infection and Immunity Research & Career Perspectives
Location: Nicholson Catholic College, Belleville, Ontario.

2008 – An Introduction to Infection and Immunity.
Location: Georges Vanier Elementary School, Belleville, Ontario.

Recent Awards and Accomplishments

2011, John A. Thomas Award. Value = $1 500 CAD
- Awarded to the top Ph.D. Candidate in the Schulich School of Medicine and Dentistry during their last year in their program from the areas including Bacteriology, Virology, Immunology and Genetics.

2010, Wisent Biocenter Award for Excellence in Graduate Poster Presentation – 2010 Infection and Immunity Research Forum. Value = $100 CAD
- Awarded to the graduate poster presentation judged to be the strongest within its category

2010-2013, Canadian Institutes of Health Research Frederick Banting and Charles Best Canada Graduate Scholarship Doctoral Research Award. Value = $105 000 over 3 years ($35 000/yr) CAD
- Awarded to the top national Ph.D. candidates participating in health research

2010, Ontario Graduate Scholarship – Declined. Value = $15 000 CAD
- Awarded to the top graduate students across all disciplines in the Province of Ontario

2010, John Robinson Graduate Scholarship. Value = $1 200 CAD
- Awarded annually to the top second year student in the Microbiology and Immunology graduate program based on academic achievement and record of research productivity

2009, Travel Award for Abstract Excellence – 2009 International Herpesvirus Workshop, Cornell University, Ithaca, NY. Value = $1 000 USD
- Travel award given to presenters judged to have presented the best abstracts at the 2009 IHW

2009-2010, Ontario Graduate Scholarship. Value = $15 000 CAD
- Awarded to the top graduate students across all disciplines in the Province of Ontario

2009, Best Scientific Poster in Category, Travel Award – 2009 Margaret Moffat Research Day. Value = $500 CAD
- Awarded to the top poster presentation in the Biochemistry and Molecular Biology Category at the 2009 Margaret Moffat Research Day

2008, VWR Award for Best Oral Presentation – 2008 Infection and Immunity Research Forum. Value = $500 CAD
- Awarded to the top oral presenters at the 2008 IIRF

2007-2008, Roche Award. Value = $500 CAD
- Awarded to the student judged by his/her peers to have given the best Microbiology and Immunology graduate seminar each year

2007, Best Scientific Poster in Group - 2007 Infection and Immunity Research Forum. Value = $100 CAD
- Awarded to the top scientific poster presentations at the 2007 IIRF

2007-Present, Schulich Graduate Enhancement Scholarship. Value = $5 000 CAD

2007-Present, Schulich Medical Research Scholarship. Value = $2 350 CAD

2007-Present, Western Graduate Research Scholarship. Value = $4 100 CAD

2004-2007, Dean's Honor List
- Awarded from Years 2-4 of undergraduate studies

2003-2004, Western's Scholarship of Excellence. Value = $2 000 CAD
- Awarded to students with an overall average entering grade of 90%+

2002-2003, Valedictorian, Nicholson Catholic College

2002-2003, The Valedictory Scholarship. Value = $2 000 CAD
- Awarded to the student voted Valedictorian by faculty and graduating class

2002-2003, Greyhound's "Travel is Education Too" Scholarship. Value =$1 050 CAD
- Awarded to students who demonstrate overall academic excellence throughout all years of secondary school studies

Teaching Experience

September 2010 –December 2010
- Graduate Teaching Assistant for Microbiology and Immunology 2100A

September 2009-December 2009

- Graduate Teaching Assistant for Microbiology and Immunology 2100A
- **Nominated for Graduate Teaching Award**

September 2008-December 2008
- Graduate Teaching Assistant for Microbiology and Immunology 2100A

February 2005-2007, Part-time Supply Teacher, ALCDSB
- Teaching grades 1-12 in all subjects including: Biology, Chemistry, Philosophy, English, French, etc…

Volunteer / Appointed Positions

2010-Present, Graduate Student Representative – Appointments Committee, Department of Microbiology and Immunology
- Participate in the review of applications for perspective faculty and vote on short-list of applicants to be invited for formal interview. Interview candidates upon visit to the department and vote on final decision for job offer.

2007-Present, Graduate Student Chair- Outreach Committee, Department of Microbiology and Immunology
- Involved in community outreach and recruitment initiatives for the Department of Microbiology and Immunology, as well as other graduate programs within the Schulich School of Medicine and Dentistry